A cell-based NRG1-ERBB4 assay designed for high-throughput compound screening to identify small molecule modulators with relevance for schizophrenia

Dissertation

for the award of the degree

‘Doctor rerum naturalium’

of the Georg-August-Universität Göttingen

submitted by

Wilko Hinrichs

from Norderney, Germany

Göttingen, 30.09.2012

Prof. Klaus-Armin Nave Ph.D. (Reviewer)

Department of Neurogenetics, Max Planck Institute of Experimental Medicine, Göttingen

Prof. Dr. Martin Göpfert (Reviewer)

Department of Cellular Neurobiology, Schwann-Schleiden Research Center, Göttingen

Prof. Dr. André Fischer (Reviewer)

Laboratory for Aging and Cognitive Diseases, European Neuroscience Institute, Göttingen

PD. Dr. Moritz Rossner

Department of Neurogenetics, Max Planck Institute of Experimental Medicine, Göttingen

Prof. Dr. Thomas A. Bayer

Department of Psychiatry, Division of Molecular Psychiatry, UKG Göttingen

Dr. Judith Stegmüller

Department of Cellular and Molecular Neurobiology, Max Planck Institute of Experimental Medicine, Göttingen

Declaration

Herewith I declare that I prepared the PhD thesis entitled:‘A cell-based NRG1-ERBB4 assay designed for high-throughput compound screening to identify small molecule modulators with relevance for schizophrenia' on my own and with no other sources and aids than quoted.

“We are as forlorn as children lost in the woods. When you stand in front of me and look at me, what do you know of the griefs that are in me and what do I know of yours. And if I were to cast myself down before you and weep and tell you, what more would you know about me than you know about Hell when someone tells you it is hot and dreadful? For that reason alone we human beings ought to stand before one another as reverently, as reflectively, as lovingly, as we would before the entrance to Hell.”

Franz Kafka

Acknowledgments

First, I want to thank my supervisor PD. Dr. Moritz Rossner, for the great PhD project, his support, and all his brilliant ideas and good advice accumulated in this thesis.

Equally, I want to thank my co-supervisor Dr. Michael Wehr, for his friendship, for his patience, for the great discussions, the help with the projects, especially screening and biochemistry, and the proof reading of my thesis.

Dr. Sven Wichert for the help with the Hamilton robot, all bioinformatical questions, and help with all computer-related problems.

Dr. Magdalena Brzozka for discussions, help with the corrections and the deeper insight into mouse behavioural studies.

Dr. Elena Ciirdaeva for great support with cloning and supplies of DNA.

All members of the Rossner group and the Department of Neurogenetics, for friendship, help in all lab problems concerning techniques, instruments, software, and discussion of projects.

The members of the Lead Discovery Centre Dortmund, particularly Dr. Sascha Menninger for the great co-operation, and a deeper insight into HTP screening, lead discovery, and lead optimisation

The GGNB-CMPB program, specifically Prof Michael Hörner, for the fruit-full discussions and seminar series and the GGNB staff for the help with the administrative challenges.

I am grateful for my PhD committee, including Prof. Martin Göpfert , and Prof. André Fischer, and especially Prof. Klaus-Armin Nave for discussions, encouragements, and having me as PhD student in his lab.

Further thanks are to my parents, without there love, support and encouragement this thesis would not be possible.

Carolin, for her love and support in this part of my life.

All friends, fencers, and tabletop-wargamers for the life abroad the PhD.

Table of Content

1 Summary

Schizophrenia (SZ) is as severe and phenotypically as well as genetically complex neuropsychiatric disorder. Only so-called positive symptoms (e.g. hallucinations and delusions) are currently amenable to treatments with neuroleptics. Negative symptoms (such as anhedonia, social withdraw) and cognitive deficits, however, are not substantially improved by current therapies. An impaired function of the prefrontal cortex has been hypothesised as a potential cause for the latter symptoms. Impaired NRG1-ERBB4 signalling affects cortical circuits formed between inhibitory interneurons and excitatory pyramidal neurons. The corresponding dysbalance of inhibition and excitation is thought to be causative for the cognitive deficits observed in corresponding gain and loss-of-function mouse models. Importantly, genetic association studies have identified NRG1 and ERBB4 as risk factors for SZ. Therefore, NRG1-ERBB4 signalling is among the most promising targets for the development of new treatments for SZ.

This thesis describes the design and development of a split TEV-based co-culture assay to monitor several steps of the NRG1-ERBB4 signalling cascade in one integrated measurement. The assay displays high sensitivity and robustness and is applicable to high-throughput approaches. In a proof-of-principle, the assay was used to screen 727 FDA-approved drugs. Spironolactone was recovered as a major hit, acting as an inhibitor of NRG1-ERBB4 signalling and was validated by an extensive set of secondary assays including several technical controls. Moreover, specificity and first mode-of-action analyses were performed with a panel of assays with NRG and ERBB family members as well as different components of the signalling cascade.

In summary, the assay monitoring proximal aspects of the inter- and intracellular NRG1-ERBB4 signalling cascade was successfully established and a first hit was validated. The assay qualifies for high-throughput screenings with huge libraries of diverse chemical compounds and thus holds a great promise to identify and improve new lead structures to modulate NRG1-ERBB4 signalling.

2 Introduction

2.1 General characterisation of schizophrenia

Schizophrenia (SZ) is a severe brain disorder ((Lewis and Lieberman, 2000)(Lewis and Levitt, 2002), a major mental illness and a severely debilitating neuropsychatric disorder (Arnold and Trojanowski, 1996). The term SZ was first introduced in the beginning of the 20th century by Bleuler (Pratt et al., 2012). Kraepelin described the illness as “Dementia praecox”(Kraepelin, 1896).

The diagnostic criteria for schizophrenia are described in the ICD 10 (International Classification of Diseases 10) as well as DSM IV (Diagnostic and Statistical Manual of Mental Disorders). These literal classification schemes are important, since no biological marker of SZ has been identified so far. The classification is based on the categorization of behavioural phenotypes by interviews and are inherent to biases possible by the subjective evaluation of individual clinicians. Nontheless because our understanding of biomarkers based on causal genetic, biochemical or pathophysiological events remains scarce (Pratt et al., 2012) there is no alternative. Moreover, the term disorder is under debate, shifting to disease (Becker, 2005; Berganza et al., 2005; Steurer et al., 2006), taking in account the specific etiology and the discernable pathology of SZ (Tandon et al., 2008b). Further debates, to deconstruct the term SZ itself as it represents an artificial term for different diseases with similar phenotypes are on-going (Tandon et al., 2008a).

The prevalence of SZ ranges between 0.3% and 2.0%, with an average of 0.7% in the population of Western Europe. Although occurring worldwide, SZ seems to be independent of culture, political system, or religion (Saha et al., 2005). The precise determination of the number of affected subjects is impossible due to the lack of biomarkers, valid and reliable diagnosis, and precise demarcation between diseased and healthy people (Eaton et al., 2007).

The onset of the disease occurs usually after puberty or during early adulthood (age 15-45) (Fig. 1). Affected men are usually younger than women (average five-seven years earlier) when the disease starts and seem to have a slightly increased risk to suffer from SZ (up to 1,4 fold higher risk) (Aleman et al., 2003; McGrath, 2007). The onset of SZ is usually preceded by a prodromal phase with an average lengths of five years (Klosterkötter, 2008). The prodromal phase often includes the manifestation of cognitive deficits, impairments in social functions, and a drop in job or school related performance (Tandon et al., 2009).

After the prodromal phase chronic SZ starts mostly by a psychotic episode. The “phenotype” of the disease can further be classified by course (continuous or episodic) onset (acute, progressive or stable), and outcome (mild, severe or recovery). The most abundant type is an episodic course with distinct psychotic episodes.

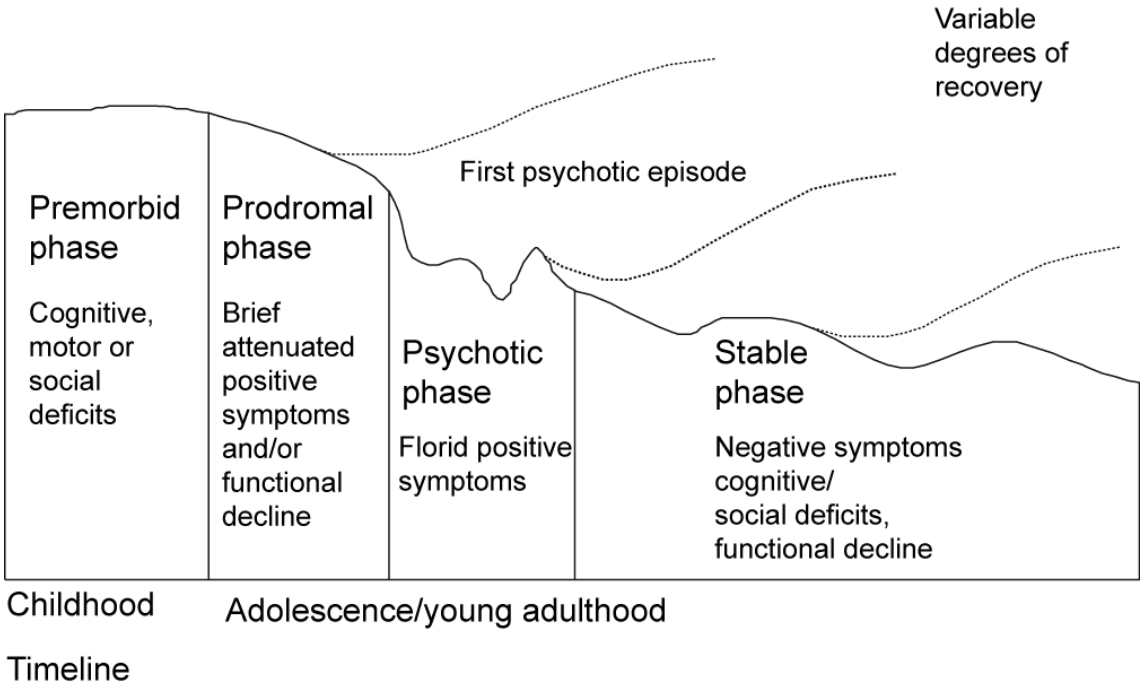

Figure 1: Schematic representation of the course of schizophrenia, modified from (Tandon et al., 2009)

SZ is characterised by three subsets of symptoms: positive symptoms, negative symptoms, and cognitive deficits (Fig. 2).

2.3 Positive symptoms

Positive symptoms are the prominent phenotypic symptoms during an acute psychotic episode where patients may suffer from different sorts of hallucinations (e.g. visual, audio, tactile, olfactory, or gustatory hallucinations), delusions or thought disorders. Patients might suffer upon e.g. hearing of a voice keeping up a running commentary on the persons behaviour or thoughts or experience olfactory hallucinations like the smell of dead people. The patients usually develop more complex delusions (bizarre delusions, delusions of control, organisations) severely altering or modifying the perception of reality. As a part of this, single symptoms are reported, such as the feeling of thought insertions or thought withdrawal, thought echos and thought broadcasting. This leads to feelings of suspiciousness or persecution, extending to attempts of suicide. In contrast, even grandiosity or hostile behaviour is observed depending on the perception content of the delusions. The behaviour of the patients is furthermore impaired by disorganised speech and/or disorganised behaviour, which can be catatonic, but also a complete disorganisation of conceptual thinking. In 75% of patients these positive symptoms can be reduced by the use of anti-psychotic drugs. At least 25% of patients do not respond to the treatment at all (Tandon et al., 2010; Tandon et al., 2009; Keshavan et al., 2008; Tandon et al., 2008b; Tandon et al., 2008a).

2.4 Negative symptoms

Negative symptoms are not as prominent as positive symptoms. However, negative symptoms can start years before the first psychotic episode and often persist after the decline of the psychotic episode. Patients may suffer from social withdrawal, reduced, flat or inappropriate affect, alogia (poverty of speech), avolition (generalized lack of motivation to perform tasks or undertake activities), emotional withdrawal, and poor rapport. All these symptoms distract the patients to live a normal social life i.e. they may not be integrated in networks of relationships, friends, colleagues, and even medical care personal. In particular solitude has been reported by patients to be one of the major symptoms ruining the quality of their life. The negative symptoms are poorly targeted by classical drugs (Tandon et al., 2009; Tandon et al., 2010).

2.5 Cognitive deficits

Furthermore, there is an impact of the disease on the cognitive abilities of the patients. These cognitive deficits are the most debilitating and persistent deficits in SZ. A drop in performance in every-day life regularly accompanies the progress in the development of the negative symptoms, e.g. at school, at the university or in professional life. Cognitive impairments are further impaired with the onset of psychotic episodes. Deficits in working memory, difficulties in

abstract thinking or stereotyped and inflexible thinking are usually observed. The cognitive deficits remain impaired after fading of the psychotic episode and can worsen with further episodes or over time. The cognitive deficits, as the negative symptoms, do not respond regularly to medication and remain largely resistant to treatment (Arnold and Trojanowski, 1996; Pratt et al., 2012).

Negative and cognitive symptoms are not efficiently targeted by available drugs and are factors which most significantly contribute to worsening of patients individual quality of life. SZ is laying an annual burden of 30 billion € on the European health care systems (33 billlion US dollars in 1999 worldwide (Bayer 1999)) and is among the top ten leading causes of disease related disability in the world (WHO statistics 2001, (Tandon et al., 2008b)).

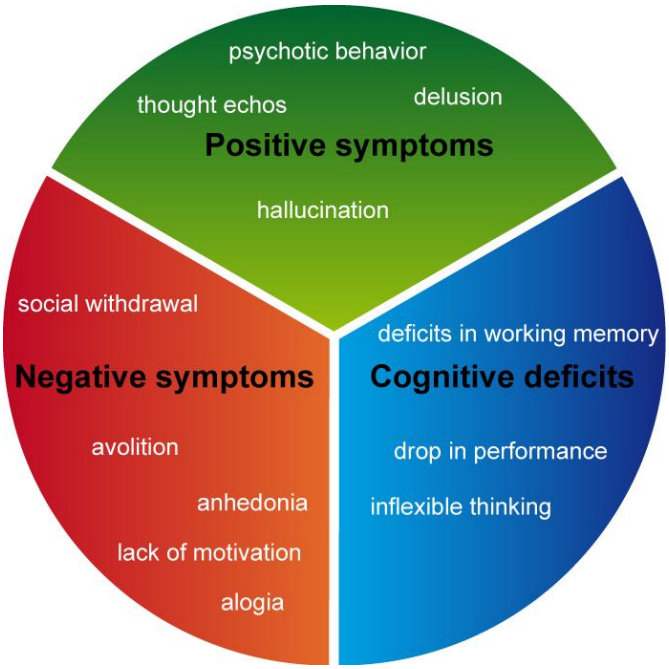

Figure 2: Triade of SZ symptoms: positive symptoms, negative symptoms and cognitive deficits are shown with exemplary phenotypes

2.6 Comorbidities

Single symptoms, or even mixtures of the symptoms described above, can also occur in various other mental diseases. For the differential diagnosis of SZ by a psychiatrist, different other illnesses e.g. depression, brain tumour, have to be ruled out as causative for the symptoms or, if occurring in parallel, separately treated. The diagnosis is further complicated by a high rate of psychiatric comorbidity in the patients. The most frequently present psychiatric comorbidities are depression, suicide tendency, substance abuse, sleep disturbances and addiction.

Diabetes mellitus, autoimmune disorders and cardiac autonomic dysregulation are the most often described non-psychiatric comorbidities. Furthermore, the medications lead often to severe side effects e.g. metabolic syndrome or tiredness, which have to be necessarily addressed in the treatment of SZ as well. In general, the health state of the SZ patients is most likely impaired in multiple ways (Ferentinos and Dikeos, 2012; Kodesh et al., 2012).

2.7 Residual symptoms

There is a set of residual symptoms, which occur with an acute psychotic episode and remain present thereafter. This has been described for most negative symptoms like social withdrawal or flat affect, or mild positive symptoms like eccentric behaviour or odd beliefs (de Bartolomeis et al., 2012).

Subtypes of schizophrenia

For a better diagnosis, SZ is subdivided in different phenotypic subtypes (Tab. 1). The usefulness of this diversion is debatable.

Type	**Description**
Paranoid (F20.0)	hostile or threatening auditory hallucinations, delusions
Catatonic (F20.2)	motoric immobility, stuporous catatonia or exited catatonia / excessive motor activity, echolalia, echopraxia
Disorganized (F20.1)	disorganized speech, disorganized behaviour, flat or inappropriate affect
Undifferentiated (F20.3)	mixture or emerging process of different subtypes
Residual (F20.5)	Absence of prominent delusions, hallucinations etc., presence of negative symptoms

Table 1: SZ subtypes with the most prominent behavioural phenotypes.

Depicted are the 5 common subtypes of SZ used, when diagnosed by a psychiatrist. The subtypes are diverse and the borders do not display clear demarcation lines. Modified from (ICD-10)

2.8 History of schizophrenia

The first identifications of mental illnesses and attempts to cure these are unknown but it´s history might be as old as human consciousness itself.

Symptoms of a mental disease were first mentioned 3400 years BC in the Book of Heart, an Egyptian papyrus (Okasha, 1999; Okasha, 2001; Mohit, 2001). However, whether these mentions can be linked to SZ is unclear or remains elusive, as this medical term did not exist at that time. Other descriptions, of putative SZ phenotypes, were found in the Indian vedas and in some books of the bible e.g. Nebukadnezar written ca.1400 BC. Skulls with trepanations are sometimes interpreted as early attempts to cure mental diseases (Clower and Finger, 2001).

The Greek philosophers Thales, Phytagoras, Galen, and Hippocrates provided the first theories of the mind and consciousness, and what mental diseases possibly could be at ca. 550 BC. The theories included natural courses and miss-regulations of the four humours. The function of the brain itself was poorly understood (Missios, 2007).

During the dark ages mental illnesses were regarded as evil possessions and no progress in theories could be made. Exorcisms and witch burnings were regular events. In 1357, the Bethlem asylum was founded in London, where dangerous mental diseased patients were simply chained and locked away.

In the 17th century, John Locke (1632-1704) came up with the theory that the brain is empty at birth and is filled in a process of learning by e.g. sensory input. Mental diseases are regarded as a disconnection of the relationship between the environment and the affected person.

In the 18th century Phillippe Pinel (1745-1826) began to unchain the patients in the asylums.

In the 19th century Wilhelm Griesinger (1818-1868) proposed that the brain is the origin / source of the mental diseases, and that these diseases are complex. In addition he shaped the term “unitary psychosis”.

Emil Kraeplin (1856-1926) proposed the dichotomy between “dementia praecox” and “bipolar disorder”. He also observed the symptoms in longitudinal manner and was convinced that an organic brain disease causing SZ symptoms exists.

In 1897 Alois Alzheimer published the first study on patients having SZ symptoms.

In 1911 Eugen Bleuler (1857-1939) coined the term “schizophrenia” He based it on the Greek words skhizein = to split and phren = mind.

The first half of the 20th century was dominated by eugenic and social darwinistic pseudo-science, that even lead to mass murder on mentally diseased patients in Germany (“Action T4”). In 1952 the first international congress on neuropathology in Rom concluded: “There is no neuropathology of SZ”.

In 1976 a computer tomography (CT) study on schizophrenic brains conducted by Johnstone showed an enlargement of the lateral ventricles. Meanwhile, the development of neuroleptics allowed for the first time to a state of control of the psychotic disease symptoms, which permitted ¾ of the patients to leave the asylums, e.g. in USA the number of patients in asylums decreased from 600,000 to 150,000. A wide range of treatment strategies were developed starting from lobotomy, relaxing therapies, lithium, insulin coma, to psychotherapy and psychoactive drugs (Jeste et al., 1985, Ellard, 1987). For further readings see (Russel and Cohn 2012)

2.9 Morphologic findings in schizophrenia

The cause of the disease remains unknown. Although the behavioural phenotype is strong, the morphological abnormalities in the brain are more subtle and elusive. SZ is nowadays considered as a multifactorial disease including multiple genetic and environmental components, potentially modulated by epigenetic- risk factors. (Tandon et al., 2008b; Tandon et al., 2009). In detail the following findings are validated and discussed.

Magnetic resonance imaging (MRI) showed in first episode SZ patients a reduction of the total brain volume, an enlargement of the ventricles and a reduction of the volume of the hippocampus. Analysis of high-risk individuals shows growing evidence for subtle abnormalities of hippocampal and ventricular volume in close relatives of SZ patients (Whalley et al., 2012).

Only a few degenerative processes are described for SZ (Meyer-Lindenberg, 2011). A dynamic wave of accelerated grey matter loss has been published (Honea et al., 2008). The loss is most prominent in the early phases of SZ. First, the parietal regions are affected, afterwards the temporal lobes, and subsequently changes in dorsolateral prefrontal cortices and superior temporal gyrii are observed. The yearly grey matter loss in SZ patients has a rate of 0,5% compared to 0,2% in healthy individuals (Rund, 2009).

Medical findings in SZ patients using EEG recordings are not specific for SZ. Deficits in sensory-motor gating measured as pre-pulse inhibition are observed. However, again they are not specific for SZ and are present in other psychiatric diseases as well. Moreover, SZ patients display impairments of synchronisation of different brain areas (Fig 12). A disturbance in sensory gating of the p50

wave is often found in SZ patients. A failure in the corollary discharge system is hypothesized as causative for hallucinations (Ishii et al., 2012).

Autopsies taken from post mortem brains of SZ patients show a decrease in brain weight and brain length, a decrease of the volume of cerebral hemispheres, and an enlargement of the ventricles (Kleinman et al., 2011).

In vivo neuroimaging studies revealed alterations in the ventricular system. SZ brains display abnormalities in the cavum septi pellucidi, an enlargement of the lateral ventricles, and the third ventricle. The grey matter volume is decreased in the prefrontal cortex. A decrease in the thalamus, temporal lobe structures, medial temporal lobe (hippocampus/amygdala), and the superior temporal gyrus is described. The white matter integrity is decreased in all four cortical lobes (Fornito et al., 2012).

At the cellular level microscopic studies of the hippocampus and prefrontal cortex have shown no overall change in neuron numbers, but a size reduction of the mean neuronal soma, and a higher package density of neurons in the prefrontal cortex. The thalamus displays a lower number of neurons in the mediodorsal, anteroventral, and anteromedial nuclei. The entorhinal cortex is characterised by a poorly developed layer II and a disturbance in the layer structure (Arnold and Trojanowski, 1996).

Other theories in the field link findings of auto immune reactions and micro glia malfunctions to the disease (Monji et al., 2009). For further information, see (Hanisch and Kettenmann, 2007; Chen et al., 2010).

Fast progress in individualised medicine enabled derivation of human induced pluripotent stem cells (hiPSC) from patients. The re-programming of patient fibroblasts infected with lentiviruses containing genes for the factors Oct4, SOX2, KLF4, cMYC, and Lin 28, lead to the growth and differentiation of disorder specific neurons. The SZ hiPSC display diminished neuronal connectivity and reduced expression of PSD95 and glutamate receptors. Moreover, alterations in the expression of components of cyclic AMP (cAMP) and the WNT signalling pathways have been reported. Furthermore, the neurons obtained from hiPSC of SZ patients respond to antipsychotic treatment. Experiments on hiPSC of SZ patients give for the first time an unique opportunity of investigating SZ *in vitro* which offers a tremendous potential to find new personalised treatments for SZ patients (“SZ in a box”) (Brennand et al., 2011).

2.10 Genetic studies

Adoption studies, twin studies, family-based studies, and population studies showed an increased risk to develop SZ depending on the degree of kinship

(Sullivan et al., 2003). The average prevalence in any society in any country in the world to develop the illness is 0,7% (Saha et al., 2005). For children of two SZ-positive parents, and for gene identical monozygotic twin where the other suffers from SZ the overall risk is increased to 40%-50% (Ayhan et al., 2009). The overall genetic impact on the development of SZ is estimated 70%-80% (Sullivan et al., 2003; Wexler and Geschwind, 2011). Family-based studies identified a gene that is disrupted and plays a role in the disease (disrupted in SZ: DISC1, Scottish family). However, genome-wide genetic association studies (GWAS) failed to identify a single gene or a specific subset of genes being causative for the disease. Nevertheless, it was possible to identify different single nucleotide polymorphisms (SNPs) and rare copy number variations (CNVs) in genes, which seem to be associated with brain changes leading to higher vulnerability (Sebat et al., 2009). The precise contribution of each genetic alteration remains unclear and combinatorial effects of different risk alleles are debated as effective cause (Allen et al., 2008; Jia et al., 2010). In addition, a current model suggests that a set of complex disease pathways, where various different alleles lead in different combinations to disparate neuropsychiatric disorders (Figure 3) (SZ, bipolar and unipolar depression, mental retardation, seizures and autism, no clear demarcation lines) (Karam et al., 2010). This model also emphasizes that the discovery of a single pharmacological intervention treating all symptoms at once is highly unlikely. In contrast, newly developed drugs probably target similar symptoms in different neuropsychiatric disorders (Karam et al., 2010).

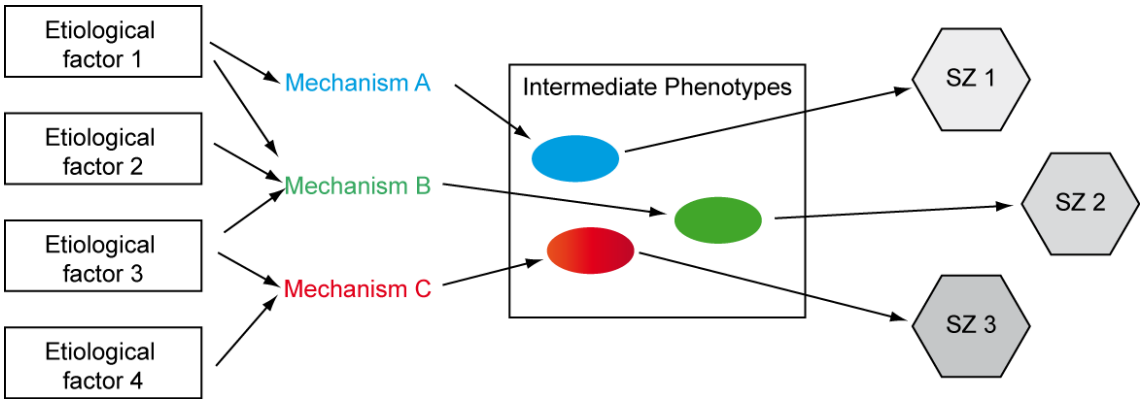

Figure 3: Model for SZ: The endpoint result is different SZ types (Tandon et al. 2008)

Some of the most frequent SZ susceptibility genes are:

2.10.1 DISC1

The DISC1 (disrupted in schizophrenia 1) gene was linked to the disease by St Clair in 1968, when he discovered a chromosomal translocation from

chromosome chr.11 to chr1 in a Scottish boy. The translocation truncated a single gene, DISC1. The truncation was present in a half of the boy's family that was diagnosed with severe mental diseases. Later linkage of DISC1 to SZ was confirmed in Finish, Caucasian and Asian populations.

DISC1 is a large scaffolding protein (93kDa), prominently expressed in the human hippocampus. It interacts with MAP1a, GSK-3β, PDE4, FEZ1, and NDEL1. DISC1 is also downstream of the NRG1-ERBB4 signalling cascade (St Clair et al., 1990; Millar et al., 2000; Kang et al., 2011; Wexler and Geschwind, 2011).

2.10.2 NRG1-ERBB4

The first findings on impaired NRG1-ERBB4 (Neuregulin1 - receptor tyrosine-protein kinase v-erb-a erythroblastic leukemia viral oncogene homolog 4) signalling were made by Stefansson and colleagues in the genome wide association studies on an Icelandic population (Stefansson et al., 2002). The identified SNP SNP8NRG243177 or 'icelandic' haplotype (HAPice) has been associated with several schizophrenia-like phenotypes, e.g impaired frontal and temporal lobe activation, deficits in cognitive functions and a predisposition for the development of psychotic symptoms (Hall et al., 2006).

Until 2009, more than 80 SNPs in the NRG1-ERBB4 receptor-ligand pair have been associated with SZ (Sebat et al., 2009). Patients with alterations in the *Nrg1* gene display endophenotypes like decrease in pre-puls inhibition (Hong et al., 2008), reduced integrity of the white matter (McIntosh et al., 2008; Winterer et al., 2008), hypofrontality, cognitive dysfunction and decreased IQ (Hall et al., 2006). Most genetic polymorphisms of the *Nrg1* gene are found in the 5' region, the regulatory element of the *Nrg1* gene (Harrison 2006). It is speculated that this alterations contribute to alterations in gene function and expression. A meta-analysis of up to 24 different studies in diverse ethnic groups successfully confirmed these findings (Munafò et al., 2006; Li et al., 2004; Li et al., 2006).

The *Nrg1* gene is a key player of numerous processes implicated and discussed in the development of SZ. NRG1 contributes to myelination, development of glial cells, migration of radial glial cells during cortical development, neuronal plasticity modulated by NMDA receptor function, development of GABAergic interneurons, and expression of dopamine and serotonin receptors and monoamine transporters (Mei and Xiong, 2008). Furthermore, NRG1 modulates the formation of dendritic spines (Chen et al., 2008), and gamma oscillations in the hippocampus (Fisahn et al., 2009). Mice heterozygous for Nrg1 show schizophrenia-related phenotypes resembling symptoms observed in SZ patients (see below).

NRG1 has been shown to increase the expression of α7-nicotinic receptors (Hancock et al., 2008). It is postulated that alterations in NRG1 mediated signalling changes the nicotinic receptor profile in presynaptic inputs, leading to deficits in pre-puls inhibition by altering glutamatergic transmission from the ventral hippocampus to the nucleus accumbens (Karam et al., 2010).

Additionally, the NRG1-ERBB4 signalling pathway is a major input for various pathways, involving PI3-kinases, PTPRZ1-RTPβ-phosphatase, BACE secretase, and the afore mentioned DISC1. Many of these are hubs at information processing, and may be suitable as future drug targets (Jaaro-Peled et al., 2009; Höistad et al., 2009).

2.11 Environmental factors

Many studies show the importance of environmental factors in onset, cause and severity of the disease. The concordance for SZ in monozygotic twins is only 50%. Therefore genes cannot be the only cause for the disease. The most prominent environmental factors contributing to development of SZ are antenatal or obstetric complications (hypoxia, maternal infections, maternal drug - intake) (Nicodemus et al., 2008)), migration (first reported by Odegard 1932, (Cantor-Graae and Selten, 2005), urbanicity (Kirkbride et al., 2006), parental age, malnutrition and psychotrauma (Keshavan et al., 2008). All these factors seem to create psychosocial stress. Just like the genetic factors, environmental factors alone fail to explain the disease (Fig. 3). The combination of genetic and environmental factors leads to the “Two Hit Hypothesis”.

2.12 Two hit hypothesis

The “Two Hit Hypothesis” of SZ integrates the genetic and environmental observations. The combination of one, or of different genetic defects, either inherited, or de novo mutated, generates a state of vulnerability e.g. a deficient neuronal network. Stressful environmental effects like viral infections, birth complications, or social stress as a second hit can subsequently trigger the outbreak of SZ by modulating the expression or function of the defective genes or proteins (Bayer et al., 1999; Maynard et al., 2001).

The proposal of a “Three Hit Hypothesis”, additionally taking in account drug effects like cannabinol (THC), as an additional player to genes and environment interaction, is under debate (Vigano et al., 2009).

2.13 Findings in animal models of schizophrenia

Animal models of diseases, reflecting the genetic findings, are highly desired and deliver valuable information about the disease. The problem with animal models of complex diseases, which cannot be associated with a single gene, or that are multifactorial disorders like SZ, is to generate a valid model for a disease.

A valid animal model has to meet the following criteria:

- *Face validity* (animal model shows the symptoms of the disease)
- *Construct validity* (animal model has the same mutation or genetic alteration underlying the mechanisms of disease aetiology)
- *Predictive validity* (animal model responds to treatments similar as patient)

As the precise cause and the multi factorial interaction remains unknown, construct validity of the different animal models in SZ is not possible. Consistent with the complexity of the disease and spectrum of symptoms, genetic research has led to the development of several animals models that are thought to mimic parts of the disease. They show a broad spectrum of endophenotypes similar to observations of a few positive symptoms, negative symptoms, and cognitive deficits in SZ but “the schizophrenia model” will not be possible to generate (Kellendonk et al., 2009).

The first mouse models in the field were drug induced ‘psychotic’ models. Mice were simply treated with Amphetamine or Phencyclidine until they show psychotic behaviour (such as motor hyperactivity) and were subsequently treated with the newlz developed putative drugs (Javitt and Zukin, 1991).

Amphetamine leads to an over activation of the dopaminergic system and Phencyclidine leads to an over activation of the glutamatergic system. The Dopamine- and Glutamate-Hypotheses sprouted from these observations. Drugs could be tested afterward with these models which lead e.g. to the discovery of antipsychotic drugs like Haloperidol (1958), which is still used to treat psychotic episodes in SZ patients. However, these setup of drug discovery remains serendipitous (Pratt et al., 2012).

2.13.1 Dopamine hypothesis of schizophrenia

Dopamine belongs to the family of monoamines and acts as neurotransmitter or neuromodulator. It is recognised via G-protein coupled receptors, localised in the prefrontal cortex, nucleus acumbens, and the striatum. Decreased Dopamin in the prefrontal cortex and increased dopamine in the mesolimbic pathwayarer key findings for SZ (Goldman-Rakic et al., 2004) The classic dopamine

hypothesis postulates that the drug class of neuroleptics (e.g. Droperidol) act as dopamine receptor antagonists (van Rossum, 1966; van Rossum, 1967). There is a correlation between affinity of these antipsychotic drugs to the Dopamine D2 receptor subtype and the clinical efficiency in countering hallucinations and delusions(Seeman and Lee, 1975). They are hypothesized to block dopamine receptors in the mesolimbic dopaminergic system. This leads to the alleviation of the positive i.e. psychotic symptoms. Unfortunately, side effects resulting from dopamine blockade in the nigrostriatal and hypothalamic-pituitary systems, phenotypically similar to Parkinson's disease, hyperprolactinemia, sedation and hypertension can be observed (Pratt et al., 2012, Vigano et al., 2009).

In 1991, a modified dopamine hypothesis was postulated (Davis et al., 1991, Biedermann and Fleischhacker, 2009) .Cortical hypoactivity, leads to negative symptoms, therefore neuroleptics show no effect. It is based on the observation that humans with frontal lobe brain damages or lobotomy show symptoms similar to SZ negative symptoms. Subcortical hyperactivity, leads to the positive symptoms, which are partially reduced by neuroleptics. Only the D2 receptor subclass, localized in the striatum (subcortical) is targeted by all relevant antipsychotics (Sanyal and Van Tol, 1997).

2.14 NRG1-ERBB4 animal models

The finding of impairments in the NRG1-ERBB4 system by GWAS, led to an increased interest in the analysis of different genetically manipulated *Nrg1* and *Erbb4* mice to study neuronal and behavioural phenotypes.

Mice that are homozygous null for *Erbb4* are dying at postnatal day (P) 10,5 - 11 because of developmental heart failure (Tidcombe et al., 2003). Heart rescued mice (to prevent developmental death) show defects in neuronal architecture.

Heterozygous knock-out (KO) mice of Nrg1 show hyperactivity and pre-pulse inhibition deficits, one of endophenotypes of SZ.

Nrg1 overexpression (Stefansson et al., 2002), altered social behaviour and increased anxiety (Desbonnet et al., 2009), memory deficits, reduced inhibitory interneuron numbers and increased ventricular volume (Chen et al., 2008). These findings resemble symptoms observed in SZ patients.

Nrg1-typeIII overexpressing mouse models and the ErbB4 heterozygous mouse model could be used to validate effects of Nrg1-ERBB4 mediating drugs.

The following table summarizes the phenotypes obtained with *Nrg1*/*Erbb* mouse models:

Mouse-model		Phenotype
Nrg1.I	Overexpression	Increased locomotor activity, non-significant trend towards decreased pre-pulse inhibition, decreased context depending fear learning (Kato et al., 2010). reduced GABAergic (parvalbumin) and myelination marker in the frontal cortex (Kato et al, 2008). Alterations in hippocampus. Hypermyelination and ataxia for high gene dosage (Brinkmann et al., 2008)
	Heterozygous KO	Behavioural phenotype linked to SZ phenotype (Stefansson et al., 2002) Fewer functional NMDA receptors, react to clozapine (Bjarnadottir et al., 2007)
	Homozygous KO	Die during embryogenesis, heart malformations (Meyer and Birchmeier, 1995)
Nrg1.III	Overexpression	Hypermyelination (Velanac et al., 2012; Michailov et al., 2004) ataxia for high gene dosage (Brinkmann et al., 2008)
	Heterozygous KO	Poor ensheathment of sensory neurons, disproportionately unmyelinated or hypomyelinated nerve fibres. Failure in myelination (Taveggia et al., 2005; Taveggia et al., 2008).
	Homozygous KO	Not separated from Nrg1.I
ErbB4	Overexpression	Generation and characterization of GAD67-ErbB4 transgenic mice. (Work in progress Lin)
	Heterozygous KO	Behavioural phenotype linked to SZ phenotype (Stefansson et al., 2002)
	Homozygous KO	Lethal at embryonic day (E) 10,5-11, failure in heart development (Tidcombe et al., 2003).
	Homozygous KO heart rescue phenotype	Defects in cranial neural crest cell migration, aberrant cranial nerve architecture, increased number of large interneurons, lactation deficits. Lack of STAT5A phosphorylation (Liu et al., 1997, Fried et al., 2002). Altered populations of hippocampal interneurons (Neddens and Buonanno, 2010).

Table 2. Shown are the effects of alterations in the Nrg1-ErbB4 signalling system in mouse animal models.

Several studies combined genetic modified animal models of SZ with environmental factors like e.g. stress (isolation stress in single caging, psychosocial stress by social defeat or maternal separation etc.). This is thought to mimic the “Two Hit” hypothesis of SZ in the respective animal model.

SZ is a human specific disorder diagnosed by a psychiatrist and obviously cannot be exactly matched in any animal model. Nonetheless, several mouse models display behavioural alterations resembling certain (endo)phenotypes of SZ (Tab. 3). The construct validity underlying these phenotypes, especially regarding modelling of positive symptoms of SZ, is often under debate.

Domain	**Schizophrenia in humans**	**Rodent phenotype**
Positive symptoms	Psychomotor agitation	Hyperlocomotion in open field
	Catatonia	Catatonia like state in bar test
	Hallucination, delusion, thought disorders	Lack of readouts
Negative symptoms	Social withdrawal	Decrease in social interaction
		Decrease in nest building ability
	Restricted interest, stereotypic behaviour	Repetitive behaviour
	Affect flattening	Lack of reliable readouts
	Anhedonia	Decrease in sucrose preference
Cognitive symptoms	Working memory deficits	Impaired performance in T-maze
		Impaired performance in 8-arm maze
		Decreased spontaneous alternation in Y-maze
	Deficit of attention	Decrease sustained attention in 5CSRTT
		Decreased set shifting ability
		Decreased spatial reversal or reversal of discriminant operant learning
	Disturbance of sensorimotor gating	Diminished pre-pulse inhibition

Table 3. Tests available for assessment of SZ-related phenotypes in rodent models

2.15 NRG1-ERBB4: from proteins to network analysis

2.15.1 Why addressing the NRG1-ERBB4 signalling system?

As described above, gene defects play the major part in the development of the vulnerability to SZ. Nonetheless, available studies fail to link the disease to a single gene or to a precise subset of genes. Therefore, the assumption that SZ is a generic term or a superordinate concept of different diseases ending up in a similar set of similar or slightly different phenotypes is presumable. If there is not “one schizophrenia” existing with one causative SZ gene, I assume that newly developed drugs, for a determined subset of patients are the auspicious novelties. The NRG1-ERBB4 signalling network seems to be one of the most promising and best accessible SZ key players to address in the development of new drugs. In detail the following subsets of information on NRG1-ERBB4 are available.

2.15.2 Protein-protein-interactions and NRG1-ERBB4 signalling

Specific protein-protein-interactions (PPI) in cells are the basic units of signalling cascades. Most cellular processes are regulated through signalling cascades or more complex structures of interlinked cascades named signalling networks or pathways (Neddens and Buonanno, 2010). Signal processing needs different regulation of information. This leads to diversification, amplification, diminution or alteration of the signal and interexchange between different cascades. The endpoints of signalling cascades are changes in expression levels of the cellular proteins thereby inducing apoptosis, proliferation, growth or other changes in cellular behaviour.

Of crucial importance for an inter-cellular communication is the reception of signals from other cells. Signals are transferred from the outside to the inside through a ligand representing the stimulus activating specific transmembrane receptors. Once activated, receptors recruit adaptor molecules and activate signalling cascades forwarding information through the cytosol to the nucleus. In the cytosol further processing takes place and different signal cascades are interlinked. In the nucleus gene activity is modulated according to the processed information, causing on and off switching of genes or modulating the gene expression (Taniguchi et al., 2006). A plurality of subsequent processes for example protein turnover and stress reactions to low oxygen levels are important parts of signal processing (Fishman and Porter, 2005).

The overall architecture of the NRG1-ERBB signalling system is organised in a bowtie or hourglass like structure (Fig. 4). A multitude of ligands binds to corresponding subtypes of ERBB receptors, thereby activating a handful of adapters and then initialising various cascades to deliver signals to the nucleus (Yarden and Sliwkowski, 2001; Oda et al., 2005). Drugs and pharmacological

substances can act through binding of receptors outside the cells, or by inhibiting the functionality of enzymes, or alter the structure of proteins and protein complexes (Oda et al., 2005; Yarden and Pines, 2012).

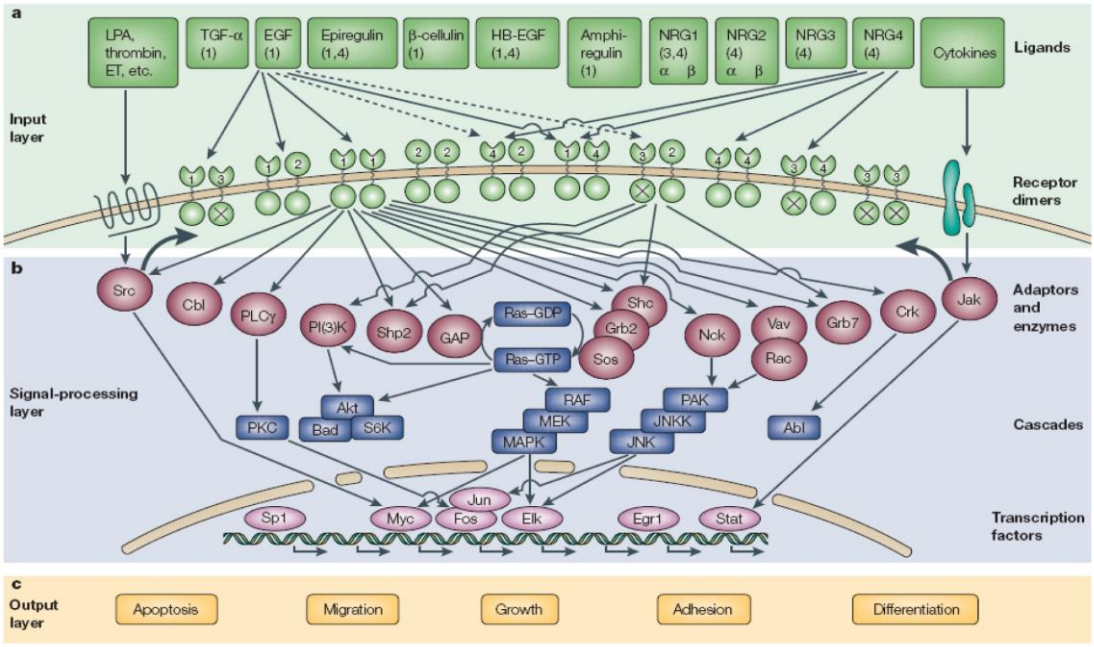

Figure 4: Bowtie structure of the ERBB signalling network (Yarden and Sliwkowski 2001)

2.15.3 Neuregulin1

Neuregulins (NRGs) are signalling molecules or ligands that bind to specific receptor tyrosine kinases (RTKs) i.e. ERBB3 and ERBB4. The Neuregulin family consist of four genes named *Nrg1-Nrg4*. The best characterised ligand is Neuregulin1 (NRG1). More than 31 isoforms of this ligand are described (Falls, 2003). The effect of the NRG1 ligand depends on the cell type, tissue context and activated receptors. NRG1 acts e.g. as differentiation factor in the peripheral nervous system (PNS) (Adlkofer and Lai, 2000) and regulates myelin sheet thickness in axon-Schwann cell interactions (Michailov et al., 2004). In the central nervous system (CNS) NRG1 promotes synaptogenesis (Kwon et al., 2008; Ozaki et al., 1997).

Historically, NRG1 was associated with various biological functions. First, it was named Heregulin/neu differentiation factor (HRG/NDF) that activates HER/neu-oncogenes or glial growth factors that promote proliferation of Schwann cells (Grossmann et al., 2009; Brockes et al., 1980). Furthermore, NRG1 was found to increase the expression of acetylcholine receptors in muscle cells (Falls, 2003).

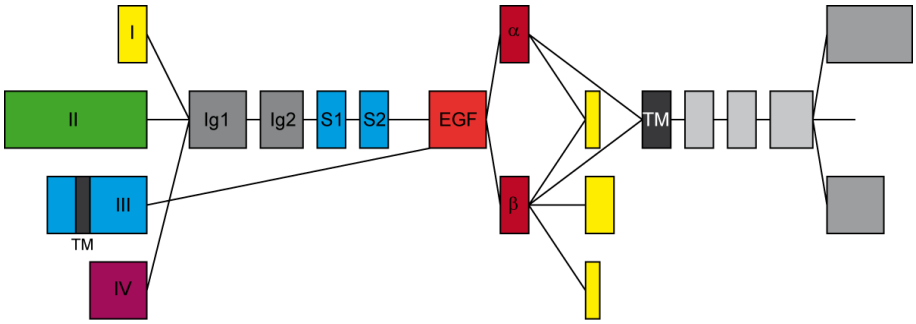

Figure 5: Splice variants of Nrg1 (modified Mei XIong 2008)

The three most abundant splice isoforms of NRG1 in mice are Nrg1-typeI-β1a, Nrg1-typeII-β1a and Nrg1-typeIII-β1a (Fig. 5). All isoforms harbour a C-terminal transmembrane domain, but differ in the N-terminus. Type I and type II harbour an extracellularly localised immunoglobulin like (Ig-like) domain. In contrast, type III contains a cysteine-rich domain (CRD) with an additional transmembrane domain. The transmembrane isoforms of NRG1 are cell type dependently processed by a set of metalloproteases, e.g. TNFalpha-converting enzyme (TACE) or beta-site APP cleaving enzymes (BACE). When cleaved, the NRG1 intracellular domain can back signal to the nucleus and the extracellular domain acts as a paracrine (type I-II) or as juxtacrine signal (type III) (Mei and Xiong, 2008).

NRG1 binding activates ERBB3 and ERBB4 receptors by inducing homo- and hetero-dimerisation of ERBB1-4 receptors, in particular NRG1 can activate ERBB1-3, 1-4, 2-3, 2-4, 3-3, 3-4, 4-4 receptor pairs (Mei and Xiong, 2008). It is postulated that a single ligand is sufficient to activate the dimers (Liu et al., 2012).

The most prominent bioactive part of all Nrg1 isoforms is the EGF like domain. The EGF like domain is 55 amino acids (AA) long (Fig. 6). A 62 AA stretch, resembling NRG1 AA Thr176–Lys238, including the EGF like domain, is commercially available via different manufactores. Thiss domain is overexpressed in bacteria and afterwards purified. It is highly active and stimulates ERBB3 and ERBB4 receptors similar to native NRGs (Liu et al., 2012).

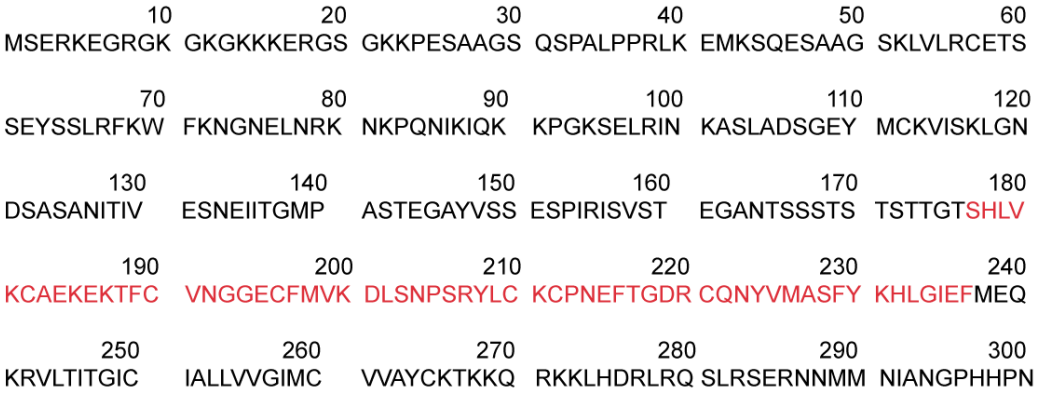

Figure 6: Amino acid sequence of NRG1. Complete precursor chain of NRG1-beta, the EGF like domain is highlighted in red. Modified from Reprokin.

2.15.4 ERBB receptor tyrosine kinase family

In humans there are four different ERBB receptors described, named EGFR, ERBB2, ERBB3, and ERBB4. Some of them have different splice variants.

ERBB receptors recognise specific signalling molecules e.g. NRGs or EGF and react by forming homo or hetero dimers. The receptor-complexes promote the signal by cross-phosporylation by tyrosine kinase activities and subsequent recruitment of phosphor-adaptor molecules, that than lead to the activation of further signalling cascades.

ERBB1	EGFR	HER1	mErbB1
ERBB2	Neu	HER2	mErbB2
ERBB3		HER3	mErbB3
ERBB4		HER4	mErbB4

Table 4. Names and synonyms for ERBB receptors. HER: human epidermal growth factor receptor.

m: murine, (Citri and Yarden, 2006; Yarden and Sliwkowski, 2001)

All ERBB receptors are glycosylated type I trans-membrane proteins characterised by four extracellular domains (I-IV) and one intracellular tyrosine kinase domain (Fig. 7 and 8). NRG ligands bind to the extracellular domains I (L1) and III (L2). The cysteine rich domains II and IV take part in the receptor dimerization (Burgess et al., 2003). After dimerization, the receptors phosphorylate each other, shift to the trans state and activate signalling cascades via adaptor recruitment. All ERBB receptors are capable of forming homo- or heterodimers with each other (Yarden and Pines, 2012).

ERBB2 lacks the ability to bind to ligands (Marmor et al., 2004, Yarden and Sliwkowski, 2001). Furthermore, the receptor shows high auto-phosphorylation levels (Lonardo et al., 1990) which leads to its constitutive activity (Di Fiore et al., 1990). ERBB2 is a classical breast cancer candidate being the first receptor ever targeted utilising an antibody (Trastuzumab, trade name Herceptin 1998) in an anti-cancer therapy (Hudis, 2007). The preferred binding partners for ERBB2 are ERBB3 and ERBB4 (Tzahar et al., 1996).

ERBB3 has no active tyrosine kinase domain. The receptor can bind to adapter molecules but its hetero-dimerisation is necessary for promoting signals (Carraway et al., 1994).

ERBB4 is the most similar receptor compared to EGFR (Plowman et al., 1993). At least 4 different isoforms of the receptor are known: ERBB4-JM-a-CYT-1, ERBB4-JM-a-CYT-2, ERBB4-JM-b-CYT-1, ERBB4-JM-b-CYT-2 (Tzahar et al., 1996).

The splice variant JM-a, has an extracellular cleavage site in the stalk-region next to the transmembrane region. The cleavage site can be processed by TACE (tumour necrosis factor-α converting enzyme) and γ-secretase (Rio et al., 2000; Ni et al., 2001). The processing cleaves the receptor into two fragments: an extracellular and an intracellular one being able to shuttle to the nucleus and acting as transcriptional activator (Williams et al., 2004; Vidal et al., 2005).

The second splice variant defined by the inclusion (Cyt1) or the exclusion (Cyt2) of exon 26. Importantly, exon 26 harbours the binding site for the regulatory domain PIK3R1, promoting PI3K signalling (Elenius et al., 1999; Carpenter, 2003).

The activation of receptor pairs is ligand-dependend and specific. NRG1 and NRG2 bind to ERBB3 and ERBB4, whereas NRG3 and NRG4 seem to bind only to ERBB4. EGF and TGFα activate EGFR only (Marmor et al., 2004,Yarden and Sliwkowski, 2001).

The expression patterns of the receptors in the brain are cell type-dependent. The receptor pair ERBB2/ERBB3 is expressed in glial cells, and the pair ERBB2-ERBB4 in neurons (Buonanno and Fischbach, 2001). ERBB4 is expressed in Parvalbumin positive interneurons (Neddens and Buonanno, 2011).

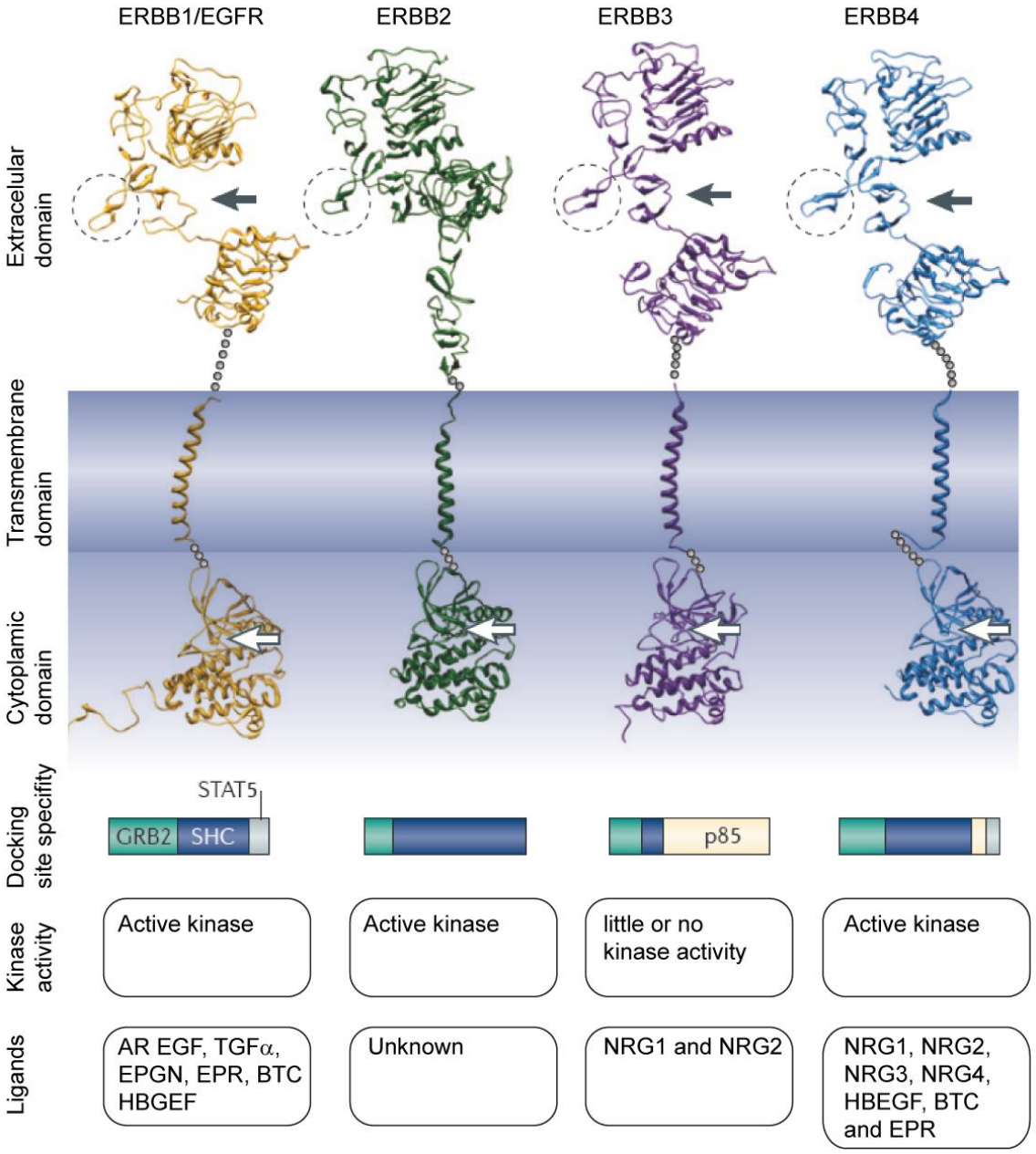

Figure 7: Functional and structural features of ERBB receptors that are unique to each receptor

The black arrows indicate the ligand-binding clefts. The dashed circles indicate the dimerisation loops. The white arrows marks the ATP binding cleft. The sizes of the coloured rectangles below the protein structures represents the fractions of docking site specifity meaning the number of binding sites for each indicated protein normalised to the total number of phosphotyrosine docking sites of each receptors. AR, amphiregulin; BTC, b-cellulin; EGF, epidermal growth factor; EGFR, EGF receptor; EPGN, epigen: EPR epiregulin; GBM, glioblastoma; GI, gastrointestinal tract; GRB2, growth factor receptor-bound protein 2; HBEGF, heparin-binding EGF-like growth factor; NRG, neuregulin; NSCLC, non-small-cell lung cancer; SHC, SRC-homology domain-containing; STAT5, signal transducer and activator of transcription 5; TGFa, transforming growth factor-a. Adapted from (Yarden and Pines, 2012).

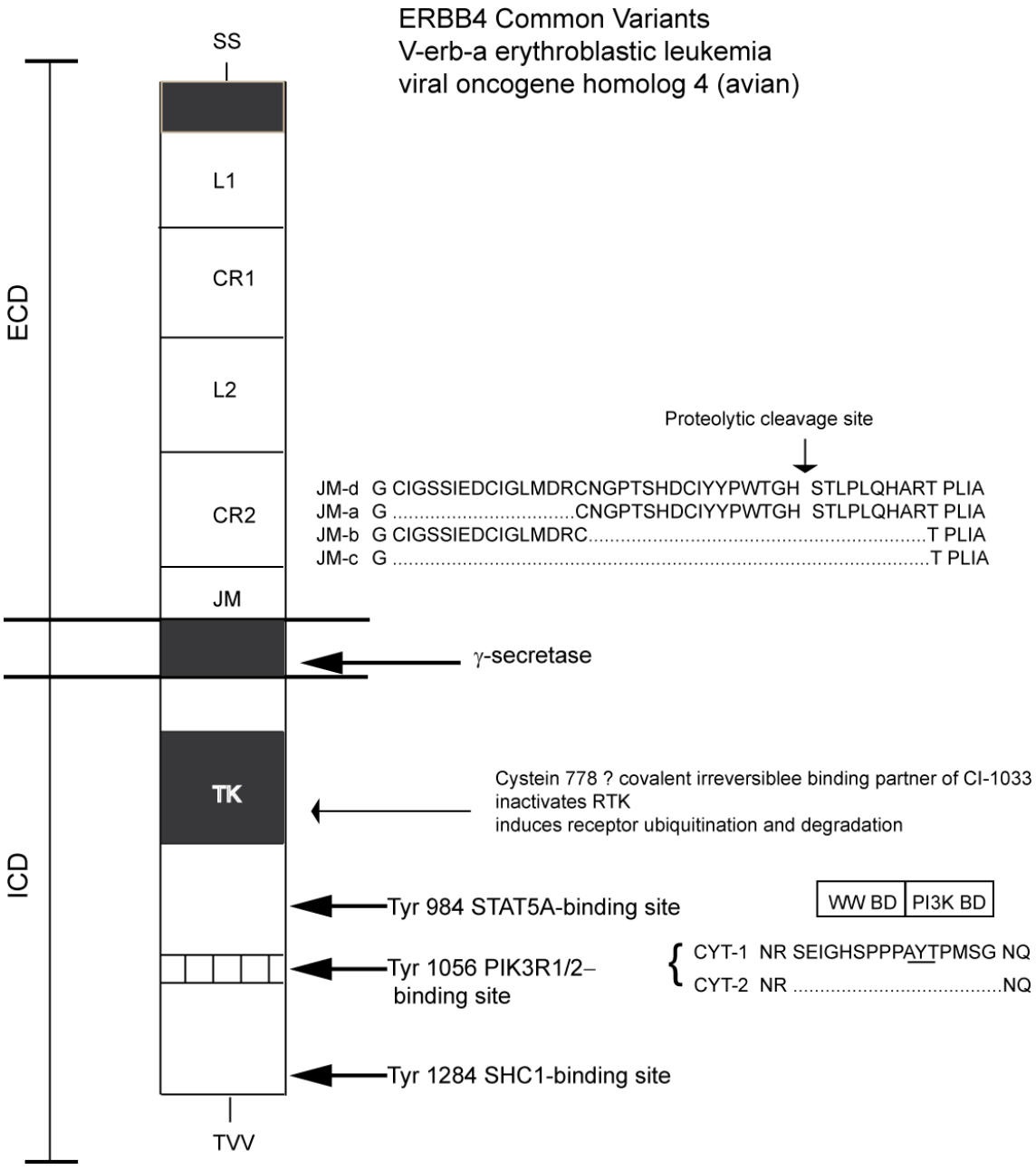

Figure 8: Schematic illustration of ERBB4 domain structure, its variants and binding sites for adapter molecules.

ECD, extra cellular ligand binding domain; ICD, intra cellular domain; SS, signal sequence; TK, tyrosine kinase domain; L1,L2, ligand interacting domains; CR1, CR2, cysteine-rich domains; modified from (Zeng et al., 2007b)

2.15.5 NRG1-ERBB4 signalling in the nervous system

The three best characterised signalling pathways initiated through ERBB receptors are the Ras-Mitogen Activated Protein Kinase Ras-MAPK pathway, the PI3K-Akt/PBK pathway and the Phospholipase C/Protein Kinase C pathway. The STATs (Signal Transducer and Activator of Transcription) can be activated via direct binding to ERBB receptor pairs (Jones et al., 2006; Marmor et al., 2004; Schulze et al., 2005).

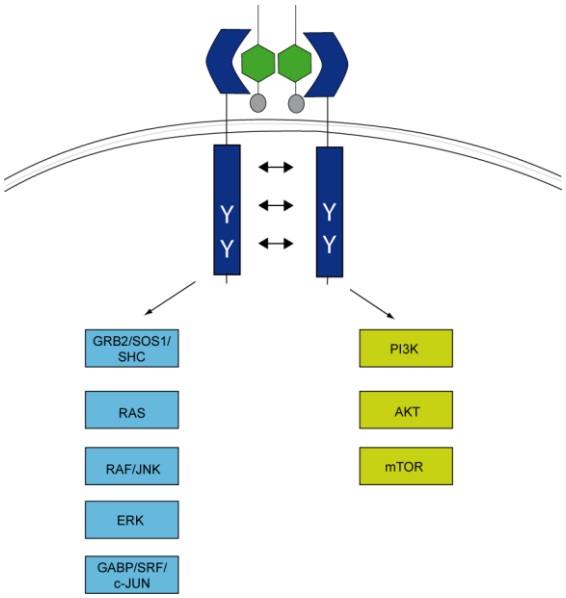

Figure 9: Schematic representation of signalling pathways initialised by ERBB4 receptors.

Modified from: Schizophrenia: Emerging targets and Therapeutic Strategieies (Karam et al., 2010).

2.15.6 Adapters of ERBB receptors

In this study 5 different phosph-adapters of ERBB-receptors system have been used.

- PIK3R1 (PI3Kp85α)

- SRC

- SHC

- STAT5A

- GRB2

2.15.7 PI3K

The phosphoinositide 3-kinase (PI3K) is a nodal point of different pathways in the cell. Its function involves cell growth, proliferation, differentiation, motility, survival and intracellular trafficking. The PI3Ks were first described by Lewis Cantley (Auger et al., 1989). A very recent study confirmed explicitly the role of ERBB4 promoted PI3K signalling in SZ (Law et al., 2012a). PI3Ks are involved in learning and memory and in long-term potentiation (Man et al., 2003). They bind to phospho-tyrosine 1056 of the ERBB4-JMA-CYT1 variant. The recruitment of PI3K to the receptors is promoted by NRG1 i.e. the EGF-like domain (Williams et al., 2009). The PI3 kinases are the central elements of the PI3K/Akt signalling pathway.

The PI3K are subdivided in 3 classes named class I, II, III (Leevers et al., 1999) (Tab. 5).

Class I PI3Ks are activated via G-protein coupled receptors (GPCRs) and receptor tyrosine kinases (RTKs). They form heterodimers and phosphorylate Phosphatidylinositol 3-phosphate (PI(3)P), Phosphatidylinositol (3,4)-bisphosphatePI(3,4)P2) and Phosphatidylinositol (3,4,5) trisphosphate ((PI3,4,5)P3).

The Class I PI3Ks consists of two subunits: catalytical subunit p110 with three variants (p110a, p110b and p110c) and the regulatory subunit p85. The regulatory subunit has five variants: the highest expressed are p85a and p55a, followed by p50a, p85b, p55y.

group	gene	protein	aliases
class I catalytic	*PIK3CA*	PI3K, catalytic, alpha polypeptide	p110-a
	PIK3CB	PI3K, catalytic, beta polypeptide	p110-b
	PIK3CG	PI3K, catalytic, gamma polypeptide	p110-g
	PIK3CD	PI3K, catalytic, delta polypeptide	p110-d
class I regulatory	*PIK3R1*	PI3K, regulatory subunit 1 (alpha)	p85-a
	PIK3R2	PI3K, regulatory subunit 2 (beta)	p85-b
	PIK3R3	PI3K, regulatory subunit 3 (gamma)	p85-g
	PIK3R4	PI3K, regulatory subunit 4	p150
	PIK3R5	PI3K, regulatory subunit 5	p101
	PIK3R6	PI3K, regulatory subunit 6	p87
class II	*PIK3C2A*	PI3K, class 2 alpha polypeptide	PI3K-C2a
	PIK3C2B	PI3K, class 2 beta polypeptide	PI3K-C2b
	PIK3C2G	PI3K, class 2 gamma polypeptide	PI3K-C2g
class III	*PIK3C23*	PI3K, class 3	Vps34

Table 5. Different classes and variants of the catalytic and regular subunits of the PI3-kinases.

2.15.8 STAT5A

The signal transducer and activator of transcription 5α (STAT5A) is a member of the family of seven structurally and functionally related transcription factors (STAT1, STAT2, STAT3, STAT4, STAT5A, STATB, STAT6). Normally STATs are activated by Janus Kinases (JAKs), respond to cytokines (JAK/STAT pathway) and can be phosphorylated by RTKs e.g. EGFR. After phosphorylation STATs homo- or hetero-dimerise and translocate to the nucleus to act subsequently as transcription factors. STAT signalling cascades are associated with cellular transformation (Kisseleva et al., 2002). Disturbed phosphorylation of STATs was found in ErbB4 homozygous KO mice (Tidcombe et al., 2003). STAT5A binds to pY984 ERBB4-JM-a-CYT1 and its increased binding to mErbB4 after Nrg1 stimulation was shown (Wehr, unpublished).

2.15.9 SHC1

The SH2 domains containing transforming protein 1 (SHC1) is the 46kDa variant expressed by the *ShcA* mRNA. It is an ubiquitously expressed adapter protein that signals through the mitogen activated protein kinases (MAPK) pathway and takes part in the regulation of apoptosis and drug resistance. The SHC1 protein contains a SH2 domain, a PTB domain and a central region bearing various phosphorylation sites. Null mutant mice homozygous for Shc dye at E11.5 because of heart defects (Ravichandran, 2001; Pelicci et al., 1992). SHC1 binds to phosphorylated Tyr1284 of the ERBB4-JM-a-CYT1 and its increased binding to ErbB4 after Nrg1 stimulation was showen (Wehr, unpublished).

2.15.10 GRB2

The growth factor receptor bound protein 2 (GRB2) is an phospo-adaptor protein. It is involved in signal transduction, transformation, cell communication and proliferation. The protein contains one SH2 two SH3 domains. It links the EGFR RTKs to the activation of Ras and the MAPKs ERK1 and 2 (Schulze et al., 2005).

2.15.11 SRC

The proto-oncogene SRC is a tyrosine kinase. C-Src phosphorylates SHC and STAT5a. For the discovery of this kinase as the first oncogene kinase J. Michael Bishop and Harold E. Varmus were awarded with the Nobel Prize in 1989 (Olayioye et al., 1999; Keely et al., 2000; Sato et al., 2000).

2.16 Downstream pathways

2.16.1 PI3K/ AKT pathway

The phosphatidylinositide 3-kinase (PI3K)-AKT-mammalian target of Rapamycin (mTOR) pathway is a key regulator for proliferation, growth, survival, protein synthesis, and glucose metabolism.

PI3Ks convert PIP2 to PIP3. This activates AKT (acute transforming retrovirus (AKT-8) also known as protein kinase B or RAC-PK) a central serine/threonine kinase. AKT is upstream to both mTOR and of GSK3β (Yap et al., 2008) (Fig. 10).

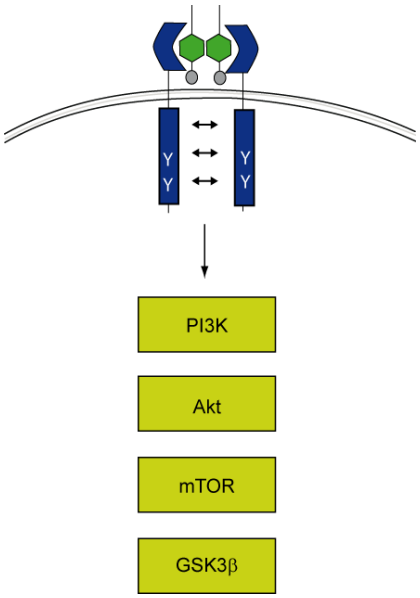

Figure 10: The PI3K, AKT, mTOR pathway

2.16.2 MAPK /ERK pathway

The mitogen-activated protein kinase (MAPK) pathway (Fig. 11) is an important central pathway linked to growth, proliferation, differentiation, and survival of various cell types. In general the “MAPK pathway” is a cassette of three kinases, which are sequentially activated. Starting point of the cascade might be e.g. a growth factor.

The very downstream kinase MAPK is activated via phosphorylation through MAPKK (MAPK kinase), which is activated through MAPKKK (MAPKK kinase). The MAPKs are deactivated via MAPK phosphatases (MKPs). In eukaryotic cells at least twelve different MAPKKKs, seven MAPKKs and eight MAPKs active in at least four different modules are described. For example one module

is the RAF/MEK/ERK cassette. The most upstream kinase is activated by membrane recruitment, usually mediated by adapter molecules, such as Grb2 Sos1 and Shc1. These are recruited to the membrane by an activated RTK. MAPKK is named MEK and the MAPK “extracellular signal-regulated kinase” is called ERK for historical reasons.

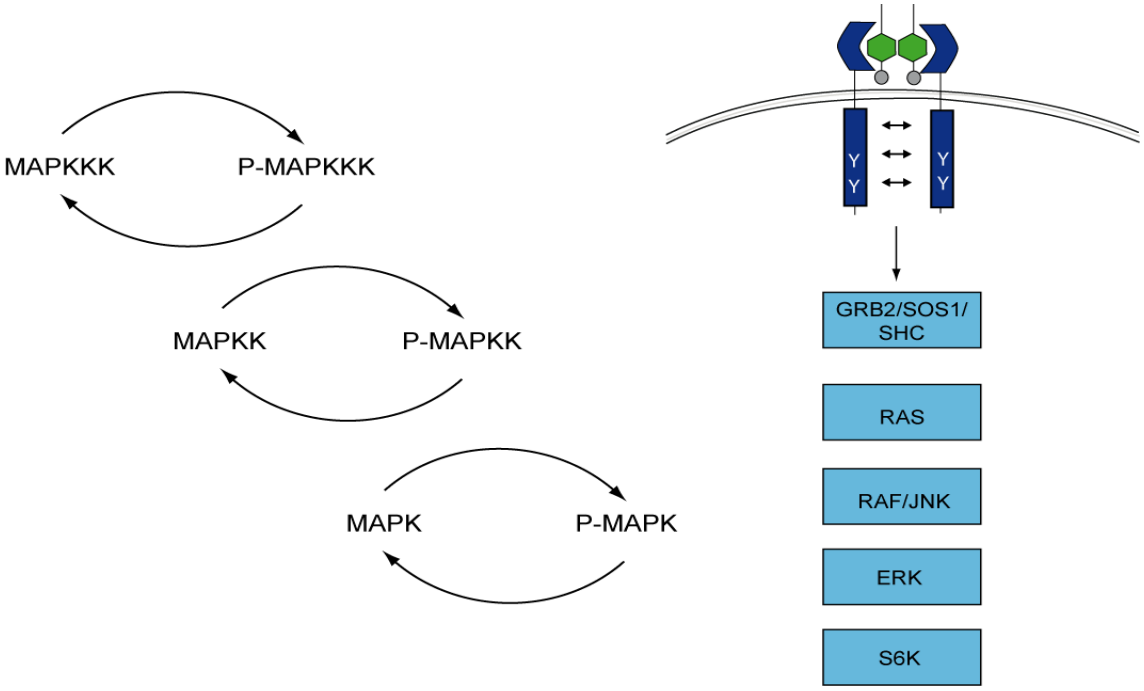

Figure 11 MAPK pathway

2.17 Localisation of NRG1-ERBB4 signalling in the neuronal architecture

2.17.1 Glutamate hypothesis of SZ

Glutamate is the most common neurotransmitter in the mammalian brain. Glutamate receptors have excitatory properties and are important for neural development, neuronal survival and synaptic plasticity.

The glutamate receptors in the mammalian CNS are subdivided in:

Ionotropic recptors	NMDA	ligand gated ion channels
	AMPA	
	Kainate	
Metabotropic	mGluRs	G-protein coupled

Table 6. Overview of the different Glutamate receptors

2.17.2 NMDA

Increasing evidence suggests that NMDA hypo-function is involved in the pathophysiology of SZ (Homayoun and Moghaddam, 2007). Low doses of NMDA antagonists like PCP, MK801 or Ketamine can induce SZ-like psychotic symptoms (Bian et al., 2009). PCP and Ketamine lead to decrease parvalbumin (PV) stained interneurons. Reduction of parvalbumin or somatostatin stained interneurons and decrease of mRNA expression of somatostatin, parvalbumin and glutamate acid decarboxylase (GAD 67) are key findings for SZ (Konradi et al., 2011). PCP and Ketamine lead to increased cortical glutamate level. Elevated levels of glutamate are observed in some brain regions of SZ patients.

"At the Network level, psychomimetic doses of NMDA antagonist may favour the balance of excitation over inhibition by blocking NMDA-dependent excitatory inputs to GABAergic interneurons" (Christoph Ott, 2012 personal communication).

"Subcortical NMDA receptor dysfunction, leading to elevated cortical glutamate levels and potentially to excitotoxic processes, may be important, particularly in the early stages of the disease" (Christoph Ott, 2012 personal communication).

mGLu2/3

Recent findings suggest that the compound LY404039 and its oral prodrug LY2140023 targets the metabotropic glutamate system. The effective treatment of SZ patients is still under debate (Mezler et al., 2010).

2.17.3 Hyper- and hypo-frontality in SZ

The gamma frequency oscillations of SZ patients performing working-memory tasks are disturbed. Responsible for this is most likely loss of inhibition of parvalbumin positive (PV+) interneurons (Uhlhaas and Singer, 2010; Haenschel et al., 2009; Barr et al., 2010).

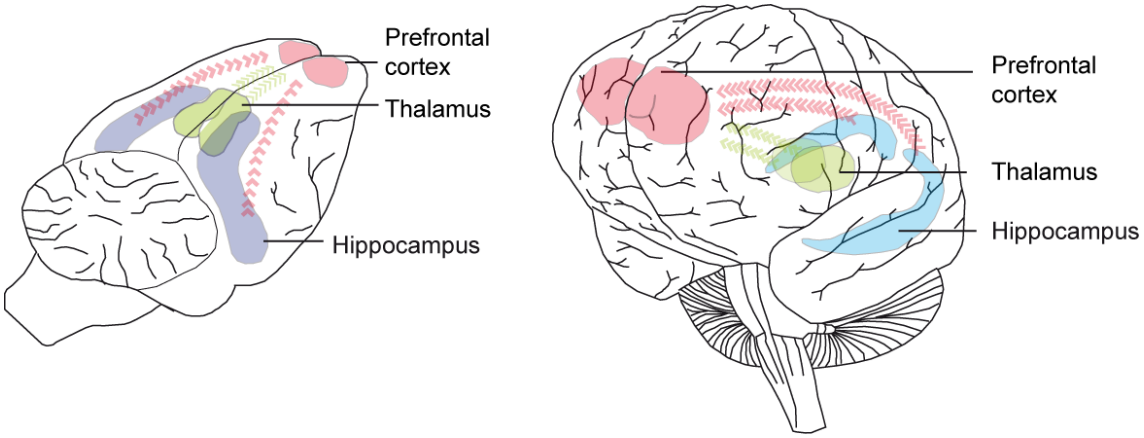

Figure 12: Prefrontal cortex, Thalamus and Hippocampus, connections in mice and man, modified by (Pratt et al., 2012).

Dysfunctional connectivity in schizophrenia. Aberrant activity in both rodent models of the disease (left panel) and in patients (right panel) is centred on prefrontal – hippocampal – thalamic networks.

2.17.4 From neuronal circuits to single synapses

A small functional substructure of the brain is a simple neuronal circuit. A neuronal circuit is defined as a hierarchical network of inhibitory and excitatory neurons. In the cerebral cortex excitatory glutamatergic pyramidal cells and inhibitory GABAergic neurons form a micro-network (Fig. 13). The pyramidal cells are specialised in the transfer of information between cortical areas and to other parts of the brain. The interneurons function as breaks and oscillation fine tuners to the pyramidal cells. Disturbance of the balance lead to circuit miss-function. In SZ a certain class of interneurons seem to be affected. The PV+ interneurons, including Basket cells and Chandelier cells, localised in the dorsolateral prefrontal cortex show a decrease in Glutamate decarboxylase isoform 67 kDa (GAD67) expression in SZ (Akbarian et al., 1995; Hashimoto et al., 2003; Marín, 2012). Expression of ERBB4 protein in humans and monkeys is restricted to the somatodendritic compartments of interneurons and is absent from pyramidal cells (Neddens et al., 2011; Neddens and Buonanno, 2011; Buonanno, 2010). The precise localisation of ERBB4 in CNS has not been

described systematically yet and has to be further analysed. For further information see: (Neddens and Buonanno, 2011).

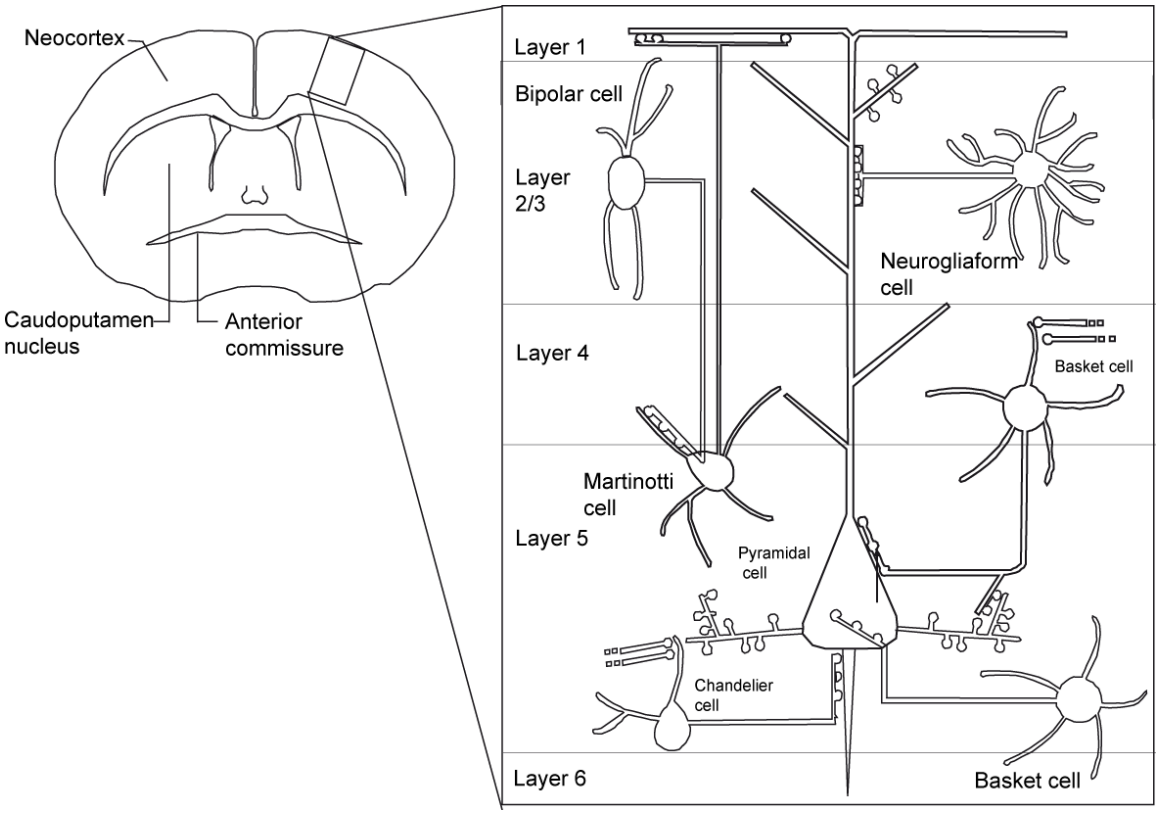

Figure 13: Cortical interneuron network

Different classes of cortical interneurons are distinguished by morphology, neurochemical content, intrinsic electrophysiological properties and pattern of connectivity. Interneurons i.e. Basket cells target the soma and basal dendrites of pyramidal cells, Chandelier cells contact the axon initial segment and Martinotti cells and neurogliaform cells primarily contact the dendrites of pyramidal cells. The cells form a complex network of inhibition and excitation synchronised to a distinct oscillation. Modified from (Marín, 2012).

2.17.5 Alterations found in the neuronal circuit

Two different reasons are hypothesised to be responsible for the reduced activity of the PV+ interneurons in SZ.

A loss of function of interneurons might be caused by (I) a reduction of inhibitory synapses number (Woo et al., 1998), or (II) by a failure in the recruitment of the interneurons to their correct final localisation, thereby preventing functional excitation of these inhibitory interneurons (Grunze et al., 1996; Gunduz-Bruce, 2009).

NMDA receptor antagonists or the conditional deletion of NR1 subunit of NMDAR lead to the dis-inhibition of excitatory pyramidal cells and a loss of synchrony, showing SZ like symptoms (Belforte et al., 2010; Carlén et al., 2012).

2.17.6 NRG1-ERBB4 in the development of PV+ interneurons

ERBB4 directs the migration of PV+ interneurons in response to NRG1 (Flames et al., 2004). NRG1-ERBB4 signalling controls the integration and synapse formation of PV+ interneurons with pyramidal cells in neuronal circuits (Fazzari et al., 2010). Moreover, PV+ interneurons deficient in ERBB4, receive less input by pyramidal cells than normal ones (Ting et al., 2011). Interestingly, mice lacking ERBB4 specific in PV+ Interneurons have an impaired working memory phenotype (Wen et al., 2010) resembling cognitive deficits observed in SZ.

An overview of the location and implication of the findings is given in (Fig. 14) for neuronal circuits and in (Fig. 15) for synapse.

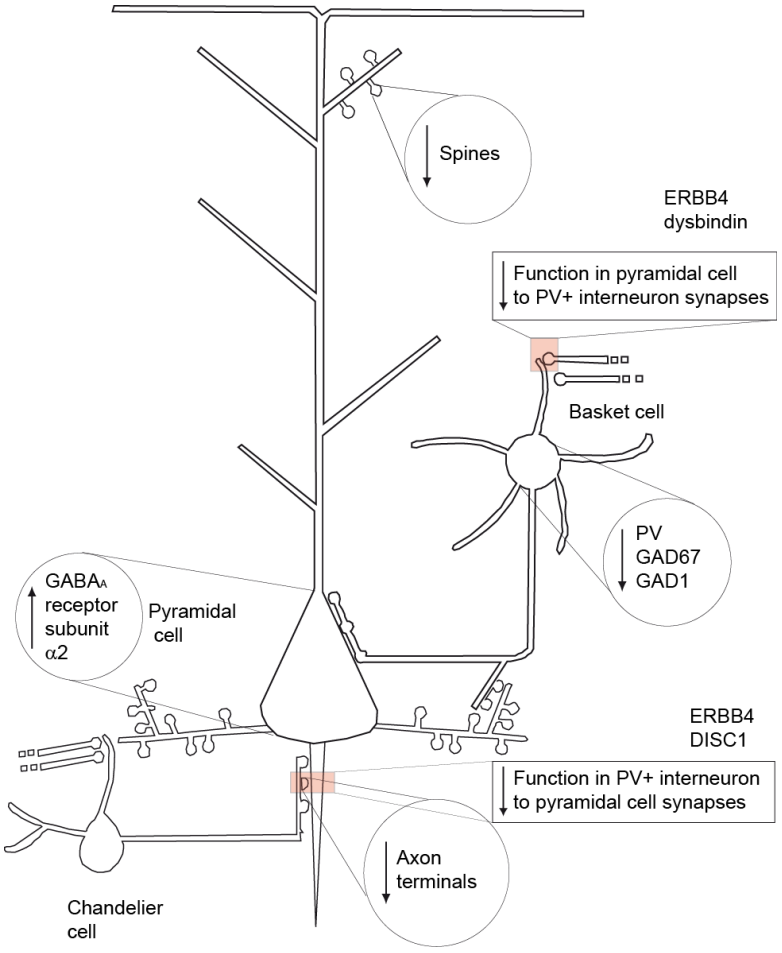

Figure 14: Alterations found in cortical circuits SZ patients and animal models

Spines and 67kDa glutamate decarboxylase (Gad67) are reduced. Loss of ERBB4 alters presynaptic functions of the Chandelier cells and post synaptic the functions of the Basket cells, resulting in a loss of inhibitory function and synchrony. The Pyramidal cell responds with asynchronous hyperactivity.

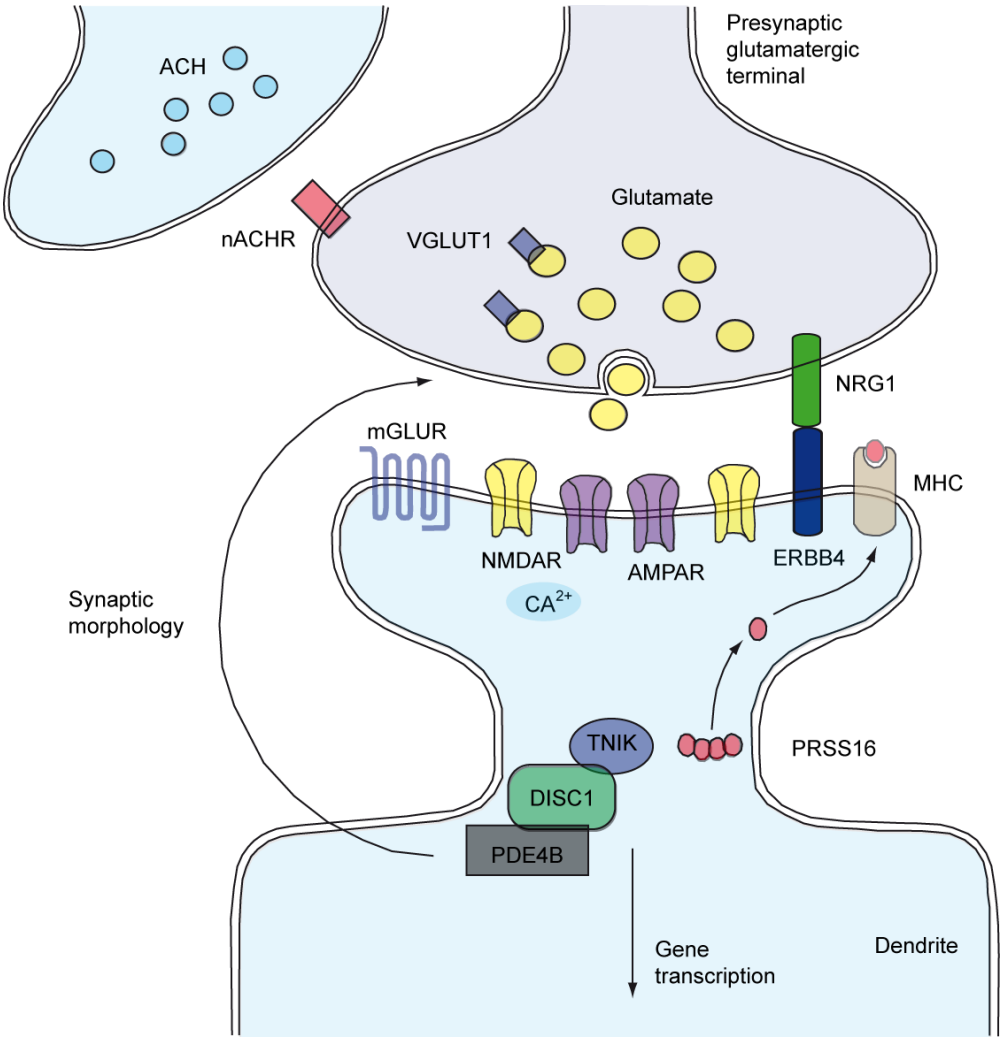

Figure 15 Synapse, modified (Pratt et al., 2012)

The picture shows the most prominent genes implicated in the aetiology of schizophrenia. NRG1-ERBB4 signalling regulates the function and morphology of the synapse. DISC1 coordinates signalling pathways that regulate synaptic structure (DISC1 with phosphodiesterase 4B (PDE4B) and TRAF2 and NCK–interacting kinase (TNIK)) a7 subunit containing nicotinic acetylcholine receptors (nAChRs) are strongly implicated in disease risk via gene copy number variations. Major histocompatibility complex (MHC) molecules have some role in the maintenance and plasticity of synaptic connections. AMPA: (a-amino-3hydroxy-5methyl-4-isoxazole propionic acid receptor (AMPAR); mGluR: metabotropic glutamate receptor; NMDAR: N-methyl-D-aspartate receptor; PRSS16: serine protease 16; VGLUT1: vesicular glutamate transporter 1.

2.18 Targeting NRG1-ERBB4 with protein-protein interaction assays

2.18.1.1 First generation drugs

The first class of drugs also named ‘typical’ drugs used in the treatment of SZ is termed neuroleptics and act as antipsychotic drugs. Neuroleptics were found in MDMA (3,4-methylenedioxy-N-methylamphetamine) and PCP (Phencyclidine) induced psychotic mice models. All of these drugs target the dopamine system. They bind to the dopamine D2 receptor subtype and block them in the mesolimbic dopaminergic system.

Prominent first generation drugs are Chlorpromazine (first synthetised in 1950) and Haloperidol (1958).

These drugs display severe side effects. The dopamine blockade in the nigostratial and hypothalamic-pituitary systems lead to extrapyramidal side effects mimicking Parkinson’s disease, hyperprolactinaemia, sedation metabolic-syndrome and hypotension. The patients have to take the drugs for their whole life. Moreover, the first generation drugs are used only for symptomatic treatment and they do not affect the cause of the disease (Hudepohl and Nasrallah, 2012).

2.18.1.2 Second generation drugs

Second generation drugs, also named ‘atypical’ drugs, are multi-affinity receptor target agents targeting specific D2 receptor subtypes or compounds with a balanced activity against serotonin (5-hydroxytryptamine) versus dopamine.

Atypical drugs, even if failing to treat all symptoms of SZ, treat a broader set of symptoms than first generation drugs and display a diminished side effect profile due to reduced extrapyramidal side effects. They also target specifically dopamine receptors in various degrees to perform the therapeutic action. Prominent representatives of atypical drugs are Clozapine (Barros 2011), which reverses altered spine formation in NRG ERBB2-4 mice, Olanzapine and Risperidone (Penzes et al., 2011).

Typical and atypical drugs that target dopamine receptors support the dopamine hypothesis of SZ. Nevertheless, they fail in curing SZ and treat only some symptoms with occasionally tremendous side effects. Principally, no accelerated progress in SZ-drug development in the past 50 years has been observed. As the construct validity of SZ in animal models cannot be fully accomplished, the complexity of an animal model obscure smaller effects, costs for animal experiments and maintenance are high and usability of animals in

HTP screenings are limited, animal models seem not to be the right system for large compound screening.

At least, knowledge of the genetic risk factors of SZ should be tried to be translated into artificial systems, resembling partially valid models to perform HTP screens identifying chemical lead compounds to develop new classes of substances which subsequently need to be active in the corresponding translational/genetic mouse model.

2.18.2 Classic hit to lead discovery

Most screens have been performed with *in vitro* assays. Substance libraries were tested against “naked” proteins. A hit generated in this kind of assay has to be evaluated extensively afterwards and may i.e. often not enter cells or tissues.

Hit confirmation means first retesting of the hits in the same assay system with the same assay conditions. Than, dose-response curves are generated to determine key pharmacological hallmarks (sensitivity, efficacy etc.). Orthogonal testing follows. The hits are tested in different assays or with different technologies. In a secondary screening the hits are tested in a cellular environment to ensure membrane permeability. Chemical amenability /accessibility has also to be ensured. Intellectual property is the next ever-present issue for commercial screens.

Biophysical testing is used to access if the compound binds to the target, i.e. nuclear magnetic resonance or isothermal titration calorimetry.

After hit confirmation, hit expansion follows. Compound clusters from the screen are chosen and expanded. The clusters contain compounds with high target affinity (below 1uM), low molecular weight and moderate lipophilicity. The compounds should not interfere with the P450 enzymes or bind to the human serum albumin. The compounds should also be stable, soluble in water, and should be cell permeable, they should further not exhibit cytotoxicity and should not be rapidly metabolised.

The compounds have to show significant biological activity in cellular assays and selectivity versus other related targets.

Lead optimization is the later process of chemical modification of lead (hit) compounds to get more potent leads with less off-target active structures (Bleicher 2003, Astle2010).

2.18.2.1 Compound screens

Compound screens give the opportunity to test large numbers of drugs, compounds or lead structures for primary effects on proven therapeutically relevant targets. For subsequent structural modifications (medicinal chemistry), it is important to identify the exact mechanism or mode of action. For HTP-compound screens an assay should be reliable, robust, scalable, fast in response, easy to readout, and mimicking the mechanism observed as close as possible.

Proximal outputs of the NRG1-ERBB4 signalling system can be monitored with PPI assays i.e. at the level of receptor dimerization or the phospho-adapter recruitment. For these types of analyses the following assay-systems should be discussed.

2.19 Cell based assays

PPIs can be analysed with genetic or biochemical methods. Genetic methods contain e.g. FRET (Fluorescence Resonance Energy Transfer), BRET Bioluminescence Resonance Energy Transfer) or complementation systems like yeast to hybrid. Biochemical methods include e.g. protein complex immunoprecipitation (Co-IP) (Boute et al., 2002; Uetz and Hughes, 2000). The accurate method depends on the questions asked and the usability e.g. in high throughput or fully automated systems.

2.19.1 Biochemical methods e.g. Co-IP

The Co-IP is based on a classical immunoprecipitation. A protein of interest is pulled down from a lysate via a specific antibody. If the protein is interacting with a second protein this protein is bound to the first protein. A second antibody is then used to probe against the second protein and so to detect the PPI. Unfortunately, the interaction can take place in vitro in the lysate which might lead to artefacts in the detection. A quantification of the PPI can be done via ImageJ or other image programs. The method is cost and labour intensive and difficult to automate in bigger scales.

2.19.2 Affinity columns

A peptide is bound to an affinity column. If a cell lysate is loaded on the column and proteins interacting with the peptide sequence bind to the peptide and can be purified afterwards. The putative interaction partners can be further analysed via MALDITOF etc.

2.20 Protein fragment complementation assays

2.20.1 Yeast two hybrid

The Yeast two-hybrid (Y2H) assay is a protein fragment complementation assay to measure PPI or protein-DNA interactions. In the classical version, the LacZ reporter gene is under the control of the upstream activating sequence UAS. The UAS transcription factor Gal4 is fragmented in an UAS binding domain and a transcriptional activator domain. Both domains can be fused to two putative interacting proteins of interest (pray and bait), and if these proteins come to close proximity, modify the Gal4 transcription factor and activate the reporter gene. The Y2H is a fast and scalable low-tech assay.

On the other site yeast is not the ideal organism to express mammalian proteins due to lack of specific chaperons and localisation mechanisms: Furthermore, interactions that take place beside the nucleus cannot be detected and this method produces a high false positive failure rate. In conclusion, Y2H is not suitable to detect interactions of huge mammalian membrane proteins (Stagljar et al., 1998).

2.21 Split TEV

The split TEV method is a protein fragment complementation assay, based on the NiA inclusion protease from the *tobacco etch virus* (TEV). The protease is split into an N- and a C-terminal part (NTEV + CTEV), thereby setting apart the catalytic residues. When NTEV and CTEV are fused to proteins of interest, which are capable of interacting with each other, the TEV protease activity is reconstituted as the fragments come into close proximity. In turn, the protease activates an artificial reporter by cleaving at a highly specific site encoded by ENLYFQ’G/S. Artificial reporters can be of transcriptional nature or reporter protein-based(Wehr et al., 2006).

A direct reporter protein is i.e. an inactive luciferase enclosed by two mutated Estrogen receptor domains (ERT2) domains bound via TEV cleavage sites (tevS). The two large ERT2 domains prevent luciferase from proper folding to functional form. TEV protease activity releases the luciferase from the ERT2 domains, it folds to a functional confirmation and the activity of luciferase as a readout can be measured(Wehr et al., 2006).

Transcription based system use i.e. the artificial transcription factor galactose 4-viral protein 16 (GV). The GV is bound with the tevS to one of the to interacting proteins with split TEV protease halves. Reconstitution of TEV-protease activity cleaves the tevS and releases the GV to shuttle to the nucleus and activate a

reporter protein under the control of the upstream activator site of five GAL4 responsive elements (UAS) site. A reporter protein can be i.e. a fluorescent protein like enhanced green fluorescent protein (EGFP) or an enzyme like the *Firefly* luciferase. Using a transcription factor and an enzyme as read out allowes also a high magnification of the signal.

The assay is robust, scalable, and was shown to be highly specific for ERBB receptors. It constitutes an optimal assay to access the intercellular NRG1-ERBB4 signalling cascade potentially adaptable to a HTP-screen (Wehr et al., 2006; Wehr et al., 2008a; Djannatian et al., 2011).

2.22 z'-Factor

For HTP screening, the z'-factor is a statistical determinant of the robustness and reliability of the assay. It links a large number of single measurements of unknown effects and effect sizes to a set of positive and negative controls. The z'-factor is calculated for small (or pilot) screens to predict if the assay is qualified for HTS. Four parameter are used, the means (μ) and the standard deviations (σ) of the positive (p) and the negative (n) controls (μp, σp and σn, μn).

$$z'\text{-factor} = 1 - \frac{3\,(\sigma p + \sigma n)}{\left|\,\mu p - \mu n\,\right|}$$

2.22.1 The interpretation of the z'-factor:

- 1 is the ideal z'-factor. It can never exceed and is impossible to matched.
- 1-0.5 is an excellent assay. 0.5 is the value when σp = σn, μp and μn show a separation of twelve standard deviations.
- 0.5-0 is a marginal assay. The assay is not automatically qualified for HTP screening. For complicated but stable assays lower z'-factors of e.g. 0.4 can be defined as limit.
- 0 is a yes/no assay with no separation window, overall not suitable for HTP screening.
- Less than 0, the assay is not qualified for HTP screening, as positive and negative controls do not have any separation window and overlap (Zhang et al., 1999; Zhang et al., 2008; Zhang, 2008; Sui and Wu, 2007).

2.23 Aim of the thesis

SZ is a severe disease. To date there are no drugs available, which mediate or attenuate the negative symptoms and cognitive deficits. Genetic studies showed that the NRG1-ERBB4 signalling system is altered at least in a subgroup of SZ patients. Moreover, the NRG1-ERBB4 signalling system most likely influences biological processes that are central to the diseases (i.e. interneuron migration and function with an impact on the excitatory-inhibitory balance and associated working memory and cognitive deficits). Therefore, addressing NRG1-ERBB4 signalling is one of the most promising targets for the development of new drugs for SZ.

The first main aim of the thesis is the design, development and characterisation of a split TEV-based co-culture assay to monitor the most proximal steps of the NRG1-ERBB4 signalling cascade. The assay must be sensitive, robust and adaptable to high-throughput approaches for future screenings of huge compound libraries. The second main aim is the engineering and validation of the secondary assays useable to analyse putative hits from larger screens.

As a pilot study, the developed assay will be used to screen 727 FDA approved drugs obtained from the NIH collection. The recovered hits will be further validated by an extensive set of secondary assays containing different Nrgs, ERBB receptors and adapter proteins, to get a fast and clear insights into the specificity of drug function, and to discard false positive hits. The aims of the screening project are (1) the detection of unknown therapeutic potentials in drugs available already on the market, and (2) the identification of new lead structures from tested substances for further lead optimisation processes.

3 Chemicals and Reagents

Chemicals were received from Amersham Biosciences, BD Falcon, BioRad, Carl Roth, Eppendorf, Invitrogen, Merck, Riedel de Haen, Roche, Serva, Sigma and VWR.

3.1 Laboratory suplies

Consumable supplies, which are not mentioned separately were purchased from commercial sources as BD Falcon, Eppendorf, Gilson, Greiner-Nunc and Menzel-Gläser.

Cell culture dishes	BD-Falcon
15cm	
10cm	
5cm	
6 well	
12 well	
24 well	
Cryo tubes	Nunc
ECL hyperfilms	Amersham Bioscience
Electroporation cuvettes (1,2,4 mm)	Biorad
NuPAGE 4-12%Bis-Tris Gels	Invitrogen
PVDF Membrane Hybond P	Amersham Biosciences
Reaction tubes	Eppendorf

3.2 Laboratory equipment

Hardware

Atroum 611 Water Putification System	Sartorius
Gene Pulser Xcell	Biorad
Hood	Heraeus
Microplate reader Mithras LB 940	Berthold Technologies
Microscopes	Leica
Leica DM IRBE (invers)	
Leica DM RXA	
Leica TCS SP5 X (confocal)	
Nucleofector	Amaxa
SDS PAGE gel electrophoresis system	Invitrogen
Xcell SureLock NuPAGE system	Invitrogen
Sonicator Bandelin Sonoplus	Bandelin
X-ray film developer KODAK XOMAT	Kodak
CellStarRoboter	Hamilton

EDV Hardware

Canon iRC3580	Canon

HP Color Laserjet 4550	Hewlet Packard
Laptop Lenovo T61	
iMac 11,2	Apple

EDV Software

Adobe package	Adobe
DNASTAR Lasergene	DNAStar
Firefox	Mozilla Foundation
Microsoft Office 2003	Microsoft
Microsoft Office X	Microsoft
Zotero	www.zotero.org
Chemsketch	ACD Labs

Kits

Calf intestine phosphatase (CIP)	Roche
Nucleobond PC 20	Machery-Nagel
NucleoBond Xtra Midi EF	Machery-Nagel
Nucleobond PC 500 EF	Machery-Nagel
Nucleobond PC 10.000 EF	Machery-Nagel

3.2.1 Antibodies

Name	Anti	Supplier
Phospho-Akt (Ser473)	Rabbit	Cell Signaling Technology
Akt	Rabbit	Cell Signaling Technology
FLAG M2	Mouse	Sigma Aldrich
HA	Rat	Roche
c-Myc	Mouse	Santa Cruz Biotechnology
V5	Mouse	Invitrogen
Phospho-p70 S6 Kinase (Thr389) (108D2)	Rabbit	Cell Signaling Technology
p70 S6 Kinase	Rabbit	Cell Signaling Technology
Phospho-HER4/ErbB4 (Tyr984)	Rabbit	Cell Signaling Technology
p-ErbB4 (Tyr 1056)	Rabbit	Santa Cruz Biotechnology
Phospho-p44/42 MAPK (Erk1/2) (Thr202/ Tyr204) (D13.14.4E) XP	Rabbit	Cell Signaling Technology
p44/42 MAPK (Erk1/2) (137F5)	Rabbit	Cell Signaling Technology
ErbB-4 (C-7)	Mouse	Santa Cruz Biotechnology
Phospho-HER4/ErbB4 (Tyr1284) (21A9)	Rabbit	Cell Signaling Technology
GSK-3? (27C10)	Rabbit	Cell Signaling Technology
Phospho-GSK-3?/? (Ser21/9)	Rabbit	Cell Signaling Technology

Table 8. Antibodies used

3.2.2 Oligonucleotides

Were synthezised in house by MPI-EM core facility
Primers

Delivery concentration	50 pmol/ul
f.c. in the PCR	0,2uM

3.2.3 Plasmids

Adapters

HS306	PIK3R1-CTEV-2HA	KanR
HS309	SRC-CTEV-2HA	KanR
HS310	GRB2-CTEV-2HA	KanR
HS311	STAT5A-CTEV-2HA	KanR
HS316	SHC1v2-CTEV-2HA	KanR

RTKs

HS275	ERBB4-Glink-NTEV-tevS-GV-2HA	AmpR
HS276	ERBB4-Glink-CTEV-2HA	KanR
HS322	EGFR-Glink-NTEV-tevS-GV-2HA	AmpR
HS323	EGFR-Glink-CTEV-2HA	KanR
HS324	ERBB2-Glink-NTEV-tevS-GV-2HA	AmpR
HS325	ERBB2-Glink-CTEV-“HA	KanR
HS326	ERBB3-Glink-NTEV-tevS-GV-2HA	AmpR
HS327	ERBB3-Glink-CTEV-2HA	KanR

Split TEV

TC118	TM-TEV	KanR
TC97	TM-tevS-GV	KanR
TC84	pCMV-GV	KanR

NRGs

V368	Neuregulin1.I-beta1a
V369	Neuregulin1.II-beta1a
V370	Neuregulin1.III-beta1a

Other

TM-FRB_IRES_FKBP
HTR5A-NTEV-tevS-GV-2HA
β-Arrestin2δ-CTEV-2HA

Gateway backbone vectors

pDest-F
pDest-HA
pDest-V5
pDest-Glink-NTEV-tevS-GV-2HA
pDest-Glink-CTEV-2HA

3.2.4 Bacterial strains

E. coli DH5a	Invitrogen
E. coli DH10B	Invitrogen
E. coli XL1-blue	Statagene
E. coli One shot Mach 1-T1	Invitrogen
E. coli DB3.1 ccdb survival	

3.2.5 Mammalian cell lines

HEK293	Human Embryonic Kidney immortalised cell line (ATTC) (DuBridge et al., 1987)
HEK293FT	Human Embryonic Kidney immortalised cell line (ATTC) (Javanbakht et al. , 2003)
PC12	Rat adrenal pheochromocytoma cell line (ATTC) (Grene and Tischler. 1976)
PC12TO	expresses TetR-VP16 transactivator (Clontech)
PC12	
Neuroscreen-1	optimised for screening PC12 cells (Thermo Fisher Scientific.
Oli-neu	Murine oligodendroglial precursor immortalised cell line (Jung et al.,1995)
NIH3T3	mouse embryonic fibroblasts (Todaro and Green, 1962)
SHSYY5	Neuroblastoma cells)

3.2.6 Solutions and buffers

PBS (Phosphate buffered saline) 10x

NaCL	100g
KCl	2,5g
NA2HPO4 x 2H2O	7,2g
KH2PO4	2,5g

Disolve, adjust pH to 7,2 with NaOH, add H2O to 1000ml

TBS (TRis buffered saline), 10x

Tris-Base (1M; pH 8)	50ml	(f.c. 50mM)
NaCL (5 M)	30ml	(f.c. 150mM)

3.2.7 Buffers for molecular biology

DNA sample buffer, 10x

Bromphenolblue	0,25%
Xylencyanol	0,25%
Ficoll (Type400)	15%

In ddH2O

TAE (Tris /Acetat/EDTA) buffer, 50x

Tris-Base pH 8	242g (2M)
EDTA (0,5 M; pH 8)	100ml (1mM)

Add ddH2O to 1000ml

TE (Tris - EDTA) buffer,

Tris-Base pH 7,4	10mM
EDTA (0,5 M; pH 8)	1mM

Ethidiumbromid

EtBr 1% in ddH2O	10mg/ml
Final concentration in the gel	1ug/ml

dNTP mix 50x

dATP, dCATP, dGTP, dTTP	10mM (2,5 mM each)
f.c. in the PCR	200uM (50uM each)

LB-medium (Luria and Bertani medium / Luria brooth) (BERTANI, 1951)

Bacto Yeast extract	0,5%

Bacto Peptone	1%
NaCl	1%
Optional Agar	1% for plates

SOC - medium

Bacto Yeast extract	0,5%
Bacto Peptone	2%
NaCl	10mM
Glucose	20mM
KCl	2,5mM
MgSO4	10mM

Antibiotics — f.c. in agar plates

Kanamycin	50ug/ml
Ampicilin	100ug/ml
Chloramphenicol	
Gentamycin	
Zeocyn (low salt agar)	

3.2.8 Luciferase assay buffers

Lysis-buffer

Passive lysis buffer (5x) Promega (Cat# E1941)
Dilute 30ml of 5x Buffer in 120 ml ddH_2O

Firefly-luciferase-assay buffer (Gaunitz and Papke, 1998)

		500 ml	1500 ml
Tricine	20 mM	1792 mg	5376 mg
$(MgCO_3)_4$*$Mg(OH)_2$*$5H_2O$ (Magnesiumcarbonat-Hydroxid-Pentahydrat)	1,07 mM	260 mg	780 mg
$MgSO_4$	2,67 mM	161 mg	483 mg
EDTA	0,1 mM	100 µl (0,5 M)	300 µl
DTT	33,3 mM	2570 mg	7710 mg
Coenzym A	270 µM 1	05 mg	315 mg
D-Luciferin, free base	470 µM	66 mg	198 mg
ATP	530 µM	146 mg	438 mg

For dissolving of $(MgCO_3)_4$*$Mg(OH)_2$*$5H_2O$ titrate the pH with HCL until the solution is clear.
Afterwards adjust the pH with 5M NaOH to7.8
Ad Luciferin and ATP at last. Control pH
Storage of the Buffer ad -20°C without light, thaw at room temperature

Renilla-luciferase-assay buffer

		500 ml	1500 ml
NaCl	1,1 M	32,15 g	96,45 g
Na_2-EDTA (Disodium ethylenediamine tetraacetate)	2,2 mM	2,2 ml (0,5 M)	6,6 ml
$KxPO_4$ (pH 5,1)	0,22 M	110 ml 1 M KH_2PO_4	330ml
BSA	0,44 mg/ml	220 mg	660 mg
NaN_3	1,3 mM	42,25 mg	126,75 mg
Coelenterazin (in 100% EtOH)	1,43 mM	300 µl Stock	900 µl

$KxPO_4$ (pH 5,1): 1M KH_2PO_4, Adjust the pH with KOH to 5.1
add Coelenterazin as last ingredience
Coelenterazin stock is 1mg in 1ml EtOH, Storage at -20°C
Adjust the pH of the Buffer to 5.0
Storage of the Buffer ad -20°C without light, thaw at room temperature

All substrates are from PJK (http://www.pjk-gmbh.de).

D-Luciferin, free acid:	No. 260150
Co-Enzyme A:	No. 260809
ATP:	No. 260920
DTT:	No. 260710
Coelenterazin:	No. 260350

3.2.9 Solutions for cell culture

2x freezing medium for eukaryotic cells

DMEM	55%
DMSO	20%
FBS	45%

PLL 250x

Poly-L-Lysine in ddH2O	5mg/ml
f.c. for coating PC12 plates	0,02mg/ml

Penicillin-Streptomycin 100x

Potassium Penicillin	10,000 U / ml
Streptomycin Sulfate	10,000 ug / ml

Trypsin-EDTA 10x

Trypsin	5g
EDTA	6,85 mM

Transfection medium

OptiMEM-Medium (Gibco)

Nutrition media

DMEM 1g Glucose/l Lonza	phenol red
DMEM 4,5 g Glucose/l Lonza	phenol red
DMEM 1g Glucose/l Lonza	
DMEM 4,5 g Glucose/l Lonza	

Horse Serum HS, heat inactivated for 45'' at 56°C
Fetales Bovines Serum FBS, heat inactivated for 45'' at 56°C
PenStrep
GlutaMAX-I (stable L alanine-L-glutamine-dipeptide)

Cell line	Glucose	Percent FCS	Percent HS	PSG
HEK	4,5%	10%	----	1%
PC12	1%	10%	5%	1%

Standard IP buffer (1% NP40)

For 250ml	Final concentration []
12.5ml 1M Tris pH7.5	50 mM
7.5ml 5M NaCl	150 mM
2.5ml NP40 (or 25 ml 10% NP40)	1 %
0.5ml 0.5M EGTA	1 mM

or Hepes-based Lysis buffer

Add freshly:

Complete tablet (Roche)(mini for 10 ml)
Phosphatase inhibitor II and III (Sigma): 10 µl/ml each
NaF (0.5M): 200 µl/ml (f.c. 100 mM)
Optional:
Na_3VO_4 (0.2M); 5µl/ml (f.c. 1mM)
PMSF (100 mM): 10 µl/ml
DTT (1M): 10 µl/ml

IP buffer for anti-Flag IP (with 1% Triton-X100):

For 250ml	Final concentration
12.5ml 1M Tris pH7.5	50 mM
7.5ml 5M NaCl	150 mM
2.5ml Triton-X100 (or 25 ml 10% Triton-X)	1 %
0.5ml 0.5M EGTA	1 mM

0.5M EGTA: 50 ml titrate with 5M NaOH (ca. 8 ml), or with 10M NaOH ca. 4 ml).

1X Running buffer:

3.03 g Tris
14.4 g Glycine
1 g SDS
add water to 1 l

1X Transfer buffer:

3.03 g Tris
14.4 g Glycine
200 ml Methanol
add water to 1 l

Sucrose buffer for brain lysates

sucrose 80%	4°C	320mM	1,37ml
1M Tris		10mM	100µl
2M NaHCO3	4°C	1mM	5µl
2M MgCl2		1mM	5µl
H2O			8,134ml
protease inhibitor			1 tablet
Phosphatase inhib.		Na4P2O7	225µl
(-20°C freezer)		NaF	200µl
		Na3VO4	50µl
		ZnCl2	10µl
total volume			10ml

4x LDS sample buffer (NUPAGE)

40% glycerol	4.6ml 87% glycerol
564 mM Tris-Base	0.682g
424 mM Tris-HCl	0.666g
LDS (lithium dodecyl =lauryl sulphate)	0.8g
2.5% (v/v) phenol red (1%solution)	250ul
7.5% (v/v) Serva Blue G250 (1%solution)	750ul
2mM EDTA	40ul 0.5M EDTA or 0.006g

1x buffer should be pH 8.5. Do not adjust the pH.

2x Freezing medium for mammalian cells

	10 ml	15 ml
DMSO (20%)	2 ml	3 ml
FCS (25%)	2,5 ml	3,75 ml
DMEM (55%)	5,5 ml	8,25 ml

3.3 The Clinical Collection

The NIH Clinical Collection (NCC) is a plated array of 281 (NCC201) and 446 (NCC003) small molecules with a history of human clinical trials. The substances are distributed by Molecular Libraries Small Molecule Repository (MLSMR) Evotec San Francisco. The collection was assembled by the American National Institutes of Health (NIH). Similar collections of Food and Drug Administration (FDA) approved drugs have been used to detect undiscovered bioactivity and therapeutic potentials. The aim of the collection is to do likewise, to provide excellent starting points for chemical lead optimisation or even to discover treatment effects in new diseases areas.

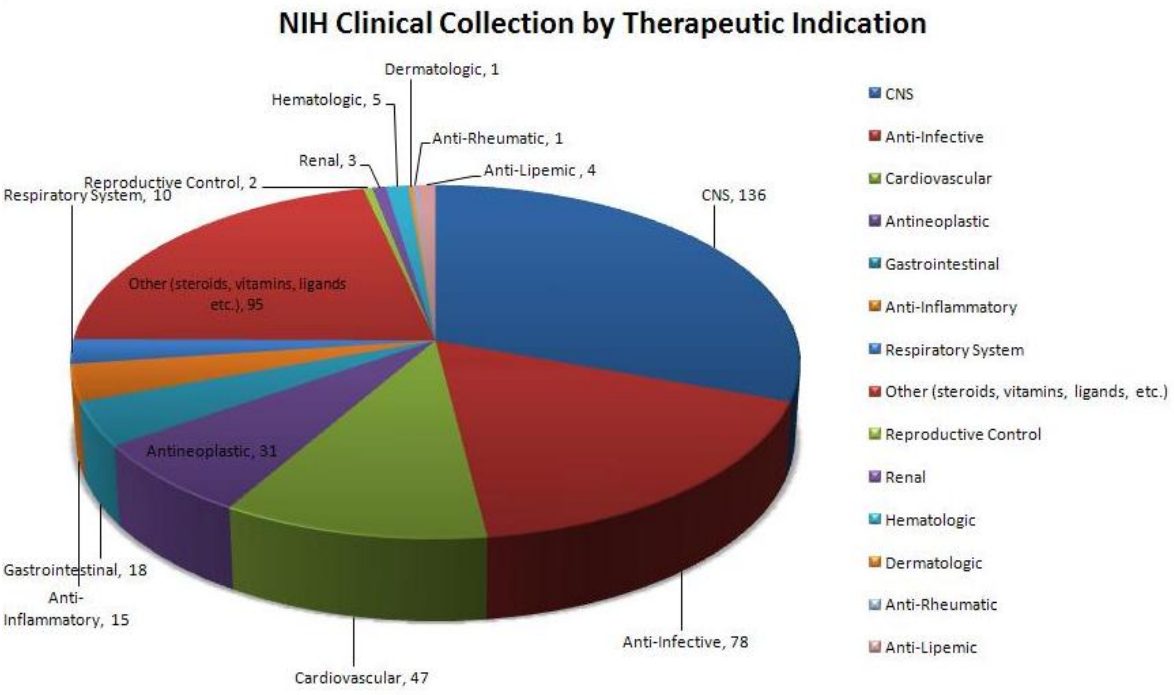

Figure 16: NIH Clinical colection

Image by Evotec

http://www.nihclinicalcollection.com/NCCAnnotatedChartVP.JPG

For the screen all chemicals are solved in DMSO and used in a final concentration of 10µM if possible. All substances were purity checked at 16.11.2007 aliquoted at 10.12.2010 or 29.09.2011. For a detailed list of drugs see apendix.

3.3.1

3.4 Drugs for validation

Name	Manufacturer	Amount	Order number
Lapatinib	Axon	10mg	1395
CI-1033	Axon	5mg	1433
Staurosporin	Cayman	100µg	81590
SB-431542 hydrate	Sigma	5mg	S4317
EGF-like domain	Reprokine	50µg	RKQ02297
mEGF	Reprokine	50µg	RKP01132
Rapamycin	Calbiochem	100µg	533210
MK-801 (Dizocilpine)	Sigma	25mg	M107
Spironolactone	Sigma	1G	S3378
Eplerenone	Sigma	10mg	E6657
Canrenone	Santa Cruz	1g	205616
Topotecan	Selleckchem	50mg	S11231
SN38	Tocris	10mg	2684
Vincristine	Tocris	10mg	1257
Mevastatin	Sigma	5mg	M2537
Albendazole	Sigma	10g	A4673
CCPA	Tocris	10mg	1705
K252a	LC Laboratories	1mg	K-2151

Table 11. Drugs ordered for validation purpose

4 Methods

4.1 General lab routine

Methods not described in detail were performed according to “Molecular cloning: A Laboratory Manual” (Maniatis,1982). Molecular biology standard methods were performed according to Sambrook and Russel (Sambrook and Russell, 2001) and to the manufacturer´s instructions if not indicated otherwise.

4.2 Transformation of chemically competent bacteria

Aliquots of transformation-competent bacteria (*E.coli*, strain XL1 blue, DH5α, Mach1) were thawed on ice or on the way. 2.5-30µl of a ligation or recombination reaction was added to 50-100µl cells (for retransformation of existing plasmids 1ul DNA and 10ul bacteria is sufficient), followed by an incubation step on ice for 5-30 min. The bacteria were heat-shocked at 42°C for 30 sec, and then cooled on ice for 2 min. 600µl cold LB medium or SOC medium without antibiotics was added, and the mix was incubated at 37°C for 45 min without or with moderate shaking. During this incubation the cells start expressing the appropriate antibiotic resistance. Then, 100-800µl were plated on pre-warmed LB-agar plates containing the appropriate antibiotics. Sterile glass beads were used to equally distribute the bacteria. The plates were incubated overnight at 30-37°C depending on the encoded genes. (Note ERBB constructs should be expressed on not more than 32°C).

4.3 Electroporation of bacteria

The commercially available electro-competent *E.coli* strain DH10B was diluted 1:4 with sterile 10% glycerol, and 20µl aliquots were made. For electroporation, the bacteria were thawed on ice, 2-2.5µl of a recombination or ligation reaction was added, and the mix was transferred into a 1mm electroporation cuvette (BioRad).

Be aware of to high concentrations of salt in the DNA. In case of producing an electric arc dilute the DNA further with the 10% glycerol. The electroporation was performed using the ‘GenePulserII’ (BioRad) with the following settings: 1.75kV, 25µF capacitance and resistance of 200Ω. The cells were resuspended in 600µl cooled LB, or alternatively in SOC medium, without antibiotics and incubated at 37°C for 45 min with moderate shaking. The bacteria were plated as described above in the section ‘Transformation of chemically competent bacteria’.

4.4 Plasmid purification

Plasmid DNA preparations are based on a modified protocol of Birnboim and Doly (Birnboim and Doly, 1979), depending on the alkaline cell lysis followed by SDS precipitation of proteins and genomic DNA. The plasmid DNA was bound to a silica membrane under appropriate high-salt conditions, washed and finally eluted with buffer TE or H_2O. Plasmid DNA was isolated from fresh overnight bacterial LB cultures grown to an OD of 2 to 3 using the Plasmid DNA Purification Kits (Mini, Midi, Maxi, Maxi EF and Giga scale) provided by Macherey-Nagel. Detailed description of the procedures can be found in the manuals provided by the manufacturers.

4.5 Plasmid DNA mini preparations

In brief, the pelleted bacteria (2-4 ml of the overnight culture) were resuspended in 250µl buffer A1 with RNAse. Cell lysis was performed by adding 250µl lysis buffer A2. After 5 min incubation the reaction was stopped by adding 300µl neutralization buffer A3. The mix was centrifuged for 10min to pellet genomic DNA as well as proteins, and the clear supernatant was then loaded onto the column. The resin membrane was washed with 600µl buffer AQ, dried by centrifugation for 2 min, and finally, the plasmid DNA was eluted in 100µl H_2O or TE buffer.

4.6 Plasmid DNA midi preparations

In brief, pelleted bacteria (200ml of the overnight culture) were resuspended in 4 ml buffer S1 with RNAse. 4ml buffer A2 was added to lyse the cells and after 5 min incubation at RT cell lysis was stopped by adding 4ml buffer S3 pre-chilled to 4°C. The suspension was incubated on ice for 5-15min. In the meantime, the column was equilibrated with 2.5ml buffer N2. The cleared and filtered lysate was loaded on the column. The column was washed twice with 10 ml buffer N3, and the DNA was eluted in 5ml buffer N5. Finally, the DNA was precipitated using 35% f.c. isopropanol, and it was re-suspended in 100 µl TE buffer. The expected amount of plasmids is 200-500µg. The f.c. in stock is adjusted to 1µg/µl.

4.7 Photometric concentration determination of nuclear acids

Concentration and purity of a nucleic acids solution can be analysed by spectrophotometry. According to the Lambert-Beer law, the concentration of a solution is directly proportional to its extinction or absorption, that is

$A=\varepsilon*c*l$

with ε representing the molar extinction coefficient (unit M-1cm-1), c being the

concentration (unit M) and l being the optic path length (cuvette thickness) that the light passes through the sample (unit cm). The extinction coefficients for nuclear acids at λ = 260nm are:

guanine: ε = 12010 M-1cm-1

cytosine: ε = 7050 M-1cm-1

adenine: ε = 15200 M-1cm-1

thymine: ε = 8400 M-1cm-1

(uracile: ε = 8111 M-1cm-1)

Using a spectrophotometer, the absorption at 260nm (maximum of absorption of nucleic acids) and 280nm (maximum of absorption of aromatic amino acids in proteins) of the nucleic acid solution was determined. For a reliable measurement, it is of importance that the value for the absorption at 260nm is set between 0.1 and 1 to fit the linear range of the photometer. Therefore, a proper dilution of the sample was necessary. To determine the concentration the following relation was applied:

1 OD260 (optical density at 260nm) = 50mg/ml for double stranded (ds) DNA

1 OD260 = 40mg/ml for single stranded (ss) RNA

1 OD260 = 33mg/ml for ss oligonucleotides

The equation to determine the concentration of dsDNA was

c (µg/µl) = OD260 * 50 * dilution factor/1000

The purity of a given sample was assessed by the relative absorption values of 260 nm over 280nm. Clean preparations of DNA and RNA would return values between 1.8 and 2.0 whereas significantly lower values indicated a protein contamination.

4.8 Agarose gel electrophoresis

Agarose gels of 0.8%-4% were used to separate DNA fragments between 0.1kb and 15kb of size. The proper amount of agarose was added to 1x TAE buffer, and the suspension was heated, in the microwave, for appr. 5min, or longer, until the agarose was completely dissolved. In case of ethidium bromide gels the solution was allowed to cool to 60°C to minimise evaporation of gases, and ethidium bromide was added to a final concentration of 1µg/µl. Be aware of ethidium bromide evaporating in to hot agarose. Don´t breath the fumes!

In case of acrydin orange nothing is added to the agarose

The fluid agarose was poured into a gel-casting form, and combs were

inserted to define the pockets for sample loading. The agarose needed 20-120min to solidify depending on the room temperature. Solid agaros gel is storable for 4 weeks at 4°C. The gel was placed in a chamber containing 1x TAE buffer. The DNA samples were prepared by adding the proper volume of 10x loading dye (ethidium bromide gel) or 10x OrangeG and GelRed containing loading dye (ethidium bromide free gels) and loaded into the pockets of the gel. The voltage applied was 30-180V (5-10 V/cm), depending on the size of the gel chamber and the agarose concentration used. For 1.5% agarose gel to analyse restriction digests the following settings were used:

small 120V

medium 150V

large 180V

DNA molecules migrate to the positive electrode as the phosphates in the DNA backbones are negatively charged. The speed of the migration is lowered by the size of the DNA molecule and the obstruction by the fishnet like structure of the agarose gel, resulting in their size-dependent separation. The DNA could be visualised by the fluorescence of the incorporated ethidium bromide when exposed to UV light source emitting 260nm.

OrangeG could be visualized via a BioDoc Analyzer

The 100bp marker or 1kb marker (Fermentas, St. Leon-Rot) were used as molecular size standards. Gel chamber, casting form and combs were produced by the workshop of the Max-Planck-Institute.

4.9 Isolation of DNA from agarose gels

To isolate DNA from agarose gels the Gel and PCR clean up kit provided by Macherey-Nagel was used. The area of the gel containing the desired DNA was excised under UV light (356nm, Intas UV systems, Heidelberg) with a scalpel. The step should be as fast as possible, cause UV light will crosslink DNA and therefore cause mutations. The excised Gel was weighted and transferred to an Eppendorf reaction tube. The DNA was purified according to the manufacturer's instructions. In brief, for each 100mg of agarose gel, 200µl of buffer NTI was added. The mix was incubated for 5-20min at 50°C until the agarose was dissolved completely. The sample was loaded onto a silica membrane, washed with 600µl buffer NT3, dried, and finally eluted in 30-50µl buffer NE prewarmed to 60°C. Concentration and size of the DNA was then checked via agarose gel electrophoresis.

4.10 DNA digest with restriction endonucleases

DNA restriction digests were performed using type II restriction endonucleases in reaction volumes of 20-200µl. Type II restriction endonucleases induce cleavage mostly within their palindromic recognition sequences of 4-8 nucleotides, and yield in 5´- or 3´-DNA overhangs or blunt ends depending on the enzyme. Most enzymes were supplied with one of four standard 10x reaction buffers (NEB, New England Biolabs). 0.5 to 1µg of DNA were used for analytical digests, 5-25µg of DNA were used for preparative digests, respectively. The restriction enzyme unit 'U' defines the amount of enzyme that is required to cut 1µg DNA in 1 hour at 37°C. Usually, 2- to 3-fold the amount of enzyme was used in digests and the digests were incubated for two hours. To save enzymes larger digests were incubated for longer than two hours e.g. overnight.

4.11 DNA sequencing

DNA sequencing was performed at the Institute's DNA Core Facility (Department of Neurobiology, MPI of Experimental Medicine, Göttingen) lead by Dr. Fritz Benseler. DNA sequencing is based on a modified dideoxy chain reaction termination method according to Sanger (Sanger et al., 1977). The approach is based on a linear DNA amplification in the presence of a sequencing primer, a DNA-polymerase, normal deoxynucleoside triphosphates (dNTPs), and modified nucleotides (dideoxyNTPs) that terminate DNA strand elongation. DideoxyNTPs stochastically incorporate into the newly synthesized DNA by replacing the normal dNTPs thereby terminating the synthesis. The products of different length are separated by capillary electrophoresis. As each of the four dideoxyNTPs is coupled to a different fluorescent dye the DNA fragments can be characterised by size, and the terminal nucleotide is identified. Through a repetitive procedure, the DNA sequence is determined.

4.12 Sequence analysis of DNA

Sequencing data was analysed using the DNAstar software, version 8, provided by Lasergene. The obtained sequences were also aligned to databases of the 'National Center for Biotechnology Information' (NCBI, http://www.ncbi.nlm.nih.gov) and ENSEMBL (http://www.ensembl.org).

4.13 Modification of DNA

Ligation of DNA The enzyme DNA ligase derived from the bacteriophage T4 catalises the formation of covalent phosphodiester bonds between free 3'-hydroxy and 5'-phosphate overhangs of double stranded DNA. Cofactors

needed for this reaction are Mg^{2+} ions and ATP. The cloning of DNA fragments, that is the ligation of insert and vector, was performed for 2h at room temperature or overnight at 4°C. The 10-20µl of a ligation reaction contained 50-100ng vector DNA, 150-300ng insert DNA (molar ratio 1:3), 1.5U T4 DNA-ligase, and the ATP-containing 10x buffer provided by the manufacturer. (Note: ATP decays over time. If the Ligation is not working ATP is probably gone). The reaction was stopped by incubation at 65°C for 10min. Standard ligation reaction:

x µl	vector	(50-100ng DNA)
x µl	insert	(150-300ng DNA)
1µl	10x buffer	
0.5µl	T4 ligase	(1.5U)

Add up to 10µl ddH2O

4.14 Dephosphorylation of 5'-DNA fragment overhangs, vectors only

The terminal 5'-phosphate groups of dsDNA can be removed by phosphatase treatment using the enzyme calf intestinal alkaline phosphatase (CIP). This helps to reduce the likelihood of unwanted vector re-ligations. As CIP is compatible with NEB-, Roche- and Promega-buffers 1-2µl of the enzyme was added to a completed DNA digest and incubated at 37°C for maximal 20 min. To stop the reaction the digested DNA fragment was heat inactivated and/or purified by agarose electrophoresis.

4.15 Cloning of PCR products

PCR products were purified by agarose electrophoresis and using the Gel and PCR clean up kit (Macherey-Nagel). The PCR products were, if they contained terminal restrictions sites, first cut with the appropriate restriction enzyme(s), purified, and then used for ligation into the designated vector. PCR products amplified with Taq-polymerase were also directly sub- cloned into the pGemT or pGemTeasy vector (Promega) through so-called TA cloning. The technique is based on the property of the Taq-polymerase to attach an additional nucleotide (preferentially adenosine) to the 3'-end of the completed PCR product. The pGemT vectors can be purchased in a linearised form with complementary 5'-thymine overhangs which bind to the PCR fragment. If a proofreading polymerase with 3'-exonuclease activity (e.g. Pfu-polymerase, Stratagene) was used in the PCR, the adenosine overhangs had to be added in a second reaction using the Taq-polymerase. To do this, 25µl of the purified PCR product were incubated with 5µl 10x buffer, dATP (f.c. 0.2mM), and 5U Red Taq-polymerase in a final reaction volume of 50µl

incubated for 10min at 37°C. The reaction was purified with the help of the Gel and PCR clean up kit (Macherey-Nagel). Therefore, 200µl buffer NTI was added per 100µl PCR reaction volume, the mix was applied onto the column, washed with buffer NT3 dried, and finally eluted in 30-50µl buffer NE. 5-7µl was used for ligation.

4.16 Amplification of DNA by polymerase chain reaction

The polymerase chain reaction (PCR) was developed by Kary Banks Mullis (Mullis et al., 1992; Mullis and Faloona, 1987), and is now a commonly used method for selective in vitro amplification of defined DNA fragments. The DNA synthesis begins with the annealing of two DNA oligonucleotides (primers), which flank the DNA stretch that is supposed to be amplified. One primer anneals as a sense primer to the plus strand of the DNA, the other primer binds as an anti-sense primer to the minus strand. The polymerase recognises the dsDNA (primer and template) and exponentially amplifies the DNA region flanked by the primers. The synthesis is catalysed by thermostable Taq-polymerases (derived from the thermophilic bacterium Thermus aquaticus) or proofreading polymerases (e.g. Pfu-polymerase, Stratagene, derived from the thermophilic archaea bacterium Pyrococcus furiosus). The latter one helps to reduce the mutation rate by its 5'-3'-exonuclease activity by one power to about one mutation in 106 nucleotides.

Standard PCR reaction (20µl):

x µl template (10-100ng)

1µl sense (forward) primer (10pmol/µl)

1µl anti-sense (reverse) primer (10pmol/µl)

2µl 10x reaction buffer (including MgCl2)

1-5µl dNTP mix (dATP, dCTP, dGTP, dTTP; f.c. 0.2mM each)

0.8µl Taq polymerase (5 U/µl) Add ddH2O to 20µl

A PCR reaction consists of three main steps:

1. denaturation,

2. primer annealing

3. elongation.

The PCR steps are run at different temperatures, and they are repeated multiple times in cycles. At the beginning of the PCR, an initial denaturation at 95°C was used to remove any DNA secondary structures followed by a primer annealing step between 50-60°C where the primers are supposed to bind to their complementary DNA sequence. The annealing temperature was 2-4°C

lower than the computed melting temperature of the primers. At 72°C the elongation was performed, which is the optimum temperature for the Taq-polymerase. The extension time was calculated depending on the template length and the polymerase used. Non proofreading polymerases require up to 30sec per 1kb template, whereas proofreading enzymes need about 1min per 1kb. The PCR ended in a final elongation step at 72°C to ensure complete synthesis. Depending on the DNA template and the purpose (cDNA, plasmid DNA, genomic DNA) 15-36 cycles were run. The volume of the PCR reaction was 20µl (genotyping) or 50µl (preparative PCR).

Standard PCR protocol

3 min → 95°C, initial denaturation

30 sec → 56°C, annealing

60 sec → 72°C, elongation

30 sec → 95°C, denaturation

60 sec → 55°C, final annealing

10 min → 72°C, final elongation cycle

Designing primer sequences

Primers were designed with melting temperatures (T_m) of 60°C. Primer melting temperature can be roughly calculated with the help of the following formula: T_m = (A+T)2+(G+C)4, with A, T, G and C indicating the numbers of the corresponding nucleotides in the primer sequence. For a more precise T_m determination, an online algorithm developed by Warren A. Kibbe (Kibbe, 2007) was used (http://www.basic.northwestern.edu/biotools/oligocalc.html).

Site-directed mutagenesis

This method of PCR-based in vitro mutagenesis presents a fast approach to exchange and manipulate one or more nucleotides, also simultaneously, in a DNA molecule. Following aspects for the design of the mutagenesis oligonucleotides have to be considered: The length of the oligonucleotide is supposed to be in the range between 24bp and 45bp.

The T_m of the oligonucleotide should be higher than 78°C and is calculated by using the following formula: T_m = 81.5+0.41 (% GC)-675/N-% mismatch (with N being the length of the oligonucleotide in bp and % GC reflecting the GC content in per cent).

The mutation, deletion or insertion should preferentially lie in the middle the oligonucleotide and flanked by each side with 10-15bp which exhibit 100% complementarity to the target sequence The GC content of the

oligonucleotide should not be below 40%.

The oligonucleotide should start and end with at minimum one G or C.

The mutagenesis PCRs are exclusively performed using proofreading polymerases. The PCR product was digested with DpnI, a restriction endonuclease, which specifically recognises the methylated sequence 5'Gm6ATC 3', and therefore cuts only the parental template DNA generated in *E.coli.* The mutated sample was gel purified and transformed into bacteria for amplification.

4.17 One-way gateway

The gateway recombination system is based on site-directed recombination and uses enzymes derived from the bacteriophage lambda that are able to transfer DNA fragments between vectors (Hartley et al., 2000) This cloning strategy works with much higher efficiency than the conventional cloning technique that is based on type II endonucleases and T4 DNA- ligase. For detailed information on gateway cloning see Invitrogen's web page (http://de.invitrogen.com/site/de/de/home/ProductsandServices/Applications/Cloning/Gateway- Cloning.html). To clone an ORF or other DNA fragments of interest specific recombination sites (attB1 and attB2) have to be added to both ends via PCR. The PCR product was recombined in a 'BP reaction' with a 'donor' plasmid, termed pDONR, containing attP1 and attP2 recognition sites. The BP reaction is catalised by the Gateway BP clonase II enzyme mix.

Each BP reaction contained:

3µl	attB-PCR product	(10-100ng/µl)
1µl	pDONR	(100ng/µl)
1µl	BP clonase II	

BP reactions were incubated overnight at RT. To optimize conditions for transformation, 1µl of proteinase K was added and incubated at 37°C for 10 min, followed by a heat-inactivation step at 95°C for 10 min. 1µl of the inactivated BP reactions was taken for electroporation in DH10b bacteria or for chemical transformation in XL1blue bacteria. Clones were selected by the appropriate antibiotic, and the insert was sequenced.

One major feature of the gateway system is that bacteria harbouring a not recombined donor vector after a recombination reaction are not supposed to survive as the pDONR vector contains the toxic gyrase inhibitor encoded by the ccdB gene flanked by the recombination sites. The ccdB gene is only replaced by an insert when the recombination event was successful, ensuring that only properly recombined clones survive and produce colonies.

Constructs containing the pDONR backbone and the DNA insert represent ‘entry clones’ (pENTR). These constructs carry attL sites (the product of recombination of attB and attP sites). To generate the final ‘expression clones’, abbreviated pEXPR, the attL sites of the Entry clones are recombined with attR sites of a ‘destination vector’, or pDEST, in an ‘LR’ reaction, catalysed by the Gateway LR Clonase II enzyme mix.

Each LR reaction included:

1 µl pENTR (25-100ng/µl)

1µl pDEST (100ng/µl)

1µl LR clonase

2µl H2O

The reaction was incubated at RT overnight followed by a proteinase K digest. 1µl of the reaction was transformed into DH10b electro-competent or DH5α chemical competent bacteria. The resulting pEXPR clones were then analysed by restriction digest and sequencing and functionally tested by transient transfection in cell culture followed by luciferase assays, fluorescence assays or western blotting.

4.18 Subculturing of eukaryotic cells

Eukaryotic cells (HEK293, HEK293FT, PC12, etc) were cultivated on 15 cm dishes or cell culture flasks at 37°C in a humidified incubator containing 5% CO2. After reaching 70-90% confluence, cells were subcultured by washing with PBS and mild treatment with 2.5 ml trypsin/EDTA for 1-5 min at 37°C until they detached from the culture dish. The reaction was stopped by adding 5ml serum-containing culture medium, the cells were resuspended and the cells were pelleted by centrifugation for 3 min at 800g. The supernatant was discarded, the pellet resuspended in fresh medium, and an appropriate inoculum (typically, a dilution of 1/10 to 1/5) was plated onto new dishes.

4.19 Thawing and cryopreservation of cell lines

Frozen stocks of cell lines were kept at -196°C submerged in liquid nitrogen in 2ml cryovials. Aliquots were quickly thawed in a water bath at 37°C, suspended with 3 ml pre-warmed growth medium, and centrifuged for 3 min at 800g to remove the DMSO with the supernatant. The pellet was resuspended in fresh medium and plated onto a 15 cm culture dish.

For cryopreservation cells were grown on 15 cm dishes until reaching 90% confluency. The medium was removed, and the cells were detached using trypsin as described above. The cells were counted using a Neubauer

counting chamber, and, after centrifugation, resuspended in an appropriate volume of ice-cold growth medium to obtain a concentration of about 4 million cells per 1 ml. 500 µl of the cell suspension was transferred into a cryovial already containing an equal volume of the ice-cold 2x freezing medium.

The samples were mixed gently by inverting the tubes three times and quickly frozen at -20°C. After two hours the cells were transferred to –80°C for one day and finally to liquid nitrogen for long term storage.

4.20 Coating with poly-L-lysin

For PC12 cells, it is important to coat the dishes with poly-L-lysin (PLL). The negatively charged polysaccharid structures on the cell surface bind to the positively charged PLL allowing better adherence of the cells. For coating, dishes were incubated with 0.02 mg/ml PLL in ddH2O for 20 min at RT, then washed twice with sterile water, air-dried, and stored at 4°C until further use.

96 well plates were coated using the Hamilton Lab Star robot. 30µl of PLL solution were pipetted in each well. The PLL solution incubated for 20''. Afterwards the wells were washed twice with ddH2O. The coated plates were sterilized via UV light for 1h

4.21 Transfection of mammalian cells

DNA-transfer in eukaryotic cells with lipofectamine2000

The transient transfection of plasmid DNA in eukaryotic cells was done using lipofectamine2000 (Invitrogen). The approach is based on the formation DNA-containing liposomes that are endocytosed by the cell. Cells were typically transfected in 96-well plates for reporter gene assays. Depending on the cell line different numbers of cells were plated:

Cell line	**96well**	**6well**	**15cm**
PC12TO	40.000	1.000.000	5M
PC12WT	40.000	1.000.000	
PC12 Neuroscreen	50.000		
HEK293	20.000	500.000	5M
HEK293FT			5M

The protocol provided by the manufacturer was modified to obtain optimal results. For a single well of a 96-well plate, both the 10-200ng (mini or midi prep) of DNA and 0.2µl of lipofactamine2000 were diluted in 15µl OptiMEM each. The solutions were mixed separately, incubated for 5min, and then

combined, resulting in 30µl. The mix was vortexed for 20sec. and incubated for 20 min at RT. The growth medium was completely removed from the cells, and 30µl of the OptiMEM containing DNA/lipofectamine complexes were applied onto the cells. After two hours, 30µl of regular growth medium was added to each well. The cells were allowed to express the plasmids for 24-48h, and subjected to a given procedure, i.e. western blots or reporter gene assays.

4.22 DNA transfer in eukaryotic cells with electroporation

During electroporation a brief current pulse induces a transmembrane electric field in the cells, which leads to local instabilities of the cell membrane (electro-pores). In this short period macromolecules such as DNA are able to enter the cell. With optimal setting of the parameters, cells recover and can be subcultured. For the generation of stably transfected Hek293 cells, 5M cells were mixed with 20µg linearised plasmid and transferred into an electroporation cuvette (4 mm).

Parameters for electroporation were the following: 950µF, 220 V. After electroporation, cells were incubated under standard conditions.

4.23 Generation of stable cell lines

Cells were transfected and selected with the indicated drug selection concentrations corresponding to the repsective resitance encoded on the expression plasmid.

Hek293

Puromycin	200ng/ml	
Hygromycin	100µg/ml selection	50µg/ml maintaining
G418	400µg/ml selection	200µg/ml maintaining

Hygromycin Co integration

Vector MSCV Hygro	Hygromycin 50µg/ml	1-5;000,000 cells
2 µg pMSCV Hygro	10 µg Plasmid of interest linearised	

Electroporate the cells and plate the cells on a PLL coated cell culture Plate

Start the selection 24h after transfection. After 5 days nearly all cells are dead

After 2 weeks positive survival clones should be visible by eyesight Alternatively, transfection via Lipofectamin 2000 (Invitrogen cat.-no.: 11668-019) It isn’t necessary to linearize the plasmid of interest

Transfection scheme for a 10 cm dish:

	O-MEM	LF2000	DNA
DNA tube:	1,5 ml	20 µl -	1,2µg

Add the OptiMEM to both tubes; mix well through pipetting and incubate 5 min at room-temperature (RT). Mix the LF/OptiMEM mixture and the DNA/OptiMEM, incubate 20min at RT. Change the medium with 3ml of LF/DNA-mix per dish, incubate for 1-2 h at 37°C, then add 3 ml of fresh 2x growth medium. Start selection 24h after transfection

PC12TO

Hygromycin Co integration

Vector MSCV-hygro Hygromycin 200µg/ml 1-5,000,000 cells

2 µg pMSCV Hygro 10 µg Plasmid of interest linearised

50µg /ml Hygro is not enough!

Important for freezing and thawing of stable cells:

When you freeze the cells change 3h before freezing the growth-media to media without selection antibiotics. For freezing use a freezing medium with the double amount of serum at least. Don't forget the DMSO. When thawing let the cells grow for 24h in a growth medium without selection antibiotics. After 24h you can add the selection antibiotics.

4.24 Luciferase reporter gene assays

4.24.1 Single assay 16x6 measurement points

Luciferases are enzymes which catalytic activity leads to the emission of visible light upon substrate conversion. The most commonly used luciferase is the firefly luciferase that catalyses the following reaction:

luciferin + ATP → luciferyl adenylate + PPi

luciferyl adenylate + O2 → oxyluciferin + AMP + light

Transcriptional activity of a given promoter can be investigated by transfecting the cells with a reporter construct carrying a luciferase ORF under the control of this particular promoter. Expression level, of the luciferase reporter gene, is then quantified by adding luciferase substrate and ATP to the cellular lysates and measuring the intensity of the emitted light. Luciferase reporter gene assays were performed in HEK293 cells and PC12 cells in 96-well plates. 12-48 h after transfection the medium was removed and 30-40 µl of 1x passive

lysis buffer (Promega) was added to each well. The plates were incubated for 20 min at RT under moderate or fast shaking (200-1400 rpm) and assayed immediately, stored at 4°C up to 6h or frozen at -20°C. Prior to analysis the samples were transferred to black, white or black and white plastic microtiter plates. White wells increase the signal. Black plates decrease the noise. Black and white plates combine both features.

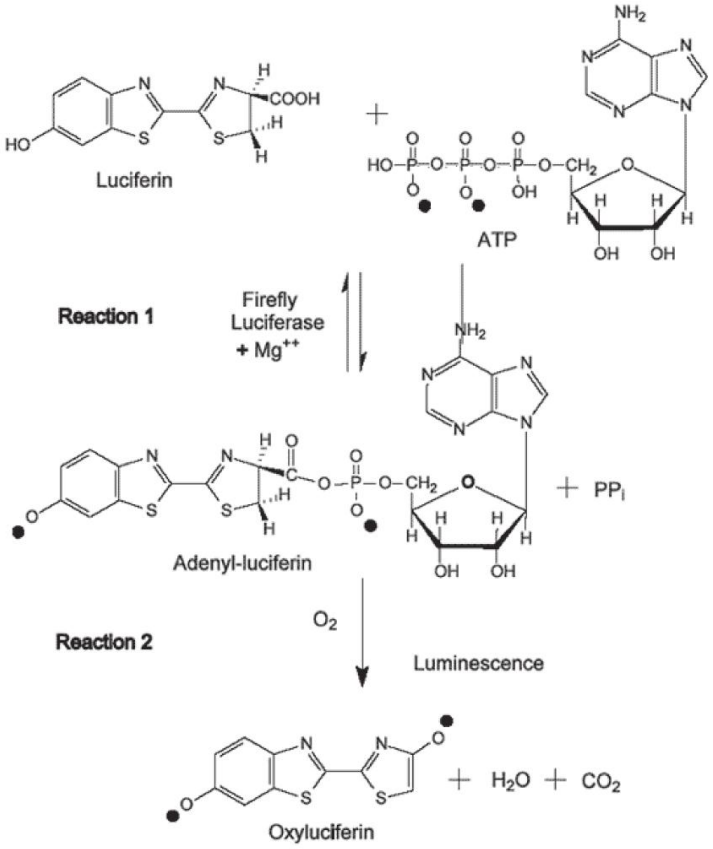

Figure 17: Reaction of D-Luciferine with the firefly luciferase (modified from sigmaaldrich.com)

4.24.2 Normalisation and transfection control

Measurements of the firefly luciferase (*Photinus pyralis*) activity are commonly normalized to the activity of a different reporter, e.g. *Renilla* luciferase (*Renilla reniformis*) that is expressed under a constitutively active promoter. This is done to rule out differences in cell number, transfection efficiency, and RNA and protein expression from well to well.

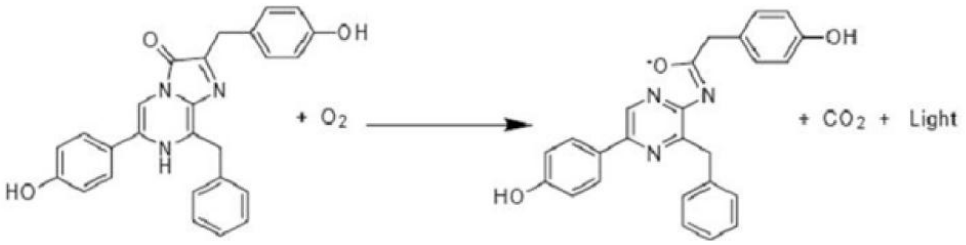

Figure 18: Reaction of Coelenterazine with the *Renilla* luciferase (modified from Komabiotech.co.kr).

A mix of three different plasmids encoding *Renilla* luciferas under control of different promoters was used. To visually control transfection efficiency an equal amount of pEYFPnuc, a construct for CMV promoter-driven expression of the nuclear localized enhanced yellow fluorescent protein was used.

TC34	SV40	-Rluc
TC35	TK	-Rluc
TC33	CMV	-Rluc
TC48	CMV	-EYFPnuc

The plasmids were mixed at the following ratio: SV40:TK:CMV = 10:2:1 to compensate for the different potency of the promoters.

The R*enilla* mix is prepared with the following recipe

pSV40_*Renilla*	100µg	
pTK_*Renilla*	20µg	
pCMV_*Renilla*	*1*0µg	
pEYFPnuc	13µg	in 1300µl

Final concentration of all 110ng/µl

(100ng *Renilla* plasmids and 10ng EYFPnuc).

Dependent on the assay the *Renilla* mix has to be modified to meet the requirements or to prevent usage of promoters which react to the assay. The TK-promoter seems to be promoter of choice for NRG1-ERBB4 assays.The fluorescent protein can be exchanged with other colours e.g.

pEYFP, pEYFPnuc, pECFP CI, DSRed, pCherry

20ng of the *Renilla* mix was cotransfected per well along with any firefly reporter gene assay, if not indicated otherwise. For standard luciferase reporter gene assays six technical replicates were analysed to enhance statistical reliability. Transfection efficiency was checked via fluorescent protein expression. Bioluminescence measurement was performed with the help of the Microplate reader Mitras LB940 or Microlumat Plus 96V (Berthold Technologies) and the associated software MicroWin 2000 using the following protocol:

1) Injection of 40-75 µl firefly luciferase substrate, 2-60 sec reaction time, 1-10sec measurement of light signals

2) Injection of 40-75 µl *Renilla* luciferase substrate, 2-60 sec reaction time, 1-10 sec measurement of light signals

The firefly and the *Renilla* luciferases display high substrate specificity and do not cross-react. Moreover, firefly luciferase activity is blocked by the pH conditions of the *Renilla* substrate.

4.24.3 Statistical analysis

Data were exported from MicroWin 2000 and analyzed with Excel or GraphPadPrism. For normalisation, the firefly-value was divided by the corresponding *Renilla*-value to get the relative luciferase unit (RLU). Mean, standard deviation (SD) and standard error of the mean (SEM) of the six technical replicates were calculated.

4.25 Screening of high throughput assays 96 well formats

4.25.1 Automated PLL coating

The Hamilton Labstar robot was programed to coat 96 well plates. The plates were opened than 30ul of PLL/H_2O were pipetted. The plates were incubated for 20 min., than washed with 2 times 50ul H_2O. The dried plates were sterilised by one hour UV-light exposition.

4.25.2 In solution transfection of PC12 cells

To transfect huge amounts of equal cells with equal plasmids we used the following protocol per one 96well plate. 4,000,000 cells were harvested and diluted in 5ml phenol red free DMEM. The following plasmids were diluted in 2,5ml Optimem and mixed.

2µg	ERBB4-NTEV-tevS-GV_2HA
2µg	PIK3R1-CTEV_2HA
2µg	UAS firefly luciferase
2µg	TK-*Renilla* luciferase
0,5µg	pECFP CI

20ul of Lipofectamin2000 were diluted in 2.5ml Optimem and mixed.

Both Optimem aliquots were mixed and incubated for 20min. Afterward the 5ml Optimem and the cells in DMEM were carefully mixed, and incubated at 37°C at 5% CO_2 for 2h.

4.25.3 Plating of cells

10ml solution, containing 4,000,000 in solution transfected cells, per 96well

plate, were stored in the bubble paddle reservoir of the Hamilton Cellstar robot. 100ul per well were pipetted using the 96er pipet head. The homogeneity of the solution over time is sustained by mild paddeling of the reservoir. Keep in mind that the reservoir has a “death volume” of 50ml/5 plates. The finished plates were stored in the cytomat automated cell culture (34 plates maximum).

4.25.4 Handling of stable Nrg1-type-I expressing cells

1,000,000 Nrg1-type-I expressing PC12 cells per plate were harvested and diluted in 10ml phenol red free DMEM. The cells were placed in the Cellstar robot in the bubble paddle reservoir (see above). 10,000 cells/well were plated in each well. Note, stable cell lines grow slower than normal PC12 cells, probably due to Hygromycin. Start in time with growing the cells.

4.25.5 Dispension of drugs

The drugs of the NCC library were diluted in DMSO to an f.c. of 1mM. 80 drugs were used per 96well-plate using the collums 2-11 (blue). 1A-D is further stimulated with 10mg/ml EGFld (yellow). 12A-D is inhibited with 100nM CI-1033 (red) and 12E-H with 10µM Lapatinib (lilac).

24h after in solution transfection the plates were processed with the Cellstar robot. They were driven out of the incubator, opened, and stimulated with 2ul of Drug/DMSO. 30min. after the drug stimulation, the cells were stimulated with 100ul DMEM with 10,000 Nrg1-typeI expressing cells per well, automatically pipetted with the 96well head from the bubble paddle reservoir. Afterwards the cells were automatically incubated for another 24h.

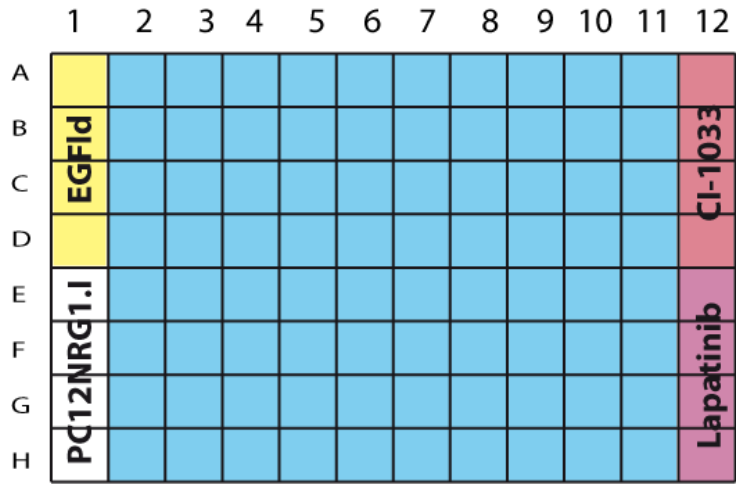

Figure 19: Layout of a 96 well-plate for HTP screen

4.25.6 Automated dual luciferase assay

Plates were emptied of medium. The cells were lysed by application of 35ul of passive lysis buffer and high speed shaked for 10 min. The plates were measured in the LB plate reader. 30ul of firefly substrate were pipetted in each well, the plate was shaken for ten sec. and than firefly luciferase activity was measured. Than 30µl *Renilla* substrate were pipeted in each well, the plate was shaken for ten sec. and than *Renilla* luciferase activity was measured. The data was automaticly exported as text file and analysed using the following TinR script.

4.25.7 Analysis of results with TinR

The data was analysed with TinR using the following script:

```
library("cellHTS2")

 # Script to analyse Luci Screens with cellHTS2
 # part 1 creates all folders and fiules wich are neccesary to run the cellHTS2 package
 # part2 runs cellHTS2
 # part1

   # Please specify Replicate number and number of substance plates
    subPlates=as.numeric(winDialogString("How many Substance Plates were used", "4"))
    reps=as.numeric(winDialogString("How many replicates", "3"))
    experimentName <- studyName <- winDialogString("Name of the study?", "screen1")
    #create new folder with studyName
    datadir<-paste("Z:/User/Systasy project NEW/Operative Business/ERBB4 PI3Kp85a split TEV Compound screen/Analysis with R/",studyName,sep="")
    dir.create(datadir)
    dir(datadir)
    setwd(datadir)
    #create SUBFOLDERS
    dir.create(paste(datadir,"/logRatio",sep=""))
    dir.create(paste(datadir,"/rawdata",sep=""))
    # choose all rawdatafiles and copy them to Study folder
    csa<-choose.files(default = "Z:/User/Systasy project NEW/Operative Business/ERBB4 PI3Kp85a split TEV Compound screen/Analysis with R", caption = "Select the LUCI rawdata files",multi = TRUE)
    file.copy(csa,paste(datadir,"/rawdata",sep=""))
    allfiles <- dir(paste(datadir,"\\rawdata\\",sep=""))    # place all raw data files into a RawData subfolder
    f2r<- allfiles[grep("TXT",allfiles)]

  # go through all rawdata files and extract relevant data and create new files
  for(fi in f2r){
  te<-read.table(paste("rawdata/",fi,sep=""),skip=9)
  ff<-te[1:96,]
  ffname=paste(strsplit(fi,".TXT")[[1]],"_FF",sep="")
  ff<-cbind(rep(ffname,times=96),ff)
  rn<-te[101:196,]
  rnname=paste(strsplit(fi,".TXT")[[1]],"_RN",sep="")
  rn<-cbind(rep(rnname,times=96),rn)
  write.table(ff,paste(ffname,".TXT",sep=""),quote=F,row.names=F,col.names=F,sep="\t")
  write.table(rn,paste(rnname,".TXT",sep=""),quote=F,row.names=F,col.names=F,sep="\t")
  }
```

```
 # generate platelist.txt file
 allfiles <- dir(datadir)    # place all raw data files into a RawData subfolder
 f2r<- allfiles[grep("TXT",allfiles)]
 ma<-matrix("NA",nrow=length(f2r),ncol=4)
 Filename=NULL
 for(i in 1:subPlates ) {
 print(i)
    FileNamesRNTemp = f2r[seq(reps*(i-1)*2+2,reps*i*2,by=2)]
    FileNamesFFTemp = f2r[seq(reps*(i-1)*2+1,reps*i*2,by=2)]
    Filename = c(Filename,FileNamesRNTemp,FileNamesFFTemp)
 }

 Plate = rep(1:subPlates,each=reps*2)
 Replicate = rep(1:reps,subPlates*2)
 Channel =   rep(rep(1:2,each=reps),subPlates)
 ma<-cbind(Filename,Plate,Replicate,Channel)
 write.table(ma,"Platelist.txt",row.names=F,quote=F,sep="\t")

 # part2

 if(subPlates == 4) {
    file.copy("Z:/User/Systasy project NEW/Operative Business/ERBB4 PI3Kp85a split TEV Compound
screen/Analysis with R/ScreeningLibraries/Ncc-201/Plateconf.txt",datadir)
    file.copy("Z:/User/Systasy project NEW/Operative Business/ERBB4 PI3Kp85a split TEV Compound
screen/Analysis with R/ScreeningLibraries/Ncc-201/Description.txt",datadir)
    file.copy("Z:/User/Systasy project NEW/Operative Business/ERBB4 PI3Kp85a split TEV Compound
screen/Analysis with R/ScreeningLibraries/Ncc-201/drug list.txt",datadir)
 }
 if(subPlates == 6) {
    file.copy("Z:/User/Systasy project NEW/Operative Business/ERBB4 PI3Kp85a split TEV Compound
screen/Analysis with R/ScreeningLibraries/Ncc-003/Plateconf.txt",datadir)
    file.copy("Z:/User/Systasy project NEW/Operative Business/ERBB4 PI3Kp85a split TEV Compound
screen/Analysis with R/ScreeningLibraries/Ncc-201/Description.txt",datadir)
    file.copy("Z:/User/Systasy project NEW/Operative Business/ERBB4 PI3Kp85a split TEV Compound
screen/Analysis with R/ScreeningLibraries/Ncc-003/drug list.txt",datadir)
 }

x <- readPlateList("Platelist.txt", name=experimentName, path=datadir)

x <- configure(x,
   descripFile="Description.txt",
   confFile="Plateconf.txt",
   path=datadir)

table(wellAnno(x))

xn <- normalizePlates(x, scale="multiplicative", method="median",
varianceAdjust="none")

ctoff <- quantile(Data(xn)[, , 1], probs = 0.05, na.rm = TRUE)

xn1 <- summarizeChannels(xn, fun = function(r1, r2, thresh = quantile(r1,
 probs = 0.05, na.rm = TRUE)) ifelse(r1 > thresh,
 r2/r1, as.numeric(NA)))

xn1 <- normalizePlates(xn1, scale = "multiplicative",
 log = TRUE, method = "median", varianceAdjust = "none")
```

```
xsc <- scoreReplicates(xn1, sign = "-", method = "zscore")
xsc <- summarizeReplicates(xsc, summary = "median")
xsc <- annotate(xsc, geneIDFile="drug list.txt",       # enter annotation file name
path=datadir)

par(mfrow = c(1, 2))
ylim <- quantile(Data(xsc), c(0.001, 0.999), na.rm = TRUE)
boxplot(Data(xsc) ~ wellAnno(xsc), col = "lightblue",
outline = FALSE, ylim = ylim)
imageScreen(xsc, zrange = c(-2, 4))

 negControls <- vector("character", length = dim(Data(x))[3])
  negControls[1] <- "(?i)^PC12 Nrg1-typeI$"                    ## neg controls for channel 1, Renilla, PC12
Nrg1.typeI cells are baseline
  negControls[2] <- "(?i)^Lapatinib$|^CI-1033$"      ## neg controls for channel 2, Firefly
  posControls <- vector("character", length = dim(Data(x))[3])
  posControls[2] <- "(?i)^EGF-like domain$"          ## pos controls for channel 2

setSettings(list(platelist = list(intensities = list(include = TRUE)),
screenSummary = list(scores = list(range = c(-4, 4)))))

negControls <- "(?i)^Lapatinib$|^CI-1033$"
posControls <- "(?i)^EGF-like domain$"

out <- writeReport(raw = x, normalized = xn1, scored = xsc,
outdir = "logRatio", map = TRUE, posControls = posControls,
negControls = negControls)

browseURL(out)

save(xsc, file = paste(experimentName, ".rda", sep = ""))
```

4.25.8 Preparation of dose response dilutions for 96well format.

To prepare a master plate start by solving the drug in DMSO. Prepare 150ul of 10mM stock solution. Prepare 2 stripes of a 96 well plastic plate with following DMSO amounts.

Pipette 100ul stock solution in 1a, pipette 34ul stock solution in 1b, mix by pipetting 10times up and down. Transfer 10ul from 1a.→2a., mix, transfer 10ul from 2b.→2c., repeat top down pipetting for all wells except 7b. that remains pure DMSO. 8a. and b. remains empty for assay stimulation controls.

Dose response curves from f.c. 100µM to 0.0001µM can now be generated by pipetting 2ul to wells containing final 200ul co-culture or cell culture buffer. Note pipetting of small amounts (2ul) with 8 channel pipets is inaccurate 12ul are needed for 6 wells. Plan with 150-200% as master mix. 90µl will only be secure enough for 5*96 well plates.

4.26 Biochemical methods

4.26.1 Western Blot

Western blotting is a classical method for immunological detection of proteins in biological samples (Towbin et al., 1992).

4.26.2 Sodium dodecyl sulphate polyacrylamid gel electrophoresis (SDS-PAGE)

Unlike DNA, proteins may be positively or negatively charged or neutral and do not have a linear relationship between weight and charge due to differences in amino acid composition. To enable directed migration of proteins in the electric field SDS is used to produce a negative charge. After heat denaturation at 70°C the polypeptide chains unfolds to expose the hydrophobic regions which can non-covalently bind SDS hydrophobic tails at the stochiometry of 1 SDS molecule per 2 amino acids. Additional treatment with dithiotreitol (DTT) reduces all intra- and intermolecular disulfide bonds.

Protein lysates were mixed with 4x LDS sample buffer and 10% DTT (f.c. 0.1M) and incubated at 70°C for 10 min. 2- 5µg were used for western blotting. For SDS-PAGE NuPAGE Novex Bis- Tris Gels (Invirtogen) were used with Xcell SureLock NuPAGE buffer chambers (Invitrogen) according to the manufacturer´s protocol. The electrophoresis was performed at 200V for 45-60min.

4.26.3 Transfer of proteins on membranes

The transfer of proteins from the gel to a PVDF membrane was performed with the Xcell SureLock Western Blot System (Invitrogen) according to the manufacturer´s instructions. Prior to transfer PVDF membranes were activated for 3min in 100% methanol and afterwards rinsed in transfer buffer. The transfer was done at 30V for 2h while the chamber was placed in ice water.

4.26.4 Detection

When the transfer was completed the membrane was incubated in blocking buffer (5% non fat milk powder in TBS-T for normal antibodies or 5% BSA in TBS-T for α-phospho antibodies) for at least 30min at RT. The primary antibody was applied in the appropriate dilution in blocking buffer at 4°C overnight. The membrane was rinsed twice with TBST and than washed with TBST three times for 10min and was subsequently incubated with the appropriate horse-radish peroxidase (HRP)-conjugated secondary antibody for 1h at RT. After two times rinsing and three wash steps for 10 min in TBS-T the membrane was treated with enhanced chemiluminescence (ECL) detection solution for 1 min according to the manufacturer´s recommendations and enclosed in plastic foil. In a dark chamber an ECL-hyperfilm was exposed to the membrane and developed with KODAK-O-MAT. For reprobing the membrane was incubated with 0,5M NaOH for 3min at RT or Restore WB stripping buffer according to the manual. The membrane was then washed in TBS-T and blocked again as described above. All incubation steps were performed under constant moderate shaking or rolling.

4.27 The MK801 mouse model

NMDA antagonists are tools to produce SZ-like symptoms in animal models and human subjects (Eyjolfsson et al., 2006). This is based on the first findings (Luby et al., 1959) that Phencyclidine induces a psychotic state with positive and negative symptoms in healthy humans (Snyder, 1980). The underlying mechanism of glutamate receptor blockage was discovered in 1982 (Lodge and Anis, 1982). The dysfunction of the combined dopaminergic and glutamatergic transmitter system in the pathogenesis of SZ has been broadly discussed (Javitt and Zukin, 1991; Olney and Farber, 1995; Flores and Coyle, 2003; Carlsson et al., 1999). The disturbance of glutamatergic neurotransmission, has been reported in patients with distinct negative symptoms and cognitive deficits (Harrison and Weinberger, 2005; Goff and Coyle, 2001; Tsai and Coyle, 2002). All known SZ susceptibility genes act on glutamatergic synaptic transmission (Harrison and Weinberger, 2005), and

reduced GABA synthesis has also been described in SZ patients (Lewis et al., 2005).

Therefore, MK801, the most potent non-competitive NMDA receptor complex antagonist, is used to model SZ symptoms in animal models. MK801 binds to a site in the ion channel and blocks cat ion flow. Therefore, the receptor acquires the open confirmation that is dependent on the agonist MK801.

The drug produces locomotor hyperactivity in rodents that may correspond to positive symptoms of SZ (Nilsson et al., 2004), social withdrawal that is a core phenotype of negative symptoms (Sams-Dodd et al., 1997), pre-pulse inhibition deficits, and maybe cognitive deficits (Arnt, 1998).

MK801 is reported to trigger auditory hallucinations (Allen and Young, 1978).

In addition, MK801-elicited effects were studied on hippocampal and prefrontal GABAergic interneurons in rodent animal models (Braun et al., 2007).

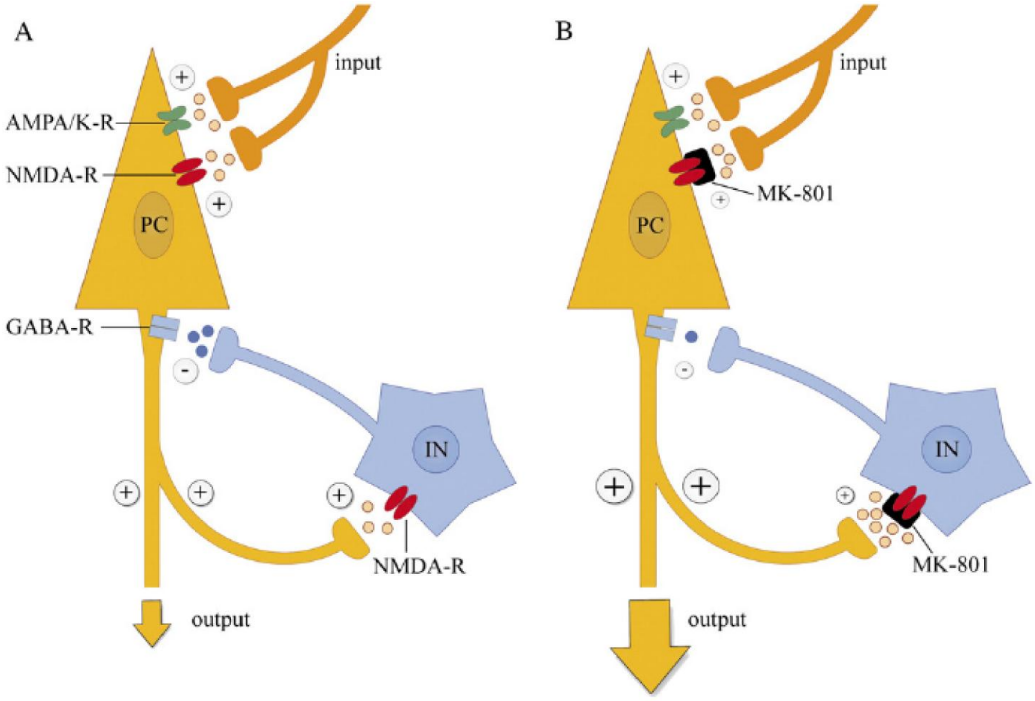

Figure 20: Model of the local neuronal circuit dis-inhibition in response to MK801 in the cortex.

A) An inhibitory GABAergic interneuron (IN, i.e. Chandelier cell or Basket cell) receives input from the excitatory pyramidal cell (PC) thereby exerting an inhibitory control by recurrent projections to the pyramidal cell. B) In presence of the NMDA receptor antagonist MK801, this local feedback inhibition becomes disrupted, whereas the excitatory input is sustained via non-NMDA (AMPA/kainate) receptors, which do not respond to MK801. Due to this imbalance the total excitatory output is predicted to be enhanced. Image taken from (Braun et al., 2007).

4.28 Drug tests in mice

4.28.1 Drugs and treatments

Spironolactone (Sigma-Aldrich) was dissolved in 0.9% NaCl with 1% DMSO and 0.002% Tween®20. MK801 (Sigma-Aldrich) was dissolved in 0.9% NaCl with 1% DMSO. Drugs were stored in DMSO at -20°C and diluted freshly before experiments. Spironolactone (20mg/kg), MK801 (0.5mg/kg), and vehicle (0.9% NaCl with 1% DMSO) were injected i.p. in volumes of 10ml/kg.

4.28.2 Mice

C57Bl6/N male mice were purchased from Charles River (Sulzfeld, Germany) at the age of three weeks. After arrival, animals were housed in standard plastic cages with food and water ad libitum in the colony room, with a 12 hours light-dark cycle (lights switched on at 8:00 a.m.). One week prior experiments, mice were placed in single cages and habituated to experimental rooms. Experiments were conducted with nine weeks old animals. Treatment groups were analysed at balanced time points during the light phase to exclude an interference of circadian rhythm on drug actions.

4.28.3 Behavioral studies

To assess the effects of Spironolactone on MK801-induced hyperactivity mice were injected with corresponding drugs according to the protocol depicted in (Fig. Figure 55 A) Animals were divided randomly in one of the following four treatment groups: Group 1 was injected twice with vehicle ([veh+veh], n=13), group 2 was administered with Spironolactone and vehicle ([Spiro+veh], n=14), group 3 treated with vehicle and MK801 ([veh + MK801], n=12), and group 4 injected with Spironolactone and MK801 ([Spiro+MK801], n=14). 100min after the first injection (vehicle or Spironolactone) each animal underwent the open field test. The open field test was conducted in a Plexiglas arena (45 x 45 x 55 cm high). Each mouse was placed individually in an open field box and was allowed to explore freely the test arena for 20 min to determine baseline activity. After 20min, the experiment was stopped for 4min to administer the second injection (vehicle or MK801 according to the protocol in (Figure 55 A) Subsequently, animals were placed back to the open field box and left undisturbed for 120min. The distance travelled, the time which each mouse spent active, and the time spent in the centre of the arena (defined as 70% of central area) were analysed as an indicator of anxiety. The numbers of rearings were taken as a sign of exploratory drive. All movements were monitored by infrared sensors and analysed by the ActiMot software (TSE Systems, Bad Homburg, Germany).

5 Results

5.1 Design of a screening platform for Nrg1-ERBB4 signalling

A cell-based assay that can be used for HTP screening approaches has to meet specific criteria, such as scalabilty and, robustness. Moreover, it has to provide a simple but quantifiable readout.

The screening assay described here is mimicking proximal aspects of the Nrg1-ERBB4 signalling using a co-culture assay of two different cell populations (Figure 25). The first population represents PC12 cells expressing constitutively active mouse-derived Nrg1-typeI-β1a (Figure 26, Figure 27). The second population represents also PC12 cells but expressing human ERBB4 fused to the N-terminal part of the TEV protease (NTEV) that is linked via a TEV protease cleavage site (tevS, sequence: ENLYFQ'G) to the artificial transcription factor Gal4-VP16 (GV). As ERBB4 is a type I transmembrane receptor, GV is anchored to the membrane as long as no functional TEV protease is present. Activated ERBB4, i.e. Nrg1 ligand-bound and dimerised ERBB4, is auto-phosphorylated at several specific Tyr residues in the C-terminal region that act as binding sites for phospho-adapter molecules, such as the regulatory subunit of the PIK3, PIK3R1, that binds to phosphorylated Tyr residues within YXXM motifs. Therefore, PIK3R1 fused to the C-terminal part of the TEV protease (CTEV), is also expressed in the second cell population. In this assay, activated ERBB4 binds to PIK3R1 initiating the formation of TEV protease activity as both TEV protease fragments get into close proximity, which allows the refolding of the inactive fragments into a functional TEV protease. The protease can cleave at the tevS to release the artificial transcription factor GV that in turn translocates to the nucleus. Here, GV induces the transcription of a firefly luciferase reporter gene that is under the control of upstream activating sequences (UAS-Fluc). UAS-Fluc is the third component that has to be introduced into the second cell population to complete the assay. Using a firefly luciferase as readout allows for a linear amplification of an occurred ERBB4/PIK3R1 interaction event. In addition, the luciferase assay is an easy-to-use readout, stable, and very sensitive assay (Figure 22, Figure 28).

5.1.1 Normalisation

For normalisation purposes, the assay system is co-transfected with a *Renilla* luciferase vector. The *Renilla* luciferase is constitutively expressed under the control of the Thymidine kinase (TK) promoter. It is assumed that the transfection efficiency can be compared across all wells using the enzymatic activity of the *Renilla* luciferase. Choosing the correct promoter for the *Renilla*

luciferase is vital, as some promoters like the CMV or SV40 promoter seem to respond to growth factors, such as the EGFld and other introduced effects like shRNAs (C. Hammer personal communication). In addition, the normalisation vector in the screen is used to detect toxic substances by means of absolute *Renilla* values.

5.1.2 Concentrations of plasmids

All plasmids in the assay are regularly used in the concentration of 20ng/well. Titration assays have shown that this concentration is sufficient to yield optimal induction ratios for the Nrg1-induced ERBB4/PIK3R1 assay, which is also in agreement with a previous report using the split TEV technique for ERBB4 assays (Wehr et al, 2008).

5.1.3 Cell numbers per well

Two different cell concentrations have to be considered. First, cell numbers of population 1 have to be high enough to provide a detectable and stable signal, but adjusted to reasonable levels to prevent overcrowding as cells still divide within the 48h duration of the assay. 40,000 PC12 cells/96-well were determined to be optimal. Second, the Nrg1-typeI-expressing cells have to be adjusted. A number of 5,000-10,000 cells/96-well resulted in a stable activation of the assay that allowed both further activation or inhibition.

5.1.4 Cell types tested for the assay

We tested PC12, HEK293, and CHO cells for usability in the screen. PC12 cells performed best in transient assays. HEK293 cells gave unstable results in transient assays and, unfortunately, a triple transgenic HEK293-derived cell line stopped working reliably. CHO cells gave no stable results at all.

5.1.5 Transfection methods

We tested FuGeneHD, Lipofectamine LTX, and Lipofectamine 2000. For PC12 cells, Lipofectamine 2000 was best suitable, as it could well be used for both adherent and in-solution transfections. For screening purposes, in-solution transfection was used to increase homogeneity of transfected cells in the wells. A special steering device named “bubble paddle reservoir” available within the Hamilton Microlabstar Plus robot was used to further increase homogeneity of the cells.

5.1.6 Workflow of the NRG1-ERBB4 assay

Critical to HTP-screening are the time points applied in a workflow of a given assay. When using in-solution transfection, two time points are critical. First, the components of the assay have to be expressed and correctly localised to

the membrane, a process that occurs during the expression phase of the transiently transfected cells after plating. Second, a good time window has to be chosen for the application of the drugs and concomitant addition of the Nrg1-type1-expressing cells. We tested various setups with six hours differences between each time point and found a reasonable measurement window between 12h expression/12h stimulation and 24h expression/36h stimulation. After a total assay duration of 72h, the plates were overgrown and the cells started to die. For screening purposes, working hours also have to be considered. Therefore, a 24h expression/24 stimulation workflow was chosen.

5.1.7 Stability of the luciferase signals

To provide a robust readout the luciferase signal has to be stable over the time needed for the measurement. For HTP screening, the processing of the assay plates should be as fast as possible. Therefore, cells are lysed using an 8-well dispenser head, allowing to dispense the buffer in minimal time. In addition, the buffer used, the Promega passive lysis buffer, is formulated to provide optimal stability for luciferase enzymes. When the substrates are added to the cell lysates, the luciferase reaction starts immediately. The firefly luciferase signals are relatively stable, with 80% stability over the first 5 minutes. The *Renilla* luciferase signals decrease fast, with a reduction of 50% within two minutes. To start the measurement, luciferase substrates are dispensed across the plate, followed by orbital mixing and the measurement itself for which the detector head moves again across the plate. The minimum time required for a measurement of one plate in one run in our luciferase reader is 100 seconds for dispensing, 10 seconds for mixing, and 100 seconds for reading. Thus, firefly and *Renilla* luciferase activity is measured in each well 110 seconds after addition of the substrate. As the timing for each well regarding substrate addition and reading is the same the initial dramatic decrease in *Renilla* luciferase activity should not have an effect on the readings obtained from the screen (Figure 21).

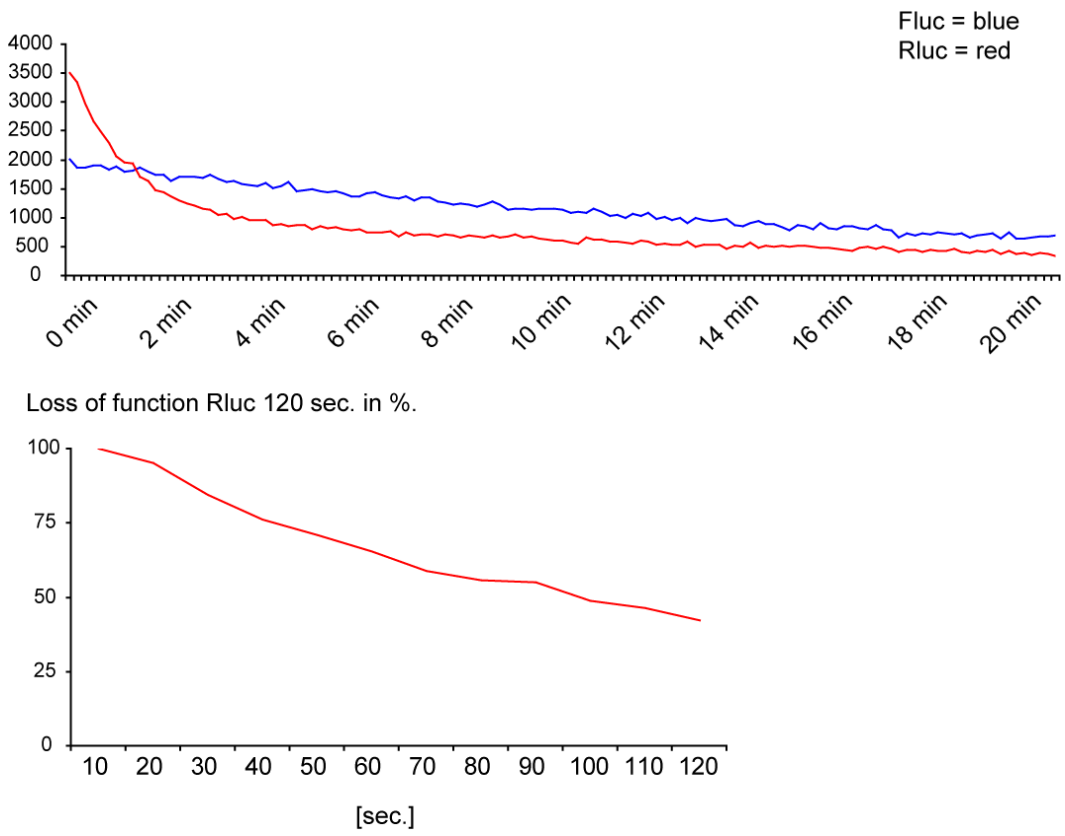

Figure 21: Kinetics of firefly and *Renilla* luciferase

Decay of firefly luciferase (Fluc, blue) and *Renilla* luciferase (Rluc, red) signal over 20 min. The Fluc signal drops regularly over 20 min, then remaining with about 50% of activity. The Rluc signal initially drops fast, losing about 50% of its activity within the first 2 min, but remains relatively stable afterwards.

5.1.8 Protocol at a glance one 96 well plate

The experiments lead to the following protocol used in the screening assay:

Transfection Protocol

1. Pipet DNA
2. Mix DNA with 1/2 volume Optimem
3. Vortex
4. Incubate 2-5 minutes
5. add LF2000 to other 1/2 volume Optimem
6. Vortex
7. Incubate 2-5 minutes
8. Combine LF2000/Optimem and DNA/Optimem mix
9. Vortex
10. Incubate 30 minutes at RT
11. Add cells (in medium, with same volume as total volume of Optimem)
12. Incubate 2h at 37°C, but no shaking/rocking
13. Plate cells on 96 well plates, 100µl/96-well. No centrifugation necessary
14. Incubate 24h for protein expression. Check expression using a GFP-transfected control plate.
15. Add drugs (2 µl in DMSO, f.c. 10µM). Controls: 10 µM Lapatinib, 0.1 µM CI-1033.
16. Add EGF-like domain (f.c.10 ng/ml; 20 ng/ml added in 100µl) or PC12 Nrg1-typeI cells (in 100µl)
17. Incubate further 24h
18. lyse cells for assay (35 µl PLB/96-well)

5.2 Component controls

5.2.1 CMV-GV

The PC12 cells are transfected with UAS-Fluc and GV. The UAS-Fluc can be activated by constitutively active expression of the GV that is under the control of the CMV promoter. In HTP screens, all substances that interfere with Fluc activity have to be eliminated to reduce false positive signals (Figure 23).

5.2.2 TM-TEV/TM-GV

The PC12 cells are transfected with TM-TEV, TM-GV, and UAS-Fluc. TEV protease and GV are bound to a membrane anchor termed TM, a transmembrane domain present in the plasmid pHOOK. Both the protease and the GV are localised to the membrane. Any substance that interferes with TEV protease activity can be removed from the screen (Figure 23)

5.2.3 Lapatinib

Lapatinib is an ERBB-specific receptor tyrosine kinase inhibitor. In the screen, it is used as control acting as an inhibitor. 10 µM of Lapatinib leads to highly decreased luciferase activity in the screen (Figure 29).

5.2.4 CI-1033

CI-1033 is a non-specific receptor tyrosine kinase inhibitor. It is used in the screen as further control also acting as a highly potent ERBB4 inhibitor. 100nM. CI-1033 results in even more decreased luciferase activity compared to 10µM Lapatinib (Figure 29).

5.2.5 EGFld

The NRG1 EGF-like domain (EGFld) is a potent activator of ERBB3 and ERBB4 activity. In the screen, it is used to further activate the assay, with levels that are above the ones induced by Nrg1-typeI-expressing cells. 10ng/ml EGFld (ca1.5nM, MW ca. 7.2 kD) are sufficient to activate the assay nearly to maximum levels. EGFld domain represents the functional domain of human NRG1 for ERBB3/4 activation. Therefore, EGFld represents the most effective way to activate ERBB3/4. Substances that are found in the screen and modulate Nrg1-ERBB4 signalling, but fail to modulate EGFld-ERBB4 signalling act as putative modulators of Nrg1 processing (Figure 24).

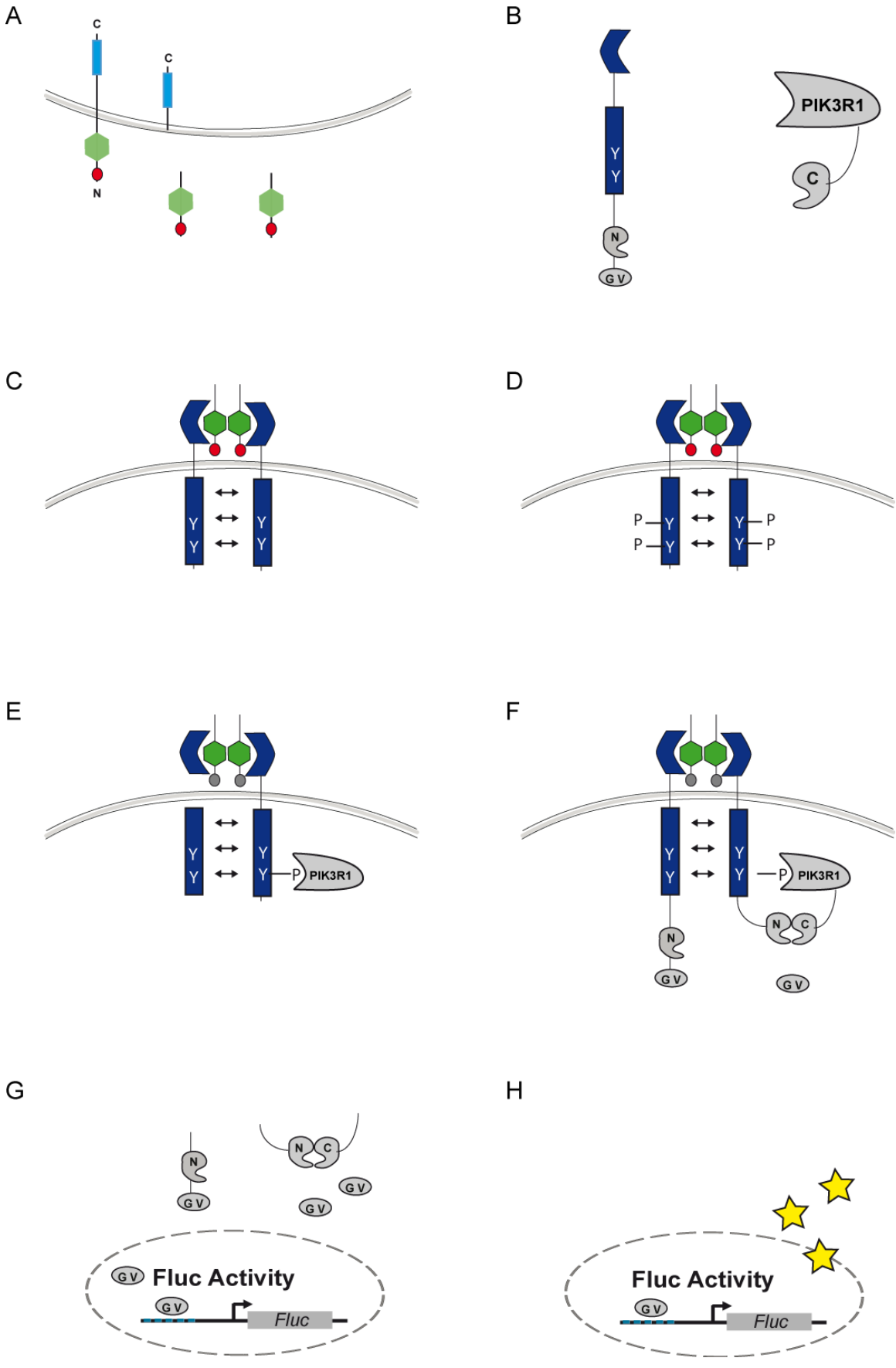
A
C
C
N
B
PIK3R1
C
Y
Y
N
G V
C
D
E
P
PIK3R1
F
N
C
G
H
Fluc Activity
Fluc

Figure 22: Schematic representation of the shape and function of the constructs used in the screen

A) Distal of the signalling cascade is a PC12 cell line stable expressing Nrg1-typeIβ1a. Nrg1 is localised in the membrane, processed, and then released into the medium. B) The ERBB4 receptor is fused to the N-terminal moiety of the TEV protease. In addition, it is fused to the GalV-VP16 transcription factor via the TEV protease-specific cleavage site ENLYFQ`G. The alpha regulatory subunit of the PI3-kinase, PIK3R1, is fused to the C-terminal moiety of the TEV protease. C) The ERBB4 receptor homodimerises after binding to Nrg1-typeI. D) After forming homodimers, ERBB4 receptor pairs auto-phosphorylate each other. E) The ERBB4 homodimer recruits the PIK3R1 to the PI3-kinase binding site at Tyr 1056.F) The recruitment of PIK3R1 to the ERBB4 homodimer brings the N- and C-terminal fragments of the TEV protease in close proximity. G) Both fragments of the TEV protease fold into the active protease and regain protease activity. The TEV protease targets the TEV-specific cleavage site and releases the Gal4-VP16 transcription factor. The transcription factor shuttles to the nucleus and activates the UAS-Fluc reporter gene. H) Activation of the UAS-Fluc reporter gene results in a higher firefly luciferase activity, which can be measured by the turnover of ATP and d-luciferine producing light.

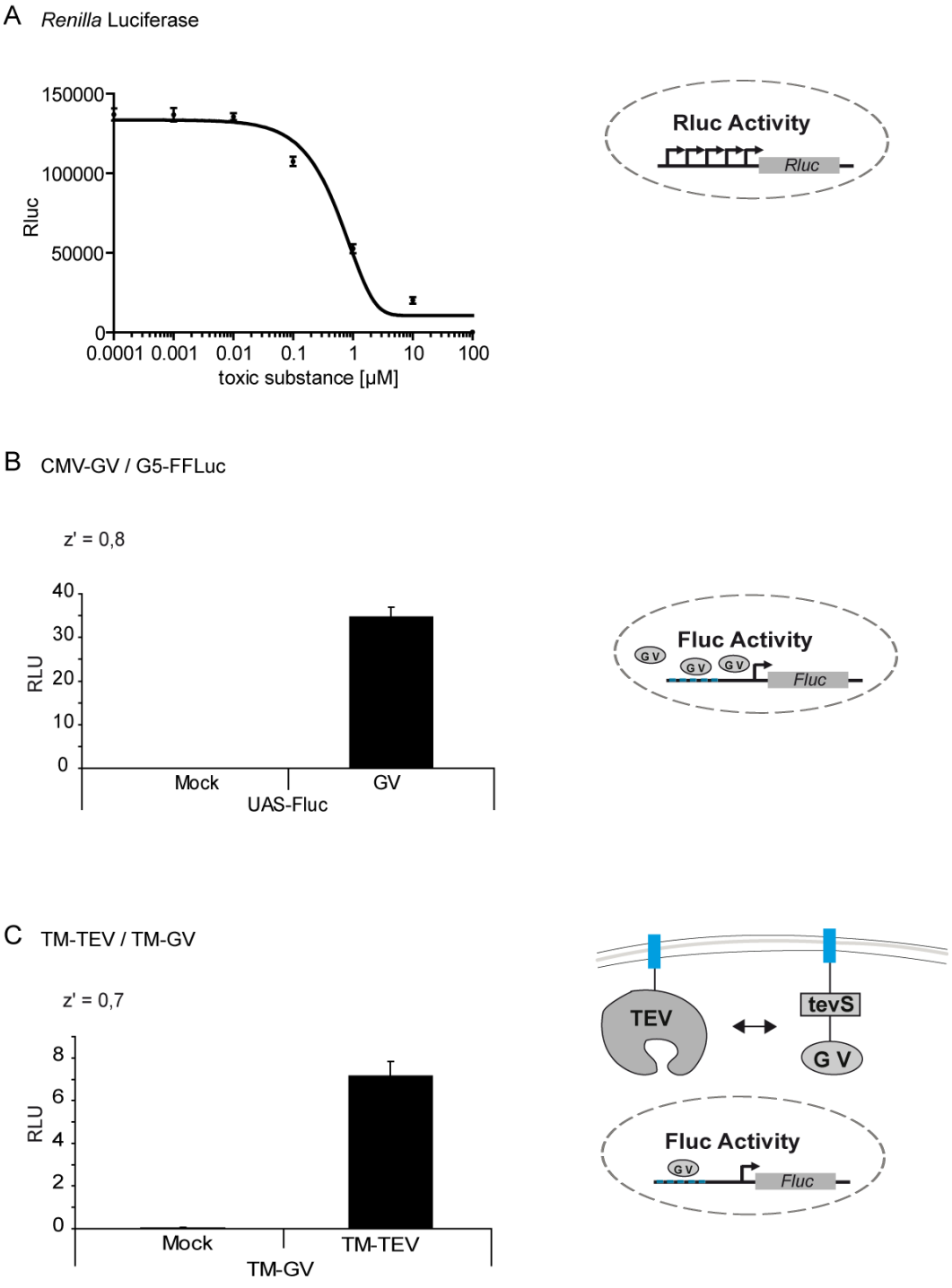

Figure 23: Controls of the screen

A) Renilla luciferase. Effect of a toxic substance. B) Constitutively active GV-UAS-firefly assay. The Cytomegalovirus promoter (CMV) was placed in front of the Gal4-VP16 (GV) artificial transcription factor. C) TM-TEV/TM-GV.A transmembrane anchor (HOOK) was fused to the TEV protease (TM-TEV) and the TEV protease cleavage site/GV fusion (TM-GV).

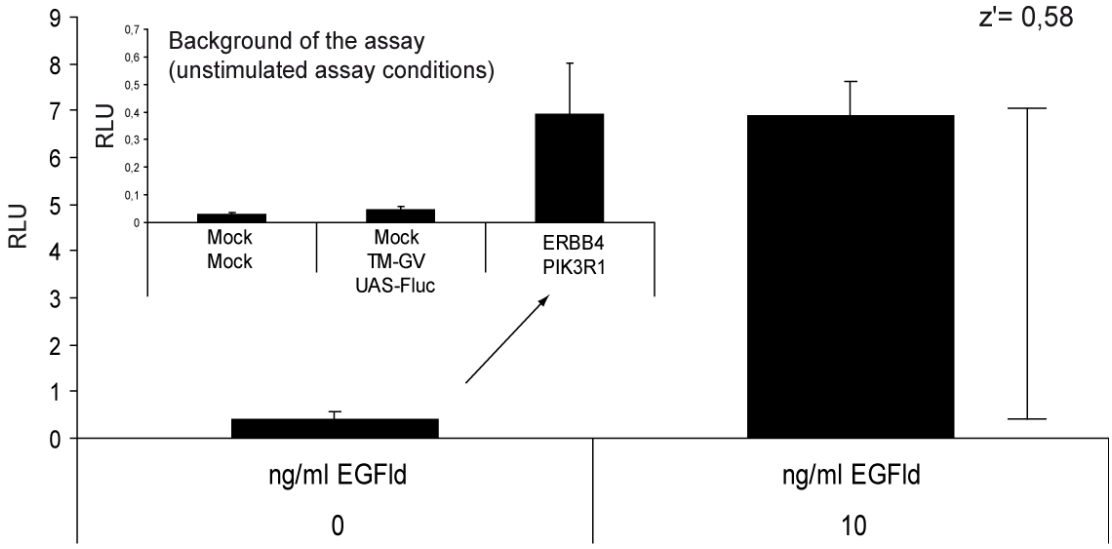

Figure 24: Background of the assay

ERBB4/PIK3R1 split TEV assay in PC12 cells. ERBB4 was fused to NTEV-tevS-GV-2HA. PIK3R1 was fused to CTEV-2HA. ERBB4 dimerises after stimulation with 10ng/ml EGF-like domain and recruits PIK3R1. Further controls (inset) show the background of the assay. The background of non-stimulated ERBB4/PIK3R1 is about ten times higher than the background of mock transfected cells or cells transfected with TM-GV/UAS-Fluc.

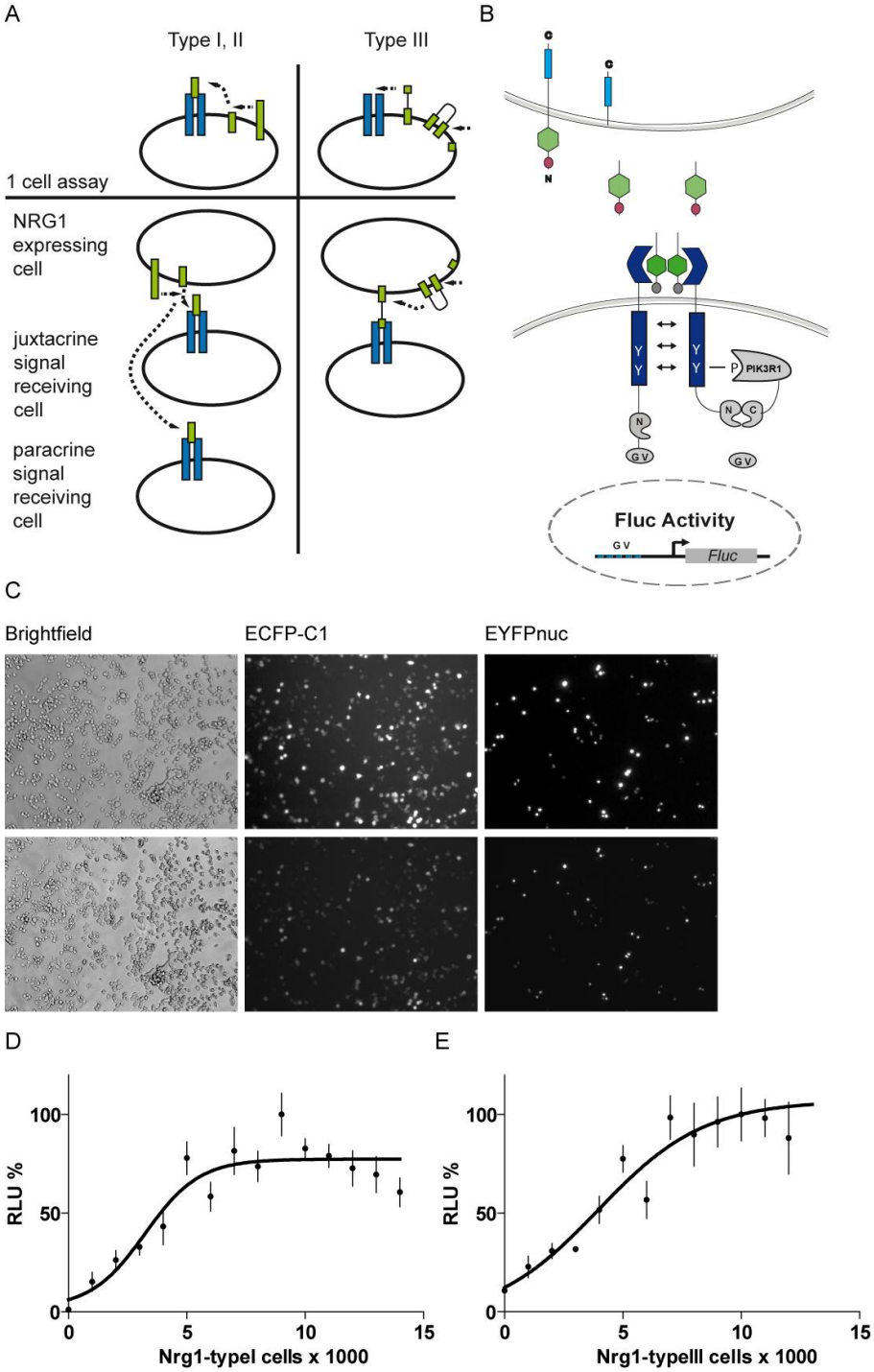

Figure 25: Design of the co-culture assay for the screen

A) Schematic representation of the differences between Nrg1-typeI- and Nrg1-typeIII-mediated signalling in co-culture assays. B) Schematic representation of the co-culture assay. Cell population one expresses Nrg1-typeI. The receiving cell, i.e. cell population two, expresses ERBB4-NTEV-tevS-GV-2HA and PIK3R1-CTEV-2HA. After binding to NRG1-typeI, ERBB4 homodimerises and recruits PIK3R1. TEV protease activity is reconstituted, cleaving at the tevS to release GV. GV translocation to the nucleus results in increasing Fluc activity.C) Microscopic images of the co-culture assay. 40,000 PC12 ERBB4/PIK3R1 cells were transfected with ECFP-C1; 10,000 Nrg1-typeI cells were transfected with EYFPnuc. D) Dose response of the Nrg1-ERBB4 assay using increasing numbers of Nrg1-typeI-expressing cells. E) Dose response of the Nrg1-ERBB4 assay using increasing numbers of Nrg1-typeIII-expressing cells.

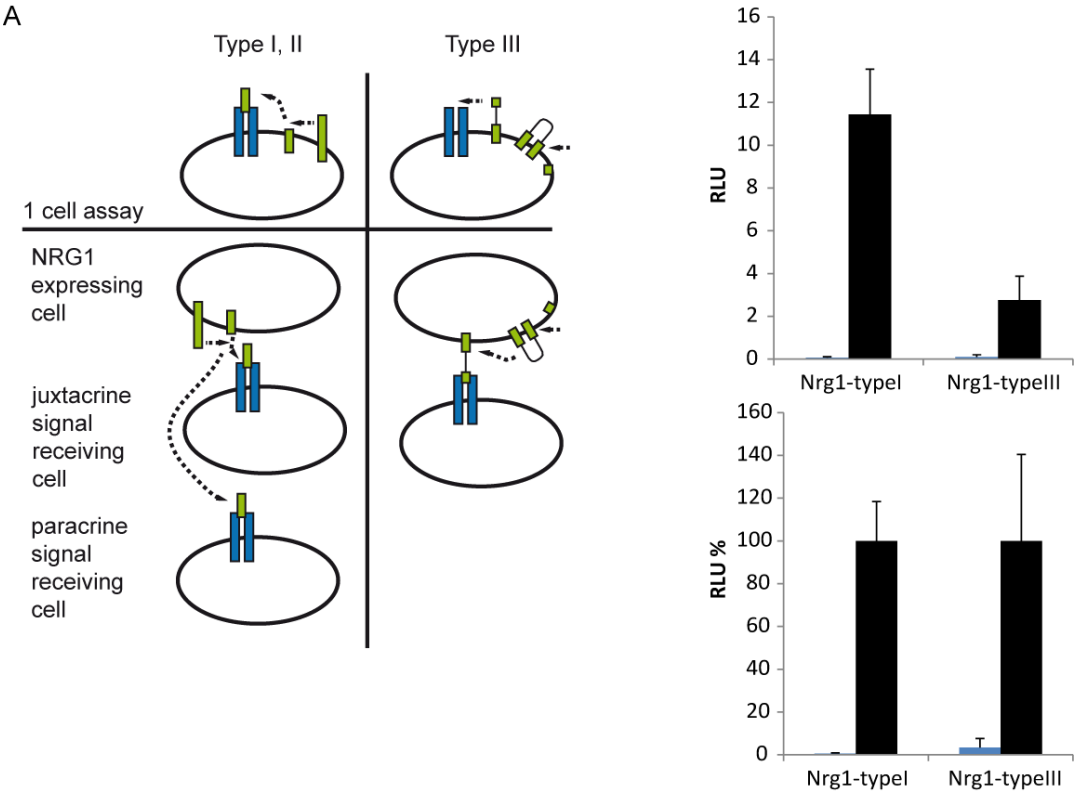

Figure 26: Difference between stimulation with Nrg1-typeI and NRG1-type III stable cell lines

ERBB4/PIK3R1 split TEV assay in PC12 cells. ERBB4 was fused to NTEV-tevS-GV-2HA. PIK3R1 was fused to CTEV-2HA. ERBB4 dimerises after stimulation with indicatednumbers of Nrg1-typeI- or Nrg1-typeIII-expressing PC12 cells, then recruiting PIK3R1.

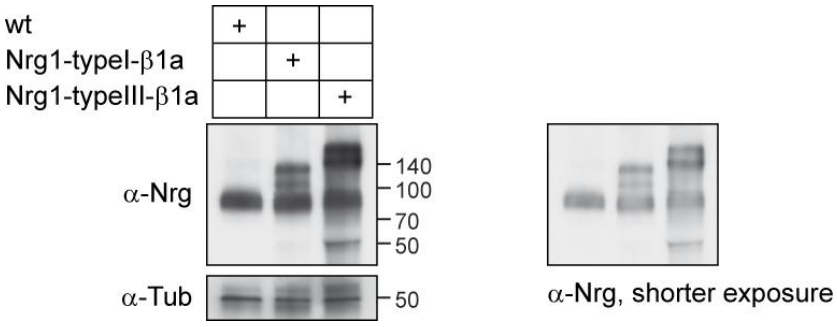

Figure 27: Western blot analysis showing stable expression of, Nrg1-typeI and Nrg1-typeIII in PC12 cells

Stable PC12 cell lines were generated using plasmids V368 (Nrg1-typeI-β1a) and V370 (Nrg1-typeIII-β1a). Plasmids were not linearised before transfection. Co-selection was performed using the Hygromycin-containing plasmid pMSCV-hyg, with a dilution of 1:10 (1 part pMCV-hyg, 9 parts Nrg plasmids) and 100µg/ml hygromycin. Maintenance of stable cells was done with 50µg/ml hygromycin in regular PC12 medium. Western blots were probed with indicated antibodies, α-Nrg targets the β1a tail of Nrg1.

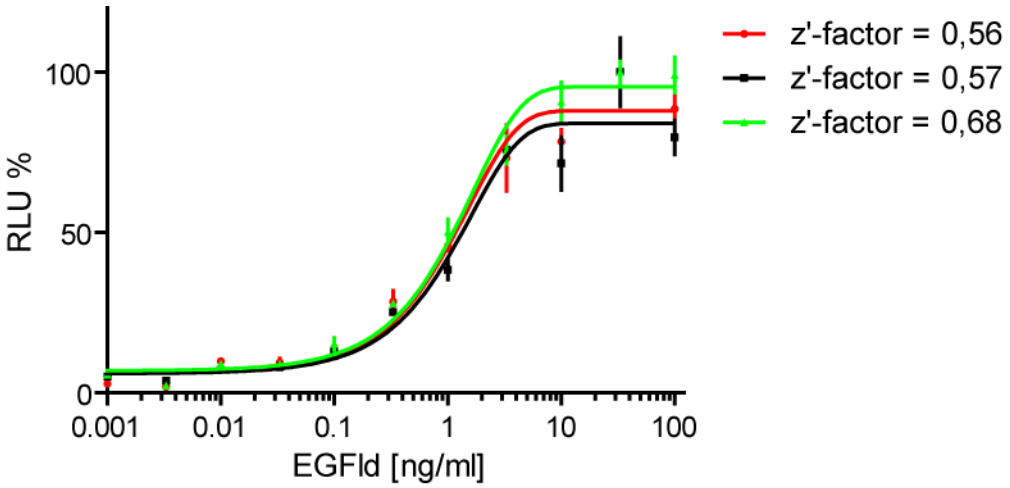

Figure 28: Robustness of the assay

Dose response of the ERBB4/PIK3R1 co-culture assay using increasing amounts of EGF-like domain. Comparison of three plate. ERBB4/PIK3R1 split TEV assay in PC12 cells. ERBB4 was fused to NTEV-tevS-GV-2HA. PIK3R1 was fused to CTEV-2HA.

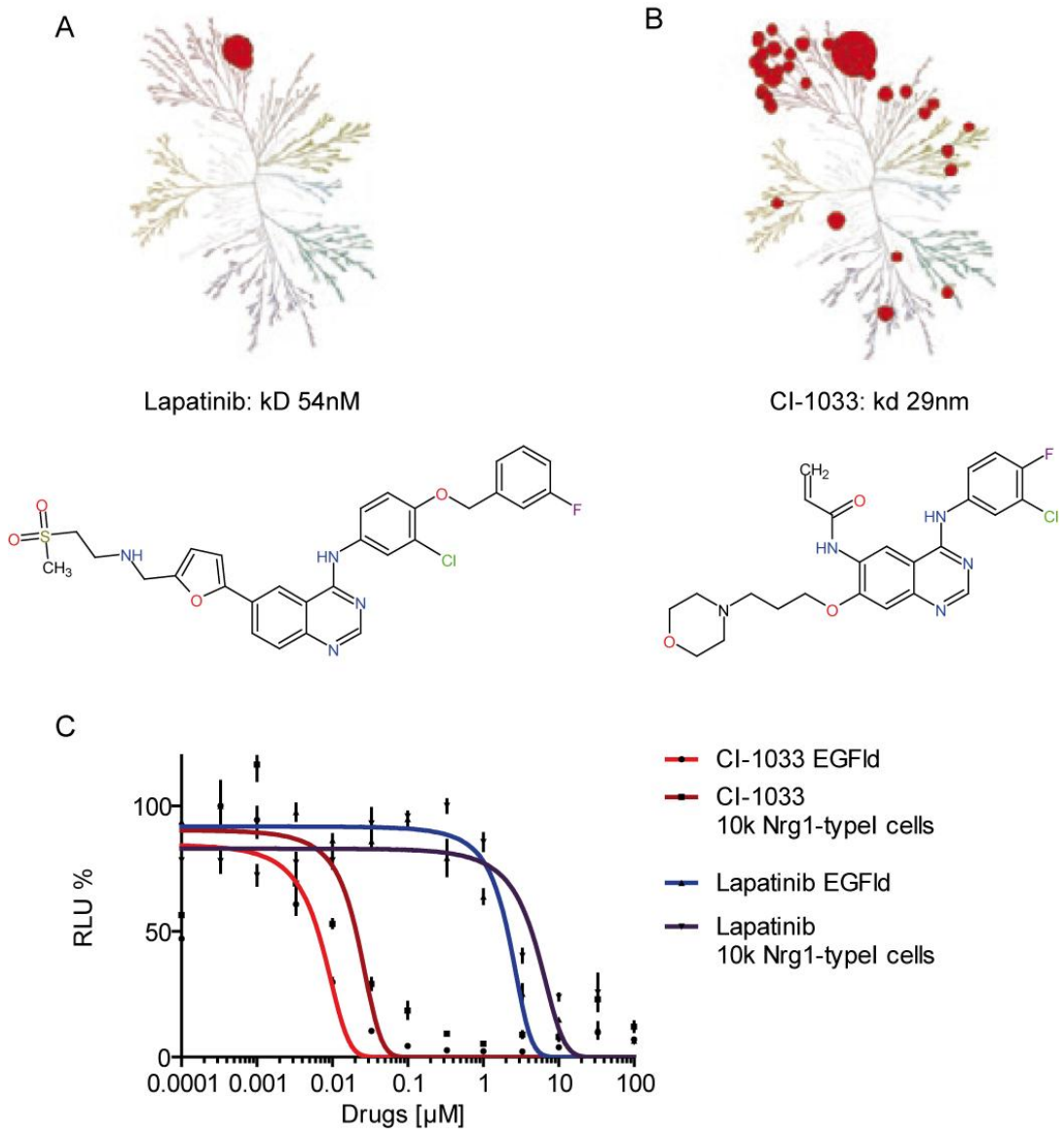

Figure 29: ERBB4 kinase inhibitor controls, Lapatinib and CI-1033

A) Lapatinib is described as an ERBB-specific kinase inhibitor. The image shows the specificity of Lapatinib against the kinases within the human kinome tree (Karaman et al., 2008). The in-vitro kD of Lapatinib on ERBB4 is 54nM. Chemical structure of Lapatinib (Karaman et al., 2008 supplements; Medina and Goodin, 2008). B) CI-1033 is described as a kinase inhibitor not specific to ERBBs. The image shows the specificity of CI-1033 against the kinases within the human kinome tree (Karaman et al., 2008). The in-vitro kD of CI-1033 on ERBB4 is 29nM. Chemical structure of CI-1033 (Karaman et al., 2008 supplements; Slichenmyer and Fry). C) Comparison of the effects of Lapatinib and CI-1033 on the ERBB4/PIK3R1 split TEV assay in PC12 cells. ERBB4 was fused to NTEV-tevS-GV-2HA. PIK3R1 was fused to CTEV-2HA.

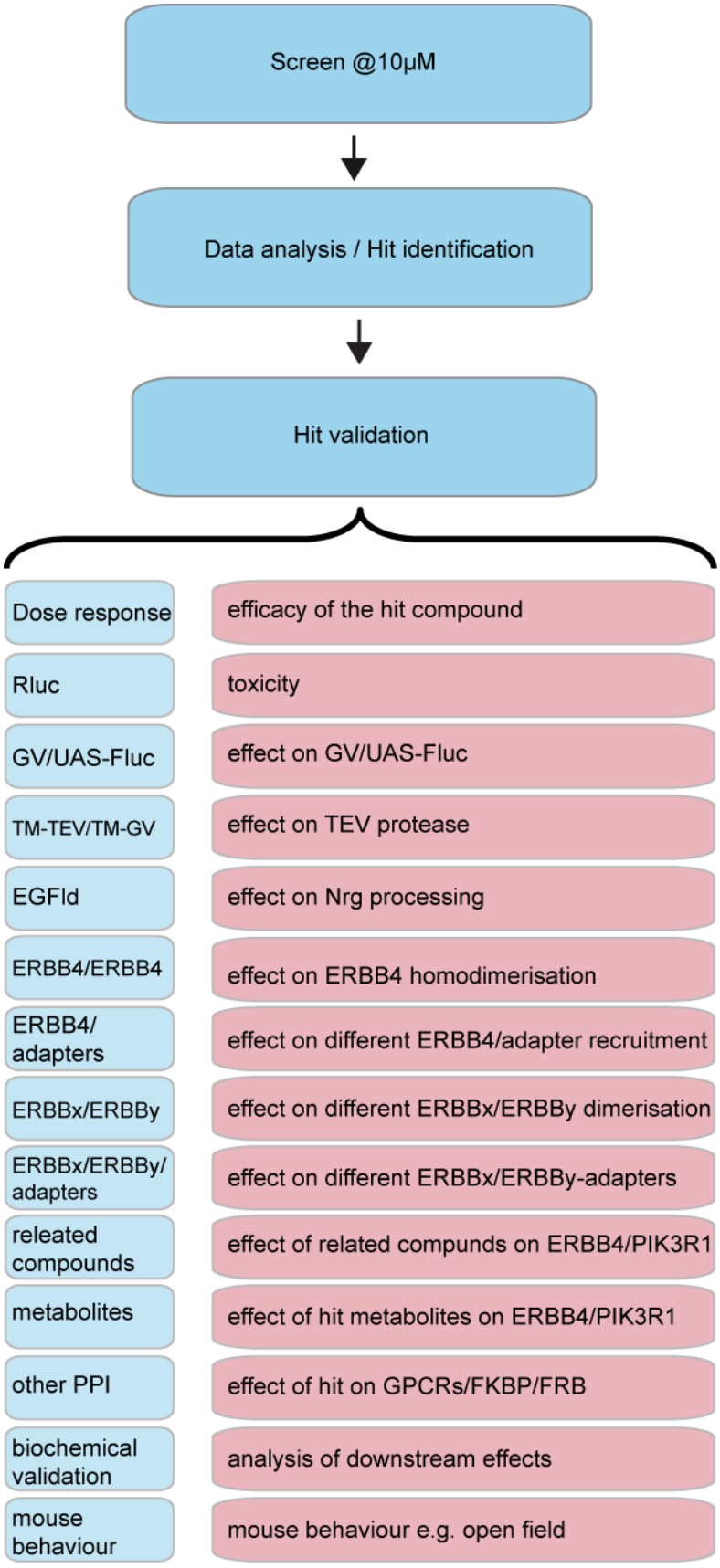
Screen @10µM
Data analysis / Hit identification
Hit validation
Dose response
efficacy of the hit compound
Rluc
toxicity
GV/UAS-Fluc
effect on GV/UAS-Fluc
TM-TEV/TM-GV
effect on TEV protease
EGFld
effect on Nrg processing
ERBB4/ERBB4
effect on ERBB4 homodimerisation
ERBB4/ adapters
effect on different ERBB4/adapter recruitment
ERBBx/ERBBy
effect on different ERBBx/ERBBy dimerisation
ERBBx/ERBBy/ adapters
effect on different ERBBx/ERBBy-adapters
releated compounds
effect of related compunds on ERBB4/PIK3R1
metabolites
effect of hit metabolites on ERBB4/PIK3R1
other PPI
effect of hit on GPCRs/FKBP/FRB
biochemical validation
analysis of downstream effects
mouse behaviour
mouse behaviour e.g. open field

5.3 The NCC201 screen

The NCC201 library was screened according to the described parameters. 5,000 (Figure 30) and 10,000 (Figure 31) PC12 Nrg1-typeI cells were used for the stimulation. A z'-factor of >0.5 was obtained when full activation was triggered using EGF-like domain and inhibition using Lapatinib and CI-1033. Both screens resulted in one putative activator and one putative inhibitor. The inhibitor was identified to be Spironolactone. It causes a highly significant decrease of the luciferase activity in the screen ($p < 0.0001$). The activator was identified to be Albendazole. It causes a highly significant increase in luciferase activity ($p < 0.0001$). Both hits were recovered from both types of screens, either run with 5,000 or 10,000 Nrg1-typeI-expressing PC12 cells. In addition, both hits showed no toxic effect in the GV-UAS-Fluc technical control screen.

The inhibitor Spironolactone is also found in a screen stimulated to maximum levels using the EGF-like domain, indicating a strong effect of the drug towards ERBB4 receptor activation, but not Nrg1-typeI processing as the EGF-like domain already represents a form that is most possibly reduced in structure but retains highest biological activity of Nrg1 (Figure 33).

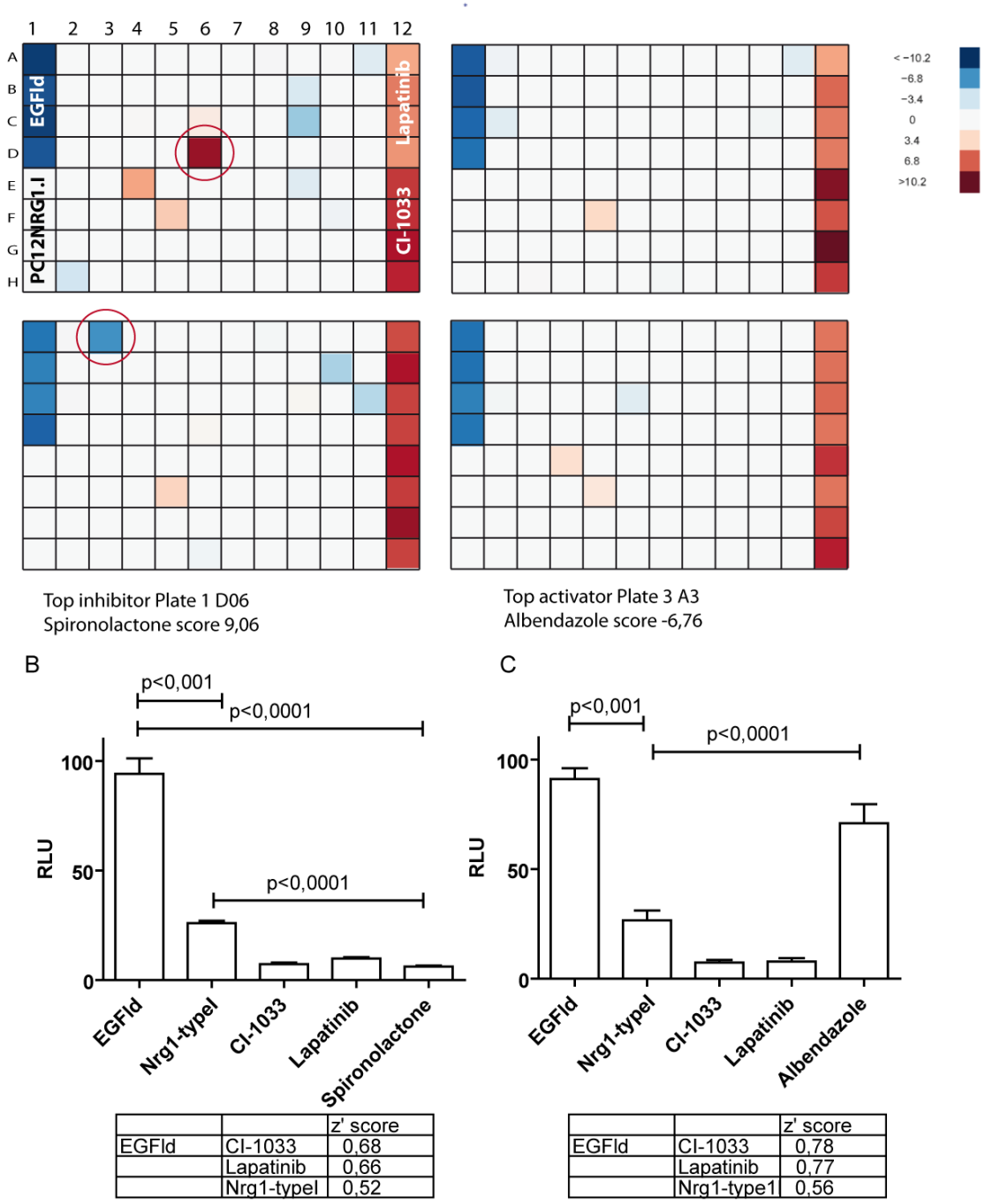

		z' score
EGFld	CI-1033	0,68
	Lapatinib	0,66
	Nrg1-typeI	0,52

		z' score
EGFld	CI-1033	0,78
	Lapatinib	0,77
	Nrg1-type1	0,56

Figure 30 Screen of the NCC201 library

A) ERBB4/PIK3R1 split TEV based screening assay in PC12 cells. ERBB4 was fused to NTEV-tevS-GV-2xHA; PIK3R1was fused to CTEV-2HA. ERBB4 dimerises after stimulation with 5.000 Nrg1-typeI cells and recruit PIK3RI. Cells were further stimulated with EGFld (10ng/ml), Lapatinib (10µM), CI-1033 (0.1µM), or 80 different compounds (see plate design). Luciferase data was analysed using tinR (see script in the methods). B) Extracted data from the screen showing the significance of the effect of the top inhibitor Spironolactone. C) Extracted data from the screen showing the significance of the effect of the top activator Albendazole (Two paired, two sided TTest).

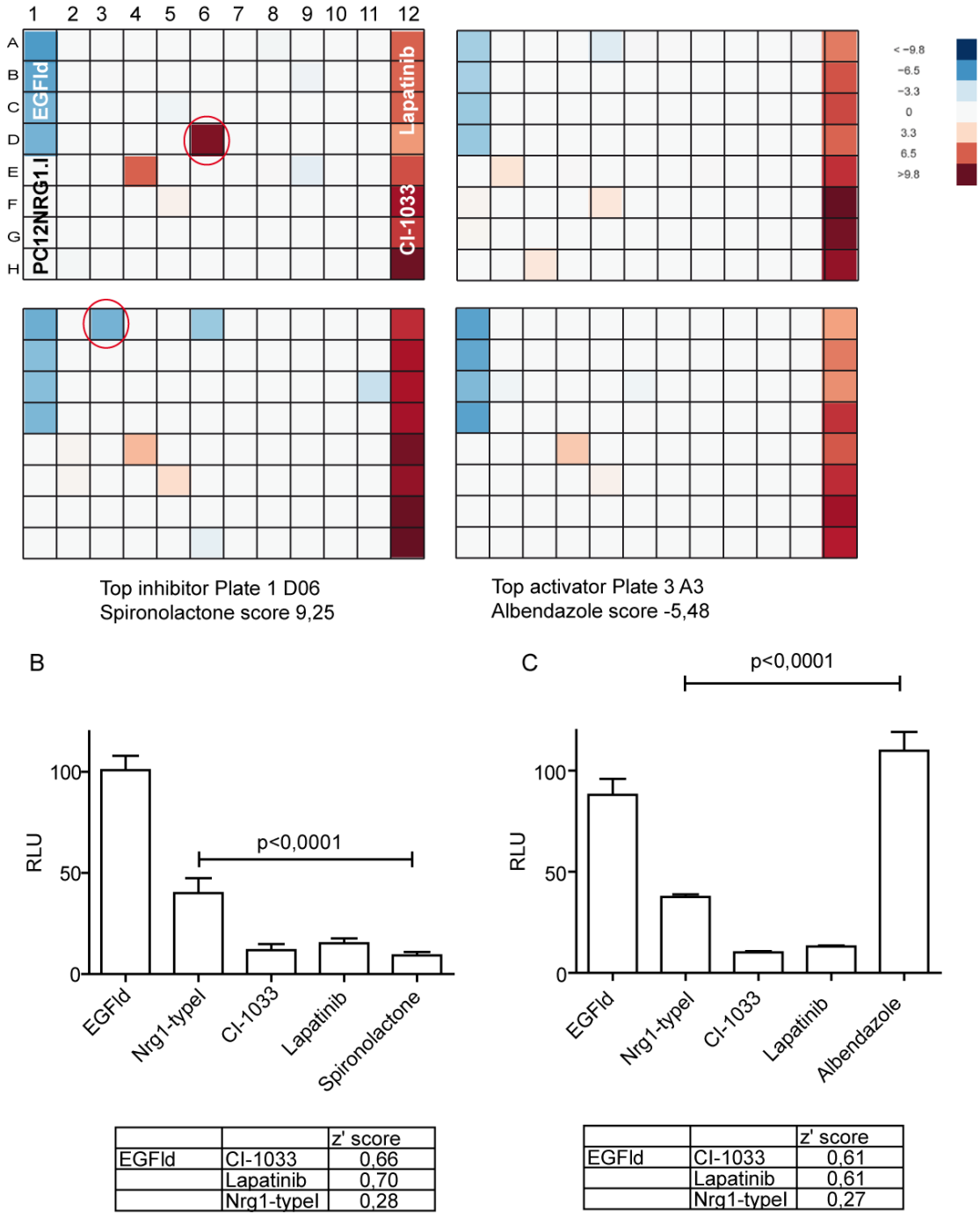

		z' score
EGFld	CI-1033	0,66
	Lapatinib	0,70
	Nrg1-typeI	0,28

		z' score
EGFld	CI-1033	0,61
	Lapatinib	0,61
	Nrg1-typeI	0,27

Figure 31: Screen of the NCC201 library 10k Nrg1-typeI cells

A) ERBB4/PIK3R1 split TEV based screening assay in PC12 cells. ERBB4 was fused to NTEV-tevS-GV-2xHA; PIK3R1was fused to CTEV-2HA. ERBB4 dimerises after stimulation with 10.000 Nrg1-typeI cells and recruit PIK3RI. Cells were further stimulated with EGFld (10ng/ml), Lapatinib (10µM), CI-1033 (0.1µM), or 80 different compounds (see plate design). Luciferase data was analysed using tinR (see script in the methods). B) Extracted data from the screen showing the significance of the effect of the top inhibitor Spironolactone. C) Extracted data from the screen showing the significance of the effect of the top activator Albendazole (Two paired, two sided TTest).

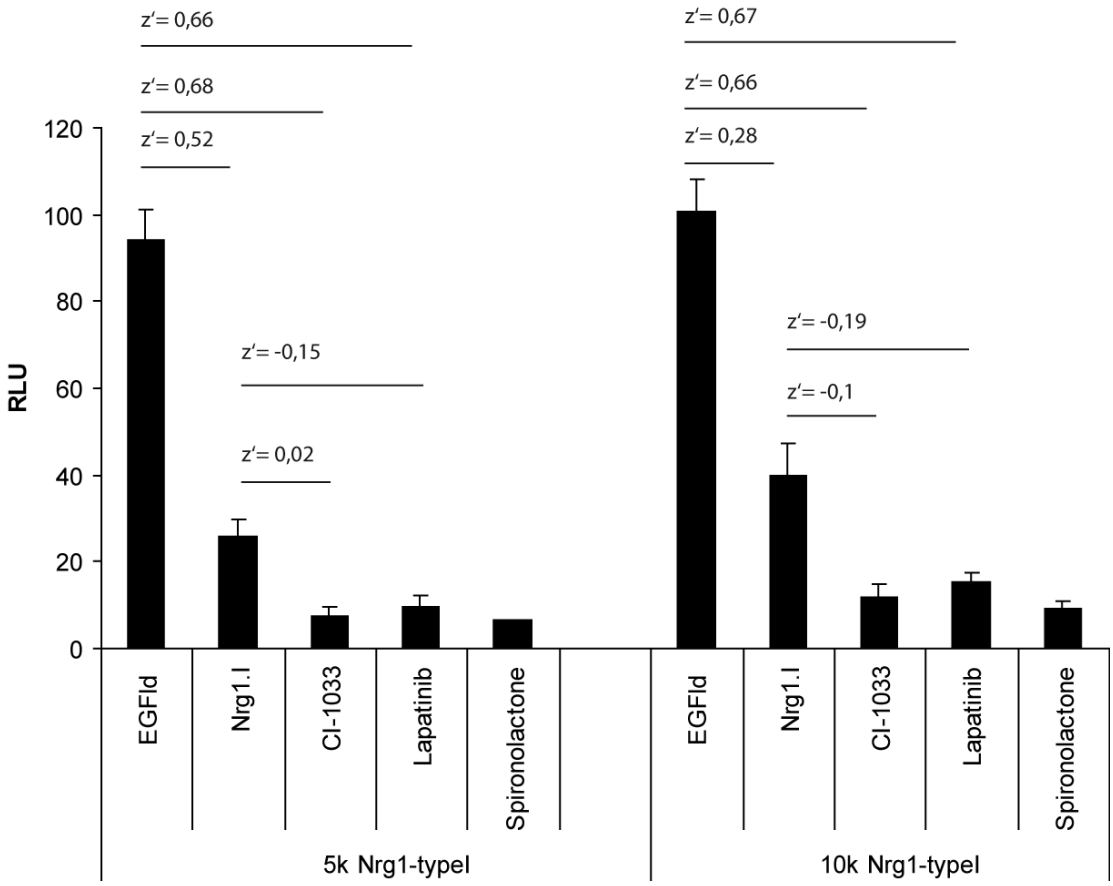

Figure 32: Detailed analysis of the functionality of the screen

Z'-factors between the different activated and inhibited states of the assay.

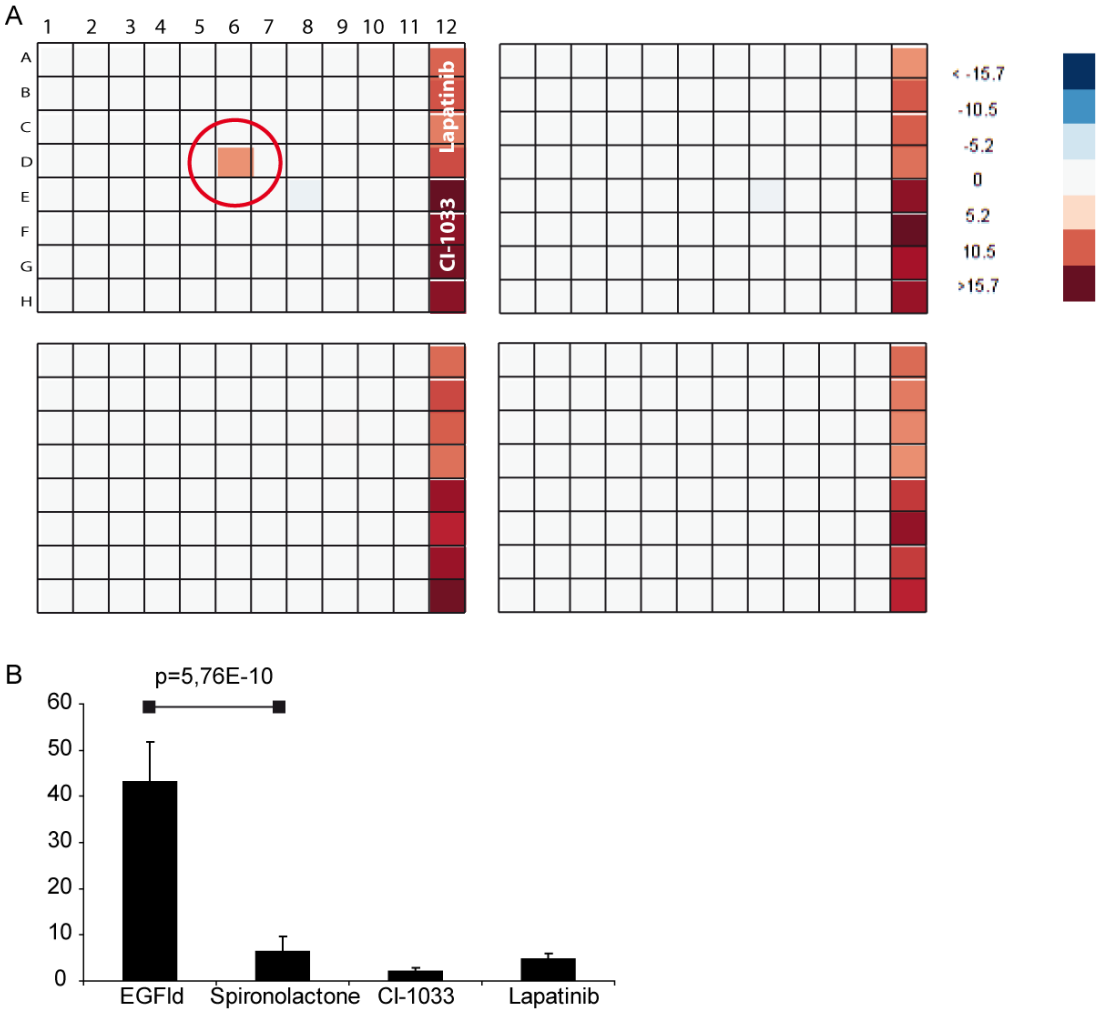

Figure 33: Counter-screen of the NCC201 library with EGF-like domain

A) ERBB4/PIK3R1 split TEV based screening assay in PC12 cells. ERBB4 was fused to NTEV-tevS-GV-2xHA; PIK3R1was fused to CTEV-2HA. ERBB4 dimerises after stimulation with 10ng/ml EGFld and recruit PIK3RI. Cells were further stimulated with Lapatinib (10µM), CI-1033 (0.1µM), or 80 different compounds (see plate design). Luciferase data was analysed using tinR (see script in the methods). B) Extracted data from the screen showing the significance of the effect of the top inhibitor Spironolactone.

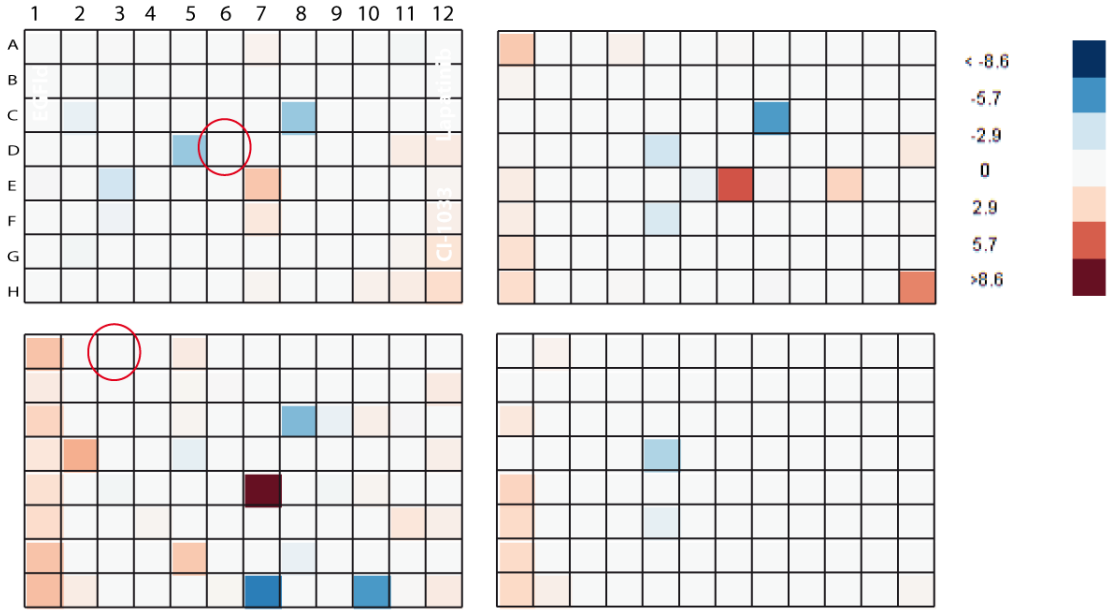

Plate 1 D06 Spironolactone
Plate 3 A03 Albendazole

Figure 34: Counterscreen of the NCC201 library with GV

PC12 cells were transfected with GV and stimulated with Lapatinib (10µM), CI-1033 (0,1µM), or 80 different compounds (see plate design). The red circles show that now effect on the UAS-firefly luciferase is measured with the indicated hits Spironolactone and Albendazole.

5.4 The NCC003 Screen

The NCC003 library was screened according to the described parameters. 10,000 PC12 Nrg1-typeI cells were used for the stimulation. A z'-factor of > 0.5 was obtained when using EGFld for activation and the Lapatinib and CI-1033 for inhibition. From this part of the library, Topotecan showed the strongest inhibiting effect.

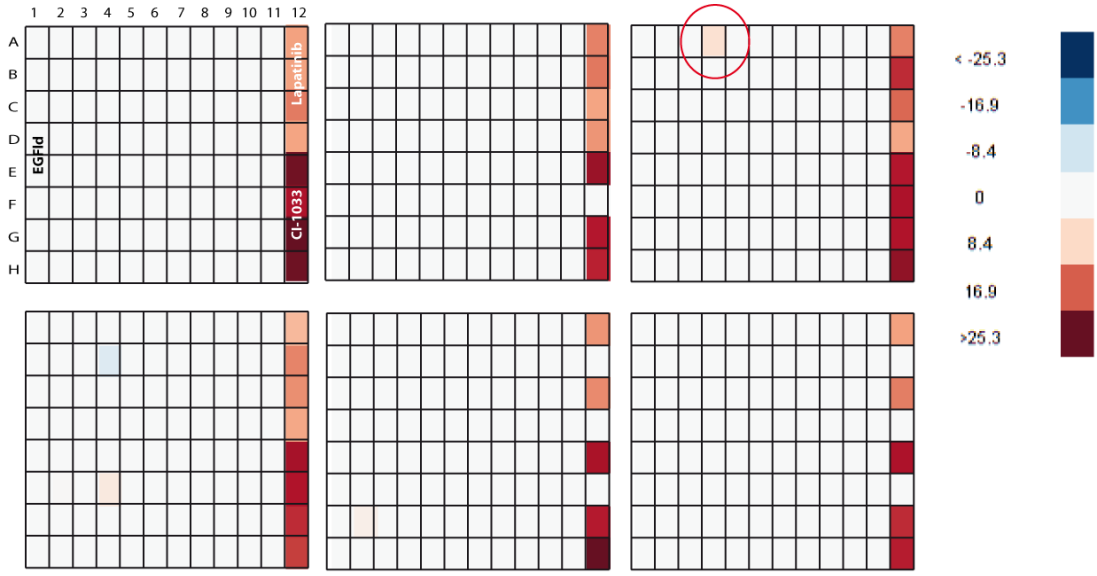

Figure 35: NCC003 screen

Split TEV-based screening assay in PC12 cells. ERBB4 was fused to NTEV-tevS-GV-2HA. PIK3R1 was fused to CTEV-2HA. The complete assay was stimulated with 10ng/ml EGFld. Lapatinib and CI-1033 are used as negative controls and inhibit kinase activity with a concentration of 10µM for Lapatinib and 0.1µM for CI-1033 (12A-H). Topotecan is highlighted by a red circle (top right panel).

5.5 Hit validation

From the NCC201 screen, two hits were recovered, the putative activator Albendazole and the putative inhibitor Spironolactone. From the NCC003 screen, one hit was recovered, the putative inhibitor Topotecan. During the development of the co-culture screen a couple of interesting substances showed alterations in the firefly activity, with minor statistical significance. These substances were chosen to test the validity of the validation concepts

.

Name	Location	Putative function
Spironolactone	NCC201 P1 D7	Inhibitor
Albendazole	NCC201P3 A3	Activator
Topotecan	NCC003 P3 A4	Inhibitor
Vincristine	NCC003 P6 B02	Inhibitor
Mevastatin	NCC003 P6 H4	Inhibitor
CCPA	NCC003 P6 B6	Activator
K252a test substance	Paper (Kuai et al. 2010)	Activator

Table 12: overview of candidate hits recovered from the screen (italics) and additionally validated substances

The hit validation is separated into three parts, named (I) vertical, (II) horizontal and (III) orthogonal validation.

(I) The vertical validation addresses at what level of the signalling cascade a candidate might be acting. In the co-culture assay, I tested whether the substance interfered with the localisation and processing of Nrg1, the binding of Nrg1 to the ERBB receptors, the homodimerisation of the receptors, the auto-phosphorylation of the receptors, the adaptor recruitment to the receptor, and all artificial components of the assay.

(II) The horizontal validation examines the specificity of the substances on Nrg1-ERBB4 signalling. Different forms of NRG1-typeI, different homo and heterodimers of ERBB receptors, and different adapters of the ERBB system can be tested, resulting in more than 200 potential combinations to test.

(III) The orthogonal validation can be sub-divided further. First, the hit substances' effects on the downstream signalling cascades were addressed using other methods, such as phospho-specific antibodies. Second, the candidates were tested in split TEV assays using related (i.e. other receptors, such as the GPCR HTR5A) and unrelated interaction partners (i.e. the model

interaction of FRB and FKBP. Third, hit compounds were searched for structurally closely related substances, and their effects on the ERBB4/PIK3R1 co-culture assay were then analysed. Finally, first attempt towards the in vivo validation of the primary hit Spironolactone in a mouse model were undertaken.

5.6 Spironolactone

Spironolactone is a synthetic, steroid like drug, which targets primarily the mineralocorticoid receptor (MCR), but it has also anti-androgen and progesterone properties. It acts as a competitive MCR antagonist (e.g. Aldosterone receptor).

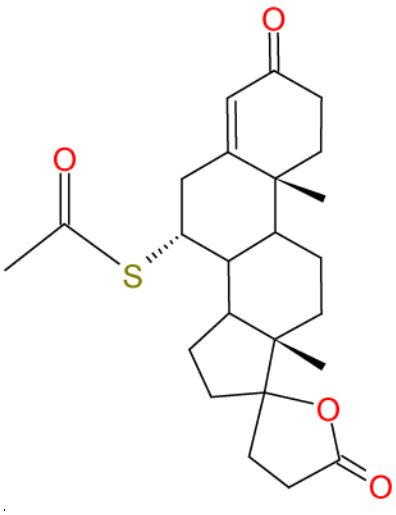

Figure 36: Spironolactone

The MCR is a cytosolic receptor bound to HSP90 proteins. After Aldosterone binding HSP90 proteins are released, causing the MCR to homodimerise and to translocate to the nucleus, where the MCR binds hormone response elements (Fuller et al., 2012; Pippal and Fuller, 2008). It has been shown that a Spironolactone-bound MCR does not translocate to the nucleus, as this inhibits the dimerisation of the receptor (Grossmann et al., 2012). A BRET study showed that a Spironolactone-bound MCR does not homodimerise, in contrast to a Aldosterone-bound MCR (Grossmann et al., 2012).

Spironolactone is used as diuretic, antihypertensive, and anti-androgen (Ogden et al., 1961). The known target profile of Spironolactone has been reported to include a much broader spectrum than the MCR only. To date, the following pharmacological inhibition or activation of the following receptors have been described (Fagart et al., 2010):

Receptor	**IC_{50}**
Mineralocorticoid receptor	24nM
Androgen receptor	77nM
Glucocorticoid receptor	2.42µM
Progesterone receptor	0.74µM

Table 13. IC_{50} values of various targets of Spironolactone (Fagart 2010)

The half-life of Spironolactone is difficult to determine (Brittain, Analytical Profiles of Drug Substances and Excipients). It is rapidly metabolised in the liver, and more than 17 metabolites were isolated from humans. It is unclear whether one or more of these metabolites are responsible for the effects observed in pharmacological studies. Spironolactone also was reported to

mildly deteriorate depressive behaviour when combined with the anti-depressant drug amitriptyline (Holsboer, 1999).

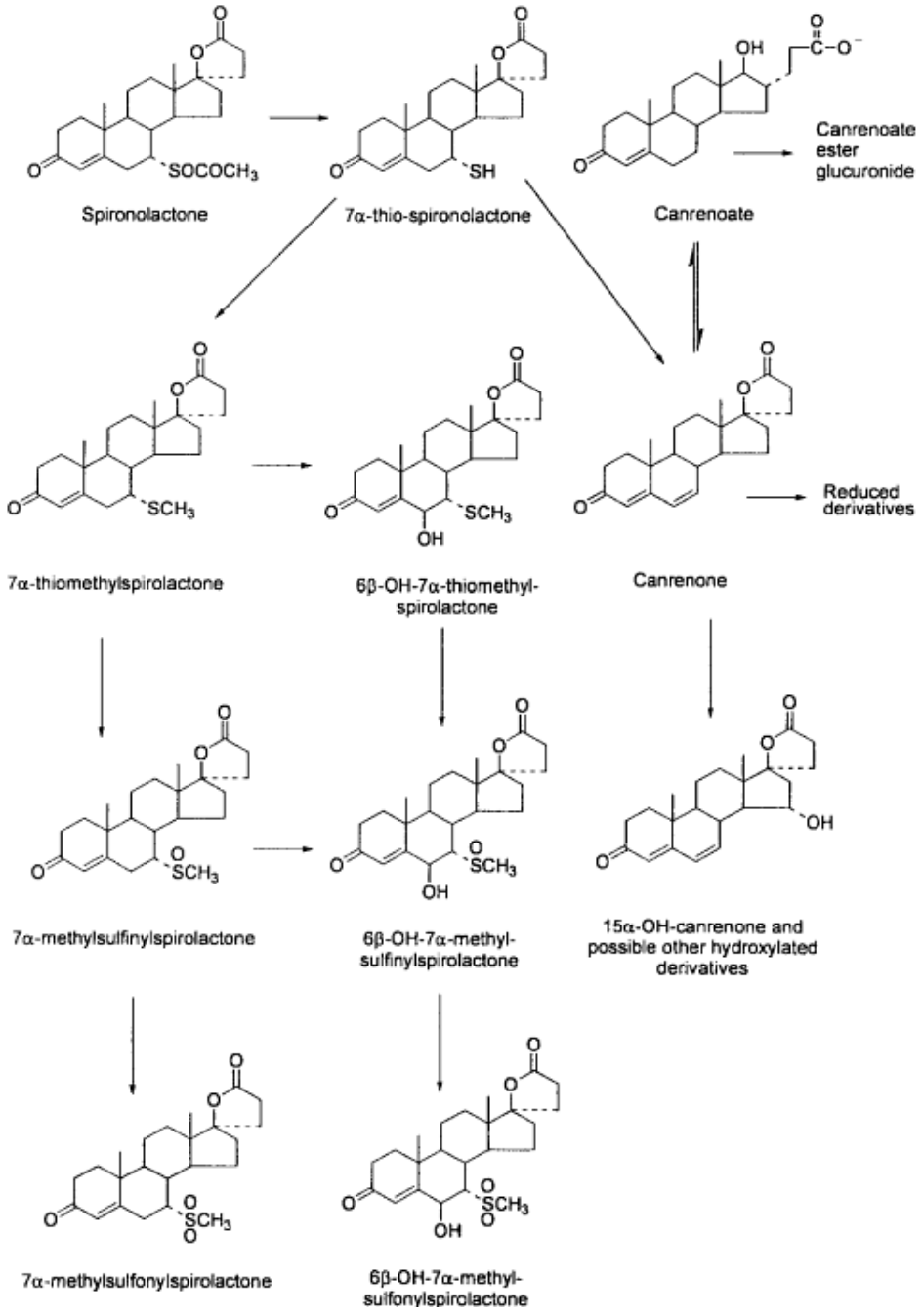

Figure 37: Map Spironolactone metabolites

Spironolactone is processed in the liver and metabolised into 17 metabolites. It is speculated that these metabolites also have an effect on the MCR, and may have other unknown functions as well. It is not known whether the structural integrity of Spironolactone is kept in a co-culture assay without liver processing (Analytical Profiles of Drug Substances and Excipients 2002 Harry G. Brittain).

In the screens performed, Spironolactone was found to decrease Nrg1-ERBB4 signalling with varying but consistent levels (5,000 and 10,000 PC12 Nrg1-typeI cells). Spironolactone was further validated in the secondary screening process where 10ng/ml EGF-like domain was used to stimulate ERBB4 signalling. The GV control screen showed that Spironolactone is not toxic for the cells at screening concentrations.

Next, possible modes of actions for Spironolactone were analysed. To do this, a vertical validation approach was used that addressed the pathway from upstream to downstream components including technical controls. In addition, a horizontal validation approach was initiated to investigate potential functions for other NRG isoforms, ERBB receptors, and adapter molecules, such as GRB2 and SHC1.

5.6.1 Vertical validation for Spironolactone

An inhibitory dose response assay was established for Spironolactone. The dose response to increasing concentrations of Spironolactone in the Nrg1-typeI-ERBB4/PIK3R1 co-culture assay showed an IC50 of 0.9 µM (

Figure 38**).**

5.6.2 Technical controls for Spironolactone validation

5.6.2.1 *Renilla* luciferase

TK-Rluc reported the toxicity of Spironolactone. Spironolactone is toxic for the cells in this assay at concentrations at an IC_{50} of 56.4µM. Figure 39

5.6.2.2 The Gal4-VP16 control assay

In a first technical control assay, UAS-Fluc was co-transfected with GV only. This setup showed the effect of Spironolactone on the GV/UAS reporter system and the firefly luciferase. The IC_{50} of Spironolactone in this assay is at a concentration of 10.7µM (Figure 39).

5.6.2.3 TEV protease control assay

To correct for any effects elicited by the TEV protease and its activity at TEV protease cleavage sites, a transmembrane version of the TEV protease (TM-TEV) was co-transfected with a transmembrane-bound GV carrying an internal TEV cleavage site (TM-GV), along with UAS-Fluc and Rluc reporters. The IC_{50} for Spironolactone in this constitutively activated TEV protease assay was determined to be at a concentration of 24.3µM. When comparing this IC_{50} value with the one obtained from the GV control assay (IC_{50}, 10.7µM),

I can conclude that Spironolactone most likely has no effect on TEV protease activity (Figure 39).

5.6.2.4 1-cell assay with soluble Nrg1-EGF-like domain

To test whether the Spironolactone effect is targeted against Nrg1-typeI expression or processing, the Nrg1-typeI-expressing PC12 cells were exchanged for the soluble EGF-like domain. The EGF-like domain was used as a surrogate for any processed Nrg1 isoforms. The replacement of Nrg1-typeI with EGF-like domain showed no functional differences in the performance of the assay, suggesting that Spironolactone does not target full length Neuregulin processing and activity (Figure 39).

The adapter proteins PIK3R1 and SRC are primarily targeted by Spironolactone

The effect of Spironolactone on the recruitment of various other adapter proteins was analysed. In the split TEV-based assay, SHC1, STAT5A and GRB2 showed an IC_{50} of roughly 5µM, SRC and PIK3R1 displayed an IC_{50} of about 0.7µM Spironolactone. These data suggest that in particular the binding of the adapter molecules PIK3R1 and SRC to the ERBB4 receptor is inhibited by Spironolactone (Figure 40, Figure 41).

5.6.3 Horizontal validation

Dimerisations of the ERBB receptor family

5.6.3.1 ERBB4 receptor dimerisations

A prerequisite for ERBB4 receptor activation is the dimerisation with itself or ERBB2, which is the preferred partner for all ERBB receptors. Therefore, split TEV assays were setup consisting of an ERBB4-NTEV-tevS-GV co-transfected with either ERBB2-CTEV or ERBB4-CTEV. Efficient activation was tested using EGF-like domain (Figure 42,Figure 43), followed by dose-response analyses for Spironolactone on the ERBB2/4 heterodimerisation and ERBB4 homodimerisation. The ERBB2/4 dimerisation yielded an IC_{50} 2.2µM, and the ERBB4 homodimerisation showed an IC_{50} of 2.4µM Spironolactone.

5.6.3.2 ERBBx/ERBBy

In addition, a complete panel of ten different ERBB receptor homo- and heterodimers stimulated with 10ng/ml EGF-like domain was measured. All combinations tested showed an IC_{50} of 2.2µM to 9.2µM Spironolactone (see table 14 below). A comparison to the ERBB4/PIK3R1 assay clearly showed a bias towards a selective inhibition for the adapter assay involving PIK3R1 (Figure 42).

5.6.3.3 ERBB2/ERBB4 dimerisation and adapters

To get further insight of Spironolactone's specificity towards the potential inhibition of ERBB2 and ERBB4, the adapter recruitment for ERBB2/4 heterodimers was analysed. The adapter recruitment of ERBB2/ERBB4 showed IC_{50} values between 0.6µM and 1.7µM (Figure 46).

5.6.3.4 ERBB2/ERBB3 dimerisation and adapters

Likewise, the adapter recruitment for ERBB2/3 heterodimers was measured. The analysis showed IC_{50} values between 0.5µM and 0.9µM. The comparison of the datasets obtained with ERBB2/3 and ERBB2/4 indicates that the effect of Spironolactone is not ERBB4-specific, but also inhibits ERBB3-mediated adaptor recruitment assays Figure 45.

5.6.3.5 ERBB4/PIK3R1 assay and effects caused by other Aldosterone derivatives

To get further insight into Spironolactone's specificity, the data from the NCC201 and the NCC003 screens were analysed for Aldosterone derivatives and structures related to Spironolactone. 25 structural related drugs were

identified. None of these drugs showed a similarly efficient inhibitory effect on the ERBB4/PIK3R1 co-culture assay (Figure 49)

5.6.3.6 ERBB4/PIK3R1 assay and effects caused by Eplerenone and Canrenone

Eplerenone, the second generation substance of Spironolactone used in the clinics, was also tested in the ERBB4/PIK3R1 assay stimulated with EGF-like domain. Eplerenone is structural and functional closely related to Spironolactone but did not show any effect in the ERBB4/PIK3R1 assay (Figure 48).

Canrenone, a metabolite of Spironolactone lacking the thioketone group was also tested in a similar ERBB4/PIK3R1 assay and showed also no specific inhibiting effect (Figure 48).

The analysis of Eplerenone and the Aldosterone derivatives suggests that the measured effect is Spironolactone-specific and not a general side effect caused by other MCR antagonists or Aldosterone derivatives (Figure 49).

5.6.4 Orthogonal validation

5.6.4.1 ERBB1/ERBB1/EGF

Spironolactone showed an effect on EGF-stimulated ERBB1/ERBB1 homodimerisation, with an IC_{50} of 1.1µM Spironolactone (Figure 50).

To address whether Spironolactone is specific to the inhibition of ERBB receptor-mediated signalling, I tested Spironolactone's effect in various other split TEV assays that also included the regulated activation of a G-protein-coupled receptor (GPCR).

5.6.4.2 GPCR Serotonin receptor 5A (HTR5A) activation

Spironolactone showed no effect on the Serotonin-stimulated HTR5A-β-arrestin (ARRB2) split TEV assay (Figure 51).

5.6.4.3 FRB/FKBP model interaction induced by Rapamycin

Spironolactone showed a minor effect on the Rapamycin-induced FRB/FKBP interaction, with an IC_{50} of 18.8µM (Figure 52).

5.6.5 Summary IC_{50} validation Spironolacone

			IC_{50} in µM
	Rluc		56.4
	GV		10.7
TM-TEV	TM-GV		24.3
NTEV-tevS-GV	**CTEV**		**IC_{50} in µM**
ERBB4	ERBB4		2.4
ERBB3	ERBB4		4.4
	ERBB3		3.1
ERBB2	ERBB4		2.2
	ERBB3		3.2
	ERBB2		9.2
ERBB1	ERBB4		4.3
	ERBB3		2.9
	ERBB2		5.8
	ERBB1		6.0
V5 tag	**NTEV-tevS-GV**	**CTEV**	**IC_{50} in µM**
	ERBB4	SHC1	4.9
		GRB2	4.8
		SRC	0.7
		PIK3R1	0.7
		STAT5A	4.6
ERBB2	ERBB3	SHC1	0.9
		GRB2	0.6
		SRC	0.9
		PIK3R1	0.5
		STAT5A	0.7
ERBB2	ERBB4	SHC1	0.8
		GRB2	0.8
		SRC	1.8
		PIK3R1	0.8
		STAT5A	0.7
NTEV-tevS-GV	**CTEV**	**Drug**	
ERBB1	ERBB1	EGF	1.1
ERBB4	PIK3R1	co-culture assay	0.9
ERBB4	PIK3R1	Eplerenone	n.c.
ERBB4	PIK3R1	Canrenone	n.c.
FRB	FKBP	Rapamycin	18.8

Table 14. Summary of IC_{50} values

These data suggest that Spironolactone affects the complete family of ERBB receptors, with a biased activity profile towards more efficient inhibition of adapter recruitment, particularly PIK3R1 and SRC.

5.6.6 Biochemistry

The biochemical, or orthogonal, validation of Spironolactone compared to Lapatinib showed the following effects:

Antibody	Lapatinib	Lapatinib / EGFld	Spironolactone	Spironolactone / EGFld
ERBB4 (Buonanno)				
ERBB4 (Santa Cruz)		activated		partial degradation
pERBB4 Y1284 (SHC)		inhibited		
pERBB4 Y1056(PIK3)		inhibited		partially inhibited
pERBB4 Y984 (STAT5A)		inhibited		
S6K				
pS6K		inhibited		
ERK1				
pERK1 T202/Y204	inhibited	inhibited		

Table 15. Results of the biochemical validation using phospho-specific antibodies

The validation shows a clear difference between Lapatinib and Spironolactone effects. Lapatinib inhibits the phosphorylation at the three adapter docking sites Y1284 (SHC1), Y1056 (PIK3R1), and Y984 (STAT5A). Spironolactone has only a mild effect on the phosphorylation at the PIK3R1 docking site Y1056.

Lapatinib inhibits phosphorylation of ERK1 independent of EGF-like domain stimulation. Spironolactone, however, has no effect on the phosphorylation levels of ERK1.

The data suggests a difference in the mode of action of Spironolactone and the Lapatinib (Figure 54).

5.6.7 Validation in HEK293 cells

Western blot analysis on HEK293 cell lysates using phospho-specfic antibodies showed a similar effect of Lapatinib and Spironolactone on the phosphorylation levels of ERBB4 at Y1284 (Figure 53).

5.6.8 Validation in a MK801 mouse model of psychosis

MK801 is an antagonist of the NMDA-type Glutamate receptor and has been shown to induce psychosis/schizophrenia-related behaviours including hyperactivity in rodents when applied experimentally (Eyjolfsson et al., 2006). The mode-of-action of MK801 is unclear but it has been suggested to act mainly on NMDA receptors located on interneurons thereby altering the balance of excitation and inhibition (Figure 20).Thus, MK801 and the Nrg1-ERBB4 signalling may modulate similar cellular circuits affected in psychiatric diseases. To assess the potential impact of the novel Nrg1-ERBB4 inhibitor spironolactone on mouse behaviour, we applied the MK801 model of drug-induced psychosis.

Mice were administered with drugs following the protocol depicted in (Figure 55 A). Their locomotor behavior in the open field, i.e. distance travelled, time which mice spent active, time spent in the centre of the test arena, and the number of rearings were analysed (Figure 55 B-F). For the analysis shown, only the time between the second injection until 60 min post injection has been taken into account, as effects are strongly attenuated later on.

MK801-treated animals showed a hyperactivity phenotype compared to controls. Mice treated with Spironolactone displayed a tendency towards less distance travelled (Figure 55 B). Interestingly, mice treated both with MK801 and Spironolactone showed a non-significant tendency towards less distance travelled compared to mice injected with MK801 only.

When the total locomotor behaviour was analysed, the non-significant tendency observed in doubly-injected mice was not visible (Figure 55 C).

Of interest, mice injected with Spironolactone only spent less time being active (Figure 55.D), and also spent less time in the centre of the open field arena compared to a control group (Figure 55 E). As reported before, MK801-injected mice displayed readily a higher activity than controls, and spent only a little amount of time in the centre. Double-treated mice, however, showed only a non-significant tendency towards less activity, and also spent only a very low percentage of the time in the centre of the test arena (Figure 55 E).

Last, I looked at rearings to assess curiosity. However, the analysis showed no significant measure compared to controls (Figure 55 F).

Taken together, our results suggest that Spironolactone reduces spontaneous locomotor activity in the open field test as adding Spironolactone on top of a MK801 treatment may lead to slightly attenuated properties on mouse behavior.

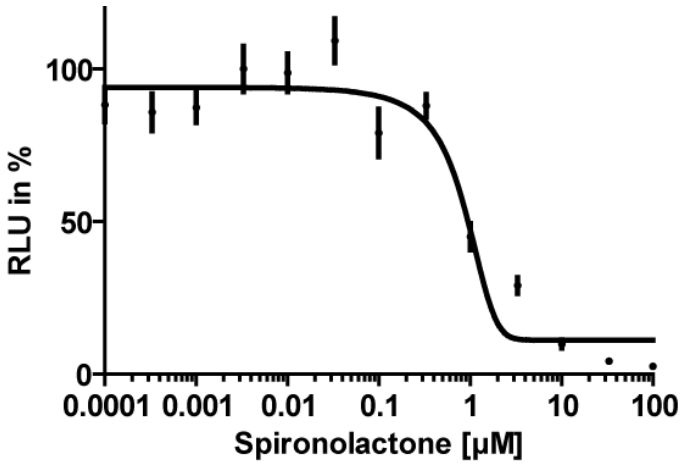

Figure 38: Dose Response of SpironolactoneSplit TEV assay in PC12 cells.

ERBB4 was fused to NTEV-tevS-GV-2xHA; PIK3R1 was fused to CTEV-2HA. ERBB4 dimerises after stimulation with 10.000 NRG1-Type I PC12 cells and recruits PIK3R1. Cells were treated with indicated concentrations of Spironolactone. Cells were harvested and analysed after 24h, n=6, error bars represent standard error of the mean.

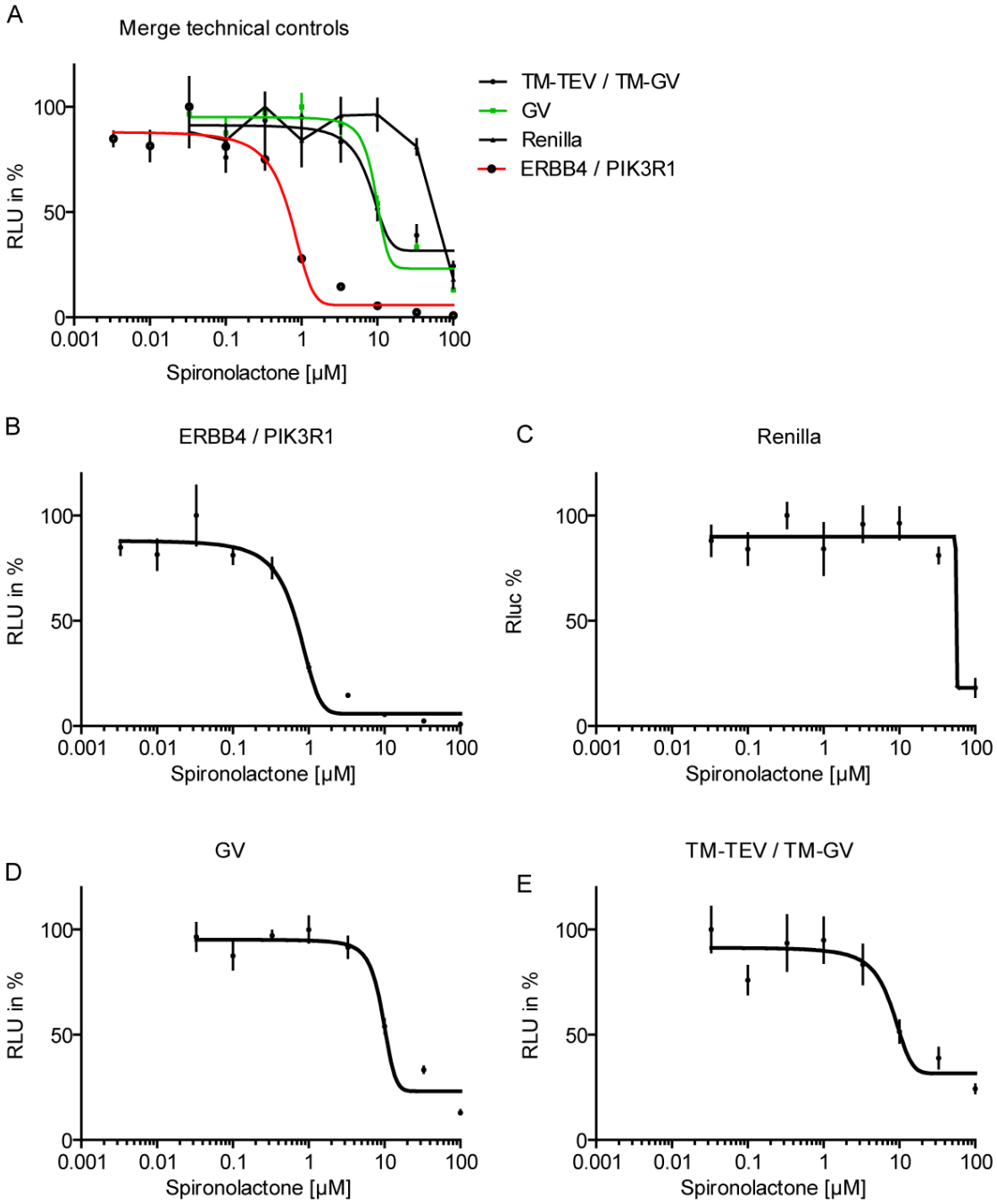

Figure 39: Technical controls

A) Merge of the results of the technical controls versus ERBB4/PIK3R1 (red).
Datasets shown from (B) to (E) were merged. B) ERBB4/PIK3R1. ERBB4 was fused to NTEV-tevS-GV-2xHA; PIK3R1 was fused to CTEV-2HA. Cells were stimulated with 10ng/nl EGFld. C) *Renilla* Luciferase assay Cells were transfected with 20ng/well TK-Rluc. D) GV assay in PC12 cells. Cells were transfected with 20ng/well CMV-GV, UAS-Fluc, and TK-Rluc. E) TM-TEV/TM-GV assay in PC12 cells. Cells were transfected with 20ng/well TM-TEV, TM-GV.

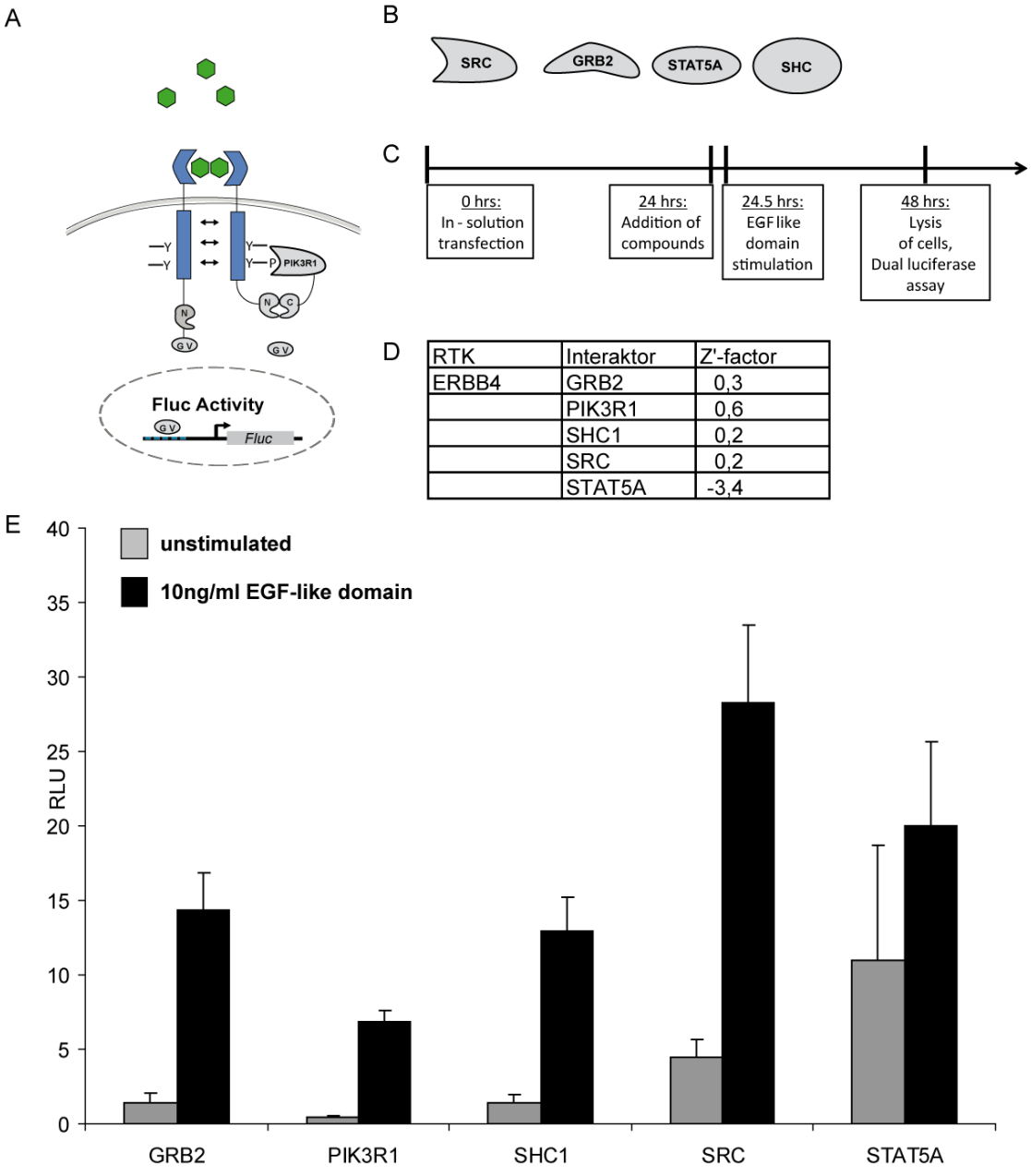

RTK	Interaktor	Z'-factor
ERBB4	GRB2	0,3
	PIK3R1	0,6
	SHC1	0,2
	SRC	0,2
	STAT5A	-3,4

Figure 40: Vertical validation Spironolactone, overview

A) Schematic depiction of the ERBB4/adapter recruitment. B) Schematic drawings of the adapters used. C) Schematic drawings of experimental time course. Cells were transfected and after 24h incubation time stimulated with 10ng/ml EGFld. Cells were lysed and analysed 24h after stimulation. D) Z'-factors obtained from the assays.
E) ERBB4/adapter recruitment. ERBB4 was fused to NTEV-tevS-GV-2xHA; adapters were fused to CTEV-2HA. Cells were stimulated with 10ng/ml EGFld.

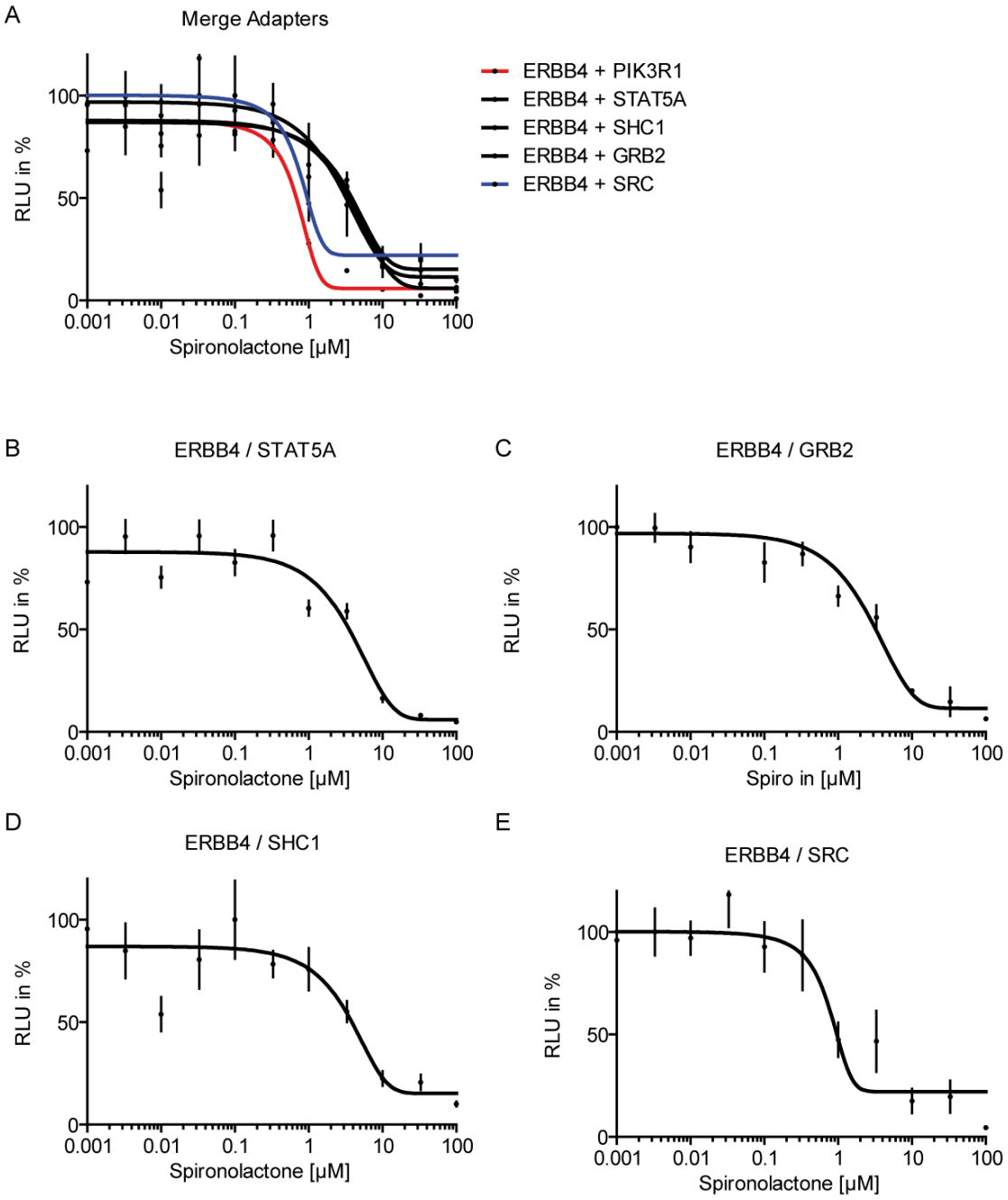

Figure 41: Vertical validation Spironolactone ERBB4/adapter recruitment

A) Comparison of ERBB4/adapter recruitment assays with ERBB4-PIK3R1 recruitment (red). ERBB/adapter recruitment for SHC1, GRB2, and STAT5a are less efficiently inhibited as compared to ERBB4/PIK3R1 recruitment. ERBB4/SHC1 is intermediate. B-E) ERBB4/adapter recruitment. ERBB4 was fused to NTEV-tevS-GV-2xHA; adapters were fused to CTEV-2HA. PC12 cells were stimulated with 10ng/ml EGFld.

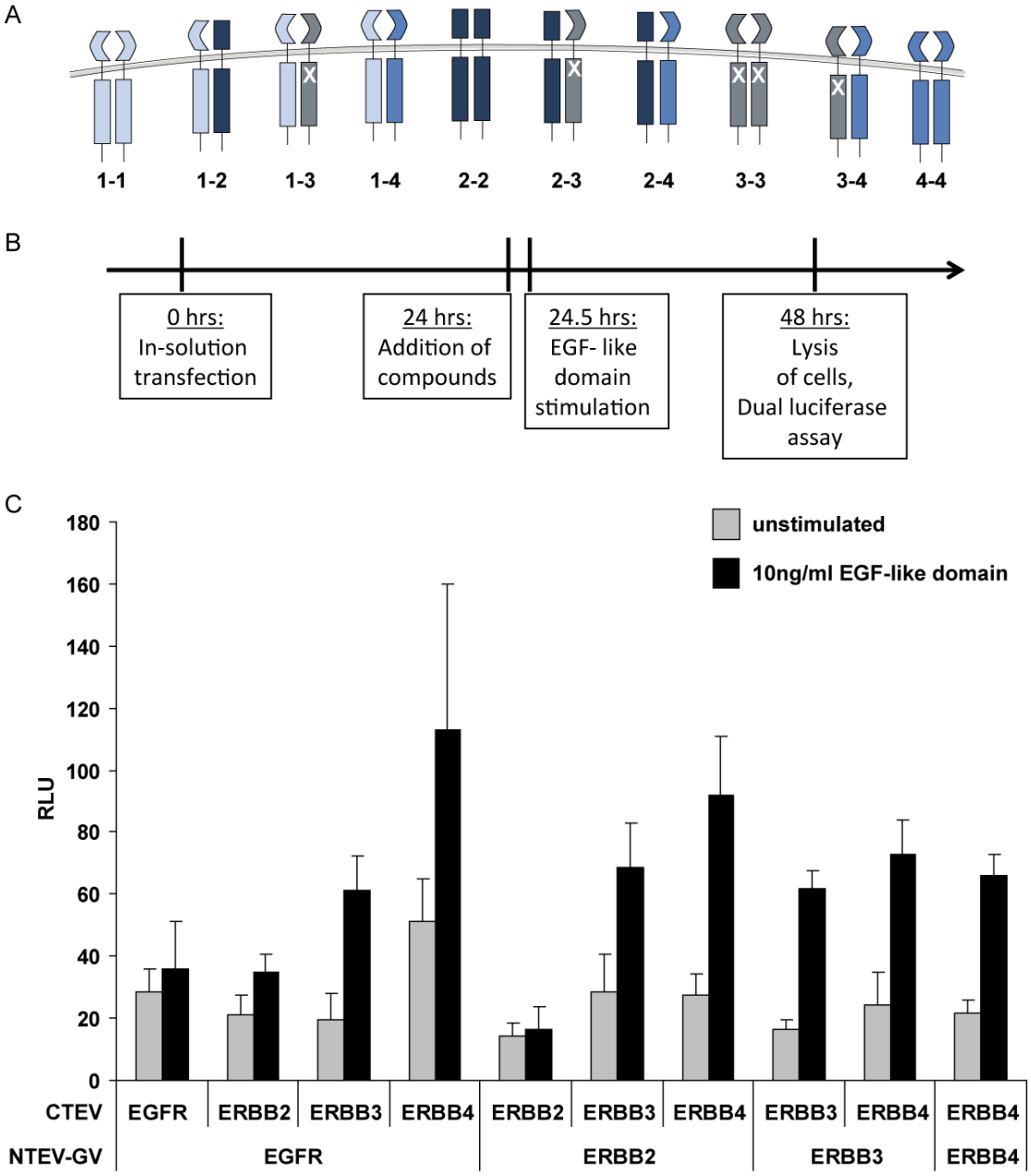

Figure 42: Homo and heterodimerisations of ERBB receptors

A) Schematic drawings of all possible ERBB homo and heterodimer combinations. Note, that ERBB1 (EGFR) is activated by EGF, and not by NRG1-typeI, and that ERBB2 lacks a NRG1-binding site whereas ERBB3 lacks intrinsic kinase activity. ERBB4 binds to NRG1 as homodimer and is able to cross-phosphorylate itself. B) Schematic drawings of experimental time course. Cells were transfected and after 24h incubation time stimulated with 10ng/ml EGFld. Cells were lysed and analysed 24h after stimulation. C) ERBB homo- and hetero-dimerisation. ERBBx/ERBBy split TEV assay in PC12 cells. ERBBx was fused to NTEV-tevS-GV-2xHA; ERBBy was fused to CTEV-2HA. Cells were stimulated with 10ng/ml EGFld.

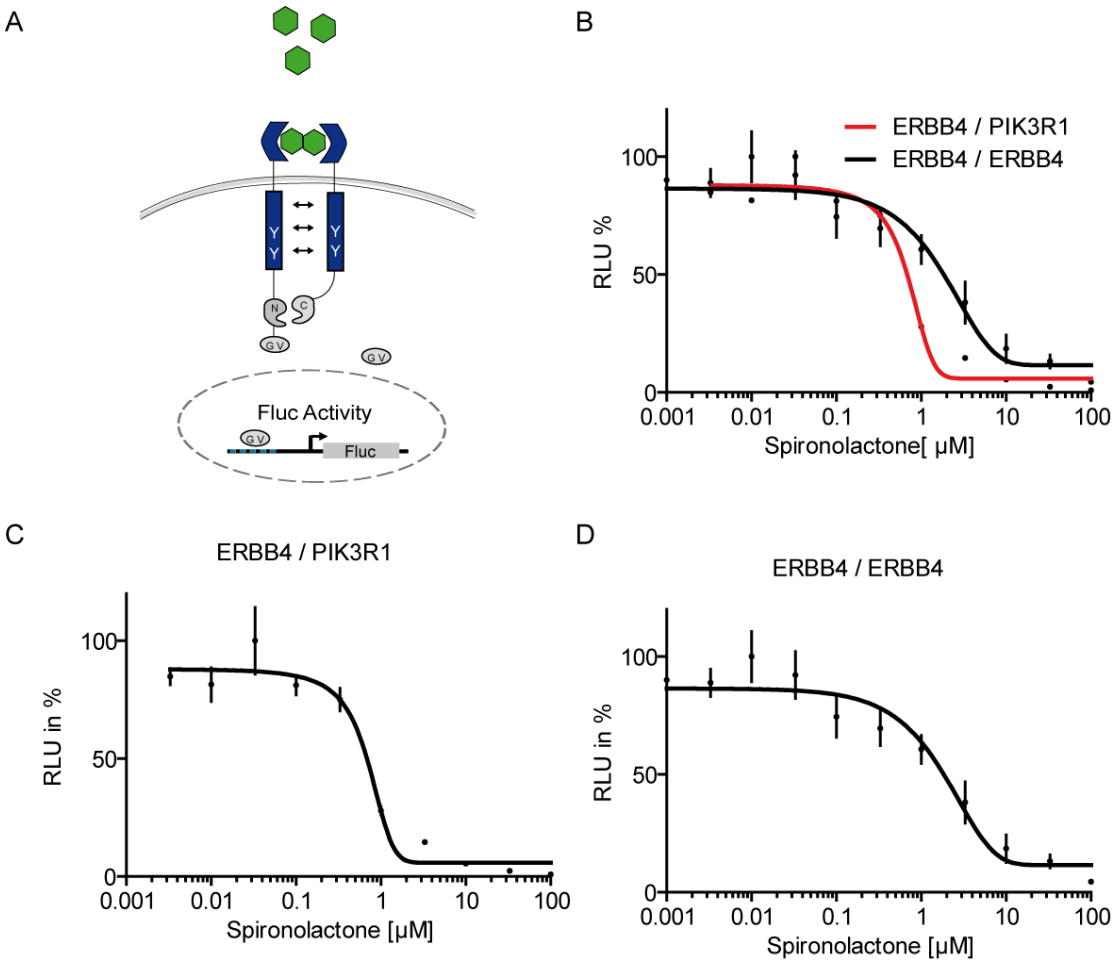

Figure 43: ERBB4 homodimerisation

A) Schematic depiction of ERBB4 homodimerisation. B) Comparison of ERBB4 homodomerisation with ERBB4/PIK3R1 interaction. C) ERBB4/PIK3R1. D) ERBB4/ERBB4. ERBB4 was fused to NTEV-tevS-GV-2xHA; PIK3R1 and ERBB4 were fused to CTEV-2HA. PC12 cells were stimulated with 10 ng/ml EGFld.

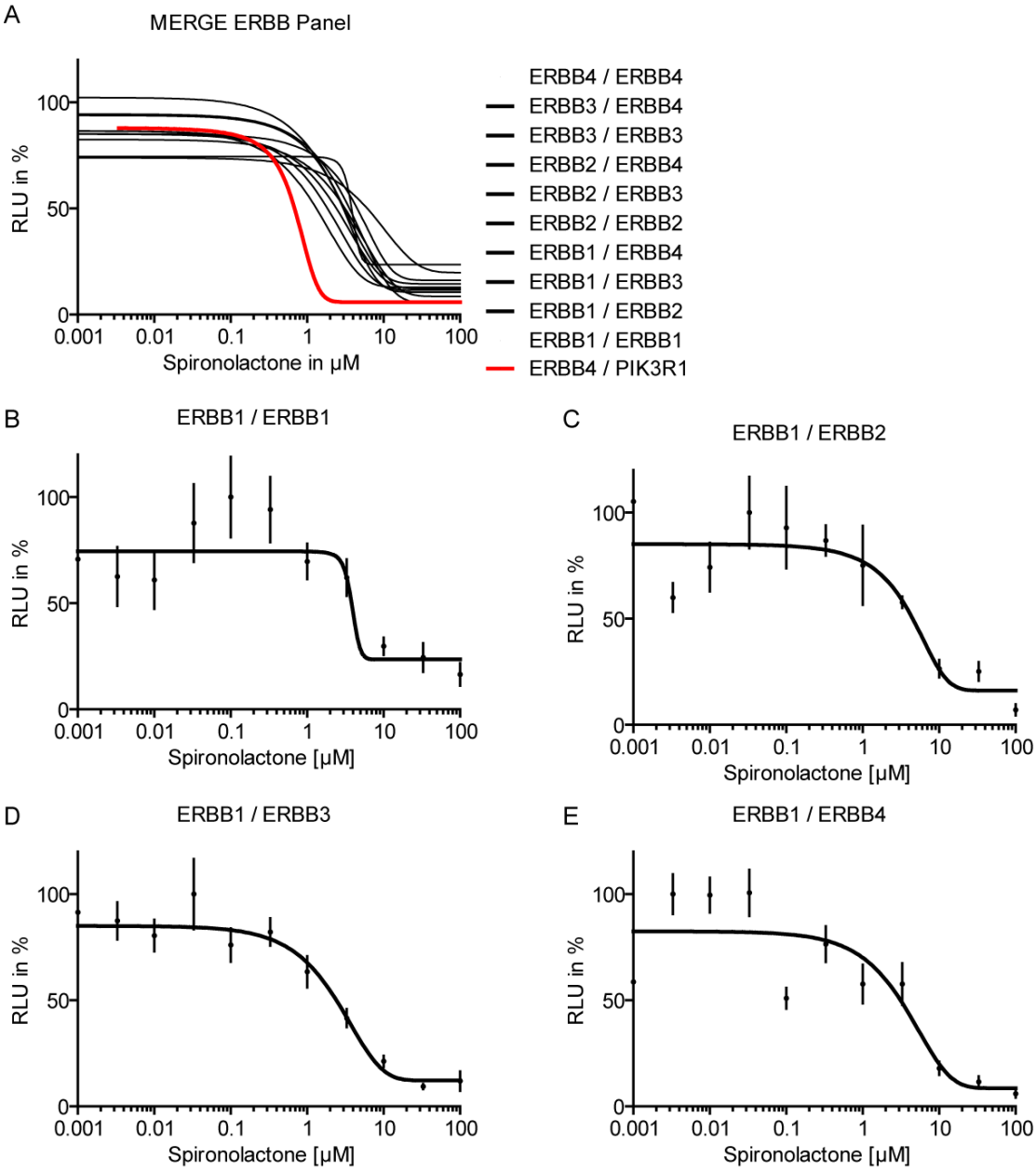
A
MERGE ERBB Panel
RLU in %
Spironolactone in µM
ERBB4 / ERBB4
ERBB3 / ERBB4
ERBB3 / ERBB3
ERBB2 / ERBB4
ERBB2 / ERBB3
ERBB2 / ERBB2
ERBB1 / ERBB4
ERBB1 / ERBB3
ERBB1 / ERBB2
ERBB1 / ERBB1
ERBB4 / PIK3R1
B
ERBB1 / ERBB1
C
ERBB1 / ERBB2
D
ERBB1 / ERBB3
E
ERBB1 / ERBB4
Spironolactone [µM]

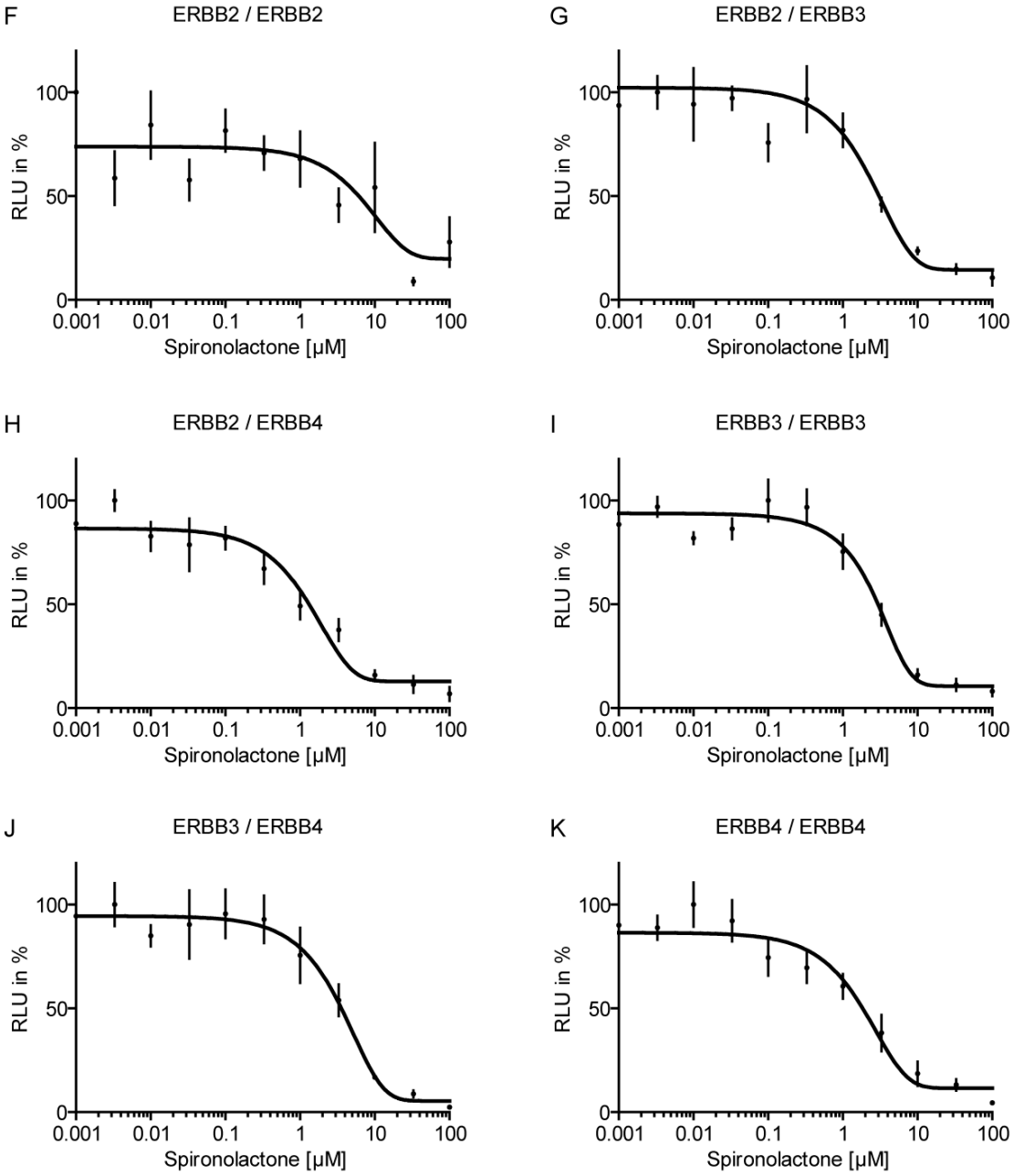

Figure 44: ERBB homo and heterodimerisation

A) Comparison of ERBB homo and heterodimerisation assays with ERBB4-PIK3R1 recruitment. ERBB homo/heterodimerisations are less efficiently inhibited as compared to ERBB4-PIK3R1 recruitment. B-K) ERBB homo and heterodimerisations. ERBBx was fused to NTEV-tevS-GV-2xHA; ERBBy was fused to CTEV-2HA. PC12 cells were stimulated with 10 ng/ml EGFld.

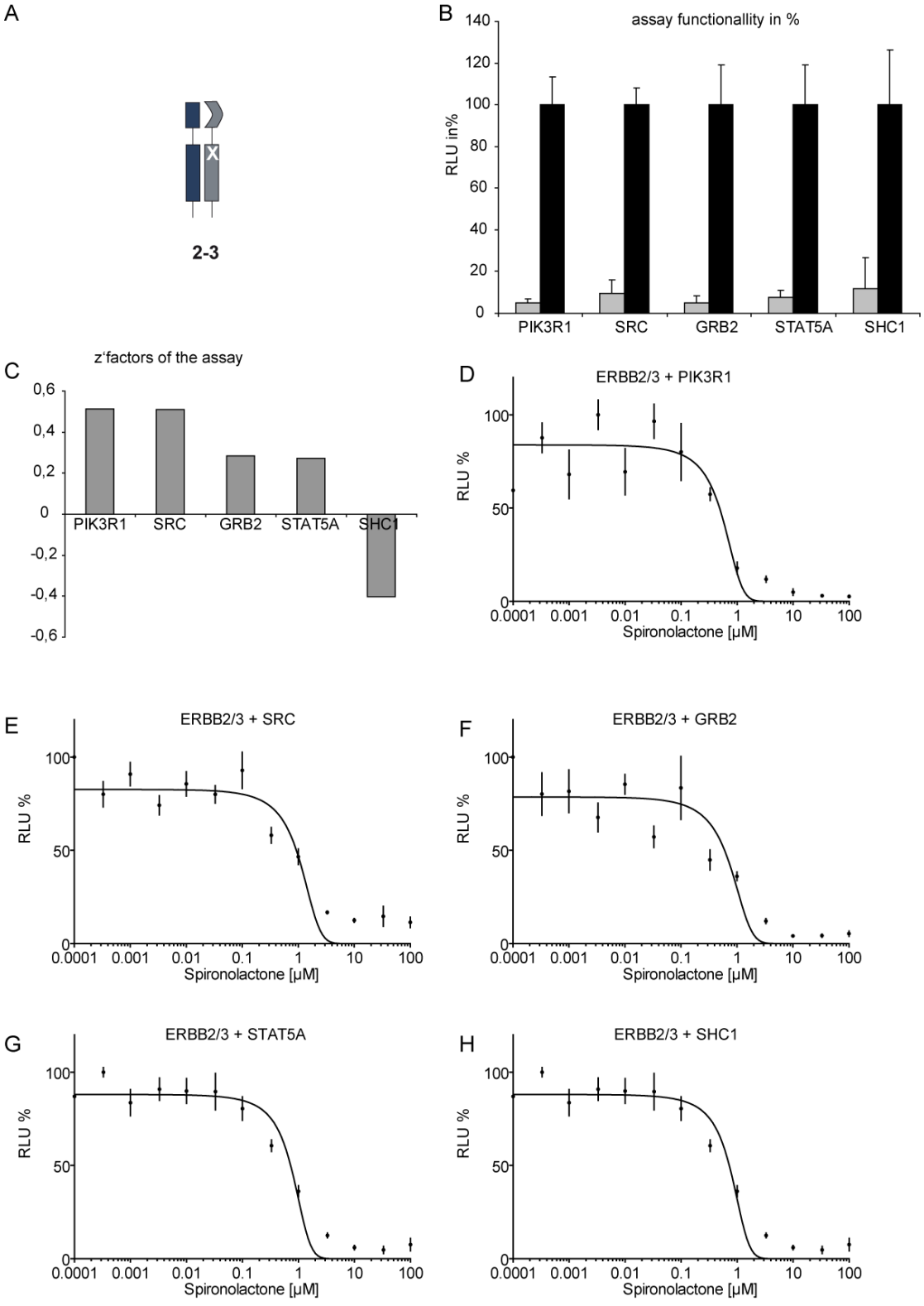

Figure 45: Horizontal validation ERBB2/3 and adapters

A) Schematic representation ERBB2/ERBB3 heterodimerisation. B) Assay performance. ERBB2/ERBB3 heterodimerise after stimulation with 10ng/ml EGFld and recruit adapters as indicated. C) Comparison of the z'-factors obtained from the assays. D-H) ERBB2/ERBB3/various adapters. ERBB2 was fused to a V5 tag, ERBB3 was fused to NTEV-tevS-GV-2xHA; adapters were fused to CTEV-2HA. PC12 cells were stimulated with 10ng/ml EGFld.

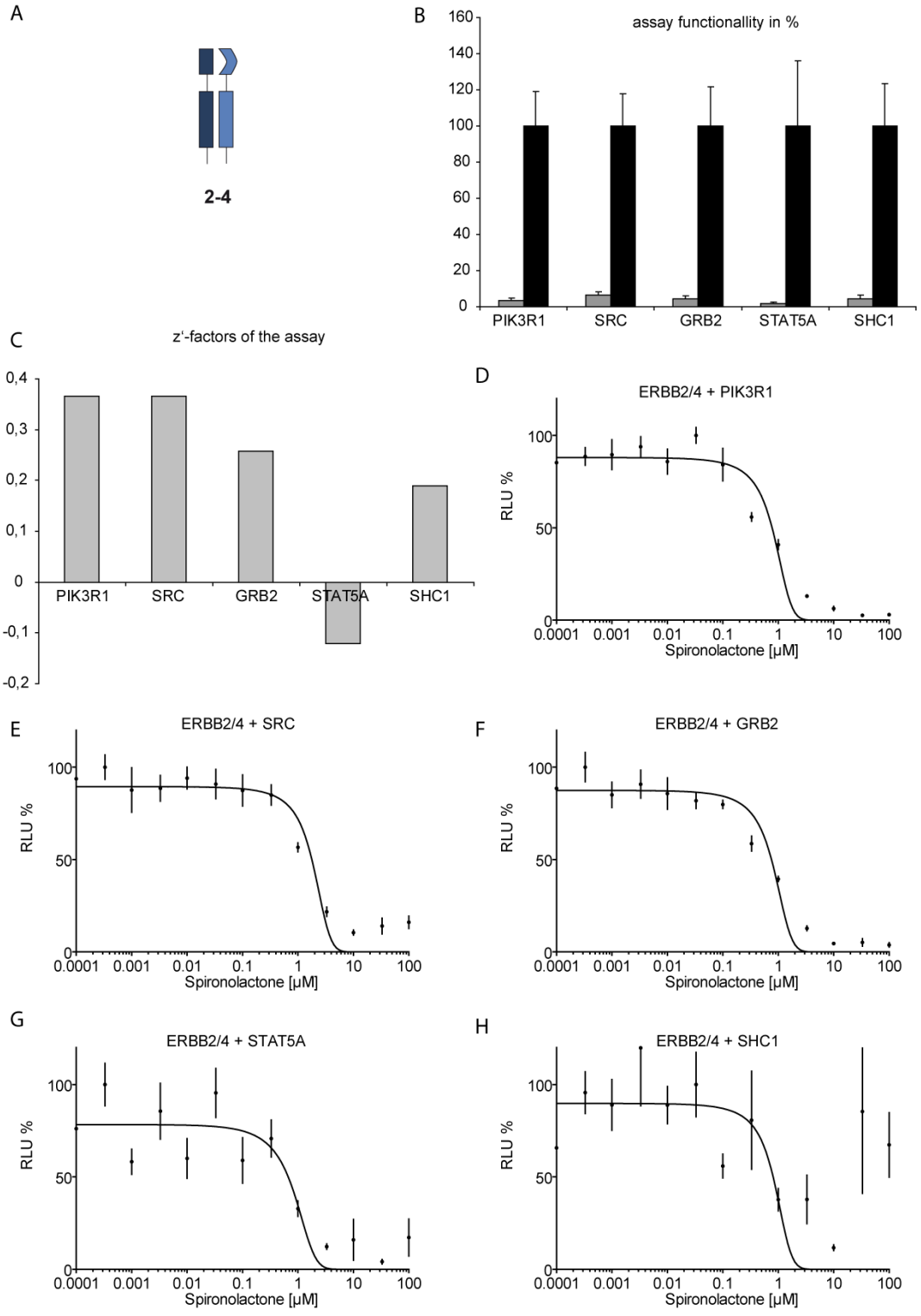

Figure 46: Horizontal validation ERBB2/ERBB4 and adapters

A) Schematic representation ERBB2/ERBB4 heterodimerisation. B) Assay performance. ERBB2/ERBB4 heterodimerise after stimulation with 10ng/ml EGFld and recruit adapters as indicated. C) Comparison of the z'-factors obtained from the assays.D-H) ERBB2/ERBB4/various adapters. ERBB2 was fused to a V5 tag, ERBB4 was fused to NTEV-tevS-GV-2xHA; adapters were fused to CTEV-2HA. PC12 cells were stimulated with 10ng/ml EGFld.

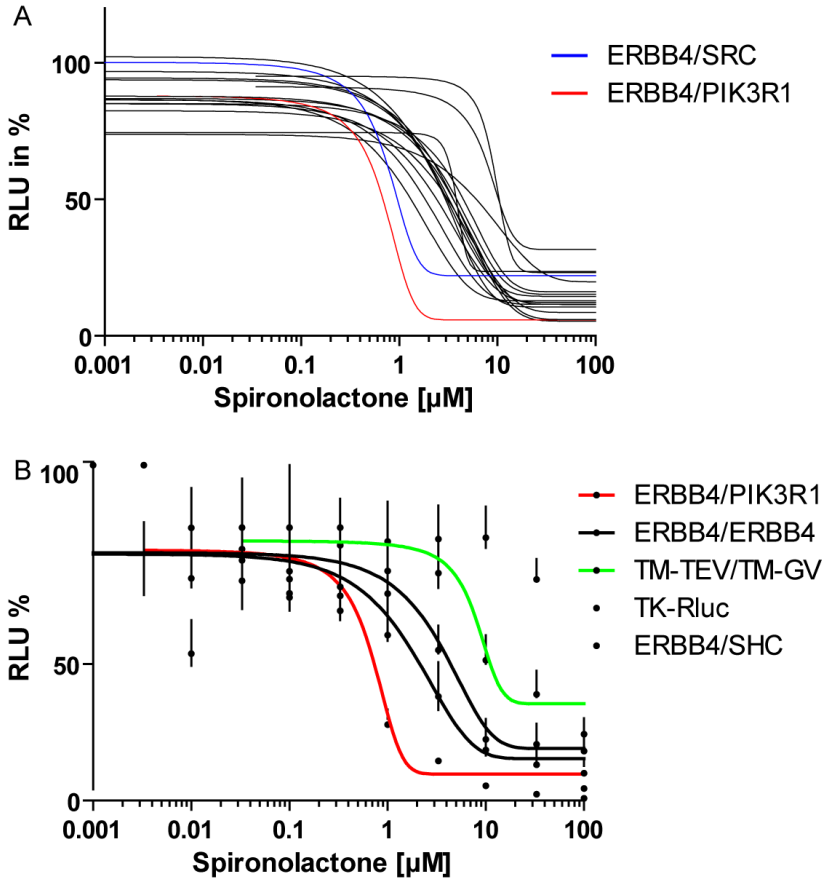

Figure 47: Data compilation of horizontal and vertical validation assays with Spironolactone

A) Detailed comparison of the datasets of the technical, vertical and horizontal validation.
B) Compilation of selected analyses of the technical, vertical, and horizontal validation.

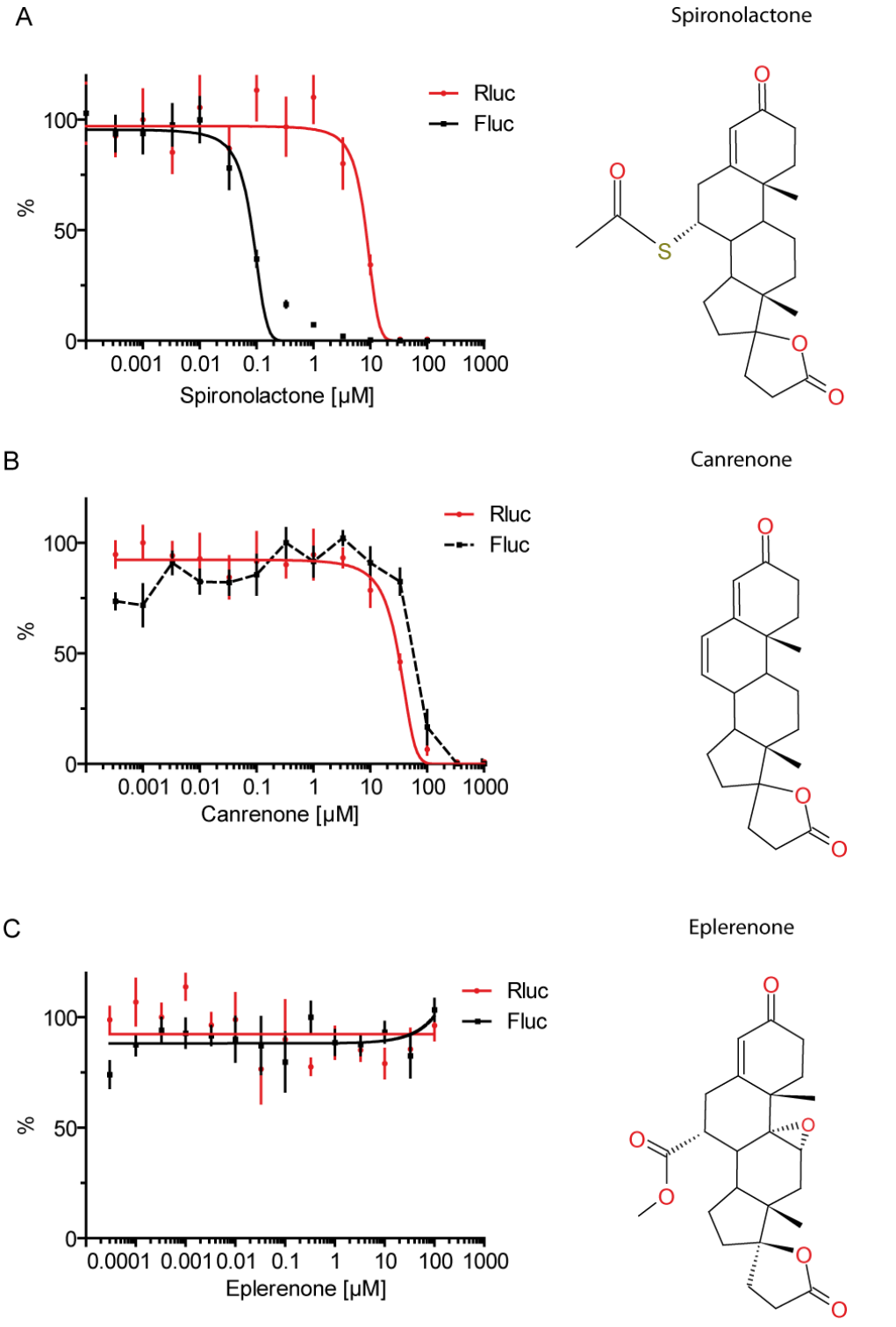

Figure 48: Comparison Spironolactone, Canrenone, Eplerenone

A) Spironolactone, exerts a strong dose-response dependent inhibitory effect on the recruitment of PIK3R1 to ERBB4 (Fluc and Rluc signal). A') Molecular structure (skeletal formula) of Spironolactone. B) Canrenone (metabolite of Spironolactone) exerts no dose-response dependent effect on the recruitment of PIK3R1 to ERBB4. B') Molecular structure (skeletal formula) of Canrenone. C) Eplerenone (2nd generation substance of Spironolactone) exerts no dose-response dependent effect on the recruitment of PIK3R1 to ERBB4. C') Molecular structure (skeletal formula) of Eplerenone. All assays are ERBB4/PIK3R1 dimerisation assays in PC12 cells, stimulated with10ng/ml EGFld.

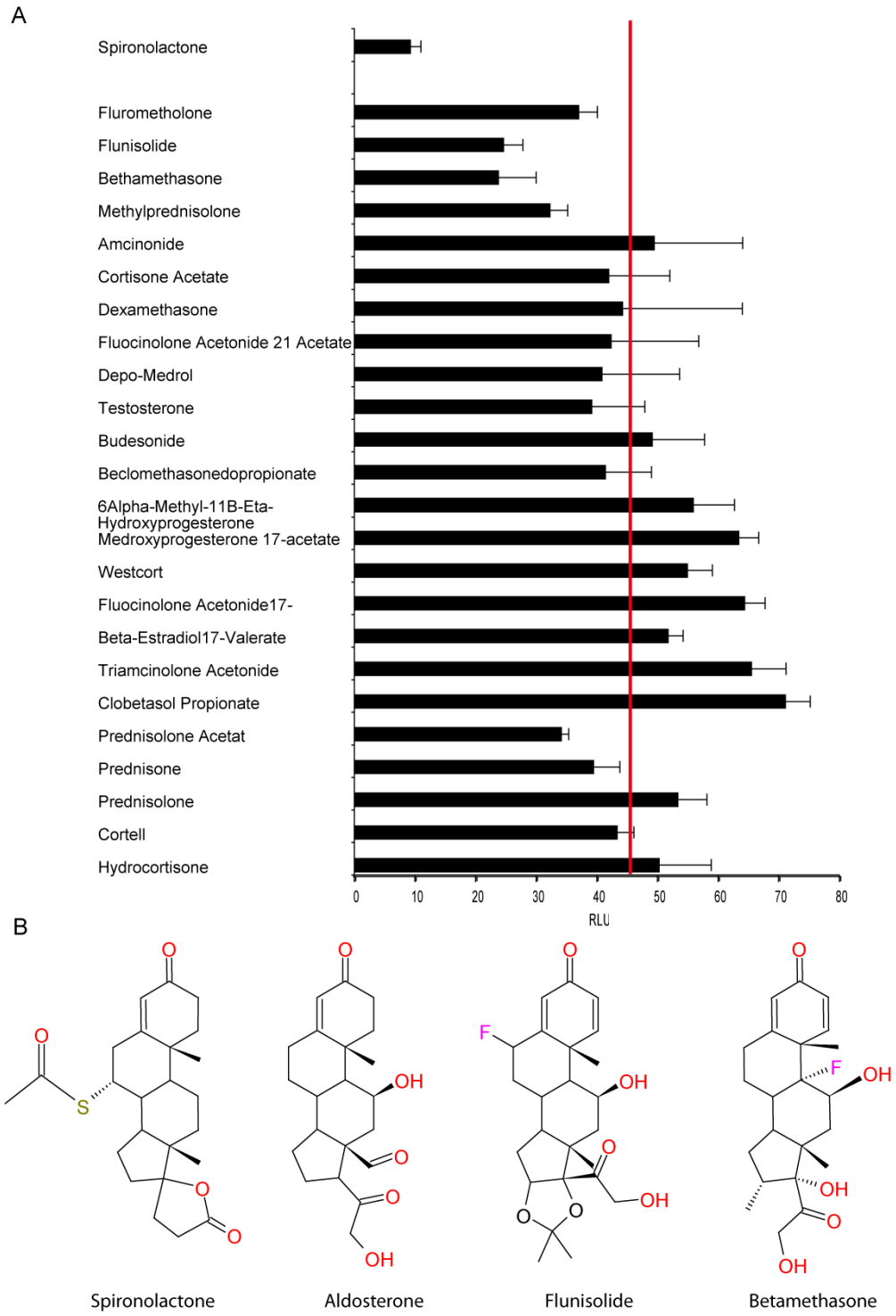

Figure 49: Analysis of substances structurally related to Spironolactone

A) Selected results from the NCC201/NCC003 screen with sterol-related substances. The 25 compounds that show the closest structural relationship to Spironolacton were analysed for inhibition of an ERBB4/PIK3R1 co-culture assay (Compounds were suggested by pupchem.org.as related compounds) The red line indicates the mean of the combined effects (RLU 46.4; 100%). Spironolactone was the most efficient substance in inhibiting the assay (RLU 9.3; 20%). B) Molecular structures of Spironolactone, Aldosterone, Flunisolide and Betamethasone. Flunisolide and Betamethasone show an inhibitory effect in the screen without reaching the detection limit.

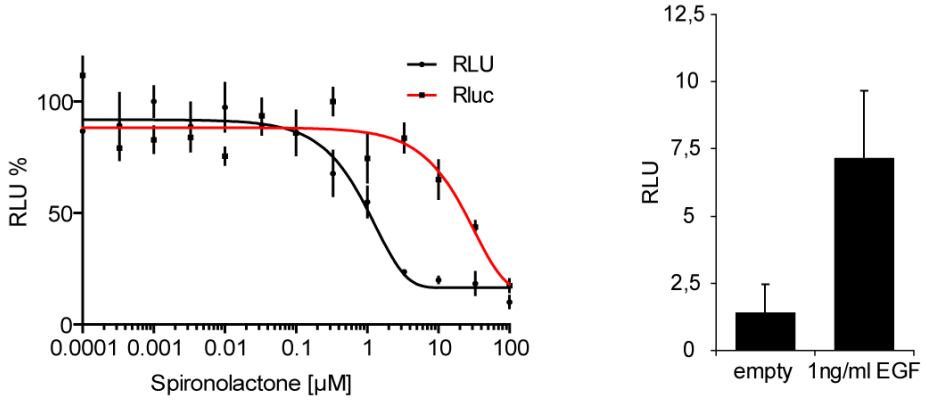

Figure 50: Effect of Spironolactone on ERBB1/1 dimerisation induced by EGF

ERBB1 was fused to NTEV-tevS-GV-2xHA; ERBB1 was fused to CTEV-2HA. PC12 cells were stimulated with 1ng/ml EGF.

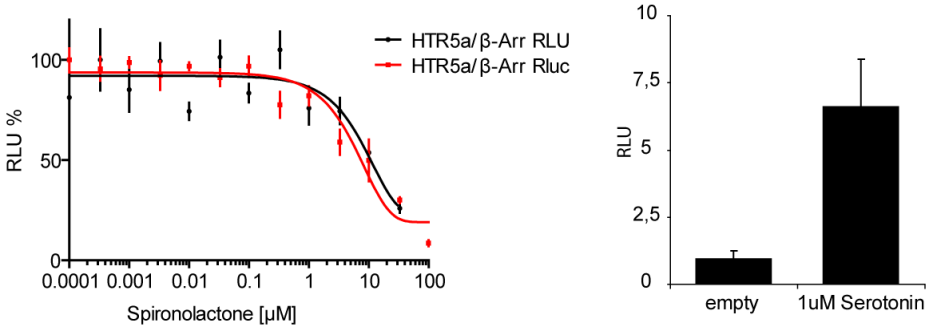

Figure 51: Effect of Spironolactone on stimulated HTR5a/β-arrestin2

HTR5A was fused to NTEV-tevS-GV-2xHA; /β-arrestin2Δ (amino acids 1-382 of ARRB2) was fused to CTEV-2HA. PC12 cells were stimulated with 1µM Serotonin.

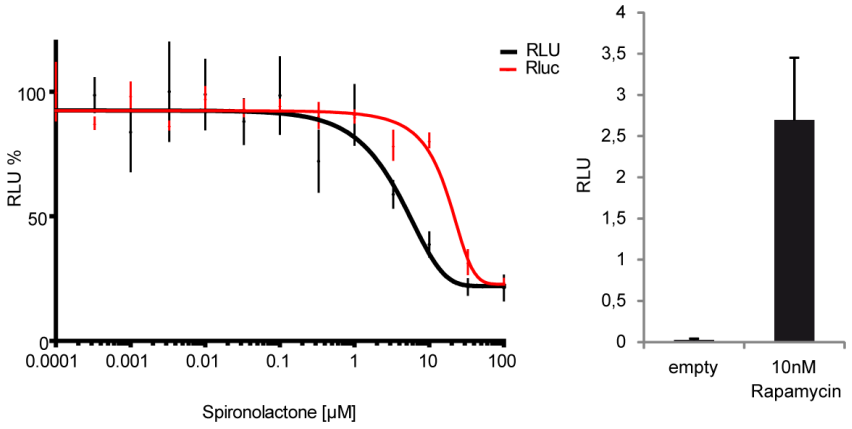

Figure 52: Effect of Spironolactone on the FRB/FKBP interaction induced by Rapamycin

TM-FRB was fused to NTEV-tevS-GV, FKBP was fused to CTEV. PC12 cells were stimulated with 10nM Rapamycin.

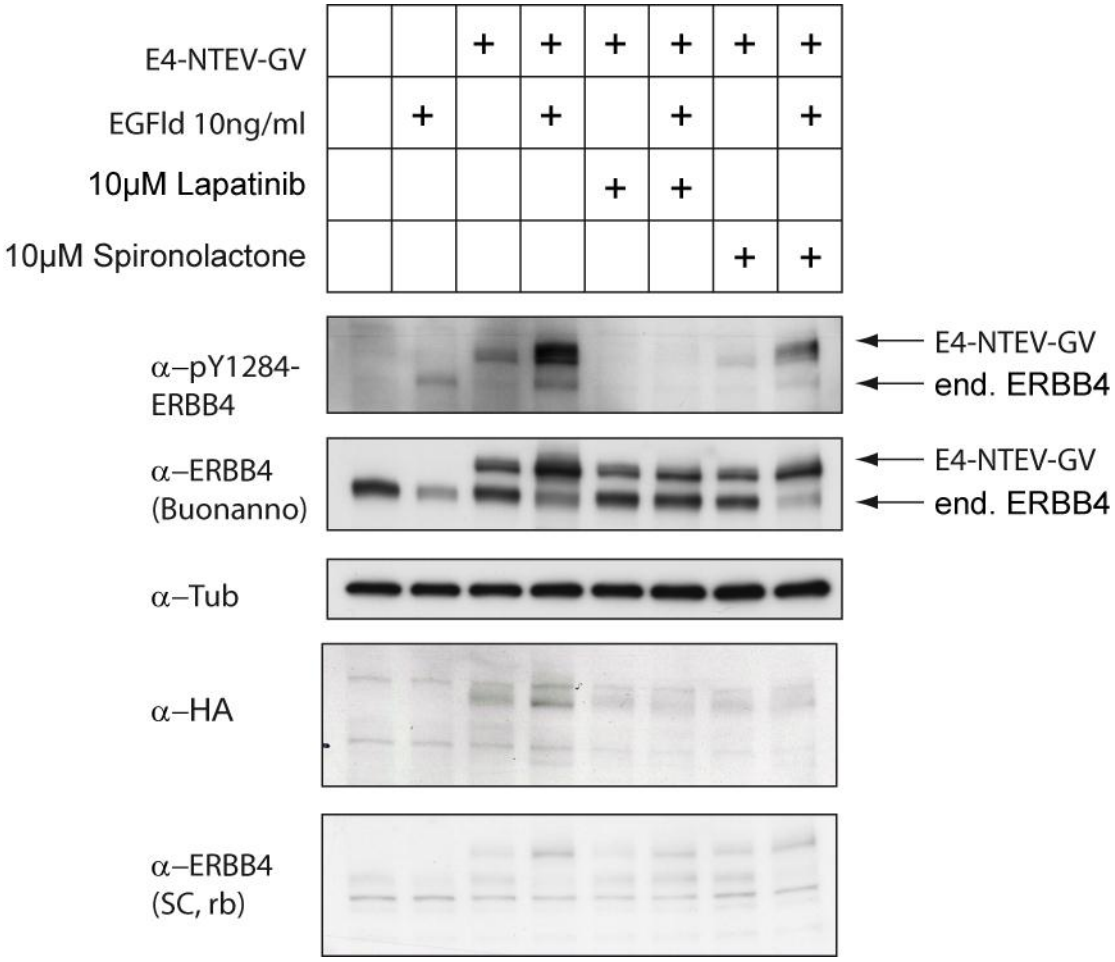

Figure 53: ERBB4 phosphorylation levels are inhibited by Lapatinib and Spironolactone

HEK293 cells were transiently transfected with ERBB4-NTEV-tevS-GV as indicated. Cells were allowed to express the vectors for 24h, and then stimulated with 10µM Lapatinib, 10µM Spironolactone (Spiro), and 10ng/ml EGF-like domain (EGFld). Cells were then incubated for additional 24h. Protein lysates were blotted and probed against antibodies as indicated. Calculated protein sizes (in kDa): ERBB4, 146.8; ERBB4-Glink-NTEV-tevS-GV-2xHA (E4-NTEV-GV), 200.

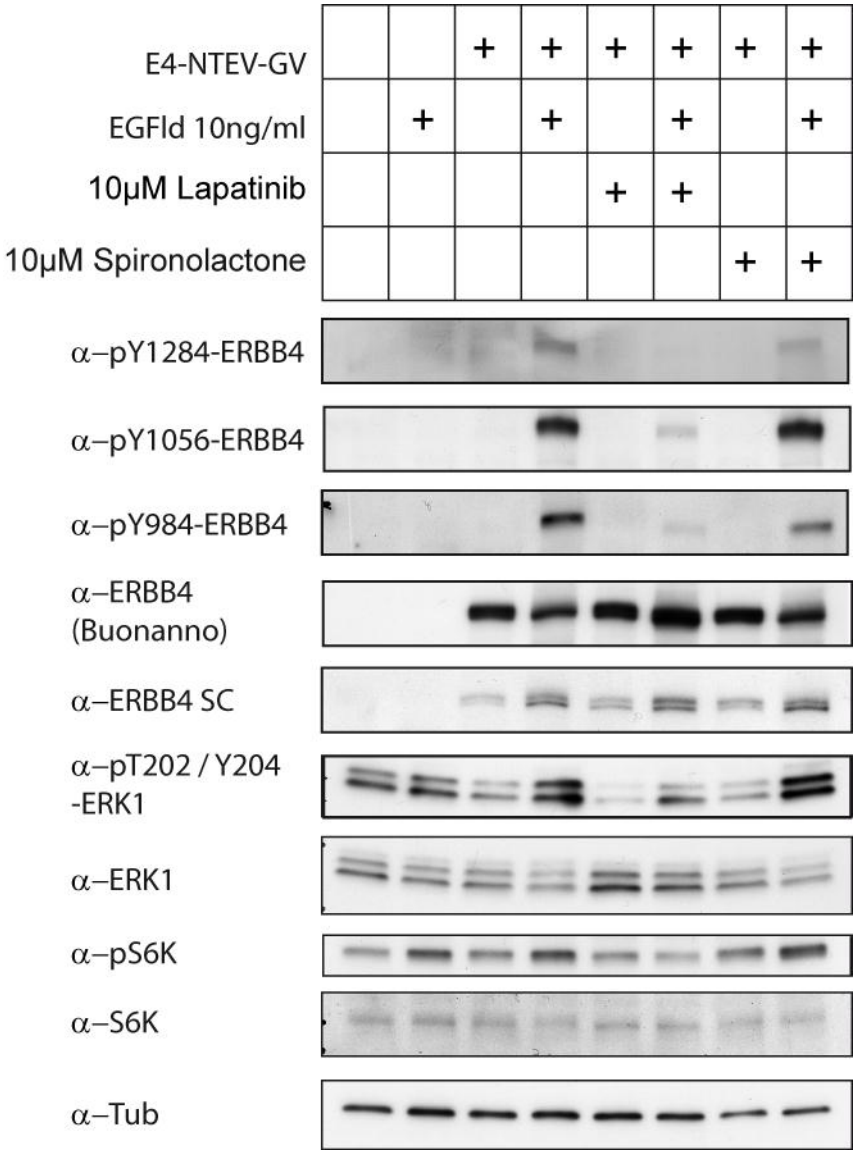

Figure 54: Analysis of phosphorylation levels of ERBB4 and major downstream signalling kinases

ERBB4 phosphorylation is inhibited by Lapatinib and Spironolactone. PC12 cells were transiently transfected with plasmids as indicated. Cells were allowed to express the vectors for 24h, and then stimulated with 10µM Lapatinib, 10µM Spironolactone (Spiro), and 10ng/ml EGF-like domain (EGFld). Cells were then incubated for additional 24h. Protein lysates were blotted and probed against antibodies as indicated. Calculated protein sizes (in kDa): ERBB4-Glink-NTEV-tevS-GV-2xHA (E4-NTEV-GV), 200. (Merge of different blots)

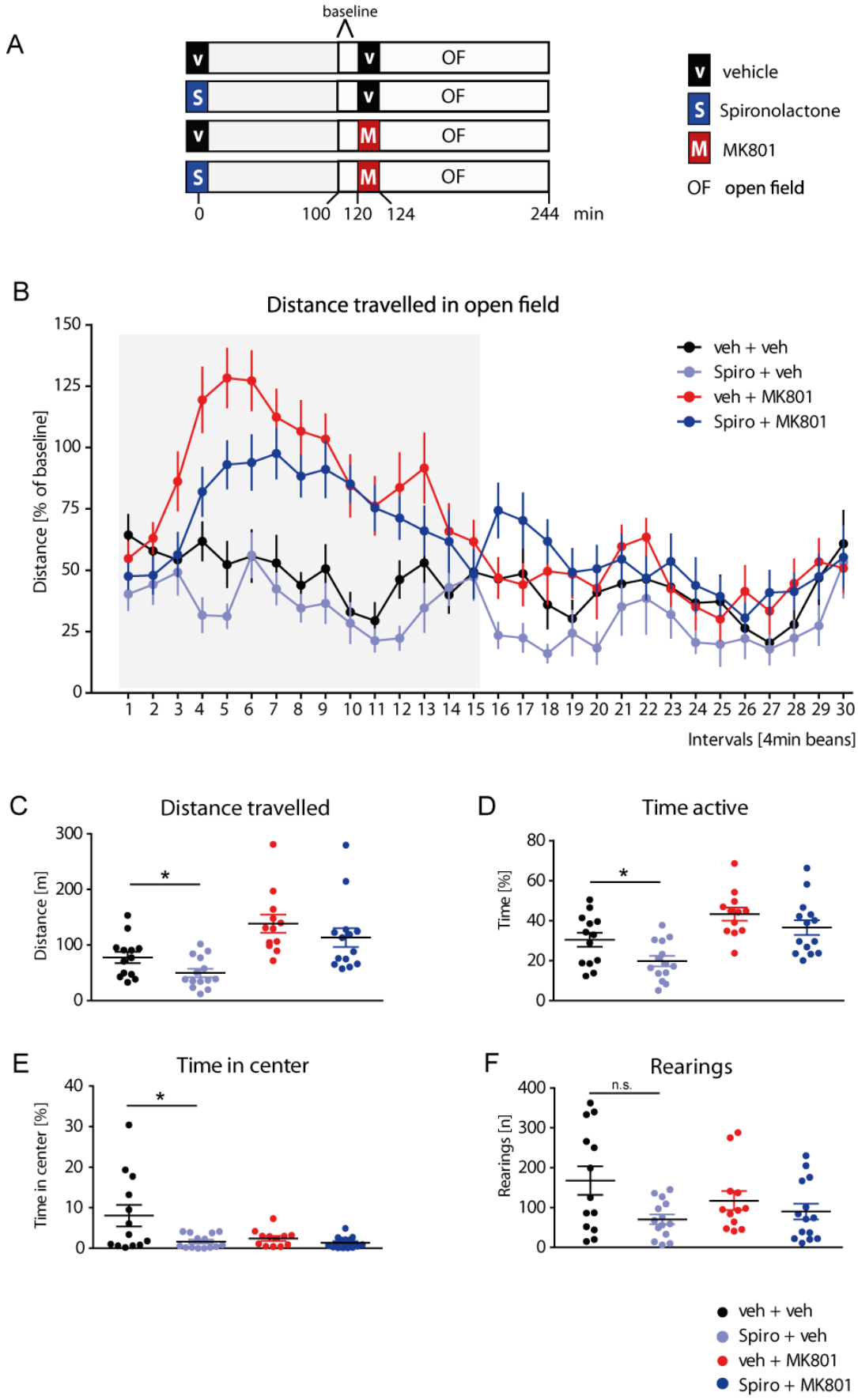
A
baseline
v
v
OF
S
v
OF
v
M
OF
S
M
OF
0
100
120
124
244
min
v vehicle
S Spironolactone
M MK801
OF open field
B
Distance travelled in open field
Distance [% of baseline]
150
125
100
75
50
25
0
1 2 3 4 5 6 7 8 9 10 11 12 13 14 15 16 17 18 19 20 21 22 23 24 25 26 27 28 29 30
Intervals [4min beans]
veh + veh
Spiro + veh
veh + MK801
Spiro + MK801
C
Distance travelled
Distance [m]
300
200
100
0
*
D
Time active
Time [%]
80
60
40
20
0
*
E
Time in center
Time in center [%]
40
30
20
10
0
*
F
Rearings
Rearings [n]
400
300
200
100
0
n.s.
veh + veh
Spiro + veh
veh + MK801
Spiro + MK801

Figure 55: Effects of Spironolactone on MK801-induced hyperactivity in mice tested in an open field setup

Effects of Spironolactone on MK801-induced hyperactivity in mice tested in open field.
A) Experimental protocol. 9 weeks old C57Bl/6N male mice were divided randomly in one of 4 treatment groups: group 1 injected twice with (v) vehicle ([veh+veh], n=13), group 2 administered with Spironolactone (S) and vehicle ([Spiro+veh], n=14), group 3 treated with vehicle and (M) MK801 ([veh+MK801], n=12), and group 4 injected with Spironolactone and MK801 ([Spiro+MK801], n=14). 100 min after the first injection, mice were placed in the open field arena for 20 min to score baseline activity. Thereafter, animals were taken out of the test boxes for 4 min, administered with a second injection, and returned to the open field arena for the next 120 min where activity was monitored.
B) Distance travelled in open field arena depicted as a percentage of mean distance travelled during baseline activity. A 2-way ANOVA was performed pairwise between different treatments during the time window between intervals 1 to 15. [Veh+MK801] animals showed hyperactivity when compared with [veh+veh] controls (interaction time × treatment $F_{(14,322)}$=5.73; p<0.0001; effect of treatment $F_{(1,23)}$=17.92; p=0.0003; 2-way ANOVA). [Spiro+veh] mice showed a non-significant tendency to travelled less distance then [veh+veh] ($F_{(1,25)}$=3.39 p=0.0774, 2-way ANOVA). Animals treated with [Spiro+MK801] displayed a slight tendency to travel shorter distance than mice with induced hyperactivity [veh+MK801] (effect of treatment $F_{(1,24)}$=2.89; p=0.1018; 2-way ANOVA).
C) Distance travelled in open field. Mice treated with spironolactone [Spiro+veh] travelled less distance than [veh+veh] controls (49.79 m ±27.93 vs 77.76 m ±36.39; p=0.0369). [veh+MK801] animals covered longer distance than [veh+veh] (138.4 m ±56.65 vs 77.76 m ±36.39; p=0.0036). [Spiro+MK801] animals showed a non-significant tendency to cover a shorter distance than [veh+MK801] mice (113.4 m ±63.49 vs 138.4 m ±56.65; p=0.0849).
D) Time which mice spent active during open field test. [Spiro+veh] animals spent less time active than control [veh+veh] group (19.79% ±9.761 vs 30.47% ±12.71; p=0.0273). [veh+MK801] displayed more activity than [veh+veh] (43.33% ±11.47 vs 30.47% ± 12.71; p=0.0240). [Spiro+MK801] treated group showed non-significant tendency towards less activity when compared with [veh+MK801] mice (36.57% ±13.92 vs 43.33% ±11.47; p=0.1166).
E) Percentage of time which mice spent in the center of the open field arena. Spironolactone administered with vehicle significantly reduced the percentage of time in which mice were scored in the centre of the open field arena compared to controls ([Spiro+veh] 1.643% ±1.706 vs. [veh+veh] 8.046% ± 9.518; p=0.0387). Similarly, groups injected with [veh+MK801] and [Spiro+MK801] spent very low percentage of time in the center of test arena (2.442% ±2.009 and 1.371% ±1.410, respectively).
F) Number of rearings performed during open field test. Mice treated with spironolactone [Spiro+veh] displayed a non-significant tendency towards less rearings when compared to [veh+veh] controls (70.36 ±46.80 vs 167.6 ±129.4; p=0.0765). The [veh+MK801] group displayed similar number of rearings to controls (117.3 ±83.32 vs 167.6 ±129.4; p=0.6053). Spironolactone did not have a significant impact on rearings in the [Spiro+MK801] treated group when compared with the [veh+MK801] group (89.93 ±74.79 vs 117.3 ±83.32; p=0.2367).
Veh, vehicle; Spiro, Spironolactone; black dots, veh+veh (n=13); light blue dots, Spiro+veh (n=14); red dots, veh+MK801 (n=12); dark blue dots, Spiro+MK801 (n=14). Data presented as mean ±S.E.M.

5.7 Validation Albendazole

The activator hit found in the screen of the NCC201 library is Albendazole. Albendazole is a Benzimidazole compound normally used as anthelmintic in the treatment of worm infections (van Schalkwyk et al., 1979). It binds to tubulin and inhibits the polymerization of microtubules (Nayak et al., 2011). There is a highly significant activation of luciferase activity in the Nrg1-typeI-ERBB4/PIK3R1co-culture assay when applying 10µM Albendazole (p<0,0001)(Figure 57 A).

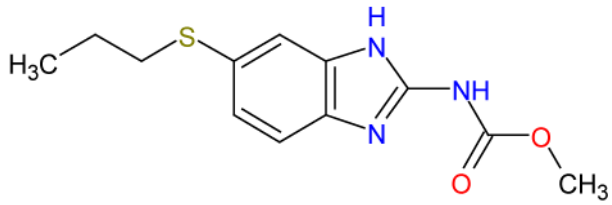

Figure 56: Chemical structure of Albendazole

5.7.1 Technical controls for Albendazole

5.7.1.1 *Renilla* Luciferase

To test for potential Albendazole-mediated toxicity, PC12 cells were transfected with the *Renilla* luciferase. The test revealed a toxic effect against the co-culture assay at concentrations between 33µM to 100µM (Figure 57 B).

5.7.1.2 The Gal4-VP16 control assay

The technical control GV/UAS-Fluc showed a 3-fold increase of 300% of the Fluc activity. The EC_{50} of Albendazole is at 0.3µM (Figure 57 G).

5.7.1.3 TEV protease control assay

To test for any stimulating effects elicited by the TEV protease and its activity at TEV protease cleavage sites, a transmembrane version of the TEV protease (TM-TEV) was co-transfected with a transmembrane-bound GV carrying an internal TEV cleavage site (TM-GV), along with UAS-Fluc and Rluc reporters. Like the GV control assay, the TM-TEV/TM-GV assay showed a comparable 2.5-foldincrease of the firefly activity, with an EC_{50} of 1.0µM Albendazole (Figure 57. F)

5.7.1.4 Co-culture assay using increasing numbers of Nrg1-typeI-expressing cells

To test Albendazole's activating effect at different pre-activated conditions, the co-culture assay ERBB4/PIK3R1 was stimulated with 1,000, 5,000, and

10,000 Nrg1-typeI-expressing PC12 cells. All three assays roughly showed a 2-fold activation of the firefly luciferase activity, with an EC_{50} of 0.3µM Albendazole (Figure 57 C).

5.7.1.5 Single cell assay with soluble Nrg1-derived EGF-like domain

The single cell ERBB4/PIK3R1 assay was stimulated with 1 or 5ng/ml EGF-like domain to get two different pre-activated conditions. Both assays showed a 1.5-fold activation of the firefly luciferase activity, with an EC_{50} of 0.6µM Albendazole at a concentration of 1ng/ml EGF-like domain, and an EC_{50} of 0.4µM Albendazole and 5ng/ml EGF-like domain (Figure 57 D,E).

The comparison of the data revealed that firefly luciferase activity was highly increased in the technical control assays when Albendazole was applied at high concentrations. For example, the GV technical control assay displayed strongly increased readings for firefly luciferase at Albendazole concentrations that were not toxic for the cells as measured by *Renilla* luciferase activity (Figure 57 D, D', D''). Therefore, Albendazole seems not to be a specific activator of Nrg1-ERBB4 signalling, but rather an unspecific activator of either GV, the UAS promoter, the activity of firefly luciferase, or a combination thereof. Further validation approaches have to be performed, for example, it should be addressed whether Albendazole has the potential to increase firefly luciferase activity when expressed under the control of the constitutively active CMV promoter (Figure 57 H).

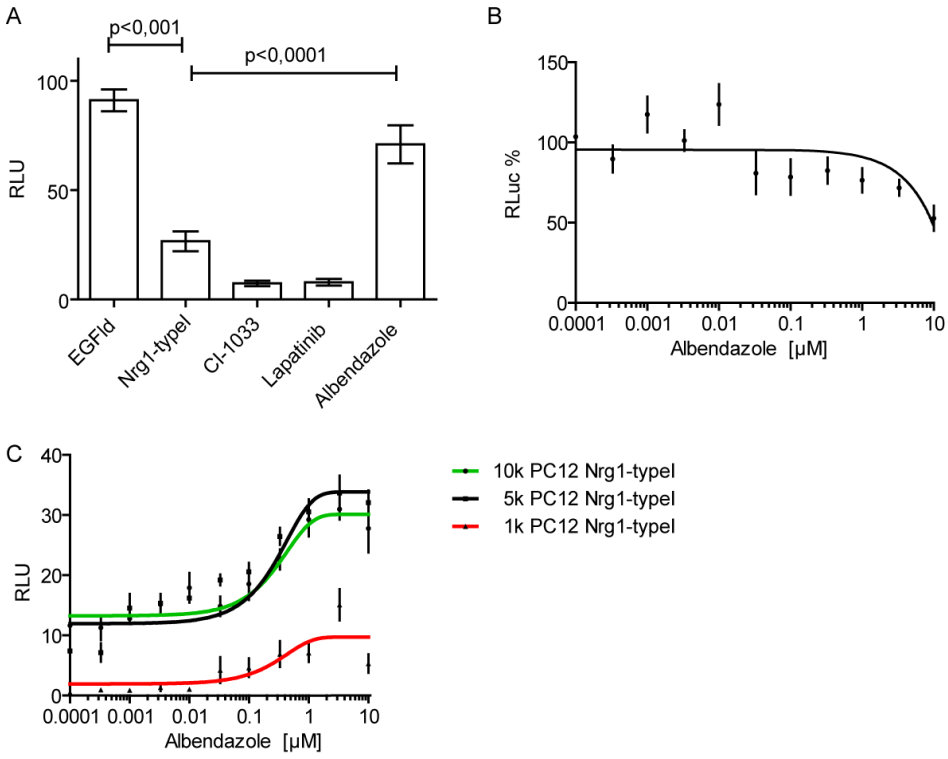

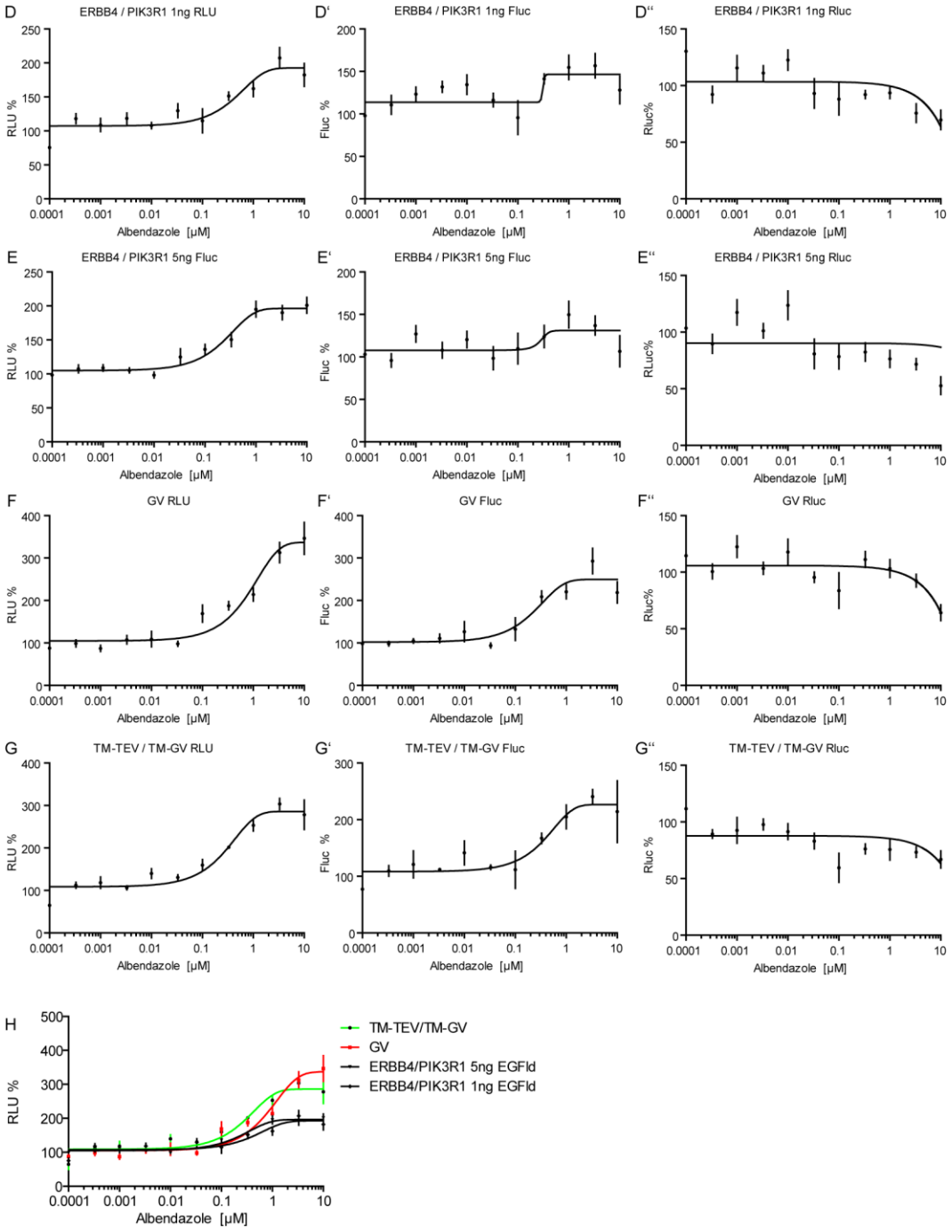

Figure 57: Validation Albendazole

A) Extracted data from the screen showing a significant activation of Nrg1-ERBB4 signalling caused by Albendazole in the co-culture assay. B) Renilla luciferase assay to test the toxicity of Albendazole. C) ERBB4/PIK3R1 co-culture assays activated with 1k, 5k, or 10k Nrg1-typeI cells. D) ERBB4/PIK3R1 single cell assay stimulated with 1ng EGFld. E) ERBB4/PIK3R1 single cell assay stimulated with 5ng EGFld. ERBB4 was fused to NTEV-tevS-GV-2HA; Adapters were fused to CTEV-2HA. PC12 cells were stimulated with indicated numbers of Nrg1-typeI-expressing cells or indicated cell numbers of EGFld. F) GV/UAS-Fluc technical control assay showing the effect of Albendazole on relative luciferase activity. G) TM-TEV/TM-GV technical control assay showing the effect of Albendazole on TEV protease function. H) Comparison of the data shown from (B) to (I). GV and TM-TEV/TM-GV control assays show the highest activation of relative luciferase activity.

5.8 Topotecan

The NCC003 screen showed a significant reduction in firefly luciferase activity for 10µM Topotecan (brand name Hycamtin, GlaxoSmithKline 2007). Topotecan is a Topoisomerase I inhibitor used as a chemotherapeutic agent for the treatment of ovarian, cervical, and small cell lung cancer.

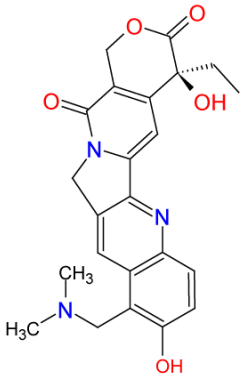

Figure 58: Chemical structure of Topotecan

Topotecan is a drug used as chemotherapeutic. It is a semi-synthetic derivative of the alkaloid Camptothecin, a substance from the bark or leaves of *Camptotheca acuminate* the Tibetian “Happy Tree”. Camptothecin is nearly insoluble in water and has to be modified to increase water solubility. One of these derivatives is Topotecan. It functions as a Topoisomerase I inhibitor, mimicking a DNA base pair, intercalating between the Topoisomerase (Arg364, Asp533, Asn 722) and the DNA (GC base pairs). This leads to a stalling of the rewinding process after the single strand break by stabilising the cleavage complex, and therefore causing double strand breaks that lead to cell cycle arrest in the S-phase, and terminal to apoptosis (Streltsov et al., 2003; Streltsov et al., 2003; Takimoto and Arbuck, 1997a; O’Leary and Muggia, 1998a; Pommier, 2006; Pommier, 2004).

Topotecan was FDA-approved in 2007 and is primarily used in the treatment of ovarian cancer and small cell lung cancer (Carol et al., 2010). It is also tested for brainstem gliomas and sarcomas (Houghton et al., 1995).

In the NCC003 screen, Topotecan was found to decrease significant the luciferase activity ($p=1,4*10e^{-10}$, two sided, two paired T-Test).

5.8.1 Vertical validation for Topotecan

The dose response to increasing concentrations of Topotecan showed an IC_{50} of 0.5µM in the Nrg1-typeI ERBB4/PIK3R1 assay. Exchanging the Nrg1-typeI cells with EGFld lead to an IC_{50} of 0.4µM (Figure 59).

5.8.2 Technical controls

5.8.2.1 *Renilla* luciferase

The technical validation showed a strong toxic effect of Topotecan between 3.3-100µM monitoring *Renilla* luciferase (Figure 60). All values above 10µM are excluded from the dose responses curves, because the decreased *Renilla* activity leads to false activation in the calculation of the relative luciferase units (RLU).

5.8.2.2 Gal4-VP16 control

In the first technical control assay, UAS-Fluc was co-transfected with GV only. There was no effect of Topotecan below 10µM on the GV/UAS-Fluc control assay. Above 10µM Topotecan PC12 cells were dead.

5.8.2.3 TEV protease control

The test showed a mild effect on the TM-TEV/TM-GV system (IC_{50} 8.5µM) but data quality and toxic effects have to be taken into account as well (Figure 60). I can conclude that Topotecan has a strong toxic effect on the cells, but it neither seems to target the firefly luciferase itself, nor to interfere with TEV protease activity.

5.8.2.4 Testing different adapter proteins

The effect of Spironolactone on the recruitment of various other adapter proteins was analysed. The vertical validation of the adapters using the split TEV-based assay showed that the IC_{50} for PIK3R1 is at 0.5µM, for SRC kinase at 0.9µM, for GRB2 at 2.8µM, for STAT5A at 2.5µM, and for SHC1 at 2.2µM. These data suggest that in particular the binding of the adapter molecules PIK3R1 and SRC to the ERBB4 receptor is inhibited by Topotecan, but the difference observed was not as strong as for Spironolactone (Figure 61).

5.8.3 Horizontal validation

The horizontal validation showed no inhibitory effect of Topotecan on ERBB1 and ERBB2 homodimers, and on ERBB1/ERBB2 heterodimers stimulated with 10ng/ml EGFld, as they are not activated (Figure 62).

However, Topotecan showed an inhibitory effect on most ERBB homo/heterodimers, with an IC_{50} of 2.7µM for ERBB1/3, 2.0µM for ERBB1/4, 0.9µM for ERBB2/3, 2.3µM for ERBB2/4, 2.3µM for ERBB3/3, 2.4µM ERBB3/4, and 1.0µM for ERBB4/4 (Figure 62). ERBB2/3 heterodimers and ERBB4 homodimers are of particular interest, displaying IC_{50} values of 0.9µM

and 1.0µM, thus having IC_{50} values that are within the range of the inhibitory effect for ERBB4/PIK3R1 and ERBB4/SRC assays (Figure 63).

5.8.3.1 ERBB2/ERBB4 dimerisation and adapters

To get further insight into Spironolactone's specificity towards the potential inhibition of ERBB2/4, the adapter recruitment for ERBB2/4 heterodimers was analysed. The validation of ERBB2/4 adapter recruitment showed IC_{50} values of 0.6µM for ERBB2/4/SHC, 0.7µM for ERBB2/4/GRB2, 0.8µM for ERBB2/4/SRC, 2.1µM for ERBB2/4/PIK3R1, and 0.7µM for ERBB2/4/STAT5A (Figure 65).

5.8.3.2 ERBB2/ERBB3 dimerisation and adapters

Likewise, the adapter recruitment for ERBB2/3 heterodimers was measured. The validation of ERBB2/3 adapter recruitment showed IC_{50} values of 0.8µM for ERBB2/3/SHC1, 2.3µM for ERBB2/3/GRB2, 1.7µM ERBB2/3/SRC, 1.1µM for ERBB2/3/PIK3R1, and 0.8µM for ERBB2/3/STAT5A (Figure 64).

Topotecan inhibits all measured ERBB homo and heterodimerisations within a comparable range. Therefore, Topotecan is not an ERBB4-specific inhibitor.

5.8.4 Orthogonal validation

5.8.4.1 ERBB1/ERBB1/EGF

ERBB1/1 (EGFR-homodimerisation) stimulated with 1ng/ml EGF showed an inhibition of the homodimerisation at IC_{50} values of 0.5µM, but the inhibition seemed to be incomplete (Figure 67).

5.8.4.2 FRB/FKBP model interaction induced by Rapamycin

To address whether Topotecan is specific to the inhibition of ERBB receptor-mediated signalling, I tested Topotecan's effect in a another split TEV assay that used the Rapamycin-regulated model interaction of a membrane-targeted FRB fused to the NTEV moiety (TM-FRB-NTEV) and a cytosolic FKBP fused to the CTEV moiety (FKBP-CTEV).

TM-FRB-NTEV and FKBP-CTEV were pre-stimulated with 10nM Rapamycin to ensure occurred interaction. Addition of Topotecan showed no effect, suggesting that it does not affect protein-protein interactions in general (Figure 68).

5.8.4.3 ERBB4/PIK3R1 assay and effects caused by Irinotecan and SN38

Irionotecan, a second-generation drug of Camptothecin (i.e. Topotecan derivative), was also present in the NCC003 library. Of interest, Irinotecan had

no effect on the ERBB4/PIK3R1 co-culture assay. Irinotecan is a pro-drug that has to be activated in the liver (Xie et al., 2003). As the co-culture assay cannot provide a metabolic functionality that is present in the liver, I tested the activated Irinotecan-metabolite SN38 (Chabot 1998). SN38 did not show any inhibitory or activatory activity in the ERBB4/PIK3R1 co-culture assay (Figure 66). The analysis of Irinotecan and SN 38 suggests that the measured effect is Topotecan-specific and not a general effect of Camptothecin analogues.

5.8.4.4 Summary validation Topotecan

Technical validation			**IC_{50}**
	Rluc		n.c.
	GV		n.c.
TM-TEV	TM-GV		8.5
NTEV-tevS-GV	**CTEV**		**IC_{50}**
ERBB4	ERBB4		1.0
ERBB3	ERBB4		2.4
	ERBB3		2.3
ERBB2	ERBB4		2.3
	ERBB3		0.9
	ERBB2		n.c.
ERBB1	ERBB4		2.0
	ERBB3		2.7
	ERBB2		n.c.
	ERBB1		n.c.
NTEV-tevS-GV	**CTEV**		**IC_{50}**
ERBB4 homodimerisation	SHC1		2.2
	GRB2		2.8
	SRC		0.9
	PIK3R1		0.4
	STAT5A		2.5
V5tag	**NTEV-tevs-GV**	**CTEV**	**IC_{50}**
ERBB2	ERBB3	SHC1	0.8
	ERBB3	GRB2	2.3
	ERBB3	SRC	1.7
	ERBB3	PIK3R1	1.1
	ERBB3	STAT5A	0.8
ERBB2	ERBB4	SHC1	0.6
	ERBB4	GRB2	0.7
	ERBB4	SRC	0.8
	ERBB4	PIK3R1	2.1
	ERBB4	STAT5A	0.7

NTEV-tevS-GV	CTEV	Drug	IC_{50}
ERBB1	ERBB1	EGF	0.5
ERBB4	PIK3R1	co-culture assay	0.4
ERBB4	PIK3R1	SN38	90.6

Table 16: Summary of IC_{50} values

From these data, Topotecan was found to be an inhibitor of ERBB dimerisation and adapter recruitment. Binding of Topotecan to ERBB receptors has to be further validated. However, the severe side effects of Topotecan, resulting from its anti-topoisomerase I effects, makes the usage of Topotecan for the treatment of psychiatric patients highly unlikely (Alimonti et al., 2004). To use the potential of Topotecan in this setting, an in-depth analysis of the underlying mechanisms related to the toxicity has to be performed. Only then, it might be worth to look at new lead structures for further developments.

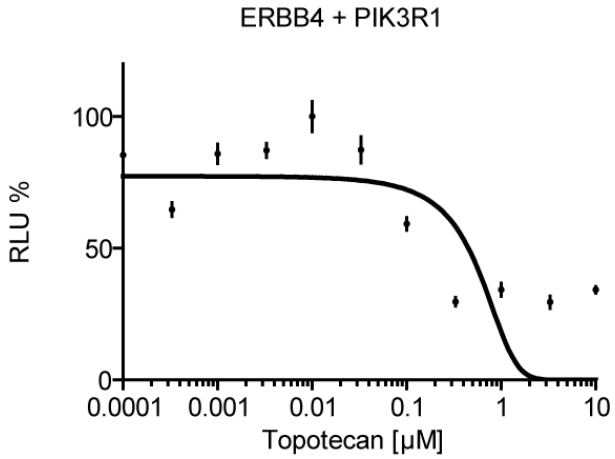

Figure 59: ERBB4/PIK3R1 co-culture assay

A) ERBB4 was fused to NTEV-tevS-GV-2HA; PIK3R1 was fused to CTEV-2HA. Cells were stimulated with 10ng/ml EGFld.

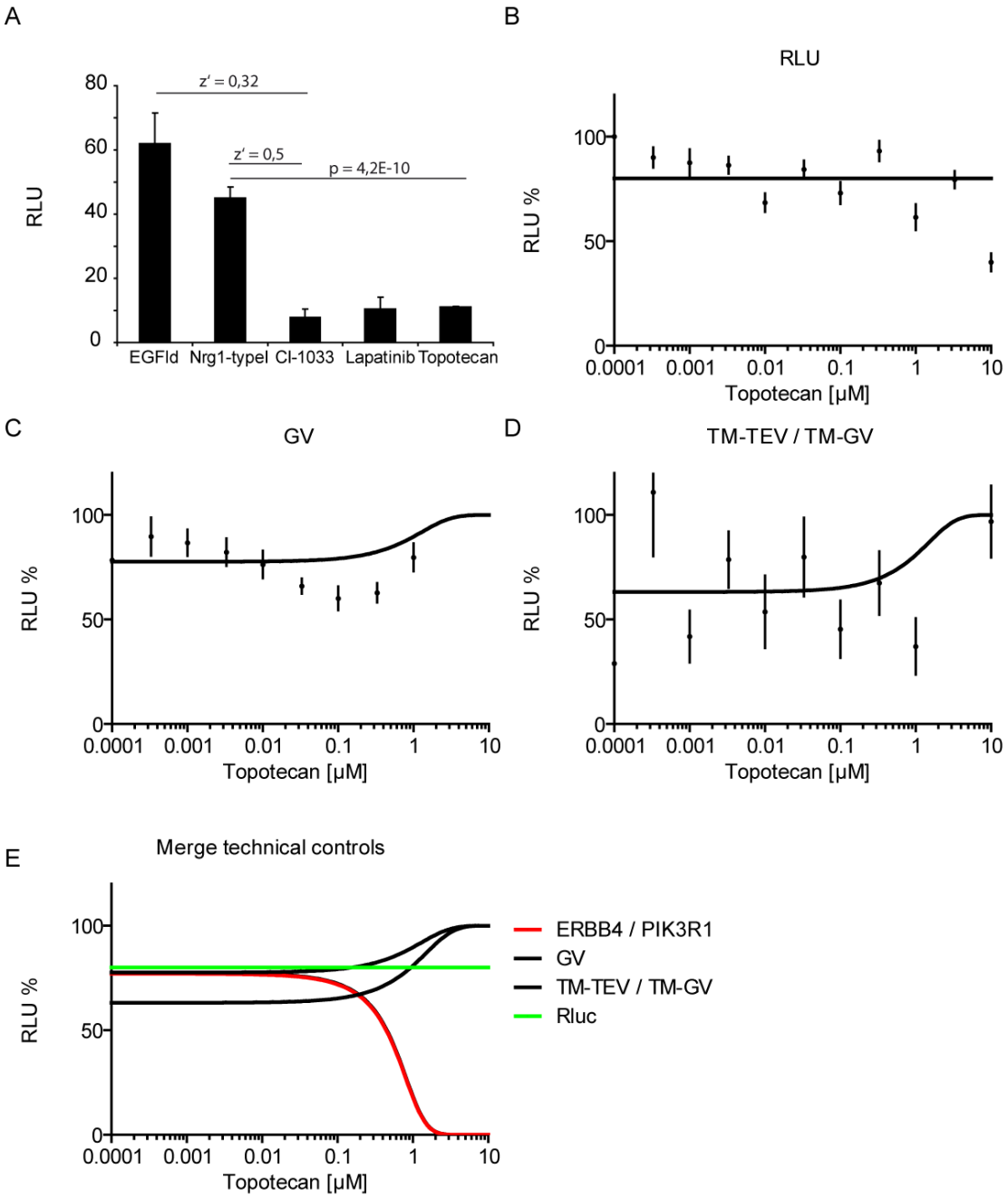

Figure 60: Technical controls for Topotecan

A) Data set from the NCC003 screen. Topotecan significantly inhibits Nrg1-typeI-stimulated ERBB4/PIK3R1signalling. B) *Renilla* luciferase assay. Cells were transfected with 20ng/well TK-Rluc. C) GV control assay in PC12 cells. Cells were transfected with 20ng/well CMV-GV, UAS-Fluc, and TK-Rluc. D) TM-TEV/TM-GV control assay in PC12 cells. Cells were transfected with 20ng/well TM-TEV and TM-GV.E) Datasets shown from (B) to (D) were merged. The ERBB4/PIK3R1 assay is shown in red.

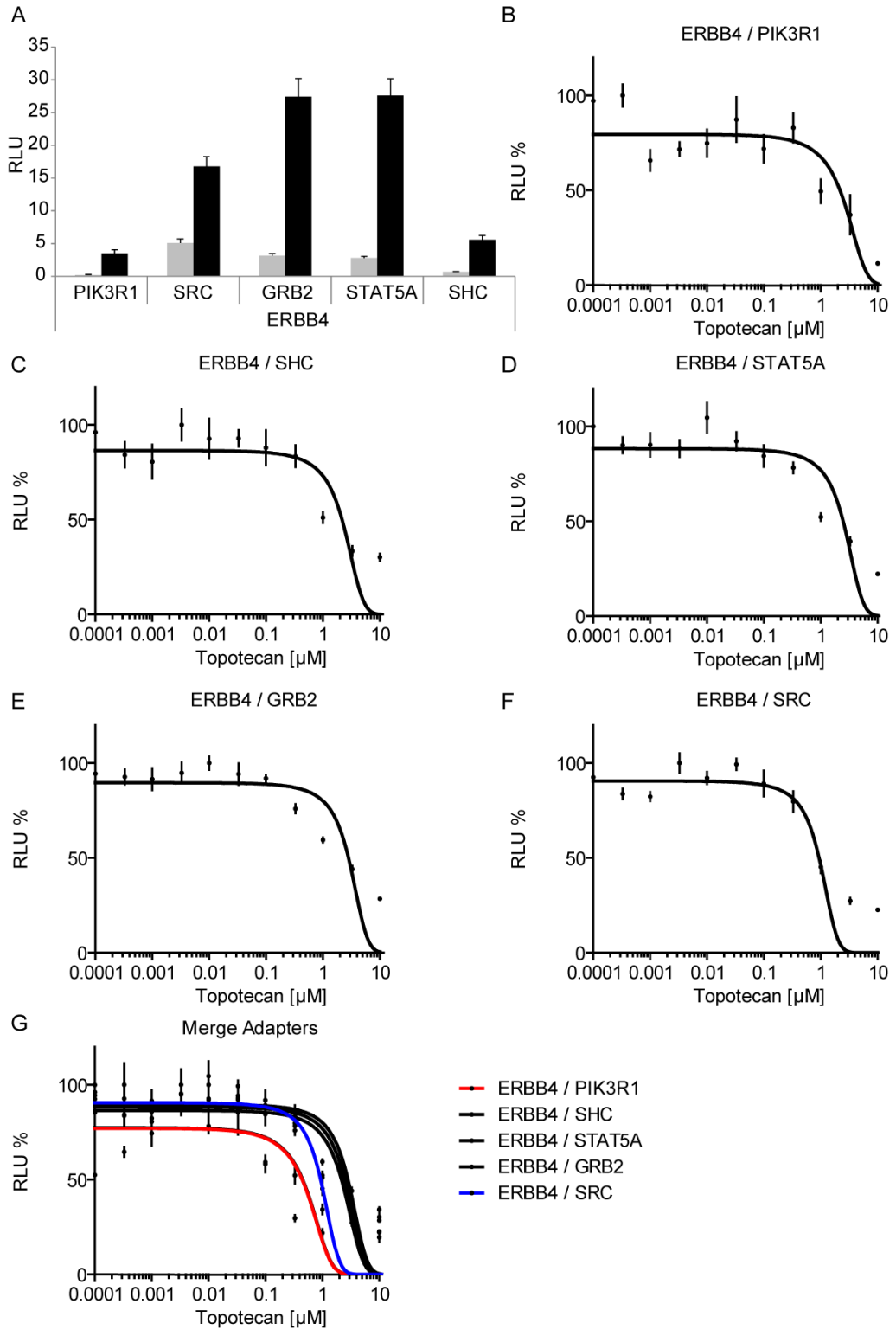

Figure 61: Vertical validation Topotecan ERBB4/adapter recruitment

A) ERBB4/adapter recruitment. ERBB4 was fused to NTEV-tevS-GV-2HA; adapters were fused to CTEV-2HA. Cells were stimulated with 10ng/ml EGFld. B-F) ERBB4/adapter recruitment. ERBB4 was fused to NTEV-tevS-GV-2HA; adapters were fused to CTEV-2HA. PC12 cells were stimulated with 10ng/ml EGFld. G) Comparison of ERBB4/adapter recruitment assays to ERBB4-PIK3R1 recruitment assay (red). ERBB/adapter recruitment for SHC1, GRB2, and STAT5A are less efficiently inhibited compared to the ERBB4/PIK3R1 recruitment.

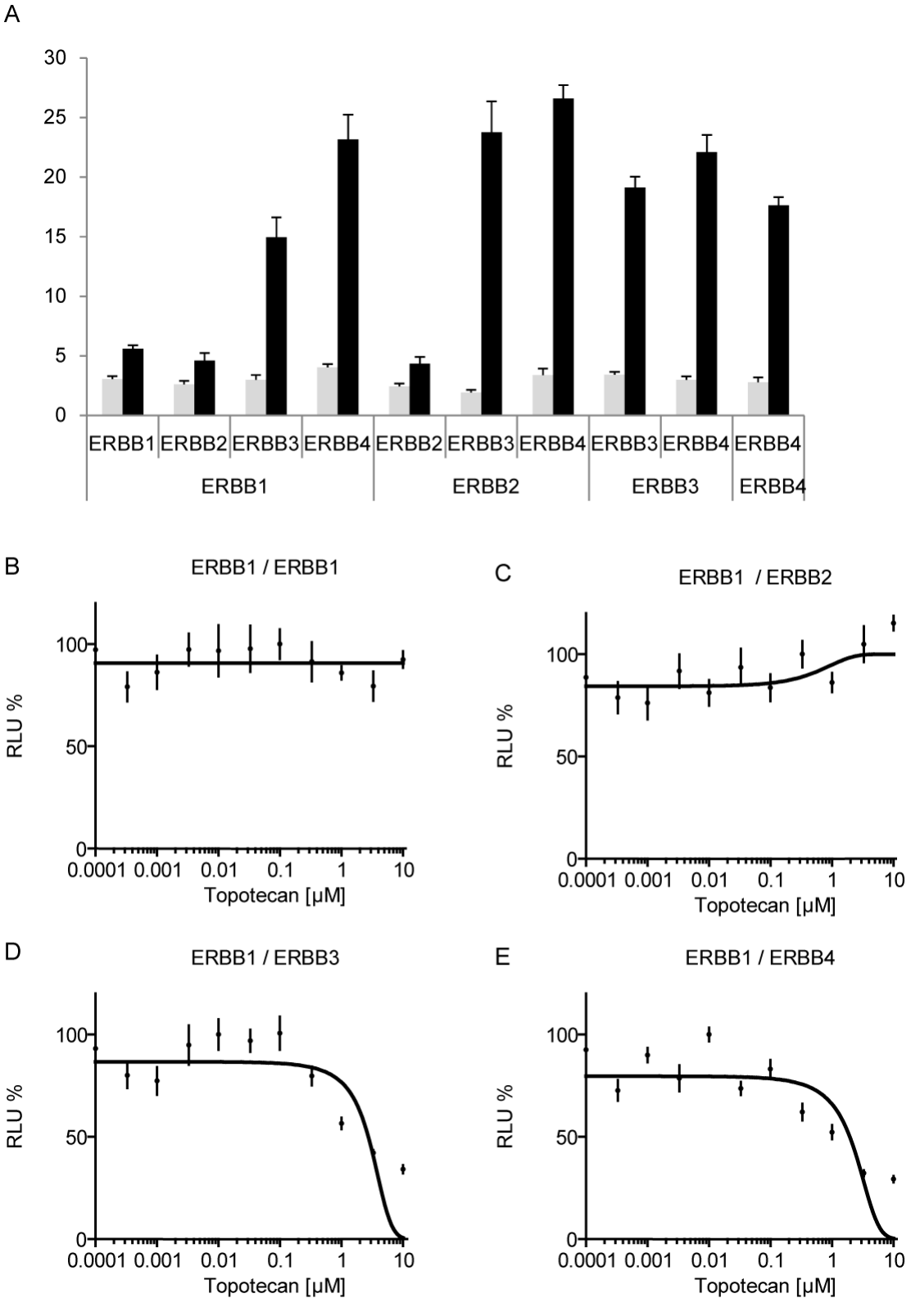
A
30
25
20
15
10
5
0
ERBB1
ERBB2
ERBB3
ERBB4
ERBB2
ERBB3
ERBB4
ERBB3
ERBB4
ERBB4
ERBB1
ERBB2
ERBB3
ERBB4
B
ERBB1 / ERBB1
RLU %
100
50
0
0.0001 0.001 0.01 0.1 1 10
Topotecan [µM]
C
ERBB1 / ERBB2
RLU %
100
50
0
0.0001 0.001 0.01 0.1 1 10
Topotecan [µM]
D
ERBB1 / ERBB3
RLU %
100
50
0
0.0001 0.001 0.01 0.1 1 10
Topotecan [µM]
E
ERBB1 / ERBB4
RLU %
100
50
0
0.0001 0.001 0.01 0.1 1 10
Topotecan [µM]

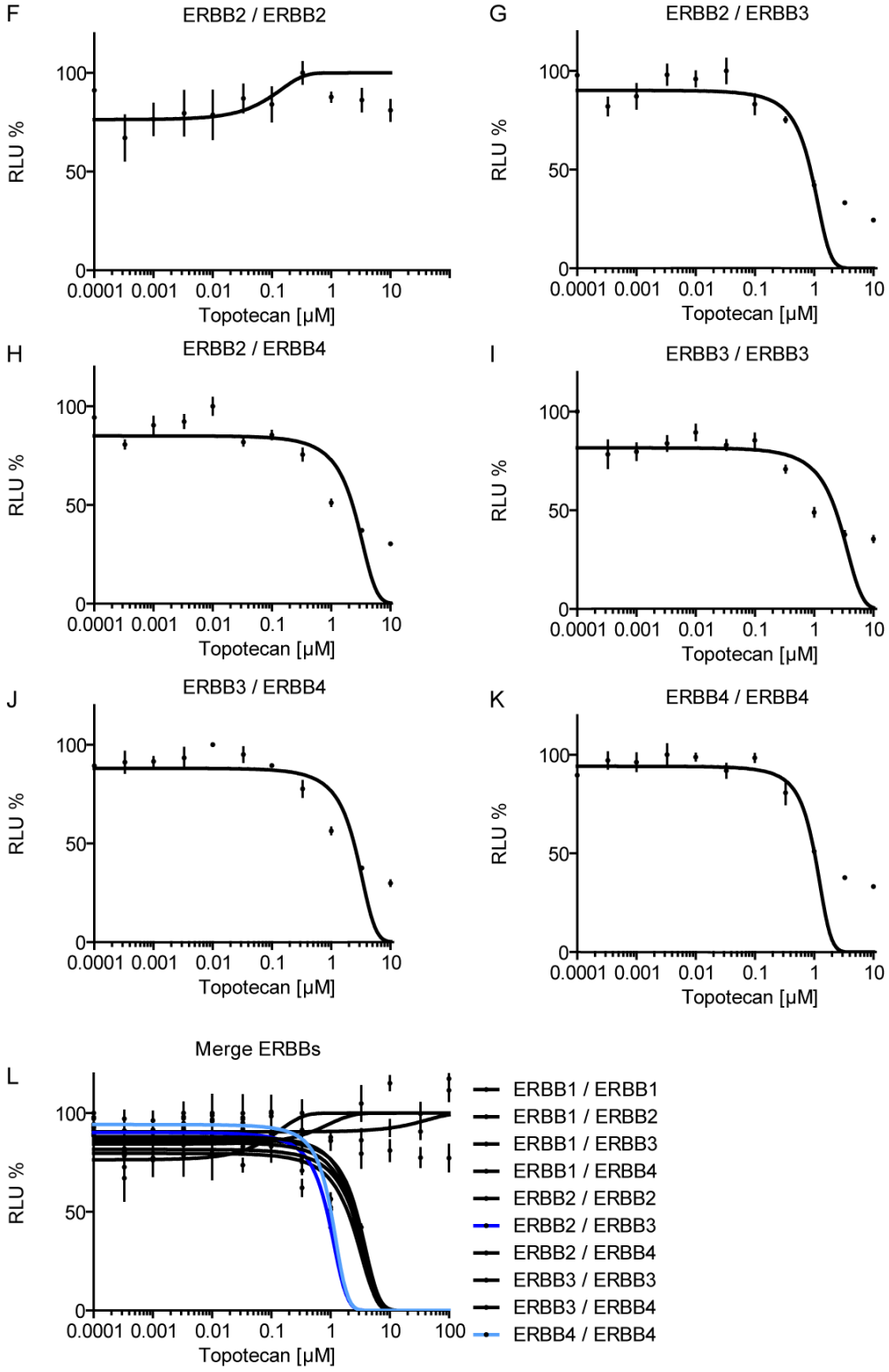

Figure 62: Homo and heterodimerisation of ERBB receptors

A) ERBB homo- and heterodimerisation. ERBBx/ERBBy split TEV assay in PC12 cells. ERBBx was fused to NTEV-tevS-GV-2HA; ERBBy was fused to CTEV-2HA. Cells were stimulated with 10 ng/ml EGFld. B-K) ERBB homo- and heterodimerisations. ERBBx was fused to NTEV-tevS-GV-2HA; ERBBy was fused to CTEV-2HA. PC12 cells were stimulated with 10 ng/ml EGFld. L) Comparison of ERBB homo- and heterodimerisation assays to ERBB4-PIK3R1 recruitment. ERBB homo/heterodimerisations are less efficiently inhibited compared to ERBB4-PIK3R1 recruitment.

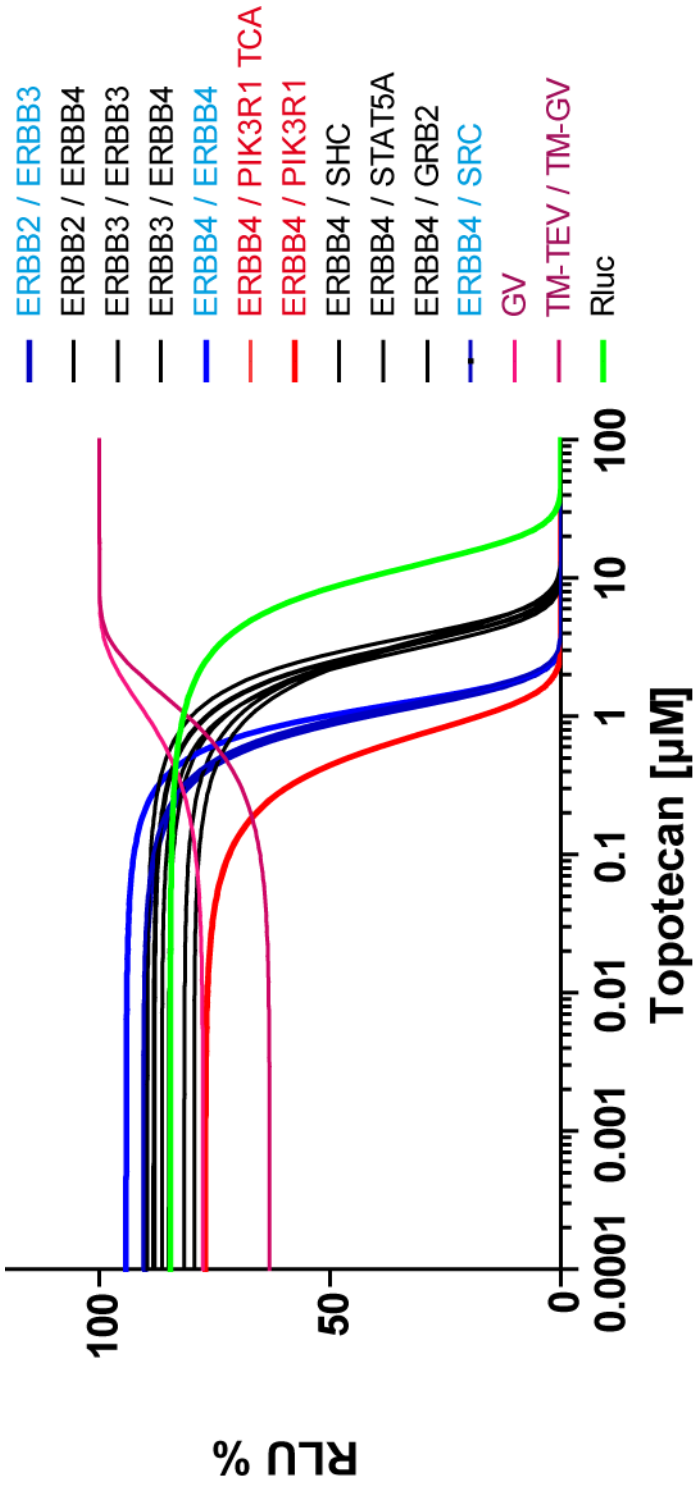

Figure 63: Summary on Topotecan validation

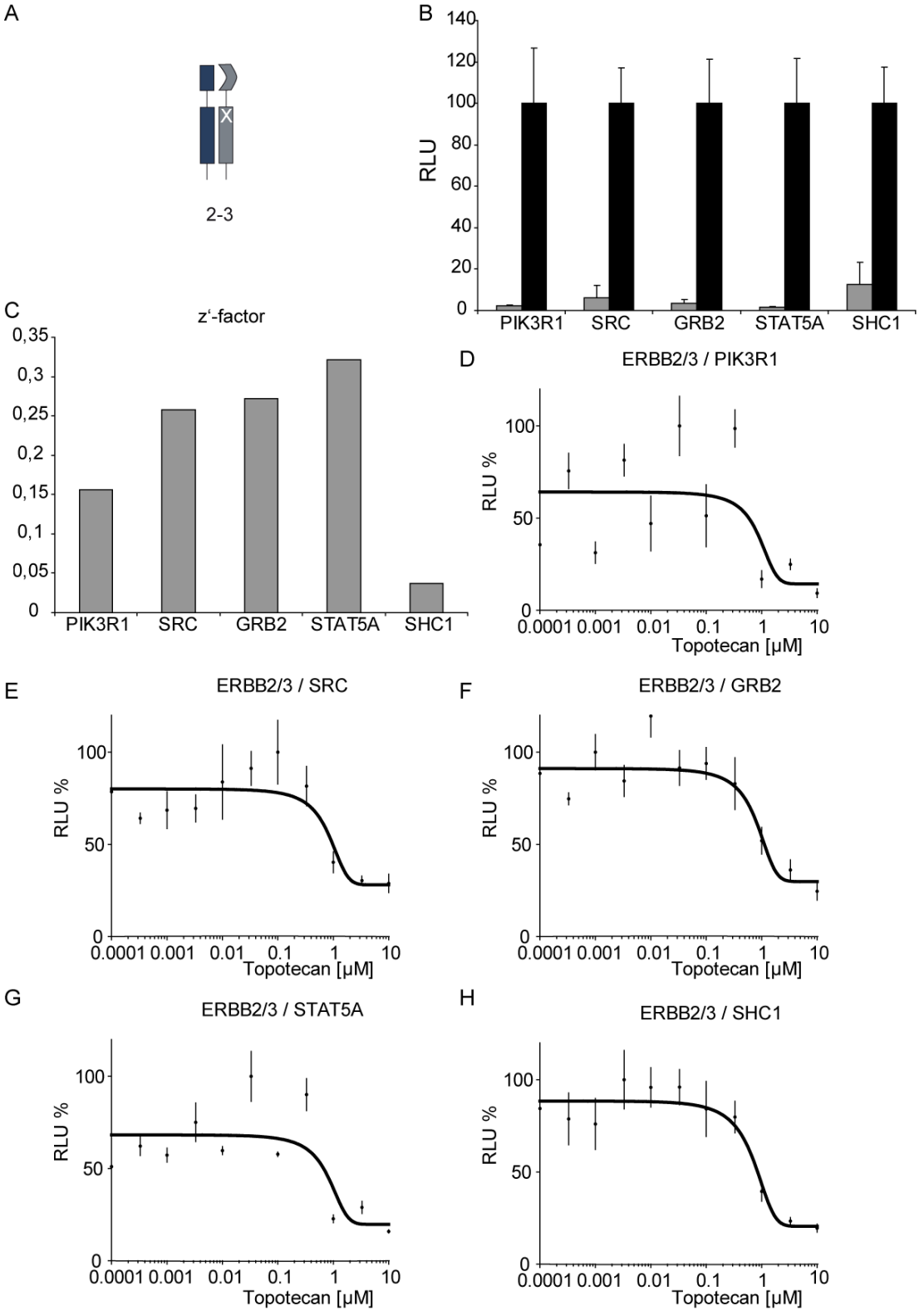

Figure 64: Horizontal validation ERBB2/ERBB3/adapters

A) Schematic representation ERBB2/ERBB3 heterodimerisation. B) Assay performance. ERBB2/ERBB3 heterodimerise after stimulation with 10 ng/ml EGFld and recruit adapters as indicated. C) Comparison of the z'-factors obtained from the assays. D-H) ERBB2/ERBB3/various adapters. ERBB2 was fused to a V5 tag, ERBB3 was fused to NTEV-tevS-GV-2HA; adapters were fused to CTEV-2HA. PC12 cells were stimulated with 10 ng/ml EGFld.

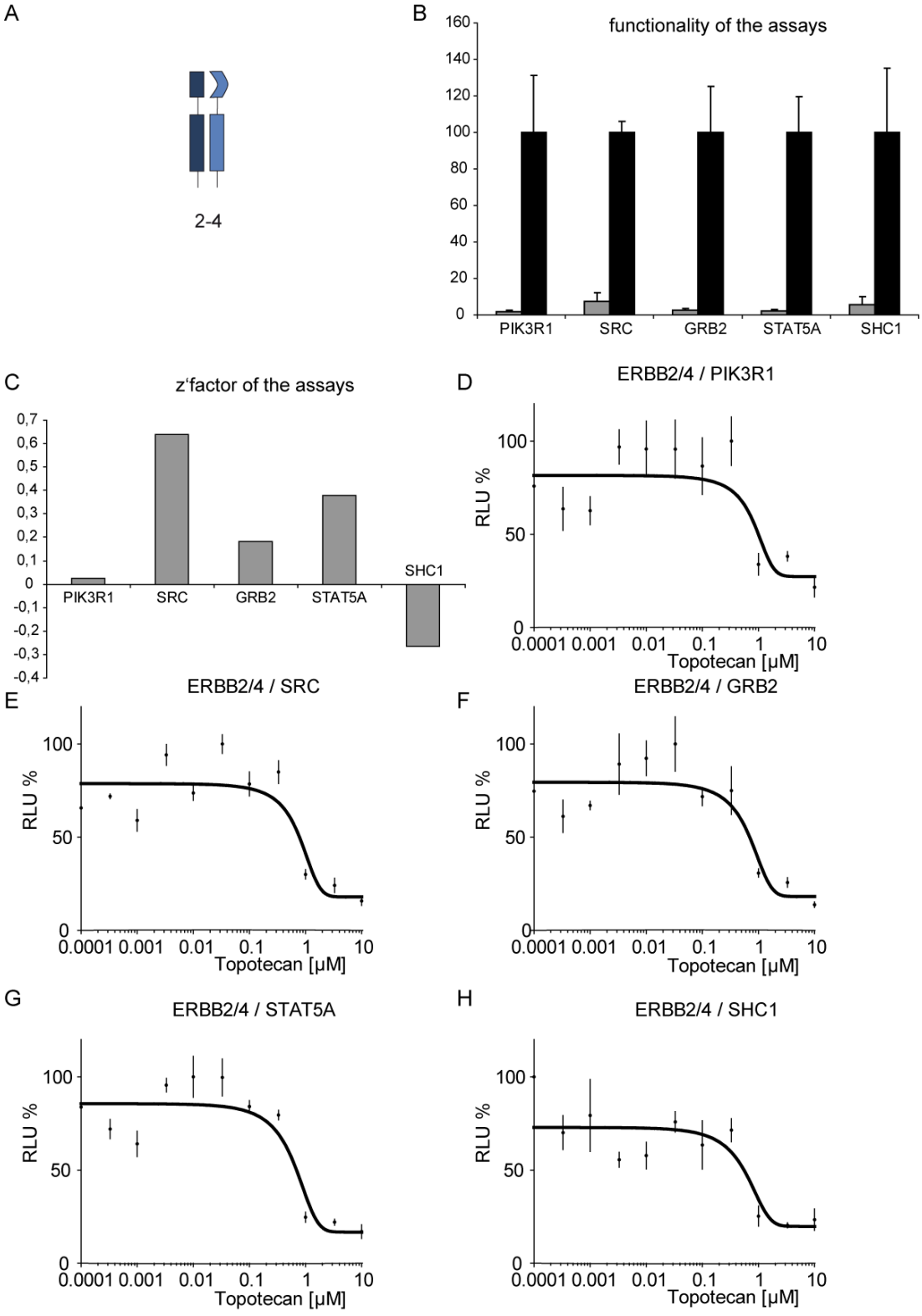

Figure 65: Horizontal validation for Topotecan's effect on ERBB2/ERBB4/adapters

A) Schematic representation ERBB2/ERBB4 heterodimerisation. B) Assay performance. ERBB2/ERBB4 heterodimerise after stimulation with 10 ng/ml EGFld and recruit adapters as indicated. C) Comparison of the z'-factors obtained from the assays. D-H) ERBB2/ERBB4/various adapters. ERBB2 was fused to a V5 tag, ERBB4 was fused to NTEV-tevS-GV-2HA; adapters were fused to CTEV-2HA. PC12 cells were stimulated with 10ng/ml EGFld.

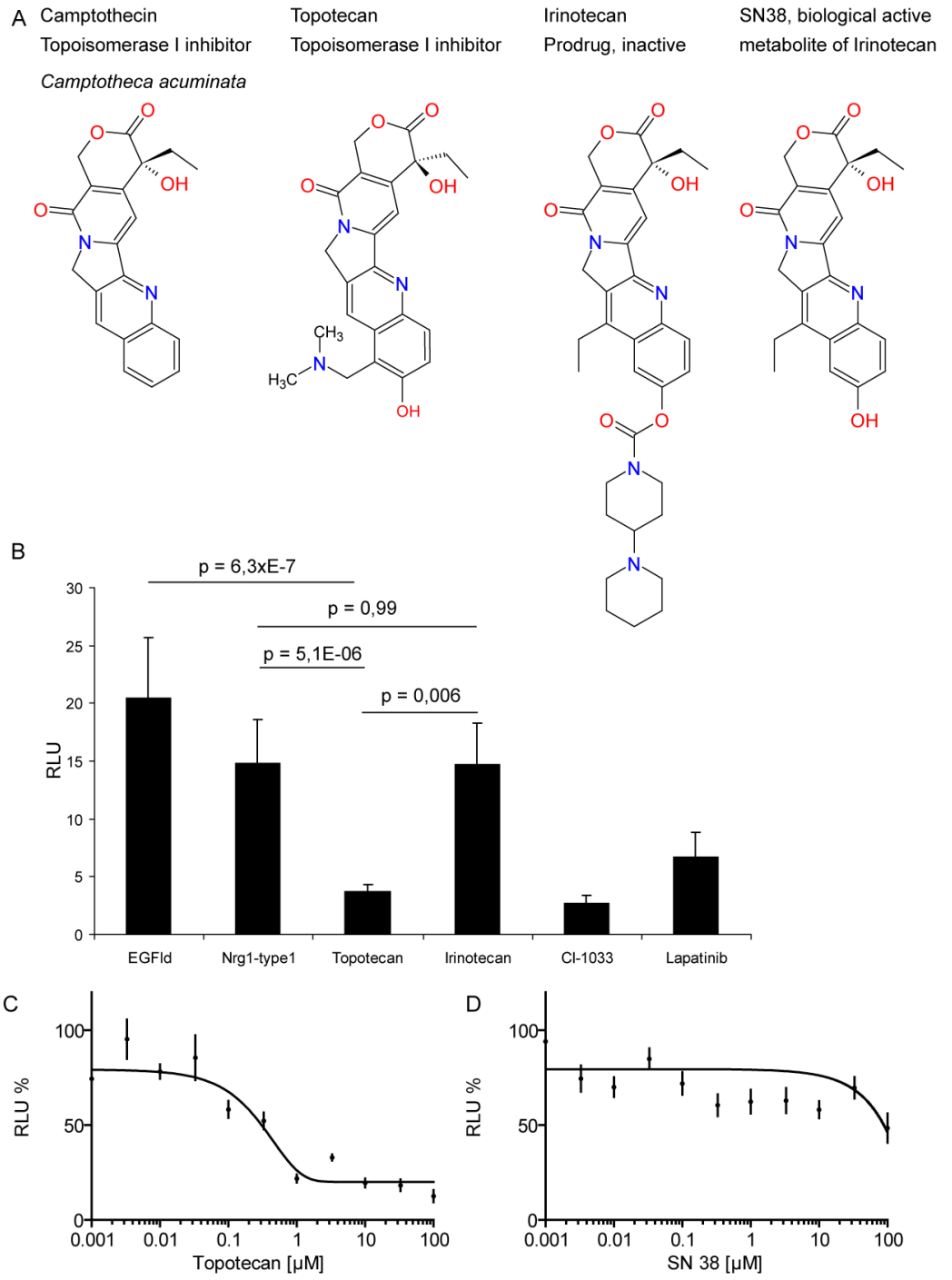

Figure 66: Effect of Topotecan derivatives Irinotecan and SN38 on the ERBB4/PIK3R1 split TEV assay

A) Comparison of the chemical structures of Camptothecin derivates. Chemical structures of Camptothecin, Topotecan, Irinotecan, SN38. B) Data set from the NCC003 screen. The difference between Topotecan and Irinotecan on the ERBB4/PIK3R1 co-culture screen is shown. C-D) Individual effects of Topotecan (C) and SN38 (D).
ERBB4 was fused to NTEV-tevS-GV-2HA; PIK3R1 was fused to CTEV-2HA. Cells were stimulated with 10ng/ml EGFld.

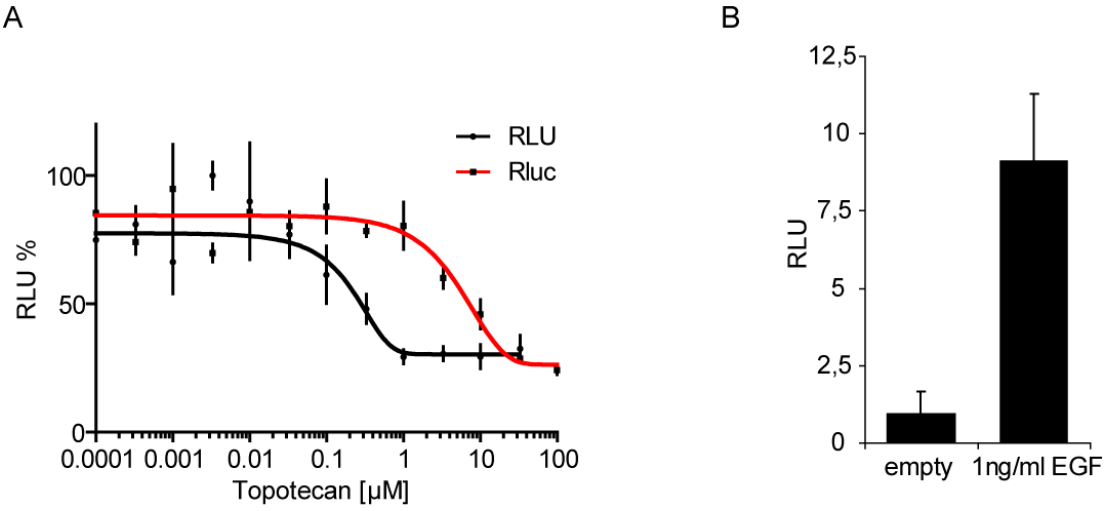

Figure 67: Effect of Topotecan on ERBB1/1 dimerisation induced by EGF

A) ERBB1 was fused to NTEV-tevS-GV-2HA; ERBB1 was fused to CTEV-2HA. PC12 cells were stimulated with 1 ng/ml EGF. B) Activation window of the EGF-induced ERBB1/1 assay. Setup as in (A).

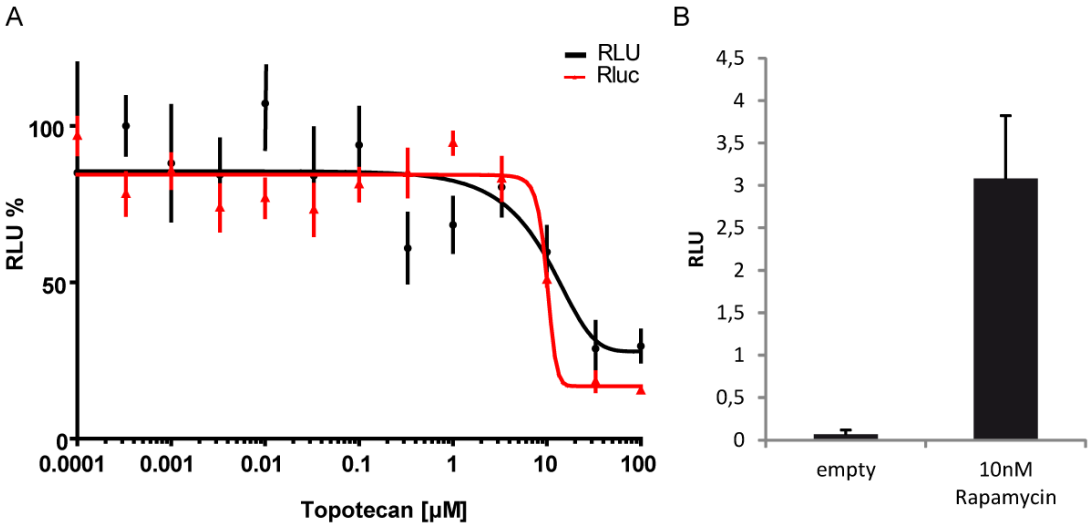

Figure 68: Effect of Topotecan on the FRB/FKBP interaction induced by Rapamycin

A) TM-FRB was fused to NTEV-tevS-GV, FKBP was fused to CTEV. PC12 cells were stimulated with 10nM Rapamycin. B) Activation window of the Rapamycin-induced FRB/FKBP assay. Setup as in (A).

5.9 Validation Mevastatin

Mevastatin (Compactin penicillium) is an antifungal metabolite from Penicillium breviocompactum. It is an HMG-CoA reductase inhibitor (cholesterol biosynthesis) with multiple side effects, which prevent the therapeutic usage.

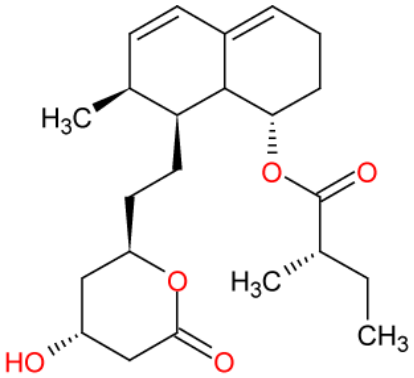

Figure 69: Chemical structure of Mevastatin

Mevastatin showed a significant activation of the firefly luciferase activity in the screen. In the ERBB4/PIK3R1 assay activated with 10ng/ml EGF-like domain it showed a 250% activation of the relative luciferase activity at an EC_{50} of 0.7µM.

5.9.1 Technical controls for Mevastatin

Renilla luciferase

In the *Renilla* luciferase assay Mevastatin showed a toxic effect wit an IC_{50} of 0.4µM.

The comparison of both datasets indicate that the activation of the relative luciferase activity is reciprocal to the toxic effect of Mevastatin on the PC12 cells e.g. the *Renilla* luciferase activity.

Mevastatin has no specific effect on the ERBB4/PIK3R1 co culture assay. The Mevastatin dataset is an excellent example for the elimination of false positive hits from the screening results.

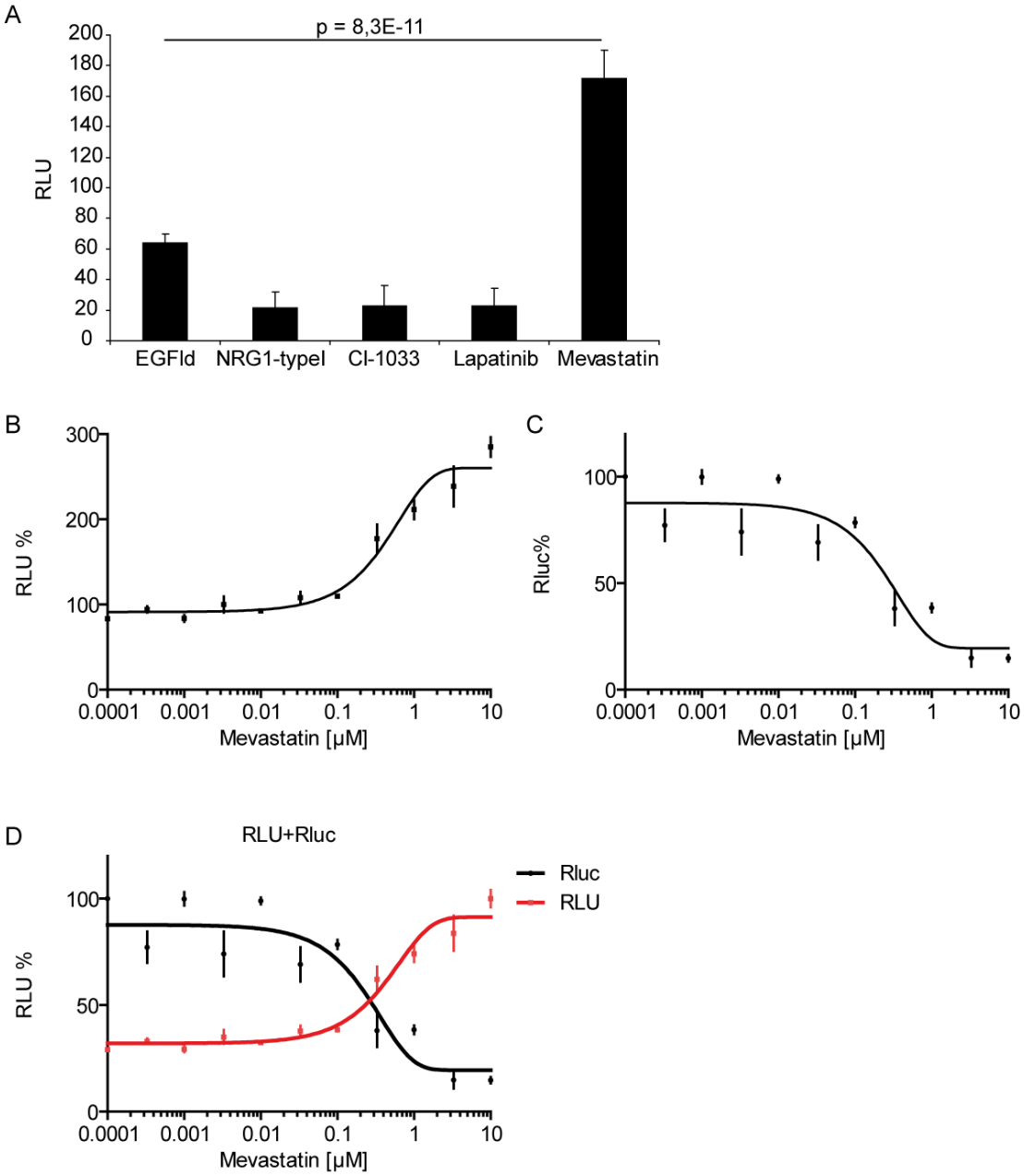

Figure 70: Validation Mevastatin

A) Data extracted from the screen. B) ERBB4/PIK3R1 10 ng/ml EGFld. ERBB4 was fused to NTEV-tevS-GV-2HA; PIK3R1 was fused to CTEV-2HA. PC12 Cells were stimulated with 10 ng/ml EGFld. C) *Renilla* luciferase assay to test the toxicity of Mevastatin. D). Comparison ERBB4/PIK3R1 and *Renilla* luciferase, the increment of growth of the RLU value is dependent on the decrease in Rluc.

5.10 Validation CCPA

2-chloro-N(6)-cyclopentyladenosine (CCPA) is a specific agonist for the Adenosin A1 receptor (Gao and Jacobson, 2002).

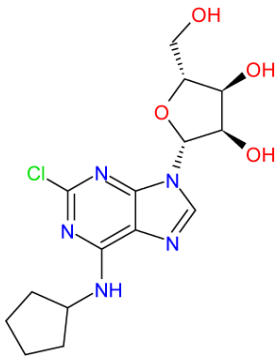

Figure 71: Chemical structure of CCPA

CCPA showed a significant activation of the firefly activity in a preliminary co-culture screen witch did not reach a z'-factor of 0.5. CCPA showed a two fold activation of the firefly luciferase activity in the ERBB4/PIK3R1 co-culture assay.

5.10.1 Technical controls for CCPA

***Renilla* luciferase**

CCPA showed no toxic effect on the *Renilla* luciferase.

The Gal4-VP16 control assay

In the technical vallidation CCPA showed an two fold activation of the firefly activity.

TEV protease control assay

In the TM-TEV/TM-GV assay CCPA showed a two fold activation of the firefly activity.

5.10.2 Vertical validation

CCPA showed although a two fold activation of ERBB4/SHC adapter recruitment and a two fold activation of ERBB4 homodimerisation.

As the technical controls indicate CCPA is not an activator of the NRG1-ERBB4 system. It interfers unspecific with the firefly activity or cell activity, activating it 2 fold between a CCPA concentration of 0.01µM and 1µM.

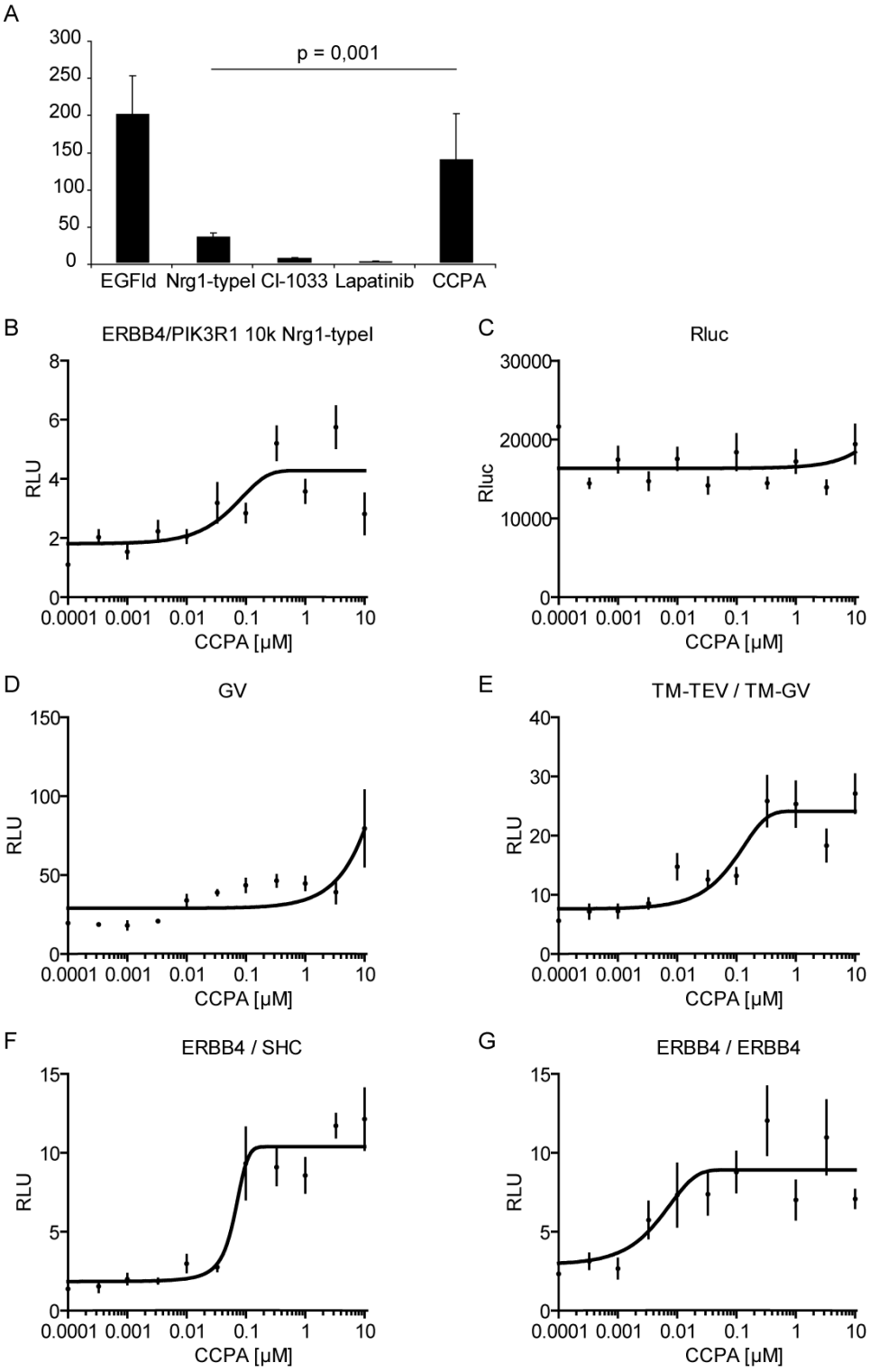

Figure 72: Validation CCPA

A) Extracted data from the screen. B) Co culture assay Nrg1-typeI-ERBB4/PIK3R1. Split TEV assay in PC12 cells. ERBB4 was fused to NTEV-tevS-GV-2HA; PIK3R1 was fused to CTEV-2HA. C) *Renilla* luciferase assay to test the toxicity of CCPA. D) GV/ UAS-Fluc. E) TM-TEV/TM-GV.F) ERBB4/SHC split TEV assay in PC12 cells. ERBB4 was fused to NTEV-tevS-GV-2HA. SHC was fused to CTEV-2HA. Cells were stimulated with 10 ng/ml EGFld. G) ERBB4/ERBB4 split TEV assay in PC12 cells. ERBB4 was fused to NTEV-tevS-GV-2HA. ERBB4 was fused to CTEV-2HA. Cells were stimulated with 10 ng/ml EGFld.

5.11 Validation Vincristine, effects on *Renilla* luciferase

Vindesine and Vincristine are vinca alkaloid derivatives from *Catharanthus roseus*. (Madagaskar Evergreen). They are antimitotic chemotherapeutics used in the treatment of cancer and as immunosuppressive drugs. The akaloids interfere with the formation of tubulin into microtubules therby inhibiting cell division. Further effects are on RNA/DNA synthesis, lipid biosynthesis, cyclic nucleotide metabolism, glutathione metabolism and calmodulin-dependent CA^{2+}-transport ATPase (Jordan et al., 1985).

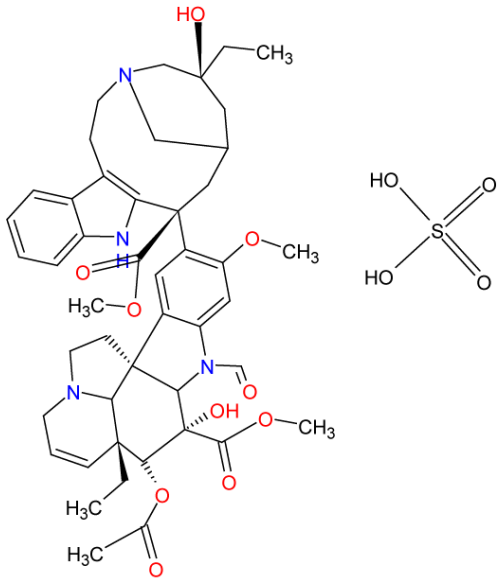

Figure 73: Chemical structure of Vincristine sulfat

Vindesine and vincristine showed a minor significant activation of the firefly activity ($p<0.009$) in a preliminary co-culture screen that did not reach a z'-factor of 0.5. Vinchristine was further analysed and showed a 10 fold activation of the firefly luciferase activity between 0.001µM and 1µM in the complete ERBB4/PIK3R1 co-culture assay. It showed a high toxic effect on the *Renilla* luciferase assay at an IC_{50} of 0.015µM reducing *Renilla* luciferase activity. In the technical vallidation Vincristine showed a ten fold activation of the GV/UAS-Fluc assay and a ten fold activation of the TM-TEV/TM-GV assay. Both increases in the relative luciferase values are due to the 90% decrease of *Renilla* luciferase activity.

Vincristine showed although a ten fold activation of ERBB4/SHC and a ten fold activation of the ERBB4 homodimers.

As the technical controls indicate Vincristine is not an activator of the Nrg1-typeI-ERBB4 signalling system. It interfers with the *Renilla* activity, decreasing the *Renilla* activity with an IC_{50} of 0.015µM. The observed activation is a pure

mathematical artefact, resulting from the calculation of relative luciferase units (RLU).

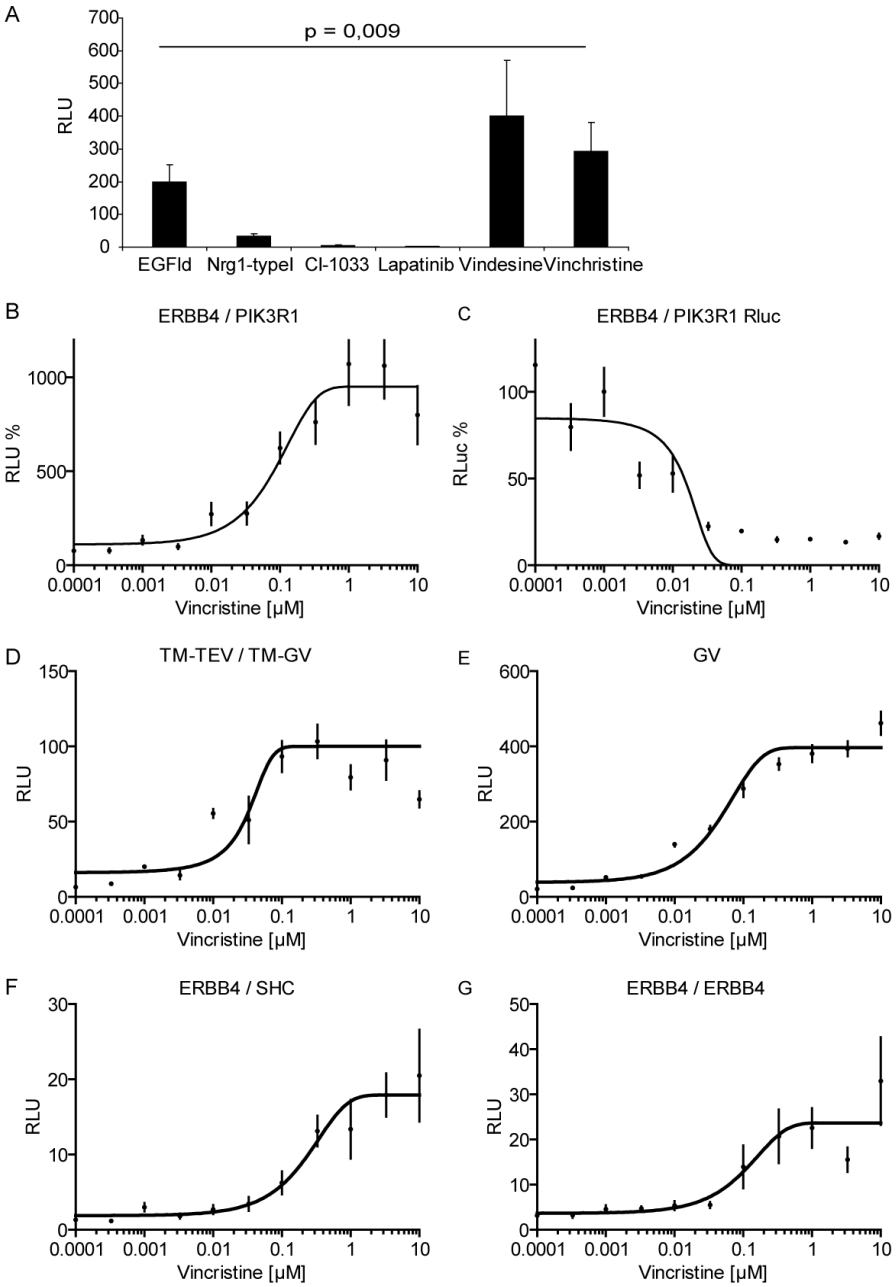

Figure 74: Validation Vincristine

A) Extracted data from the screen. B) Co culture assay Nrg1-typeI-ERBB4/PIK3R. Split TEV assay in PC12 cells. ERBB4 was fused to NTEV-tevS-GV-2HA; PIK3R1 was fused to CTEV-2HA. C) Renilla luciferase assay to test the toxicity of Vincristine. D) GV/UAS-Fluc. E) TM-TEV/TM-GV. F) ERBB4/SHC split TEV assay in PC12 cells. ERBB4 was fused to NTEV-tevS-GV-2HA. SHC was fused to CTEV-2HA. Cells were stimulated with 10 ng/ml EGFld. G) ERBB4/ERBB4 split TEV assay in PC12 cells. ERBB4 was fused to NTEV-tevS-GV-2HA. ERBB4 was fused to CTEV-2HA. Cells were stimulated with 10 ng/ml EGFld.

5.12 Validation K252a

The Indolocarbazole K252a is an alkaloid from *Nocardiopsis spec*. and a Staurosporin analogue. It is a highly specific CaM kinase and phosphorylase inhibitor (IC_{50} 1.8 and 1.7nmol) and a serine/threonine protein kinase inhibitor (IC_{50} 10 to 30nmol) (Borasio, 1990).

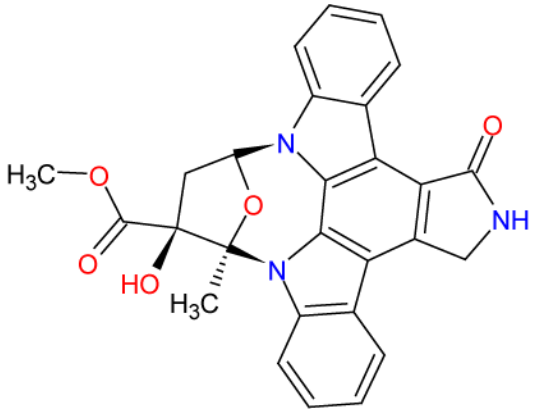

Figure 75: Chemical structure of K252a

K252a was described by Kuai (Kuai et al., 2010) to potentiate Nrg1 induced neuritogenesis in PC12 cells transfected with ERBB4. In addition, Kuai et al. showed that the effect of K252 depends on the potentiation of the localisation of ERBB4 receptors to the membrane and an elevation of ERBB4 receptors in the membrane due to altered endocytosis (Kuai et al., 2011). Therefore, I wished to test, whether K252a could activate NRG1-ERBB4 signalling using the split TEV ERBB4/PIK3R1 co-culture assay. However, K252a did not activate ERBB4 signalling, and proved only to be toxic for the cells.

Surprisingly, K252a showed an inhibition of the relative luciferase activity in the ERBB4/PIK3R1 co-culture assay, with an IC_{50} of 0.7µM. The technical control *Renilla* luciferase showed an IC_{50} of 0.2µM K252a. Thus, the reduction in relative luciferase activity was not caused by a specific effect on NRG1-ERBB4/PIK3R1 signalling, but rather through a toxic effect elicited onto the cells.

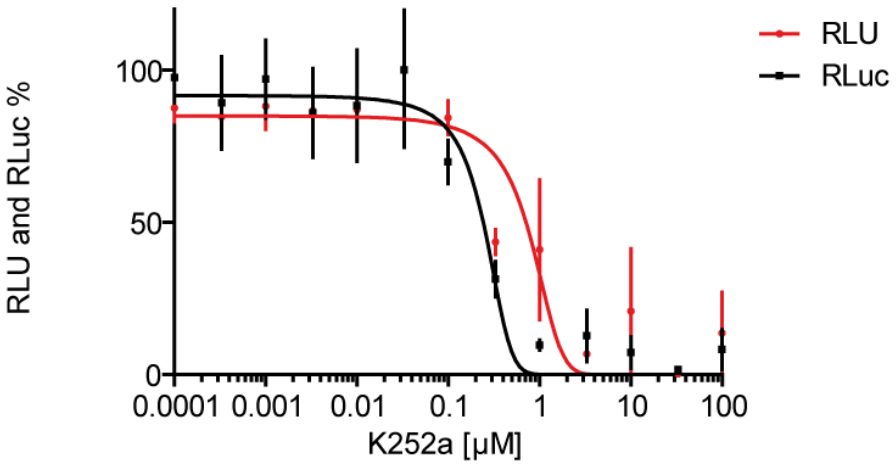

Figure 76: Validation of K252a

ERBB4/PIK3R1 10ng/ml EGFld. ERBB4/PIK3R1 split TEV assay in PC12 cells. ERBB4 was fused to NTEV-tevS-GV-2HA. PIK3R1 was fused to CTEV-2HA. Cells were stimulated with 10ng/ml EGFld. Cells were harvested after 24h and luciferase data was analysed using graph pad prism. n=6, error bars represent standard error of the mean.

6 Discussion

6.1 Technical issues of cell-based assays

6.1.1 Translational assays and using GWAS data to model SZ.

Most of the findings gained from screening assays in animal models remain serendipitous. Animal models for SZ, which mimic the entire complexity of the disease, are not available for SZ (Nestler and Hyman, 2010). Therefore, the lack of construct validity in animal models favours simpler models, with one simple model covering one aspect/genetic trait of SZ. Those molecular isolated aspects of SZ may also be modelled in cell-based assays. Various pathways are known to be involved in SZ on a molecular level, which is consistent which the hypothesis that SZ is also seen as an umbrella term for various diseases with similar disease patterns (Pratt et al., 2012; Keshavan et al., 2008; Marín, 2012).

Several genetic association studies revealed the relevance of malfunctions in the NRG1-ERBB4 signalling system for the development of (Stefansson et al., 2003; Stefánsson et al., 2003; Stefansson et al., 2002; Buonanno, 2010; Li et al., 2004 Lu et al., 2010 Weickert et al., 2012). To address this signalling pathway in more detail, I designed a cell-based co-culture assay that could partially mimics the communication between two distinct neurons via Nrg1-ERBB4. Hits resulting from this compound screen were shown to target the Nrg1-ERBB4 signalling pathway and could be used in the future to treat SZ mouse models to prove the hits' in vivo relevance.

6.1.2 Rational design of the assay workflow

Critical to compound screenings are the time points of measurements(Macarron et al., 2011; Ohlmeyer and Zhou, 2010). Large screens imply the usage of huge substance libraries. These libraries are expensive in maintenance and the costly and laborious handling and storage forces the user to test an individual compound in a primary screen only once. Therefore, only a compound's single effect of a single administration can be usually measured without exceeding available budgets.

This requires assays of highest quality and reliability. Moreover, the handling of the cells and the screening time points have to be adjusted further to get an optimal window for the measurements. This includes several technical issues, such as enzyme activity, instrument availability, and manpower. The applied assay is a transcriptional-based assay with the activity of the firefly luciferase as readout. Firstly, the transfected cells need time to express the components required for the cell-based assay. In our cell-based assay, the cells need 12h

to sufficiently express the components. This is especially important for the correct localisation of the ERBB4 receptor. Secondly, after stimulation, the cell needs 12h time to express the reporter protein to get satisfying levels that can be measured. After testing various combinations and protocols, I decided to apply a 24h/24h measurement cycle, i.e. the cells were allowed to express the assay components for 24h, then stimulated with compounds and controls, and 24h later they were lysed for luciferase assay analysis. This implies a 12h/12h measurement cycle. Also, measurement cycles are possible between 12h–12h and 36h–36h. To integrate the screen in daily working hours a 24h-24h setup is most preferable.

6.1.3 Selection of constructs

Reaching construct validity for SZ is an ambitious goal and is so far not possible. It might be partially possible in the future, when patient-derived induced pluripotent stem cells (iPSC) could be instructed to relevant neirnal lineages and using these cells e.g. in phenotypic screen (Brennand et al., 2011; Brennand and Gage, 2012; Brennand and Gage, 2011). The NRG1-ERBB4 system signalling pathway itself is a proven target, but this signalling network is far more complex to be reflected used in one single assay (Mei and Xiong, 2008). NRG1 has a large number of isoforms (more than 30 are yet described). The isoforms differ in length, function, localisation, and processing properties (Fleck et al., 2011; Luo et al., 2011; Mei and Xiong, 2008; Meyer and Birchmeier, 1995).

ERBB4 consists of four major isoforms (JM-a, JM-b, Cyt1, and Cyt-2)(Zeng et al., 2007a; Yarden and Pines, 2012). To this end it is unknown, which exact isoform(s), has/have what kind of impact on SZ, and in which cell types this may be cause a specific part in SZ. Tremendous effort has been done by the GWAS studies. However, they cannot deliver this kind of information.

For the Nrg1-ERBB4 cell-based assay, I chose Nrg1.typeI-β1a mainly for the reason of assay performance. The Nrg1-typeI containing cells delivered a far better measurement window than the Nrg1-typeIII (Figure 26). The most active part of all NRGs is the EGF like domain, which is encoded in NRG1-typeI-β1a but also in typeIII, and in the corresponding murine versions.

For ERBB4 receptors, I chose the JM-a-Cyt1 variant, as it encodes a PI3K-binding site that is necessary to integrate PI3K signalling given the importance of this downstream process in the context of SZ (Law et al., 2012). All adapters tested performed well when assaying for ERBB4 receptor activation. Importantly, the PI3K adapter protein PIK3R1 performed best, and was recently reported as a SZ target (Law et al., 2012).

The subset of Nrg1-typeI-β1a/ERBB4-JMa-Cyt1/PIK3R1 was mainly chosen to meet the needs of assay performance and not as neccessarily being the most relevant for SZ. Nonetheless, SNPs enhancing the expression of the ERBB4-JMa-Cyt1 variant seems to associated with an elevated risk of SZ (Silberberg et al., 2006; Law et al., 2007).

6.1.4 Artificial and tagged proteins in the cell-based assay

The ERBB4 receptor and the adapter proteins that get recruited to the activated ERBB4 are modified (i.e. tagged) to make them applicable to the split TEV assay technique. For the split TEV system, it has been shown that the TEV fragments do not affect the function of the proteins under investigation (Wehr et al., 2008). However, it cannot be ruled out that some chemical compounds target the TEV fragments. Therefore, false positive hits that could be directed against artificial components of the cell-based assay had to be removed during the secondary analysis.

6.1.5 In vitro screens vs. co-culture screening systems

To date, many large-scale screens are done in in-vitro assays (Macarron et al., 2011; Inglese et al., 2007). These screens deliver fast and specific binding data for substances that perform excellent against a single target. However, the absence of the biological context results in high attrition rates for compounds identified in in-vitro binding assays due to unanticipated off-target effects that are detected in later phases. For example, off-target effects can be caused by unspecific activation of non-desired signalling pathways that act opposite to the desired effects.

Cell-based screens allow the integration of various signalling pathways into an overall cellular response, and toxic side effects and/or effects on downstream targets may be immediately measured (Lievens et al., 2012). However, limitations of cell-based assays are that usually only one or two different assay aspects can be addressed within a screen. Multiplexed cell-based assays, at least starting from the stage of hit-to-lead optimisation and later, may prove invaluable to increase information collected for a given compound. Therefore, the luciferase reporter has already been replaced successfully with encoded molecular barcodes that principally would allow monitoring of several cellulat parameters in parallel (Botvinnik et al., 2010).

Cell-based screens utilising engineered cell lines or transiently transfected cells may prove equally well in screens. However, overexpressing proteins and alterations thereof to match the requirements of the cell-based assay have to be carefully tested to avoid any artificial effects.

The presented co-culture assays represent a technological progress over standard cell-based assays based on a single cell poulation. Such an assay is specifically designed to monitor the communication between two populations of cells and can monitor inter- as well as intracellular signalling (Wehr et al., 2008a). These cells may be of different origin, where the first population may represent cells producing a signal-emitting ligand, and the second population may express a receptor that receives the signal. Ligands like NRG1 have to be expressed, processed, correctly localised and integrated into the plasma membrane, or even secreted to be fully functional (Falls, 2003). Likewise, the ERBB4 receptor can only signal correctly when specifically activated at the plasma membrane (Yarden and Pines, 2012). A co-culture assay using, firstly, a Nrg1-expressing and, secondly, an ERBB4-expressing cell population guarantees that the ERBB4 receptor is only activated at the plasma membrane, thereby best mimicking the natural situation.

6.1.6 Limitations of co-culture systems vs. animal models

Results obtained from cell-based assays, including co-culture assays, may have different degrees of implications for translational experiments planned thereafter in animal models. This is particularly true for cell-based assays designed to address neurobiological relevant mechanisms.

In this compound screen, I have used PC12 cells, which are pheochromocytoma cells isolated from the rat adrenal medulla (Greene and Tischler, 1976). Therefore, these cells are neither neurons, nor organised in circuits, layers or tissues, and were not cultivated in a 3D format. PC12 cells were grown in flat-bottom 96-well plates for the assays performed. Compounds tested were pipetted onto the cells, and did not have to cross the blood-brain barrier, and compounds were also not degraded by liver functions. Nonetheless, compared to the hetelogous cell lines usually engaged for HTS campaigns (such as HEK293 or CHOk1 cell lines), PC12 cells seem to be more appropriate in a neurobiological context since closely related to the sympathoadrenergic lineage of neurons.

Conversely, a given mouse model is a compromise between the very complex human brain and a rather simple cell-based co-culture assay. In addition, a mouse brain lacks several key features found in a human brain. This is particularly true for the ability to communicate in an abstract manner. For example, abnormal communication with other humans has been widely reported in SZ patients, and this phenotype can only be partially mimicked in mice, using the Open Field and other related tests (Pratt et al., 2012).

Nevertheless, a well-developed cell-based assay may provide promising initial data that can be further corroborated using a suitable animal model. This

model, in turn, may offer opportunities to conclude signalling and wiring functions up to the human situation.

6.1.7 Screening of compound libraries: The hit-to-lead process in drug discovery

When screening large compound libraries, hit compounds are most likely clustered into sets of similar substances. These hits have to be confirmed using alternative assay. To enter the next phase, i.e. the hit-to-lead process, the isolated compounds have to be modified using medicinal chemistry, and the following lead structures will be analysed and further optimised towards improved signalling characteristics. Therefore, in a prospective manner, greatest care was taken to develop and test several secondary validation assays for robustness and fast applicability (see below).

6.1.8 Screening of FDA approved drug libraries

The NCC library is a collection of FDA-approved drugs that have a history of clinical usage, and important information such as toxicity, bioavailability, side effects etc. are well described. In addition, the safety, best way of application, and maximum dosage for humans is already known for the respective application.

Therefore, using the NCC library is different from the screening of other compound libraries as putative hits are already FDA-approved drugs, which implies that a given hit could potentially be immediately used in patients. However, many drugs have a spectrum of side effects indicating that they have more targets than the one they were primarily designed for. A simple and straightforward approach is to test known drugs for yet undiscovered therapeutic potential. The NCC library was exactly designed for this purpose. All drugs in this library are well described and can be further tested investing little time and effort. However, as these drugs are already on the market patent issues may prove complicated when a given drug from this library will be applied in a new context. Pharmaceutical companies have no interest to reassess patented drugs in new clinical trials. A solution to this could be a non-profit, government-financed consortium that takes over responsibilities.

6.1.9 Transfer of the HTP screen to the LDC

Problems in assay miniaturisation from a 96-well to a 384-well format

For HTP screens of large libraries, such as for the library from LDC comprising more than 200,000 compounds, a miniaturisation of the assay is needed to optimise handling. For example, amounts of valuable drug portions should be reduced, and the number of data points per handling unit, such as a

cell culture plate, should be increased, also allowing for the generation of more data sets in less time.

The assay presented in this thesis worked well in the 96-well format, with 40,000 assay cells per well and 10,000 Nrg1-typeI cells added, with a z' factor of >0.5 indicating a good separation window for the screen. Attempts to miniaturise the assay to a 384-well format caused problems in the assay's stability, as indicated by a rather low z' factor of around 0.3. Initial tests to simply downsize each component by a factor of four did not prove helpful. Colleagues at the LDC are now devoting much of their time and energy to get the assay working. Currently, it is expected that the large compound screen will be performed in a single cell assay including a stimulation using the EGF-like domain. For secondary screening, however, it is planned to use the co-culture assay in a 96-well format.

6.1.10 Elimination of false positives

Firefly luciferase activity was used as readout in the screen, and hits were scored for increased or reduced readings. A given drug may alter these readings by influencing the viability of the assay cells or by acting on the reporter proteins themselves, e.g. by changing their expression, efficient folding and sorting, or localisation, thereby leading to the identification of a false positive hit (Sink et al., 2010). For example, a given drug may promote or inhibit the firefly luciferase activity (Cheng and Inglese, 2012), or impinge on the correct functionality of the artificial co-transcriptional activator GV or the TEV protease. To eliminate these false positive hits, we implemented several measures in the screen itself and during the secondary screening process. For the screen, a second luciferase, the *Renilla* luciferase under the control of the constitutive TK-promoter was used to assay for viability. Therefore, all highly toxic substances can be excluded from the analysis as they strongly reduce *Renilla* readings. During the process of secondary screening, further tests were run to address a given drug's effect related to the functionality of GV, the TEV protease, and the concomitant release of GV induced by TEV activity. To do this, I re-screened the entire library using (1) a setup of constitutive GV expression and the firefly luciferase reporter UAS-Fluc and (2) a membrane-anchored TEV protease, a membrane-anchored GV, and the reporter UAS-Fluc. In summary, applying these controls helped to eliminate false positives.

6.1.11 Elimination of false negatives

The elimination of false negatives is less straight forward. For example, a given drug that has an effect on ERBB4 but does not score in the chosen cell-based assay because of the chosen assay time point. For example, long-term effects of drugs cannot be monitored at the 24h time point, whereas

immediate and short-term effects may have already faded away. Each screen that we performed, however, was run in replicates, and complex statistical processing contributes to minimise false negatives. However, if the cell-based assay does not respond to a treatment, either due to a chosen readout or a given sensitivity, a selected assay time point, or a host cell, a potentially potent drug will not be recovered.

6.1.12 Reproducibility of screening results

The split TEV technique is a highly robust and sensitive method for cell-based assays (Capdevila-Nortes et al., 2012; Wehr et al., 2006; Wehr et al., 2008a, Djannatian et al., 2011) and was recently successfully used in an RNAi screen (Michael Wehr, personal communication). Here, the split TEV technique was applied for the first time in a compound screen, using the FDA-approved NCC library as template. For internal reasons, the NCC library was screened several times, i.e. to optimise protocols related to robotics and operational sequences. The library subset NCC201 was screened ten times in total, and Spironolactone was recovered each time as inhibitor of ERBB4 signalling. Other hits followed up upon in secondary screening, like Vincristin/Vindesine and CCPA scored in initial screens only, likely due to the setup process required to make the robotics unit fully functional (see table 16. for details).

Name of drug	NCC subset	Total times recovered	State of validation
Spironolactone	201-1-D06	10	animal model
Topotecan	003-3-A04	5	stopped
Vincristin	003-6-B02	1	toxic
CCPA	003-6-B06	1	unspecific
Albendazole	201-3-A03	2	unspecific
Mevastatin	003-6-H04	1	toxic

Table 16. Secondary screening and validated hits

6.1.13 Binding assays and co-immunoprecipitations

Drugs recovered from the screen need to be validated using alternative assays. For example, drug-protein binding assays are necessary to verify that a drug physically associates with its target protein. Various protein-drug binding assays like isothermal titration calorimetry, surface plasmon resonace system, plasma protein binding assays, X-ray christallography and nuclear magnetic resonance are available (Arkin and Wells, 2004).

For the precise determination of protein-drug binding crystal structures and X-ray crystallography or nuclear magnetic resonance can be used. As both

techniques are time-consuming an analysis using these methods is beyond the scope of this thesis. The following techniques are less time consuming. Surface plasmon resonance SPR (Huber, 2005) is a technique for the measurement of binding interactions. A surface bound immobilized molecule is probed against an analytic. Meassured is the change in refractive index of the surface after binding.

Isothermal titration calorimetry is a physical technique (Freyer and Lewis, 2008). Binding of small molecules to proteins can be measured using changes in Gibbs free energy and in entropy (Holdgate et al., 2010). This method has been used successfully for. ERBB Antibody binding was in addition profen by ITC (Castoldi et al., 2012).

The overexpression and purification of large membrane proteins, such as the ERBB4 receptor, however, is difficult. To study ERBB4-drug binding affinities using these methods, the receptor may be separated into various functional subunits, such as the cytosolic, a transmembrane, and an extra-cellular part, thereby circumventing purification problems.

In addition, the split TEV protein-protein interaction assay has to be complemented, i.e. by using a co-immunoprecipitation (co-IP) or a GST pull-down assay. Currently, ERBB4 and PIK3R1 are cloned into co-IP compatible vectors, and these experiments will commence shortly.

6.1.14 Testing compounds on unrelated targets

To assess target specificity of the compounds, unrelated but also closely related targets were chosen using the same cell-based assay format. To ensure the specificity of the hit compounds and to get a broader understanding of additional effects a spectrum of selected PPI was tested. The selection contained Rapamycin induced FKBP-FRB (test of general effect on induced PPI), and a GPCR mediated interaction with β-Arrestin2 (Serotonin 5a Receptor). Further tests like NTRK1 (also known as TRKA)-SHC (to study an effect on another receptor tyrosine kinase) and further kinases are scheduled to increase informations about target specificity.

6.2 Relevance for schizophrenia

The potential applicability of the candidates identified from NRG1-ERBB4 screens for treatment of SZ is unclear. NRG1-ERBB4 signalling plays a key role in the development of the brain, and this process takes place over decades (Mei and Xiong, 2008). Both, in the screen and in the dose response validation experiments end point effects are measured 24h after stimulation. It is unclear whether such an effect has an influence on brain architecture after many years post development. Nonetheless, each drug may be applied daily over long periods of time and may be functional even when half-life and on-target effects are limited. Nonetheless, at least Spironolactone, which has a favourable tox-profile and is used in the clinic, might be applied in limited treatment trials at some point in patients. Before this might ever take place, several follow-up validations are essential. Most importantly, additional behavioral analyses with appropriate animal models need to be performed in the future, addressing working memory and social interaction tests for example.

SZ is regularly diagnosed after puberty or in early adulthood. The most significant changes in brain architecture (early years and puberty) are occurring at this time point. Finding and then also applying a drug that affects brain or neuronal circuit architecture during the human childhood and puberty raises major questions. First, it is ethically inconceivable to treat a child with brain structure-modifying drugs to prevent the relatively small (1%) chance of contracting with SZ. Second, the severe side effects and unpredictable changes in the wiring of the brain do strictly bar this. In addition, to start a promising treatment scheme, a reliable biomarker that is present in children is needed, and a systematic analysis of a child’s brain wiring has to be initiated as well. However, as such a biomarker is still elusive, treating children in this perspective remains far in the future.

Recent research shows (Nitsche et al., 2012; Lewis and González-Burgos, 2008) that the neuroplasticity and the on-going change in brain architecture exhibit sufficient neuroplasticity to be a putative target for the effects induced by drugs. Hopefully, drugs modifying NRG1-ERBB4 signalling will help to specifically change the neuronal circuit of inhibitory chandelier and basket cells and activating principal neurons in adults, thus re-balancing the initially disturbed circuit architecture. However, this question cannot be answered without studies in humans.

For the treatment of SZ, a moderate activator of NRG1-ERBB4 signalling is highly desired. In schizophrenia, reduced or potentially enhanced NRG1-ERBB4 signalling (Weickert et al., 2012) leads to a loss of inhibition mediated by parvalbumin positive basket and chandelier cells (PV+ interneurons) on

principal pyramidal neurons, and an activator of NRG1-ERBB4 signalling could potentially alleviate symptoms related to this circuit architecture (Lewis and González-Burgos, 2008). However, no drug from the NCC library showed a specific activating effect on NRG1-ERBB4 signalling. Therefore, it is planned to use larger libraries of compounds to increase the chance to find an activator. For example, the analysis of the Spectrum collection (2320 compounds (http://www.msdiscovery.com/spectrum.html) was successful used by (Kocisko et al., 2003; Weissmann and Aguzzi, 2005; Sun et al., 2006; Weisman et al., 2006; Stallings-Mann et al., 2006). Moreover, the 200,000 compound library from the Lead Discovery Centre Dortmund is in progress (Eitner and Koch, 2009).

6.3 NRG1-ERBB4 – Spironolactone

The inhibitory effect of Spironolactone was several times recovered in the screen. In addition, dose-response assays for Spironolactone validated a clear concentration-dependent inhibition of NRG1-ERBB4 signalling. Spironolactone was originally described as an antagonist of the mineralocorticoid receptor MCR (Rogerson et al., 2003). MCR regulates salt homeostasis in the kidney (Brewster and Perazella, 2004), and Spironolactone is used as a diuretic in the clinics (Ogden et al., 1961). MCR plays also a role in the brain (in particular in the hippocampus)(Oyamada et al., 2008), heart vasculature (Oyamada et al., 2008), and adipose tissue (Marzolla et al., 2012). Mechanistically, Spironolactone binds to the aldosterone binding pocket of the MCR, thus preventing its translocation to the nucleus, where the MCR induces the transcription of target genes (Grossmann et al., 2012)

For Spironolactone's action on NRG1-ERBB4 signalling, I speculate that Spironolactone could prevent ERBB4 receptors from dimerising thus reducing downstream signalling, i.e. preventing activation of downstream kinases, such as PI3K and AKT. Importantly, treatment of Spironolactone showed reduced phosphorylation levels of pTyr1284 in ERBB4, concomitant with a mild decrease in phospho-AKT levels. However, this signalling needs to be addressed in more detail in the future, including other SZ-relevant kinases, such as GSK-3β (Emamian, 2012).

6.3.1 Does Spironolactone physically bind to ERBB4 receptors?

Spironolactone specifically inhibits NRG1-ERBB4 signalling. However, split TEV assays do not allow answering whether Spironolactone physically binds to ERBB4 to inhibit receptor activation. Other assays discussed above are necessary to address this question.

6.3.2 Spironolactone derivates and metabolites

The secomd generation drug of Spironolactone Eplerenone showed no effect on ERBB4/PIK3R1 co-culture assay. The metabolite Canterenone showed also no effect.

This leads to the assumption that the thioketone (Acetylthio) group of Spironolactone is part of the mode of action. The entire description of the structure function relationship is beyond this thesis.

The penetration of the blood-brain barrier (BBB) is vital for any drug used for psychiatric treatment. Until now it is not known if Spironolactone passes the BBB (Geerling and Loewy, 2009).

6.3.3 Preliminary validation in a mouse model

An analysis of Spironolactone effects counteracting MK801 induced psychosis (see MK801 mouse model) showed that Spironolactone shows only a non-significant tendency to reduce spontaneous locomotor activity. The administered Spironolactone concentration was 20 mg/kg, relatively high compared to concentrations in humans (20-200 mg/75kg (average human)). As the effects are measured in two hours, they are supposably not based on Spironolactone's primary action against MCR and the resulting changes in gene expression (48h).

The MK801 mouse model is not the perfect model to validate putative NRG1-ERBB4 inhibitors. A mouse model constitutively overexpressing Nrg1-typeIII is in the validation phase and will soon be available ((Velanac et al., 2012) personal communication M. Schwab).

The effect of Spironolactone on the mouse brain has also to be shown in Western-Blots on mouse brain lysates and will be performed as soon as the model is available.

6.4 Topotecan shows strong toxic effects

Topotecan is a semisynthetic variant of Camptothecin. Camptothecin is a pentacycline quinolone alkaloid found in the bark seeds, and fruits of the Chinese happy tree *camptotheca acuminate* (Xi Shu). Parts of the tree were regularly used in the treatment of different diseases in traditional Chinese medicine wheras no reports for the use in psychiatric treatments are available. In a screen for cancer therapeutics performed in 1966 by M. E. Wall and M. C. Wani camptothecin was isolated. It is not water-soluble and has severe side effects including unpredictable toxicity. Camptothecin acts as a topoisomerase I inhibitor (O'Leary and Muggia, 1998b; Redinbo et al., 1998; Morton, 1968).

Topoisomerases are enzymes that are localised to the nucleus, and are responsible for the relaxation of positive and negative supercoiled DNA strands. Camptothecin inhibits the breakage re-joining reaction of DNA–topoisomerase I. The inhibition is specific and results in the accumulation of reversible intermediate DNA-Camptothecin-topoisomerase I ternary complexes. Camptothecin only binds to the DNA-topoisomerase I complex, but not to DNA or the enzyme alone. (Gromova 1993, Hsiang 1989) (Gromova et al., 1993; Hsiang et al., 1989)

Topotecan is made water-soluble by a basic chain at carbon 9. It is used against small lung cancer and ovarial cancers. It acts as Topoisomerase I inhibitor by stalling the DNA-topoisomerase I complex, and therefore acts cytostatic. For Topotecan, the penetration of the blood brain barrier, the localisation to the CNS, and cerebrospinal fluid concentrations of 32% in serum levels have been reported (Takimoto and Arbuck, 1997b)

Irinotecan (FDA-approved in 1998) is a pro-drug and undergoes hydrolysis by carboxylesterase, primarily in the liver. This conversion results is SN-38, which is the biologically active form of Irinotecan, with an increased activity of 1000-fold (Kawato et al., 1991; Redinbo et al., 1998; Kuhn, 1998; Zamboni et al., 1998). Irinotecan is used in the clinics to treat colorectal cancer.

Irinotecan has severe side effects including diarrhoea associated with abdominal cramping, vomiting, flushing, and diaphoresis. This is mediated by increased cholinergic activity, and this is reversible with atropine (Abigerges et al., 1995; Rowinsky et al., 1994).

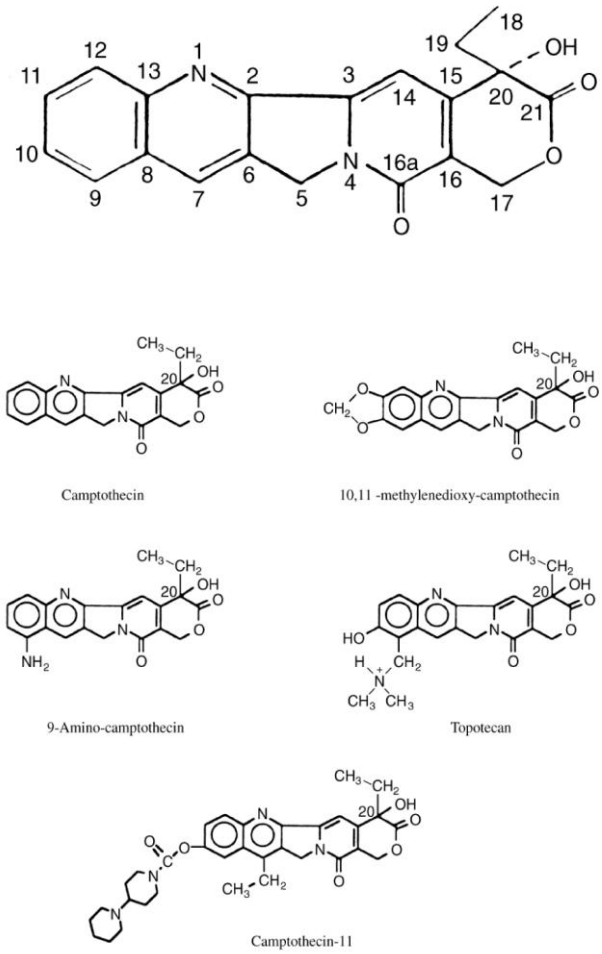

Figure 77: Immage. Campothecin derivatives (O'Leary and Muggia, 1998)

Camptothecins are toxic to the bone marrow and cause mucositis and diarrhoea (Irinotecan) in humans (O'Leary and Muggia, 1998a). They are only used as chemotherapeutics in live-threatening cancers (Taguchi et al., 1990). Therefore, usage of Topotecan in psychiatric patients is not recommended unless a lead optimisation processes results in lead structure with reduced toxicity i.e. reduced DNA-Topoisomerase I binding. On a chemical basis, it has already shown that binding of an amino group at C12 abolishes topoisomerase I inhibiting function and that specific stereochemistry at C20 is necessary. Only the (S) isomer is active, racemic mixture shows 50% activity and the (R) isomer is completely inactive (O'Leary and Muggia, 1998a). This combined with the inactivity of SN 38 may serve as template for a putative starting point of a leadoptimisation process, given the modified compounds remain inhibitory to NRG1-ERBB4 signalling.

Topotecan shows nicely the dilemma of the used co-culture assay systems. The time dimensions of an effect cannot be measured directly. Topotecan is strongly toxic for all fast-dividing cells, but the effect is not prominent in a 24h assay. Toxic effects can accumulate and strike over time and remain hidden in short termed assays.

6.5 Conclusion

Activators of NRG1-ERBB4 signalling are highly desired to compensate for SZ-induced loss of function phenotypes but remain elusive. The NCC library containing FDA-approved compounds was applied to address this issue. However, with Spironolactone and Topotecan, only inhibitors of NRG1-ERBB4, were identified. As the NCC library only contains not far more than 700 drugs, larger collections, such as the Spectrum Collection containing 2300 compounds, will be used in the in the future. In addition, the LDC library, with more than 200,000 compounds, will be used to screen for activators of NRG1-ERBB4 signalling. Once an activator is identified, medicinal chemistry will be applied to generate new molecular entities in a lead optimisation process, with the aim to find a structure that activates NRG1-ERBB4 signalling, is not toxic, and fulfils the requirements to proceed into the preclinical stage of drug testing.

7 Abbreviations

BACE	Beta-site APP cleaving enzyme
BRET	Bioluminescence resonance energy transfer
BBB	Blood-brain-barrier
Chr	Chromosome
CIP	Calf intestinal alkaline phosphatase
CMV	Cytomegalovirus
CNS	Central nervous system
CNV	Copy number variations
CO-IP	Immunoprecipitation
CRD	Cystein rich domain
DISC1	Disroupted in schizophrenia
DMSO	Dimethylsulfoxide
DNA	Desoxyribonuclein acid
DSM IV	Diagnostic and Statistical Manual of Mental Disorders
DTT	Dithiothreitol
e.g.	For example/exempli gratia
ECL	Enhanced chemiluminescens
EDTA	Ethylenediaminetetraacetic acid
EGF	Epidermal growth factor
EGFP	Enhanced green fluorescent protein
ERBB4	Receptor tyrosine-proteine kinase v-erb-a erythroblastic leukemia viral oncogene homolog 4 (avian)
ERT2	Mutated Estrogen receptor domains
f.c.	Final concentration
FDA	Food and Drug Administeriation
FRET	Fluorescence Resonance Energy Transfer
GABA	Gamma-Aminobutyric acid
GAD67	Glutamat acid decarboxylase 67kd
GRB2	Growth factor receptor bound protein 2
GV	Galactose4.viral protein 16; artificial transcription factor
GWAS	Genome wide genetic association studies
HTP	High throughput
i.e.	That is/id est
IQ	Inteligence quotient
k	Kilo
kb	Kilo bases
KO	Knock out
M	Molar
MAPK	Mitogen activated protein kinases
MDMA	3,4-methylenedioxy-N-methylamphetamine
min	Minutes
MRI	Magnetic Resonance imaging
n	Nano
n.c.	Not calculated

NCC	NIH clinical colection
NIH	National Institute of Health
NMDA	N-methyl-D-aspartate
NRG1	Neuregulin1
PCP	Phencyclidine
PCR	Polymerase chain reaction
PI3K	Phodphoinositide 3.kinase
PLL	Poly-L-Lysin
PNS	Peripheral nervous system
PPI	Protein-protein-interaction
PTPRZ1	Receptor-type tyrosine-protein phosphatase zeta
PV	Parvalbumin
RLU	Relative luciferase units
RTK	Receptor tyrosine kinase
SD	Standard deviation
sec	Seconds
SEM	Standard error of the mean
SHC1	SH2 domains containing transforming protein
SNP	Single nucleotide polymorphisms
SRC	Sarcoma tyrosine kinase
STAT5A	Signal transducer and activator of transcription 5a
SV40	Simian virus 40
SZ	Schizophrenia
TACE	TNFalpha converting enzyme
TEV	*Tobacco etch virus*
THC	Tetra hydro canabinol
TK	Thymidine kinase
UV	Ulta violet
V	Volt

8 Curriculum vitae

Personal data

Name	**Wilko Hinrichs**
Place of birth	**Norderney**
Nationality	**German**

Education

2008-currente	**Graduate student GGNB** Prof. Nave, Department of Neurogenetics Max-Planck-Institute of Experimental Medicine, Göttingen
2008	**Diploma in biology** Speciality in Genetics, Biochemistry, Historic Anthropology Georg-August-University, Göttingen
2007-2008	**Diploma student** Prof. Nave, Department of Neurogenetics Max-Planck-Institute of Experimental Medicine, Göttingen
2002-2007	**Student GAU** Biology Georg-August-University Göttingen
2001-2002	**German Airforce** Hptm. Wenninger 5.LwAusbRgt1 Budle Netherlands
2001	**Abitur**
1998-2001	**Gymnasium** Ulrichs Gymnasium Norden
1992-1998	**Kooperative Gesamtschule** KGS Norderney
1988-1992	**Grundschule / Primary school** Grundschule Norderney

Professional Qualifications

2003	**Research assistant** PD Dr. Friedhard Raschke Institut für Rehabilitationsforschung LVA Klinik Norderney
2004-2007	**Research assistant** Prof. Nave, Department of Neurogenetics Max-Planck-Institute of Experimental Medicine, Göttingen

9 Own publications

Velanac, V., Unterbarnscheidt, T., Hinrichs, W., Gummert, M.N., Fischer, T.M.,Möbius, W., Nave, K.-A., and Schwab, M.H., 2012, Bace1 processing of NRG1 type III produces a myelin-inducing signal but is not essential for the stimulation of myelination: Glia, v. 60, no. 2, p. 203–217, doi: 10.1002/glia.21255.

10 Apendix, List of Drugs NCC201/NCC003

10.1.1 NIH1–NCC201

NCC_SAMPLE	Pl.	Well	Supplier	NCC_STRUCTURE_SYNONYMS[2]
SAM002264608	1	A02	LightBiologicals	DOXEPIN HYDROCHLORIDE
SAM002264609	1	B02	LightBiologicals	DIPYRIDAMOLE
SAM002264610	1	C02	LightBiologicals	Propofol
SAM002264611	1	D02	LightBiologicals	ETHACRYNIC ACID
SAM002264612	1	E02	LightBiologicals	FLUTAMIDE
SAM002264613	1	F02	LightBiologicals	FENOFIBRATE
SAM002264614	1	G02	LightBiologicals	FUROSEMIDE
SAM002264615	1	H02	LightBiologicals	5-FLUOROURACIL
SAM002264616	1	A03	LightBiologicals	Folic acid
SAM002264617	1	B03	LightBiologicals	HYDROCORTISONE
SAM002264618	1	C03	LightBiologicals	Cortell
SAM002264619	1	D03	LightBiologicals	IBUPROFEN
SAM002264620	1	E03	LightBiologicals	KETOPROFEN
SAM002264621	1	F03	LightBiologicals	MINOCYCLINE HYDROCHLORIDE
SAM002264623	1	G03	LightBiologicals	MICONAZOLE NITRATE
SAM002297829	1	H03	LightBiologicals	METYRAPONE
SAM002264625	1	A04	LightBiologicals	NORFLOXACIN
SAM002264627	1	B04	LightBiologicals	NADOLOL
SAM002264628	1	C04	LightBiologicals	Disipal
SAM002264629	1	D04	LightBiologicals	OFLOXACIN
SAM002264631	1	E04	LightBiologicals	PINDOLOL
SAM002264632	1	F04	LightBiologicals	PRAZIQUANTEL
SAM002264634	1	G04	LightBiologicals	Benzenebutanoic Acid
SAM002264635	1	H04	LightBiologicals	PREDNISOLONE ACETATE
SAM002264636	1	A05	LightBiologicals	Phenergan
SAM002264637	1	B05	LightBiologicals	PERPHENAZINE
SAM002264639	1	C05	LightBiologicals	Prednisolone
SAM002264640	1	D05	LightBiologicals	PRILOCAINE HYDROCHLORIDE
SAM002264641	1	E05	LightBiologicals	Prednisone
SAM002264642	1	F05	LightBiologicals	DL-PENICILLAMINE
SAM002264643	1	G05	LightBiologicals	PIPERACILLIN SODIUM SALT
SAM002264644	1	H05	LightBiologicals	Quinidine hydrochloride monohydrate
SAM002264645	1	A06	LightBiologicals	Ranitidine hydrochloride
SAM002264646	1	B06	LightBiologicals	RIFAMPICIN
SAM002264647	1	C06	LightBiologicals	Retinoic acid
SAM002264648	1	D06	LightBiologicals	Spironolactone
SAM002264649	1	E06	LightBiologicals	Trimethoprim
SAM002264650	1	F06	LightBiologicals	Tyzine
SAM002264651	1	G06	LightBiologicals	L-THYROXINE
SAM002264652	1	H06	LightBiologicals	Artane
SAM002264653	1	A07	LightBiologicals	URSODEOXYCHOLIC ACID
SAM002554879	1	B07	LightBiologicals	Dapsone
SAM002554881	1	C07	LightBiologicals	Symmetrel
SAM002554882	1	D07	LightBiologicals	WARFARIN SODIUM
SAM002554883	1	E07	LightBiologicals	Acetazolamide

SAM002554884	1	F07	LightBiologicals	Allopurinol
SAM002554885	1	G07	LightBiologicals	ATROPINE
SAM002554914	1	H07	LightBiologicals	Nalidixic Acid
"SAM003107539	1	A08	LightBiologicals	""3
SAM002703134	1	B08	LightBiologicals	HYDROFLUMETHIAZIDE
SAM002554886	1	C08	LightBiologicals	Annoyltin
SAM002554887	1	D08	LightBiologicals	Busulfan
SAM002554888	1	E08	LightBiologicals	Chlorzoxazone
SAM002554891	1	F08	LightBiologicals	Chlorothiazide
SAM002554892	1	G08	LightBiologicals	Cimetidine
SAM002554889	1	H08	LightBiologicals	Carisoprodol
SAM002554890	1	A09	LightBiologicals	Chlorpropamide
"SAM002554894	1	B09	LightBiologicals	Bentyl
SAM002554895	1	C09	LightBiologicals	Chloroxine
SAM002554896	1	D09	LightBiologicals	Diflunisal
SAM002554898	1	E09	LightBiologicals	Econazole Nitrate
SAM002554899	1	F09	LightBiologicals	Ethionamide
SAM002554900	1	G09	LightBiologicals	Methocarbamol
SAM002554901	1	H09	LightBiologicals	Hydrochlorothiazide
SAM002554902	1	A10	LightBiologicals	Vistaril Pamoate
SAM002554903	1	B10	LightBiologicals	Hexachlorophene
SAM002554904	1	C10	LightBiologicals	Isoniazid
SAM002554905	1	D10	LightBiologicals	Duvadilan
SAM002554906	1	E10	LightBiologicals	Isuprel
SAM002554907	1	F10	LightBiologicals	Triclosan
SAM002554908	1	G10	LightBiologicals	Mefenamic Acid
"SAM002554910	1	H10	LightBiologicals	Cantil
SAM002554911	1	A11	LightBiologicals	Maxolon
SAM002554912	1	B11	LightBiologicals	Methyldopa
SAM002554913	1	C11	LightBiologicals	NITROFURANTOIN
SAM002554915	1	D11	LightBiologicals	Pamelor
SAM002554916	1	E11	LightBiologicals	Albalon
SAM002554917	1	F11	LightBiologicals	Nicotinic Acid
SAM002554918	1	G11	LightBiologicals	Norflex
SAM002554919	1	H11	LightBiologicals	Oxytetracycline hydrochloride
SAM002554920	2	A02	LightBiologicals	Novocain
SAM002554921	2	B02	LightBiologicals	Pyrimethamine
SAM002554922	2	C02	LightBiologicals	Pro-Banthine
SAM002554923	2	D02	LightBiologicals	Probenecid
SAM002554924	2	E02	LightBiologicals	PYRIDINE-2-ALDOXIME METHOCHLORIDE
SAM002554925	2	F02	LightBiologicals	Primidone
SAM002554926	2	G02	LightBiologicals	Propylthiouracil
SAM002554927	2	H02	LightBiologicals	Pyrazinamide
SAM002554928	2	A03	LightBiologicals	Pronestyl
SAM002554929	2	B03	LightBiologicals	Sulfisoxazole
SAM002554930	2	C03	LightBiologicals	Sulfamethoxazole
SAM002554931	2	D03	LightBiologicals	Sulfacetamide
SAM002554932	2	E03	LightBiologicals	Sulfinpyrazone
SAM002554933	2	F03	LightBiologicals	Sulindac
SAM002554934	2	G03	LightBiologicals	TETRACYCLINE
SAM002554935	2	H03	LightBiologicals	Theophylline
SAM002554936	2	A04	LightBiologicals	Tolbutamide

"SAM002554937	2	B04	LightBiologicals	Triamterene
SAM002554938	2	C04	LightBiologicals	Intropin
SAM002564189	2	D04	LightBiologicals	AMOXAPINE
SAM002564191	2	E04	LightBiologicals	Adenine 9-beta
SAM002564193	2	F04	LightBiologicals	ATENOLOL
SAM002703133	2	G04	LightBiologicals	Tamoxifen
SAM002564195	2	H04	LightBiologicals	BUMETANIDE
SAM002564250	2	A05	LightBiologicals	CLOBETASOL PROPIONATE
SAM002564196	2	B05	LightBiologicals	Sonazine
SAM002564200	2	C05	LightBiologicals	CEFAZOLIN SODIUM SALT
SAM002564201	2	D05	LightBiologicals	CAPTOPRIL
SAM002564202	2	E05	LightBiologicals	CHLORAMBUCIL
SAM002564251	2	F05	LightBiologicals	CEFOXITIN SODIUM SALT
SAM002564203	2	G05	LightBiologicals	DANAZOL
SAM002564204	2	H05	LightBiologicals	(+)-CIS-DILTIAZEM HYDROCHLORIDE
SAM002564205	2	A06	LightBiologicals	DIGOXIN
SAM002564206	2	B06	LightBiologicals	17-BETA-ESTRADIOL 17-VALERATE
SAM002564207	2	C06	LightBiologicals	EDROPHONIUM CHLORIDE
SAM002564208	2	D06	LightBiologicals	FLUOCINOLONE ACETONIDE
SAM002564209	2	E06	LightBiologicals	Flurbiprofen
SAM002564210	2	F06	LightBiologicals	GLIPIZIDE
SAM002564211	2	G06	LightBiologicals	GEMFIBROZIL
SAM002564212	2	H06	LightBiologicals	Glyburide
SAM002564213	2	A07	LightBiologicals	HYDROCORTISONE HEMISUCCINATE
SAM002564214	2	B07	LightBiologicals	INDAPAMIDE
SAM002564215	2	C07	LightBiologicals	IPRATROPIUM BROMIDE MONOHYDRATE
SAM002564216	2	D07	LightBiologicals	Tofranil
SAM002564217	2	E07	LightBiologicals	LABETALOL HYDROCHLORIDE
SAM002564218	2	F07	LightBiologicals	Imodium
SAM002564219	2	G07	LightBiologicals	Pro-Amatine
SAM002564220	2	H07	LightBiologicals	Medroxyprogesterone 17-acetate
SAM002564222	2	A08	LightBiologicals	19-NORETHINDRONE ACETATE
SAM002564223	2	B08	LightBiologicals	19-Norethindrone
SAM002564224	2	C08	LightBiologicals	NICOTINE
SAM002564254	2	D08	LightBiologicals	Cardene
SAM002564225	2	E08	LightBiologicals	NABUMETONE
SAM002564226	2	F08	LightBiologicals	OXYBUTYNIN CHLORIDE
SAM002564227	2	G08	LightBiologicals	Mestinon
SAM002564228	2	H08	LightBiologicals	Rythmol
SAM002564229	2	A09	LightBiologicals	Pfizerpen
SAM002564230	2	B09	LightBiologicals	Valproic Acid
SAM002564231	2	C09	LightBiologicals	Kemadrin
"SAM002564232	2	D09	LightBiologicals	Proxymetacaine
SAM002703137	2	E09	LightBiologicals	NALOXONE HYDROCHLORIDE
SAM002564233	2	F09	LightBiologicals	SPECTINOMYCIN DIHYDROCHLORIDE PENTAHYDRATE
SAM002564235	2	G09	LightBiologicals	TROPICAMIDE
SAM002564236	2	H09	LightBiologicals	TOLAZAMIDE
SAM002564237	2	A10	LightBiologicals	TRIAMCINOLONE ACETONIDE
SAM002564238	2	B10	LightBiologicals	S(-)-Timolol maleate
SAM002564239	2	C10	LightBiologicals	THIABENDAZOLE
SAM002564240	2	D10	LightBiologicals	THIORIDAZINE HYDROCHLORIDE
SAM002564241	2	E10	LightBiologicals	Altretamine

SAM002564257	2	F10	LightBiologicals	Phylloquinone
SAM002564242	2	G10	LightBiologicals	Eryped
SAM002564244	2	H10	LightBiologicals	Dibenzyline
"SAM002564258	2	A11	LightBiologicals	6ALPHA-METHYL-11BETA-HYDROXYPROGESTERONE
SAM002564245	2	B11	LightBiologicals	Thalidomide
SAM002589919	2	C11	LightBiologicals	Aminolevulinic Acid
SAM002589920	2	D11	LightBiologicals	Carbinoxamine Maleate
SAM002589921	2	E11	LightBiologicals	Demeclocycline
SAM002589925	2	F11	LightBiologicals	Westcort
SAM002589926	2	G11	LightBiologicals	DEPRENALIN
SAM002589927	2	H11	LightBiologicals	6-[2-ETHOXY-1-NAPHTHAMIDO]-PENICILLIN SODIUM SALT
SAM002589929	3	A02	LightBiologicals	Primaquine Diphosphate
SAM002589930	3	B02	LightBiologicals	Micropenin
SAM002589932	3	C02	LightBiologicals	DOXYCYCLINE
"SAM002699895	3	D02	LightBiologicals	Beclomethasone dipropionate
SAM002589934	3	E02	LightBiologicals	Cromolyn Sodium
SAM002589935	3	F02	LightBiologicals	Priscoline
SAM002589937	3	G02	LightBiologicals	Mercaptopurine
SAM002589938	3	H02	LightBiologicals	Azathioprine
SAM002589939	3	A03	LightBiologicals	Albendazole
SAM002589940	3	B03	LightBiologicals	Griseofulvin
SAM002589936	3	C03	LightBiologicals	Lincomycin hydrochloride
SAM002589943	3	D03	LightBiologicals	Methazolamide
SAM002589944	3	E03	LightBiologicals	Terbutaline Sulfate
SAM002589979	3	F03	LightBiologicals	Mupirocin
SAM002589945	3	G03	LightBiologicals	FLUOCINOLONE ACETONIDE 21-ACETATE
SAM002699894	3	H03	LightBiologicals	Mefloquine hydrochloride
SAM002589947	3	A04	LightBiologicals	Floxuridine
SAM002699896	3	B04	LightBiologicals	MITOXANTRONE
SAM002699897	3	C04	LightBiologicals	ENALAPRIL MALEATE
SAM002699898	3	D04	LightBiologicals	BUDESONIDE
SAM002699899	3	E04	LightBiologicals	RAMIPRIL
SAM002699893	3	F04	LightBiologicals	DEPO-MEDROL
SAM002699901	3	G04	LightBiologicals	(+/-)-NOREPINEPHRINE HYDROCHLORIDE
SAM002699903	3	H04	LightBiologicals	AMCINONIDE
SAM002699904	3	A05	LightBiologicals	Clomid
SAM003107541	3	B05	LightBiologicals	PHENTOLAMINE HCL
SAM002548956	3	C05	Enamine	FLUDARABINE
SAM002548950	3	D05	Enamine	Testosterone
SAM002548955	3	E05	Enamine	Isotretinoin
SAM002548951	3	F05	Enamine	Methimazole
SAM002548957	3	G05	Enamine	Zonisamide
SAM002548958	3	H05	Enamine	Brimonidine
SAM002548959	3	A06	Enamine	Mebendazole
SAM002548969	3	B06	Enamine	Duremesin
SAM002548968	3	C06	Enamine	Flecainide Acetate
SAM002548966	3	D06	Enamine	Dilantin
SAM002548945	3	E06	Enamine	Miochol
SAM002703135	3	F06	LightBiologicals	Dantrolene sodium salt
SAM002548948	3	G06	Enamine	Dexamethasone
SAM002548938	3	H06	Enamine	Cogentin Mesylate
SAM002548936	3	A07	Enamine	Ganciclovir

SAM002548937	3	B07	Enamine	Mesna
SAM002548942	3	C07	Enamine	Meclomen
SAM002589905	3	D07	Enamine	Fluconazole
SAM002548965	3	E07	Enamine	Metaproterenol
SAM002548974	3	F07	Enamine	Methoxsalen
SAM002548963	3	G07	Enamine	Chloramphenicol
SAM002548961	3	H07	Enamine	Tizanidine hydrochloride
SAM002548935	3	A08	Enamine	Paroxetine
SAM002548934	3	B08	Enamine	mirtazapine
SAM002548930	3	C08	Enamine	Etomidate
SAM002548933	3	D08	Enamine	Moban
SAM002548940	3	E08	Enamine	fluvastatin
SAM002548931	3	F08	Enamine	Urecholine
SAM002589901	3	G08	Enamine	Cefuroxime
SAM002548983	3	H08	Enamine	Cytoxan
SAM002548982	3	A09	Enamine	Eszopiclone
SAM002264598	3	B09	LightBiologicals	Bendrofluazide
SAM002548975	3	C09	Enamine	Evista
SAM002548971	3	D09	Enamine	zidovudine
SAM002548976	3	E09	Enamine	Clozapine
SAM002264590	3	F09	LightBiologicals	Ampicillin Sodium
SAM002264591	3	G09	LightBiologicals	ACEBUTOLOL HYDROCHLORIDE
SAM002264592	3	H09	LightBiologicals	AMOXICILLIN CRYSTALLINE
SAM002699891	3	A10	LightBiologicals	(+/-)-Epinephrine hydrochloride
SAM002264595	3	B10	LightBiologicals	5-Azacytidine
SAM002264597	3	C10	LightBiologicals	Buspar
SAM002264596	3	D10	LightBiologicals	Flumadine
SAM002548978	3	E10	Enamine	Podofilox
SAM002264599	3	F10	LightBiologicals	D-CYCLOSERINE
SAM002264600	3	G10	LightBiologicals	CORTISONE ACETATE
SAM002264601	3	H10	LightBiologicals	Anafranil
SAM002264603	3	A11	LightBiologicals	Carbamazepine
SAM002699890	3	B11	LightBiologicals	Memantine hydrochloride
SAM002264605	3	C11	LightBiologicals	Norpramin
SAM002264606	3	D11	LightBiologicals	Mexitil
SAM002264607	3	E11	LightBiologicals	Norpace
SAM002589948	3	F11	LightBiologicals	STAVUDINE
SAM002589981	3	G11	LightBiologicals	Doxazosin
SAM002589949	3	H11	LightBiologicals	Minoxidil
SAM002699889	4	A02	LightBiologicals	Inderal
SAM002589951	4	B02	LightBiologicals	Ribavirin
SAM002589982	4	C02	LightBiologicals	Terazosin
SAM002589983	4	D02	LightBiologicals	Chlorthalidone
SAM002589984	4	E02	LightBiologicals	METHYLPREDNISOLONE
SAM002589985	4	F02	LightBiologicals	Phenelzine
SAM002589986	4	G02	LightBiologicals	NALTREXONE HYDROCHLORIDE
SAM002589987	4	H02	LightBiologicals	Glycopyrrolate
SAM002589988	4	A03	LightBiologicals	Ethambutol
SAM002589989	4	B03	LightBiologicals	Cetirizine
SAM002589990	4	C03	LightBiologicals	DICLOXACILLIN SODIUM
SAM002589991	4	D03	LightBiologicals	Meloxicam
SAM002589992	4	E03	LightBiologicals	DAUNORUBICIN HYDROCHLORIDE

SAM002589953	4	F03	LightBiologicals	RIFAPENTINE
SAM002589954	4	G03	LightBiologicals	Penicillin V
SAM002589955	4	H03	LightBiologicals	Gatifloxacin
SAM002589956	4	A04	LightBiologicals	clopidogrel
SAM002643511	4	B04	LightBiologicals	CEFOTAXIME SODIUM SALT
SAM002589994	4	C04	LightBiologicals	LAMIVUDINE
SAM002589958	4	D04	LightBiologicals	Ondansetron
SAM002589959	4	E04	LightBiologicals	Betamethasone
SAM002589995	4	F04	LightBiologicals	Celecoxib
SAM002589996	4	G04	LightBiologicals	4-(AMINOMETHYL)BENZENESULFONAMIDE ACETATE
SAM002589997	4	H04	LightBiologicals	THIOTHIXENE
SAM002589960	4	A05	LightBiologicals	Citalopram
SAM002589961	4	B05	LightBiologicals	Azithromycin
SAM002589963	4	C05	LightBiologicals	Lovastatin
SAM002589964	4	D05	LightBiologicals	Aminoglutethimide
SAM002589965	4	E05	LightBiologicals	Prozac
SAM002589966	4	F05	LightBiologicals	FluniSOLIDe
SAM002589967	4	G05	LightBiologicals	Acyclovir
SAM002589968	4	H05	LightBiologicals	Etodolac
SAM002589969	4	A06	LightBiologicals	Simvastatin
SAM002589970	4	B06	LightBiologicals	Rifabutin
SAM002589971	4	C06	LightBiologicals	Felodipine
SAM002589972	4	D06	LightBiologicals	Quinapril hydrochloride
SAM002589973	4	E06	LightBiologicals	Acitretin
SAM002700173	4	F06	LightBiologicals	Allegra
SAM002700174	4	G06	LightBiologicals	Fluorometholone
SAM002700175	4	H06	LightBiologicals	Sertraline
SAM002703129	4	A07	LightBiologicals	CARBIDOPA

Table 9. NCC201

10.1.2 NIH2-NCC003

NCC_SAMPLE	Pl.	Well	Supplier	NCC_STRUCTURE_SYNONYMS[2]
SAM001247063	1	A02	Tocris Bioscience	Nalbuphine
SAM001247072	1	B02	Tocris Bioscience	Raclopride
SAM001247069	1	C02	Tocris Bioscience	Zacopride
SAM001247068	1	D02	Tocris Bioscience	SKF 83566
SAM001246964	1	E02	Tocris Bioscience	3'-deoxydenosine
SAM001246965	1	F02	Tocris Bioscience	AM 404
SAM001246962	1	G02	Tocris Bioscience	PILOCARPINE HYDROCHLORIDE
SAM001246963	1	H02	Tocris Bioscience	NIFEDIPINE
SAM001246961	1	A03	Tocris Bioscience	Flurbiprofen
SAM001247015	1	B03	Tocris Bioscience	3-HYDROXY-1,2-DIMETHYL-4(1H)-PYRIDONE
SAM001247061	1	C03	Tocris Bioscience	
SAM001247062	1	D03	Tocris Bioscience	d-3-Methoxy-N-methylmorphinan hydrobromide
SAM001247059	1	E03	Tocris Bioscience	Duloxetine
SAM001247060	1	F03	Tocris Bioscience	Glycine, N-[2-[(acetylthio)methyl]-1-oxo-3-phenylpropyl]-,phenylmethyl ester [CAS]
SAM001247057	1	G03	Tocris Bioscience	Benzeneacetic acid, 2-[(2,6-dichlorophenyl)amino]-, monosodium salt [CAS]
SAM001247039	1	H03	Tocris Bioscience	PROGESTERONE
SAM001247033	1	A04	Tocris Bioscience	FAMOTIDINE
SAM001246999	1	B04	Tocris Bioscience	SR 57,227A
SAM001247003	1	C04	Tocris Bioscience	Pancuronium

SAM001247010	1	D04	Tocris Bioscience	METRONIDAZOLE
SAM001246967	1	E04	Tocris Bioscience	Benzeneacetic acid, Alpha-(hydroxymethyl)-, 9-methyl-3-oxa-9-azatricyclo[3.3.1.02,4]non-7-yl ester, [7(S)-(1Alpha,2ﾃｿ,4ﾃｿ,5Alpha,7ﾃｿ)]- [CAS]
SAM001246968	1	F04	Tocris Bioscience	Benzeneacetonitrile, Alpha-[3-[[2-(3,4-dimethoxyphenyl)ethyl]methylamino]propyl]-3,4-dimethoxy-Alpha-(1-methylethyl)-, (R)- [CAS]
SAM001246969	1	G04	Tocris Bioscience	DEPRENALIN
SAM001246970	1	H04	Tocris Bioscience	Capsaicin
SAM001246971	1	A05	Tocris Bioscience	SALBUTAMOL SULFATE
SAM001246972	1	B05	Tocris Bioscience	(ｱ)-Vesamicol hydrochloride
SAM001246993	1	C05	Tocris Bioscience	Picrotin - Picrotoxinin
SAM001247000	1	D05	Tocris Bioscience	Terazosin
SAM001247027	1	E05	Tocris Bioscience	diphenylcyclopropenone
SAM001247016	1	F05	Tocris Bioscience	4-Thiazolidinecarboxylic acid, 2-oxo-, (R)- [CAS]
SAM001247051	1	G05	Tocris Bioscience	Mesoridazine
SAM001247053	1	H05	Tocris Bioscience	3(2H)-Pyridazinone, 6-[4-(difluoromethoxy)-3-methoxyphenyl]- [CAS]
SAM001247054	1	A06	Tocris Bioscience	10H-Phenothiazine, 2-chloro-10-[3-(4-methyl-1-piperazinyl)propyl- [CAS]
SAM001247055	1	B06	Tocris Bioscience	1H-Cyclopenta[b]quinolin-9-amine, 2,3,5,6,7,8-hexahydro-, monohydrochloride- [CAS]
SAM001247056	1	C06	Tocris Bioscience	CLOTRIMAZOLE
SAM001246987	1	D06	Tocris Bioscience	LORATADINE
SAM001247037	1	E06	Tocris Bioscience	PHENELZINE SULFATE SALT
SAM001246997	1	F06	Tocris Bioscience	Riluzole
SAM001247004	1	G06	Tocris Bioscience	Naltrindole
SAM001247026	1	H06	Tocris Bioscience	Nornicotine
SAM001247052	1	A07	Tocris Bioscience	Bifemelane
SAM001246973	1	B07	Tocris Bioscience	CGS 15943
SAM001246974	1	C07	Tocris Bioscience	Cinanserin
SAM001246975	1	D07	Tocris Bioscience	Cisapride
SAM001246981	1	E07	Tocris Bioscience	Indatraline
SAM001247045	1	F07	Tocris Bioscience	TRAZODONE HYDROCHLORIDE
SAM001246995	1	G07	Tocris Bioscience	Prazosin
SAM001247001	1	H07	Tocris Bioscience	URAPIDIL HYDROCHLORIDE
SAM001247007	1	A08	Tocris Bioscience	(-)-Cotinine
SAM001247014	1	B08	Tocris Bioscience	D-CYCLOSERINE
SAM001246977	1	C08	Tocris Bioscience	Fluvoxamine
SAM001246976	1	D08	Tocris Bioscience	Doxepin
SAM001247046	1	E08	Tocris Bioscience	
SAM001247023	1	F08	Tocris Bioscience	(+)-3-HYDROXY-N-METHYLMORPHINAN D-TARTRATE
SAM001247049	1	G08	Tocris Bioscience	L-Ornithine, N5-[imino(methylamino)methyl]-[CAS]
SAM001246989	1	H08	Tocris Bioscience	Maprotilline HCl
SAM001247038	1	A09	Tocris Bioscience	Pizotyline
SAM001247032	1	B09	Tocris Bioscience	BETA-ESTRADIOL
SAM001247019	1	C09	Tocris Bioscience	N,N'-DIACETYL-1,6-DIAMINOHEXANE
SAM001247024	1	D09	Tocris Bioscience	Diphenhydramine hydrochloride
SAM001246978	1	E09	Tocris Bioscience	Galanthamine
SAM001246980	1	F09	Tocris Bioscience	Ifenprodil
SAM001247028	1	G09	Tocris Bioscience	TETRAETHYLTHIURAM DISULFIDE
SAM001246994	1	H09	Tocris Bioscience	Piribedil
SAM001246983	1	A10	Tocris Bioscience	
SAM001247047	1	B10	Tocris Bioscience	TRIPELENNAMINE HYDROCHLORIDE
SAM001246996	1	C10	Tocris Bioscience	Pyrazinecarboxamide, 3,5-diamino-N-(aminoiminomethyl)-6-chloro- [CAS]

SAM001247002	1	D10	Tocris Bioscience	9-AMINO-1,2,3,4-TETRAHYDROACRIDINE HYDROCHLORIDE
SAM001247008	1	E10	Tocris Bioscience	ETHYNYLESTRADIOL
SAM001247012	1	F10	Tocris Bioscience	2(1H)-Pyrimidinone, 4-amino-1-テソ-D-arabinofuranosyl- [CAS]
SAM001246985	1	G10	Tocris Bioscience	L-Glutamic acid, N-[4-[[(2,4-diamino-6-pteridinyl)methyl]methylamino]benzoyl]- [CAS]
SAM001247043	1	H10	Tocris Bioscience	TFMPP
SAM001247006	1	A11	Tocris Bioscience	Pramipexole
SAM001247018	1	B11	Tocris Bioscience	LIDOCAINE
SAM001246982	1	C11	Tocris Bioscience	Indomethacin
SAM001246988	1	D11	Tocris Bioscience	LY 171883
SAM001246991	1	E11	Tocris Bioscience	Paroxetine
SAM001247031	1	F11	Tocris Bioscience	Epigallocatechin gallate
SAM001247020	1	G11	Tocris Bioscience	5-Amino-2-hydroxy-benzoic acid
SAM001247025	1	H11	Tocris Bioscience	Oxiranecarboxylic acid, 2-[6-(4-chlorophenoxy)hexyl]-, ethyl ester- [CAS]
SAM001246761	2	A02	Sequoia RP Ltd	Cephalexin monohydrate
SAM001246762	2	B02	Sequoia RP Ltd	PIDOTIMOD
SAM001246757	2	C02	Sequoia RP Ltd	RAMIPRIL
SAM001246642	2	D02	Sequoia RP Ltd	FENPIVERINIUM BROMIDE
SAM001246751	2	E02	Sequoia RP Ltd	
SAM001246752	2	F02	Sequoia RP Ltd	NIZATIDINE
SAM001246753	2	G02	Sequoia RP Ltd	5-FLUOROCYTOSINE
SAM001246754	2	H02	Sequoia RP Ltd	Trileptal
SAM001246756	2	A03	Sequoia RP Ltd	TROXIPIDE
SAM001246647	2	B03	Sequoia RP Ltd	ACTARIT
SAM001246645	2	C03	Sequoia RP Ltd	AZELASTINE HCl
SAM001246759	2	D03	Sequoia RP Ltd	TOCAINIDE
SAM001246760	2	E03	Sequoia RP Ltd	TAXIFOLIN-(+/-)
SAM001246758	2	F03	Sequoia RP Ltd	LEVOFLOXACIN
SAM001246643	2	G03	Sequoia RP Ltd	CEFATRIZINE PROPYLENE GLYCOL
SAM001246700	2	H03	Sequoia RP Ltd	IDEBENONE
SAM001246703	2	A04	Sequoia RP Ltd	LEVOSULPIRIDE
SAM001246706	2	B04	Sequoia RP Ltd	Pemoline
SAM001246649	2	C04	Sequoia RP Ltd	LETROZOLE
SAM001246650	2	D04	Sequoia RP Ltd	MEROPENEM
SAM001246637	2	E04	Sequoia RP Ltd	ORLISTAT
SAM001246631	2	F04	Sequoia RP Ltd	
SAM001246694	2	G04	Sequoia RP Ltd	LEVONORGESTREL
SAM001246695	2	H04	Sequoia RP Ltd	CETRAXATE HCl
SAM001246696	2	A05	Sequoia RP Ltd	Alprazolam
SAM001246697	2	B05	Sequoia RP Ltd	LAMOTRIGINE
SAM001246702	2	C05	Sequoia RP Ltd	N-Ethyl-o-crotonotoluidide
SAM001246699	2	D05	Sequoia RP Ltd	AMFEBUTAMONE HCl
SAM001246638	2	E05	Sequoia RP Ltd	ALFUZOSIN
SAM001246639	2	F05	Sequoia RP Ltd	Amisulpride
SAM001246632	2	G05	Sequoia RP Ltd	LOFEPRAMINE
SAM001246688	2	H05	Sequoia RP Ltd	PEROSPIRONE HCl
SAM001246689	2	A06	Sequoia RP Ltd	DOCETAXEL
SAM001246690	2	B06	Sequoia RP Ltd	HONOKIOL
SAM001246691	2	C06	Sequoia RP Ltd	TOLTERODINE TARTRATE
SAM001246692	2	D06	Sequoia RP Ltd	CARMOFUR
SAM001246633	2	E06	Sequoia RP Ltd	PAROXETINE

SAM001246634	2	F06	Sequoia RP Ltd	OLMESARTAN MEDOXOMIL
SAM001246635	2	G06	Sequoia RP Ltd	LOSARTAN Potassium
SAM001246636	2	H06	Sequoia RP Ltd	TEMOZOLOMIDE
SAM001246682	2	A07	Sequoia RP Ltd	Methyltestosterone
SAM001246686	2	B07	Sequoia RP Ltd	TOSUFLOXACIN TOSYLATE
SAM001246687	2	C07	Sequoia RP Ltd	MECILLINAM
SAM001246626	2	D07	Sequoia RP Ltd	ATOMOXETINE HCl
SAM001246628	2	E07	Sequoia RP Ltd	ARTESUNATE
SAM001246679	2	F07	Sequoia RP Ltd	ITRACONAZOLE
SAM001246674	2	G07	Sequoia RP Ltd	CEFPODOXIME PROXETIL
SAM001246680	2	H07	Sequoia RP Ltd	Buflomedil HCl
SAM001246614	2	A08	Sequoia RP Ltd	4-Chloro-N-(2-morpholin-4-yl-ethyl)-benzamide
SAM001246616	2	B08	Sequoia RP Ltd	HALOMETASONE MONOHYDRATE
SAM001246681	2	C08	Sequoia RP Ltd	TRICLABENDAZOLE
SAM001246617	2	D08	Sequoia RP Ltd	ROFECOXIB
SAM001246618	2	E08	Sequoia RP Ltd	BISOPROLOL FUMARATE
SAM001246623	2	F08	Sequoia RP Ltd	EZETIMIBE
SAM001246625	2	G08	Sequoia RP Ltd	TIAGABINE HCl
SAM001246676	2	H08	Sequoia RP Ltd	IDARUBICIN HCl
SAM001246685	2	A09	Sequoia RP Ltd	FLUBENDAZOLE
SAM001246677	2	B09	Sequoia RP Ltd	TACROLIMUS
SAM001246749	2	C09	Sequoia RP Ltd	VALACICLOVIR HYDROCHLORIDE
SAM001246748	2	D09	Sequoia RP Ltd	CLARITHROMYCIN
SAM001246750	2	E09	Sequoia RP Ltd	ARIPIPRAZOLE
SAM001246747	2	F09	Sequoia RP Ltd	TRIMEBUTINE MALEATE
SAM001246746	2	G09	Sequoia RP Ltd	Mestanolone
SAM001246719	2	H09	Sequoia RP Ltd	NISOLDIPINE
SAM001246720	2	A10	Sequoia RP Ltd	PICEID
SAM001246716	2	B10	Sequoia RP Ltd	1-(2-Methyl-5-nitro-imidazol-1-yl)-propan-2-ol
SAM001246717	2	C10	Sequoia RP Ltd	NIFEKALANT HCl
SAM001246721	2	D10	Sequoia RP Ltd	NATEGLINIDE
SAM001246722	2	E10	Sequoia RP Ltd	MEGESTROL ACETATE
SAM001246728	2	F10	Sequoia RP Ltd	ORMETOPRIM
SAM001246738	2	G10	Sequoia RP Ltd	ZILEUTON
SAM001246729	2	H10	Sequoia RP Ltd	STAVUDINE
SAM001246730	2	A11	Sequoia RP Ltd	
SAM001246724	2	B11	Sequoia RP Ltd	OXICONAZOLE NITRATE
SAM001246731	2	C11	Sequoia RP Ltd	KITASAMYCIN
SAM001246732	2	D11	Sequoia RP Ltd	FAMCICLOVIR
SAM001246725	2	E11	Sequoia RP Ltd	
SAM001246726	2	F11	Sequoia RP Ltd	RUFLOXACIN HCl
SAM001246778	2	G11	Sequoia RP Ltd	TAXIFOLIN-(+)
SAM001246782	2	H11	Sequoia RP Ltd	ALOSETRON HCl
SAM001246723	3	A02	Sequoia RP Ltd	BUPROPION HYDROCHLORIDE
SAM001246718	3	B02	Sequoia RP Ltd	IRSOGLADINE MALEATE
SAM001246733	3	C02	Sequoia RP Ltd	ACARBOSE
SAM001246739	3	D02	Sequoia RP Ltd	BENPROPERINE PHOSPHATE
SAM001246740	3	E02	Sequoia RP Ltd	PHENPROBAMATE
SAM001246743	3	F02	Sequoia RP Ltd	MEMANTINE HYDROCHLORIDE
SAM001246736	3	G02	Sequoia RP Ltd	Carvedilol
SAM001246741	3	H02	Sequoia RP Ltd	LOMIFYLLINE
SAM001246742	3	A03	Sequoia RP Ltd	PAZUFLOXACIN

SAM001246745	3	B03	Sequoia RP Ltd	MIGLITOL
SAM001246737	3	C03	Sequoia RP Ltd	TRANILAST
SAM001246652	3	D03	Sequoia RP Ltd	OLANZAPINE
SAM001246653	3	E03	Sequoia RP Ltd	Nefazodone
SAM001246654	3	F03	Sequoia RP Ltd	MOXIFLOXACIN HCl
SAM001246655	3	G03	Sequoia RP Ltd	NELFINAVIR MESYLATE
SAM001246656	3	H03	Sequoia RP Ltd	PRAVASTATIN Sodium
SAM001246651	3	A04	Sequoia RP Ltd	TOPOTECAN HCL
SAM001246539	3	B04	Sequoia RP Ltd	LEVETIRACETAM
SAM001246540	3	C04	Sequoia RP Ltd	PRAMIPEXOLE HCl
SAM001246595	3	D04	Sequoia RP Ltd	RISPERIDONE
SAM001246600	3	E04	Sequoia RP Ltd	PIOGLITAZONE HCl
SAM001246552	3	F04	Sequoia RP Ltd	CILASTATIN Na
SAM001246661	3	G04	Sequoia RP Ltd	ARGATROBAN
SAM001246603	3	H04	Sequoia RP Ltd	VALDECOXIB
SAM001246658	3	A05	Sequoia RP Ltd	NAFTOPIDIL
SAM001246662	3	B05	Sequoia RP Ltd	Nobiletin
SAM001246541	3	C05	Sequoia RP Ltd	FINASTERIDE
SAM001246549	3	D05	Sequoia RP Ltd	ZOLPIDEM TARTRATE
SAM001246551	3	E05	Sequoia RP Ltd	Viramune
SAM001246601	3	F05	Sequoia RP Ltd	TOPIRAMATE
SAM001246664	3	G05	Sequoia RP Ltd	VORICONAZOLE
SAM001246665	3	H05	Sequoia RP Ltd	FENOLDOPAM MESYLATE
SAM001246610	3	A06	Sequoia RP Ltd	ROSIGLITAZONE MALEATE
SAM001246668	3	B06	Sequoia RP Ltd	ESCITALOPRAM OXALATE
SAM001246609	3	C06	Sequoia RP Ltd	ZERANOL
SAM001246671	3	D06	Sequoia RP Ltd	LATANOPROST
SAM001246673	3	E06	Sequoia RP Ltd	2',3'-DIDEOXYINOSINE
SAM001246666	3	F06	Sequoia RP Ltd	Sertraline
SAM001246670	3	G06	Sequoia RP Ltd	CALCIPOTRIOL
SAM001246559	3	H06	Sequoia RP Ltd	EPIRUBICIN HYDROCHLORIDE
SAM001246612	3	A07	Sequoia RP Ltd	BICALUTAMIDE
SAM001246672	3	B07	Sequoia RP Ltd	BENIDIPINE HCl
SAM001246669	3	C07	Sequoia RP Ltd	AMLEXANOX
SAM001246554	3	D07	Sequoia RP Ltd	CERIVASTATIN Na
SAM001246560	3	E07	Sequoia RP Ltd	ICARIIN
SAM001246562	3	F07	Sequoia RP Ltd	METHYLANDROSTENEDIOL
SAM001246553	3	G07	Sequoia RP Ltd	TRIPTOLIDE
SAM001246608	3	H07	Sequoia RP Ltd	ROSIGLITAZONE HCl
SAM001246561	3	A08	Sequoia RP Ltd	FTORAFUR
SAM001246769	3	B08	Sequoia RP Ltd	OLIGOMYCIN C
SAM001246712	3	C08	Sequoia RP Ltd	BENAZEPRIL HCl
SAM001246765	3	D08	Sequoia RP Ltd	Oxymetholone
SAM001246714	3	E08	Sequoia RP Ltd	IPRIFLAVONE
SAM001246770	3	F08	Sequoia RP Ltd	OXAPROZIN
SAM001246766	3	G08	Sequoia RP Ltd	ROLIPRAM
SAM001246713	3	H08	Sequoia RP Ltd	MOSAPRIDE CITRATE
SAM001246767	3	A09	Sequoia RP Ltd	Isoquercitrin
SAM001246763	3	B09	Sequoia RP Ltd	FLUMAZENIL
SAM001246593	3	C09	Sequoia RP Ltd	
SAM001246776	3	D09	Sequoia RP Ltd	HYPEROSIDE
SAM001246589	3	E09	Sequoia RP Ltd	RIFABUTIN

SAM001246533	3	F09	Sequoia RP Ltd	ESMOLOL HYDROCHLORIDE
SAM001246586	3	G09	Sequoia RP Ltd	TADALAFIL
SAM001246587	3	H09	Sequoia RP Ltd	Modafinil
SAM001246768	3	A10	Sequoia RP Ltd	DOXORUBICIN HYDROCHLORIDE
SAM001246764	3	B10	Sequoia RP Ltd	MOXONIDINE HCl
SAM001246711	3	C10	Sequoia RP Ltd	Nitrazepam
SAM001246571	3	D10	Sequoia RP Ltd	PEFLOXACIN MESYLATE
SAM001246572	3	E10	Sequoia RP Ltd	VENLAFAXINE HCl
SAM001246591	3	F10	Sequoia RP Ltd	PANTOPRAZOLE SODIUM SALT
SAM001246583	3	G10	Sequoia RP Ltd	FLUTICASONE PROPIONATE
SAM001246588	3	H10	Sequoia RP Ltd	INDINAVIR SULPHATE
SAM001246585	3	A11	Sequoia RP Ltd	MIDAZOLAM HCl
SAM001246582	3	B11	Sequoia RP Ltd	LAMIVUDINE
SAM001246564	3	C11	Sequoia RP Ltd	PROCARBAZINE HYDROCHLORIDE
SAM001246538	3	D11	Sequoia RP Ltd	ESOMEPRAZOLE Mg
SAM001246530	3	E11	Sequoia RP Ltd	SULFASALAZINE
SAM001246567	3	F11	Sequoia RP Ltd	TORASEMIDE
SAM001246576	3	G11	Sequoia RP Ltd	TROPISETRON HCl
SAM001246534	3	H11	Sequoia RP Ltd	Ranolazine dihydrochloride
SAM001246531	4	A02	Sequoia RP Ltd	NITRENDIPINE
SAM001246578	4	B02	Sequoia RP Ltd	SAQUINAVIR MESYLATE
SAM001246775	4	C02	Sequoia RP Ltd	BIFONAZOLE
SAM001246579	4	D02	Sequoia RP Ltd	SUMATRIPTAN SUCCINATE
SAM001246574	4	E02	Sequoia RP Ltd	EXEMESTANE
SAM001246708	4	F02	Sequoia RP Ltd	NITAZOXANIDE
SAM001246536	4	G02	Sequoia RP Ltd	Diazepam
SAM001246777	4	H02	Sequoia RP Ltd	QUETIAPINE HEMIFUMARATE
SAM001246528	4	A03	Sequoia RP Ltd	RUTIN
SAM001246580	4	B03	Sequoia RP Ltd	PENCICLOVIR
SAM001246772	4	C03	Sequoia RP Ltd	CALCITRIOL
SAM001246532	4	D03	Sequoia RP Ltd	DIPHENOXYLATE
SAM001247005	4	E03	Tocris Bioscience	Felbamate
SAM001247013	4	F03	Tocris Bioscience	DROPERIDOL
SAM001247011	4	G03	Tocris Bioscience	Pentoxifylline
SAM001246596	4	H03	Sequoia RP Ltd	
SAM001246783	4	A04	Sequoia RP Ltd	RITONAVIR
SAM001246780	4	B04	Sequoia RP Ltd	VINORELBINE BITATRATE
SAM001246624	4	C04	Sequoia RP Ltd	LINEZOLID
SAM001246727	4	D04	Sequoia RP Ltd	LOMERIZINE DiHCl
SAM001246667	4	E04	Sequoia RP Ltd	EFAVIRENZ
SAM001246548	4	F04	Sequoia RP Ltd	IRBESARTAN
SAM001246546	4	G04	Sequoia RP Ltd	REPAGLINIDE
SAM001246555	4	H04	Sequoia RP Ltd	Ethylestrenol
SAM001246605	4	A05	Sequoia RP Ltd	PTEROSTILBENE
SAM001246547	4	B05	Sequoia RP Ltd	ROXATIDINE ACETATE HCl
SAM001246556	4	C05	Sequoia RP Ltd	DEXBROMPHENIRAMINE MALEATE
SAM001246604	4	D05	Sequoia RP Ltd	ANAGRELIDE HCl
SAM001246606	4	E05	Sequoia RP Ltd	TEGASEROD MALEATE
SAM001246611	4	F05	Sequoia RP Ltd	MILRINONE
SAM001246575	4	G05	Sequoia RP Ltd	LEVOCETIRIZINE
SAM001246599	4	H05	Sequoia RP Ltd	
SAM001246558	4	A06	Sequoia RP Ltd	TICLOPIDINE HCl

SAM001246594	4	B06	Sequoia RP Ltd	LOXOPROFEN SODIUM
SAM001246577	4	C06	Sequoia RP Ltd	ZAFIRLUKAST
SAM001246565	4	D06	Sequoia RP Ltd	TERBINAFINE HCl
SAM001246584	4	E06	Sequoia RP Ltd	ISRADIPINE
SAM001246581	4	F06	Sequoia RP Ltd	VALSARTAN
SAM001247048	4	G06	Tocris Bioscience	Piroxicam
SAM001246629	4	H06	Sequoia RP Ltd	Glycopyrrolate
SAM001246992	4	A07	Tocris Bioscience	Physostigmine
SAM001247050	4	B07	Tocris Bioscience	LOBELINE HYDROCHLORIDE
SAM001247030	4	C07	Tocris Bioscience	Doxylamine succinate salt
SAM001247035	4	D07	Tocris Bioscience	Milnacipran
SAM001247017	4	E07	Tocris Bioscience	5-fluoro-2-pyrimidone
SAM001247022	4	F07	Tocris Bioscience	Chlorpheniramine
SAM001246621	4	G07	Sequoia RP Ltd	DOFETILIDE
SAM001246675	4	H07	Sequoia RP Ltd	FORMOTEROL FUMARATE DIHYDRATE
SAM001246615	4	A08	Sequoia RP Ltd	RIZATRIPTAN BENZOATE
SAM001246620	4	B08	Sequoia RP Ltd	RIFAPENTINE
SAM001246630	4	C08	Sequoia RP Ltd	LOTEPREDNOL ETABONATE
SAM001246684	4	D08	Sequoia RP Ltd	ENALAPRILAT
SAM001246627	4	E08	Sequoia RP Ltd	Donepezil
SAM001246755	4	F08	Sequoia RP Ltd	Nimetazepam
SAM001246701	4	G08	Sequoia RP Ltd	
SAM001246602	4	H08	Sequoia RP Ltd	TELMISARTAN
SAM001246542	4	A09	Sequoia RP Ltd	ITOPRIDE HCl
SAM001246597	4	B09	Sequoia RP Ltd	RIFAXIMIN
SAM001246657	4	C09	Sequoia RP Ltd	MONTELUKAST Na
SAM001246779	4	D09	Sequoia RP Ltd	2',3'-DIDEOXYCYTIDINE
SAM001247073	4	E09	Tocris Bioscience	1H-Imidazol-2-amine, N-(2,6-dichlorophenyl)-4,5-dihydro- [CAS]
SAM001247077	4	F09	Tocris Bioscience	6H-Pyrido[2,3-b][1,4]benzodiazepin-6-one, 11-[[2-[(diethylamino)methyl]-1-piperidinyl]acetyl]-5,11-dihydro- [CAS]
SAM001247075	4	G09	Tocris Bioscience	1H-Indole-2-propanoic acid, 1-[(4-chlorophenyl)methyl]-3-[(1,1-dimethylethyl)thio]-Alpha,Alpha-dimethyl-5-(1-methylethyl)- [CAS]
SAM001247074	4	H09	Tocris Bioscience	1H-Imidazole-5-carboxylic acid, 1-(1-phenylethyl)-, ethyl ester, (R)- [CAS]
SAM001247078	4	A10	Tocris Bioscience	Acetamide, 2-amino-N-(1-methyl-1,2-diphenylethyl)-, (+/-)- [CAS]
SAM001247080	4	B10	Tocris Bioscience	Altanserin
SAM001247084	4	C10	Tocris Bioscience	
SAM001246563	4	D10	Sequoia RP Ltd	
SAM001247082	4	E10	Tocris Bioscience	Azasetron
SAM001247087	4	F10	Tocris Bioscience	GR 89696
SAM001246897	4	G10	Sigma CC	DELTA1-HYDROCORTISONE 21-HEMISUCCINATE SODIUM SALT
SAM001246872	4	H10	Sigma CC	DIAZOXIDE
SAM001246886	4	A11	Sigma CC	2-CHLOROADENOSINE
SAM001246873	4	B11	Sigma CC	ORNIDAZOLE
SAM001246914	4	C11	Sigma CC	1,1-DIMETHYL-4-PHENYLPIPERAZINIUM IODIDE
SAM001246893	4	D11	Sigma CC	PIRENPERONE
SAM001246866	4	E11	Sigma CC	MESTRANOL
SAM001246867	4	F11	Sigma CC	2-(2-AMINOETHYL)PYRIDINE
SAM001246868	4	G11	Sigma CC	BENACTYZINE HYDROCHLORIDE
SAM001246870	4	H11	Sigma CC	DICHLOROACETIC ACID
SAM001246806	5	A02	Sequoia RP Ltd	BESTATIN

SAM001246774	5	B02	Sequoia RP Ltd	TOREMIFENE CITRATE
SAM001246784	5	C02	Sequoia RP Ltd	GOSERELIN ACETATE
SAM001246678	5	D02	Sequoia RP Ltd	SECOISOLARICIRESINOL
SAM001246796	5	E02	Sequoia RP Ltd	RALTITREXED
SAM001246792	5	F02	Sequoia RP Ltd	DOXAPRAM HYDROCHLORIDE
SAM001247095	5	G02	Tocris Bioscience	RU 24969
SAM001246865	5	H02	Sigma CC	Brucine
SAM001246862	5	A03	Sigma CC	TRYPTOLINE
SAM001246863	5	B03	Sigma CC	
SAM001246791	5	C03	Sequoia RP Ltd	PALONOSETRON HCl
SAM001246874	5	D03	Sigma CC	NAPROXEN SODIUM
SAM001246875	5	E03	Sigma CC	MEPIVACAINE HYDROCHLORIDE
SAM001246877	5	F03	Sigma CC	3-[3,5-DIBROMO-4-HYDROXYBENZOYL]-2-ETHYLBENZOFURAN
SAM001246890	5	G03	Sigma CC	NIMODIPINE
SAM001246892	5	H03	Sigma CC	ROLITETRACYCLINE
SAM001246891	5	A04	Sigma CC	MEPIRIZOLE
SAM001246876	5	B04	Sigma CC	6-AZAURIDINE
SAM001246889	5	C04	Sigma CC	Reichsteins substance□S
SAM001246894	5	D04	Sigma CC	3-PYRIDINEMETHANOL
SAM001246979	5	E04	Tocris Bioscience	Haloperidol
SAM001247042	5	F04	Tocris Bioscience	Stiripentol
SAM001247034	5	G04	Tocris Bioscience	Fluperlapine
SAM001246887	5	H04	Sigma CC	OXYPHENONIUM BROMIDE
SAM001246869	5	A05	Sigma CC	Homoveratrylamine
SAM001246913	5	B05	Sigma CC	TINIDAZOLE
SAM001246912	5	C05	Sigma CC	XANTHINOL NICOTINATE
SAM001246896	5	D05	Sigma CC	SYNEPHRINE
SAM001246888	5	E05	Sigma CC	Resveratrol
SAM001246871	5	F05	Sigma CC	3-Hydroxy-2-methyl-4-pyrone
SAM001246854	5	G05	Sigma CC	6-AMINOINDAZOLE
SAM001246856	5	H05	Sigma CC	ENROFLOXACIN
SAM001246857	5	A06	Sigma CC	DEHYDROCHOLIC ACID
SAM001246884	5	B06	Sigma CC	CEFACLOR
SAM001246858	5	C06	Sigma CC	1-BENZYLIMIDAZOLE
SAM001246523	5	D06	Sequoia RP Ltd	DULOXETINE HCl
SAM001246573	5	E06	Sequoia RP Ltd	VARDENAFIL CITRATE
SAM001246524	5	F06	Sequoia RP Ltd	ROPIVACAINE HCl
SAM001246525	5	G06	Sequoia RP Ltd	ANASTROZOLE
SAM001246984	5	H06	Tocris Bioscience	KETOTIFEN FUMARATE
SAM001246906	5	A07	Sigma CC	MEDROXYPROGESTERONE
SAM001246907	5	B07	Sigma CC	Pinacidil monohydrate
SAM001246908	5	C07	Sigma CC	7-NITROINDAZOLE
SAM001246909	5	D07	Sigma CC	5-Methoxytryptamine
SAM001246855	5	E07	Sigma CC	PHENOTHIAZINE
SAM001246526	5	F07	Sequoia RP Ltd	2-CHLORO-2'-DEOXYADENOSINE
SAM001246527	5	G07	Sequoia RP Ltd	GRANISETRON HCl
SAM001247094	5	H07	Tocris Bioscience	Rimcazole
SAM001247092	5	A08	Tocris Bioscience	Nafadotride
SAM001246885	5	B08	Sigma CC	DESOXIMETASONE
SAM001246557	5	C08	Sequoia RP Ltd	DEXCHLORPHENIRAMINE MALEATE
SAM001247088	5	D08	Tocris Bioscience	Guanidine, N-cyano-N'-(1,1-dimethylpropyl)-N''-3-pyridinyl- [CAS]

SAM001247090	5	E08	Tocris Bioscience	L-694,247
SAM001247081	5	F08	Tocris Bioscience	AM-251
SAM001247089	5	G08	Tocris Bioscience	HTMT
SAM001247083	5	H08	Tocris Bioscience	Benzo[a]phenanthridine-10,11-diol, 5,6,6a,7,8,12b-hexahydro-, trans- [CAS]
SAM001247091	5	A09	Tocris Bioscience	Methanesulfonamide, N-[4-[[1-[2-(6-methyl-2-pyridinyl)ethyl]-4-piperidinyl]carbonyl]phenyl]-, dihydrochloride [CAS]
SAM001247076	5	B09	Tocris Bioscience	2H-Indol-2-one, 1,3-dihydro-1-phenyl-3,3-bis(4-pyridinylmethyl)- [CAS]
SAM001246898	5	C09	Sigma CC	Beclomethasone
SAM001246900	5	D09	Sigma CC	OMEPRAZOLE
SAM001246842	5	E09	Sequoia RP Ltd	DOLASETRON MESYLATE
SAM001246841	5	F09	Sequoia RP Ltd	Zolmitriptan
SAM001246852	5	G09	Sequoia RP Ltd	TREMULACIN
SAM001246846	5	H09	Sequoia RP Ltd	DACTINOMYCIN
SAM001246847	5	A10	Sequoia RP Ltd	Tramadol
SAM001246815	5	B10	Sequoia RP Ltd	CHLORDIAZEPOXIDE
SAM001246816	5	C10	Sequoia RP Ltd	CEFIXIME TRIHYDRATE
SAM001246818	5	D10	Sequoia RP Ltd	CEFDINIR
SAM001246820	5	E10	Sequoia RP Ltd	LOFEXIDINE HCl
SAM001246804	5	F10	Sequoia RP Ltd	BALSALAZIDE
SAM001246802	5	G10	Sequoia RP Ltd	OLOPATADINE HCl
SAM001246803	5	H10	Sequoia RP Ltd	ITAVASTATIN Ca
SAM001246882	5	A11	Sigma CC	CORTISONE
SAM001246883	5	B11	Sigma CC	
SAM001246822	5	C11	Sequoia RP Ltd	HOMOHARRINGTONINE
SAM001246879	5	D11	Sigma CC	CORTICOSTERONE
SAM001246821	5	E11	Sequoia RP Ltd	VECURONIUM BROMIDE
SAM001246801	5	F11	Sequoia RP Ltd	TIBOLONE
SAM001246860	5	G11	Sigma CC	NICOTINAMIDE
SAM001246861	5	H11	Sigma CC	NIALAMIDE
SAM001246568	6	A02	Sequoia RP Ltd	VINDESINE SULFATE
SAM001246570	6	B02	Sequoia RP Ltd	VINCRISTINE SULFATE
SAM001246648	6	C02	Sequoia RP Ltd	LACIDIPINE
SAM001246659	6	D02	Sequoia RP Ltd	MIRTAZAPINE
SAM001246707	6	E02	Sequoia RP Ltd	AMPIROXICAM
SAM001246710	6	F02	Sequoia RP Ltd	GLIMEPIRIDE
SAM001246705	6	G02	Sequoia RP Ltd	AMLODIPINE BASE
SAM001246619	6	H02	Sequoia RP Ltd	RABEPRAZOLE
SAM001246878	6	A03	Sigma CC	CLOFAZIMINE
SAM001246598	6	B03	Sequoia RP Ltd	IRINOTECAN HCl)trihydrate)
SAM001246544	6	C03	Sequoia RP Ltd	LANSOPRAZOLE
SAM001246545	6	D03	Sequoia RP Ltd	8-Chloro-11-piperidin-4-ylidene-6,11-dihydro-5H-benzo[5,6]cyclohepta[1,2-b]pyridine
SAM001246904	6	E03	Sigma CC	1,3,5(10)-ESTRATRIEN-3-OL-17-ONE SULPHATE, SODIUM SALT
SAM001246881	6	F03	Sigma CC	MIFEPRISTONE
SAM001246880	6	G03	Sigma CC	
SAM001247105	6	H03	Tocris Bioscience	Sibutramine
SAM001247107	6	A04	Tocris Bioscience	Clobenpropit
SAM001246851	6	B04	Sequoia RP Ltd	HUPERZINE A
SAM001246592	6	C04	Sequoia RP Ltd	SIBUTRAMINE HCl
SAM001246833	6	D04	Sequoia RP Ltd	Lorazepam
SAM001247108	6	E04	Tocris Bioscience	8-Azaspiro[4.5]decane-7,9-dione, 8-[2-[[(2,3-dihydro-1,4-benzodioxin-2-yl)methyl]amino]ethyl]-,

				monomethanesulfonate [CAS]
SAM001247106	6	F04	Tocris Bioscience	Adenosine, N-(2-hydroxycyclopentyl)-, (1S-trans)- [CAS]
SAM001246646	6	G04	Sequoia RP Ltd	AMIODARONE HYDROCHLORIDE
SAM001246644	6	H04	Sequoia RP Ltd	mevastatin
SAM001246622	6	A05	Sequoia RP Ltd	IMATINIB MESYLATE
SAM001247102	6	B05	Tocris Bioscience	Metylperon
SAM001246773	6	C05	Sequoia RP Ltd	PARECOXIB Na
SAM001247070	6	D05	Tocris Bioscience	
SAM001246793	6	E05	Sequoia RP Ltd	ATRACURIUM BESYLATE
SAM001246799	6	F05	Sequoia RP Ltd	ARTEMETHER
SAM001247071	6	G05	Tocris Bioscience	EBSELEN
SAM001247066	6	H05	Tocris Bioscience	CGS 12066B
SAM001246805	6	A06	Sequoia RP Ltd	TELITHROMYCIN
SAM001247065	6	B06	Tocris Bioscience	CCPA
SAM001247067	6	C06	Tocris Bioscience	PD 81723
SAM001246590	6	D06	Sequoia RP Ltd	Stanozolol
SAM001246641	6	E06	Sequoia RP Ltd	Zaleplon
SAM001246840	6	F06	Sequoia RP Ltd	Prostaglandin E1
SAM001246921	6	G06	Tocris Bioscience	Testosterone
SAM001246922	6	H06	Tocris Bioscience	DEHYDROEPIANDROSTERONE
SAM001247099	6	A07	Tocris Bioscience	SDM25N
SAM001247101	6	B07	Tocris Bioscience	Thiophene, 5-bromo-2-(4-fluorophenyl)-3-[4-(methylsulfonyl)phenyl]- [CAS]
SAM001247103	6	C07	Tocris Bioscience	5-Nonyloxytryptamine
SAM001247096	6	D07	Tocris Bioscience	Salmeterol
SAM001247097	6	E07	Tocris Bioscience	SB 205607
SAM001247098	6	F07	Tocris Bioscience	R(+)-SCH-23390 hydrochloride

Table 10. NCC003

11 Literature

Abigerges, D., Chabot, G.G., Armand, J.P., Hérait, P., Gouyette, A., and Gandia, D., 1995, Phase I and pharmacologic studies of the camptothecin analog irinotecan administered every 3 weeks in cancer patients: Journal of clinical oncology: official journal of the American Society of Clinical Oncology, v. 13, no. 1, p. 210–221.

Adlkofer, K., and Lai, C., 2000, Role of neuregulins in glial cell development: Glia, v. 29, no. 2, p. 104–111.

Akbarian, S., Kim, J.J., Potkin, S.G., Hagman, J.O., Tafazzoli, A., Bunney, W.E., Jr, and Jones, E.G., 1995, Gene expression for glutamic acid decarboxylase is reduced without loss of neurons in prefrontal cortex of schizophrenics: Archives of general psychiatry, v. 52, no. 4, p. 258–266.

Aleman, A., Kahn, R.S., and Selten, J.-P., 2003, Sex differences in the risk of schizophrenia: evidence from meta-analysis: Archives of general psychiatry, v. 60, no. 6, p. 565–571, doi: 10.1001/archpsyc.60.6.565.

Alimonti, A., Gelibter, A., Pavese, I., Satta, F., Cognetti, F., Ferretti, G., Rasio, D., Vecchione, A., and Di Palma, M., 2004, New approaches to prevent intestinal toxicity of irinotecan-based regimens: Cancer treatment reviews, v. 30, no. 6, p. 555–562, doi: 10.1016/j.ctrv.2004.05.002.

Allen, N.C., Bagade, S., McQueen, M.B., Ioannidis, J.P.A., Kavvoura, F.K., Khoury, M.J., Tanzi, R.E., and Bertram, L., 2008, Systematic meta-analyses and field synopsis of genetic association studies in schizophrenia: the SzGene database: Nature genetics, v. 40, no. 7, p. 827–834, doi: 10.1038/ng.171.

Allen, R.M., and Young, S.J., 1978, Phencyclidine-induced psychosis: The American journal of psychiatry, v. 135, no. 9, p. 1081–1084.

Arkin, M.R., and Wells, J.A., 2004, Small-molecule inhibitors of protein–protein interactions: progressing towards the dream: Nature Reviews Drug Discovery, v. 3, no. 4, p. 301–317, doi: 10.1038/nrd1343.

Arnold, S.E., and Trojanowski, J.Q., 1996, Recent advances in defining the neuropathology of schizophrenia: Acta neuropathologica, v. 92, no. 3, p. 217–231.

Arnt, J., 1998, Pharmacological differentiation of classical and novel antipsychotics: International clinical psychopharmacology, v. 13 Suppl 3, p. S7–14.

Auger, K.R., Serunian, L.A., Soltoff, S.P., Libby, P., and Cantley, L.C., 1989, PDGF-dependent tyrosine phosphorylation stimulates production of novel polyphosphoinositides in intact cells: Cell, v. 57, no. 1, p. 167–175.

Ayhan, Y., Sawa, A., Ross, C.A., and Pletnikov, M.V., 2009, Animal models of gene-environment interactions in schizophrenia: Behavioural brain research, v. 204, no. 2, p. 274–281, doi: 10.1016/j.bbr.2009.04.010.

Barr, M.S., Farzan, F., Tran, L.C., Chen, R., Fitzgerald, P.B., and Daskalakis, Z.J., 2010, Evidence for excessive frontal evoked gamma oscillatory activity in schizophrenia during working memory: Schizophrenia research, v. 121, no. 1-3, p. 146–152, doi: 10.1016/j.schres.2010.05.023.

de Bartolomeis, A., Sarappa, C., Magara, S., and Iasevoli, F., 2012, Targeting glutamate system for novel antipsychotic approaches: relevance for residual psychotic symptoms and treatment resistant schizophrenia: European journal of pharmacology, v. 682, no. 1-3, p. 1–11, doi: 10.1016/j.ejphar.2012.02.033.

Bayer, T.A., Falkai, P., and Maier, W., 1999, Genetic and non-genetic vulnerability factors in schizophrenia: the basis of the “two hit hypothesis:” Journal of psychiatric research, v. 33, no. 6, p. 543–548.

Becker, V., 2005, [Rokitansky and Virchow: throes about the scientific term of disease]: Wiener medizinische Wochenschrift (1946), v. 155, no. 19-20, p. 463–467, doi: 10.1007/s10354-005-0217-x.

Belforte, J.E., Zsiros, V., Sklar, E.R., Jiang, Z., Yu, G., Li, Y., Quinlan, E.M., and Nakazawa, K., 2010, Postnatal NMDA receptor ablation in corticolimbic interneurons confers schizophrenia-like phenotypes: Nature neuroscience, v. 13, no. 1, p. 76–83, doi: 10.1038/nn.2447.

Berganza, C.E., Mezzich, J.E., and Pouncey, C., 2005, Concepts of disease: their relevance for psychiatric diagnosis and classification: Psychopathology, v. 38, no. 4, p. 166–170, doi: 10.1159/000086084.

Bertani, G., 1951, Studies on lysogenesis. I. The mode of phage liberation by lysogenic Escherichia coli: Journal of bacteriology, v. 62, no. 3, p. 293–300.

Bian, S.-Z., Zhang, J., Liu, W.-L., Sun, Z.-H., Gu, Z.-L., and Jiang, X.-G., 2009, [Receptor antagonist of NMDA and animal models of schizophrenia]: Fa yi xue za zhi, v. 25, no. 6, p. 443–446.

Biedermann, F., and Fleischhacker, W.W., 2009, Antipsychotics in the early stage of development: Current opinion in psychiatry, v. 22, no. 3, p. 326–330, doi: 10.1097/YCO.0b013e328329cd73.

Birnboim, H.C., and Doly, J., 1979, A rapid alkaline extraction procedure for screening recombinant plasmid DNA: Nucleic acids research, v. 7, no. 6, p. 1513–1523.

Bjarnadottir, M., Misner, D.L., Haverfield-Gross, S., Bruun, S., Helgason, V.G., Stefansson, H., Sigmundsson, A., Firth, D.R., Nielsen, B., Stefansdottir, R., Novak, T.J., Stefansson, K., Gurney, M.E., and Andresson, T., 2007, Neuregulin1 (NRG1) signaling through Fyn modulates NMDA receptor phosphorylation: differential synaptic function in NRG1+/- knock-outs compared with wild-type mice: The Journal of neuroscience: the official journal of the Society for Neuroscience, v. 27, no. 17, p. 4519–4529, doi: 10.1523/JNEUROSCI.4314-06.2007.

Borasio, G.D., 1990, Differential effects of the protein kinase inhibitor K-252a on the in vitro survival of chick embryonic neurons: Neuroscience letters, v. 108, no. 1-2, p. 207–212.

Botvinnik, A., Wichert, S.P., Fischer, T.M., and Rossner, M.J., 2010, Integrated analysis of receptor activation and downstream signaling with EXTassays: Nature methods, v. 7, no. 1, p. 74–80, doi: 10.1038/nmeth.1407.

Boute, N., Jockers, R., and Issad, T., 2002, The use of resonance energy transfer in high-throughput screening: BRET versus FRET: Trends in pharmacological sciences, v. 23, no. 8, p. 351–354.

Braun, I., Genius, J., Grunze, H., Bender, A., Möller, H.-J., and Rujescu, D., 2007, Alterations of hippocampal and prefrontal GABAergic interneurons in an animal model of psychosis induced by NMDA receptor antagonism: Schizophrenia research, v. 97, no. 1-3, p. 254–263, doi: 10.1016/j.schres.2007.05.005.

Brennand, K.J., and Gage, F.H., 2011, Concise review: the promise of human induced pluripotent stem cell-based studies of schizophrenia: Stem cells (Dayton, Ohio), v. 29, no. 12, p. 1915–1922, doi: 10.1002/stem.762.

Brennand, K.J., and Gage, F.H., 2012, Modeling psychiatric disorders through reprogramming: Disease models & mechanisms, v. 5, no. 1, p. 26–32, doi: 10.1242/dmm.008268.

Brennand, K.J., Simone, A., Jou, J., Gelboin-Burkhart, C., Tran, N., Sangar, S., Li, Y., Mu, Y., Chen, G., Yu, D., McCarthy, S., Sebat, J., and Gage, F.H., 2011, Modelling schizophrenia using human induced pluripotent stem cells: Nature, v. 473, no. 7346, p. 221–225, doi: 10.1038/nature09915.

Brewster, U.C., and Perazella, M.A., 2004, The renin-angiotensin-aldosterone system and the kidney: effects on kidney disease: The American journal of medicine, v. 116, no. 4, p. 263–272, doi: 10.1016/j.amjmed.2003.09.034.

Brinkmann, B.G., Agarwal, A., Sereda, M.W., Garratt, A.N., Müller, T., Wende, H., Stassart, R.M., Nawaz, S., Humml, C., Velanac, V., Radyushkin, K., Goebbels, S., Fischer, T.M., Franklin, R.J., et al., 2008, Neuregulin-1/ErbB signaling serves distinct functions in myelination of the peripheral and central nervous system: Neuron, v. 59, no. 4, p. 581–595, doi: 10.1016/j.neuron.2008.06.028.

Brockes, J.P., Lemke, G.E., and Balzer, D.R., Jr, 1980, Purification and preliminary characterization of a glial growth factor from the bovine pituitary: The Journal of biological chemistry, v. 255, no. 18, p. 8374–8377.

Buonanno, A., 2010, The neuregulin signaling pathway and schizophrenia: from genes to synapses and neural circuits: Brain research bulletin, v. 83, no. 3-4, p. 122–131, doi: 10.1016/j.brainresbull.2010.07.012.

Burgess, A.W., Cho, H.-S., Eigenbrot, C., Ferguson, K.M., Garrett, T.P.J., Leahy, D.J., Lemmon, M.A., Sliwkowski, M.X., Ward, C.W., and Yokoyama, S., 2003, An open-and-shut case? Recent insights into the activation of EGF/ErbB receptors: Molecular cell, v. 12, no. 3, p. 541–552.

Cantor-Graae, E., and Selten, J.-P., 2005, Schizophrenia and migration: a meta-analysis and review: The American journal of psychiatry, v. 162, no. 1, p. 12–24, doi: 10.1176/appi.ajp.162.1.12.

Capdevila-Nortes, X., López-Hernández, T., Ciruela, F., and Estévez, R., 2012, A modification of the split-tobacco etch virus method for monitoring interactions between membrane proteins in mammalian cells: Analytical biochemistry, v. 423, no. 1, p. 109–118, doi: 10.1016/j.ab.2012.01.022.

Carlén, M., Meletis, K., Siegle, J.H., Cardin, J.A., Futai, K., Vierling-Claassen, D., Rühlmann, C., Jones, S.R., Deisseroth, K., Sheng, M., Moore, C.I., and Tsai, L.-H., 2012, A critical role for NMDA receptors in parvalbumin interneurons for gamma rhythm induction and behavior: Molecular psychiatry, v. 17, no. 5, p. 537–548, doi: 10.1038/mp.2011.31.

Carlsson, A., Waters, N., and Carlsson, M.L., 1999, Neurotransmitter interactions in schizophrenia-therapeutic implications: European archives of psychiatry and clinical neuroscience, v. 249 Suppl 4, p. 37–43.

Carol, H., Houghton, P.J., Morton, C.L., Kolb, E.A., Gorlick, R., Reynolds, C.P., Kang, M.H., Maris, J.M., Keir, S.T., Watkins, A., Smith, M.A., and Lock, R.B., 2010, Initial Testing of Topotecan by the Pediatric Preclinical Testing Program: Pediatric blood & cancer, v. 54, no. 5, p. 707–715, doi: 10.1002/pbc.22352.

Carpenter, G., 2003, ErbB-4: mechanism of action and biology: Experimental cell research, v. 284, no. 1, p. 66–77.

Carraway, K.L., 3rd, Sliwkowski, M.X., Akita, R., Platko, J.V., Guy, P.M., Nuijens, A., Diamonti, A.J., Vandlen, R.L., Cantley, L.C., and Cerione, R.A., 1994, The erbB3 gene product is a receptor for heregulin: The Journal of biological chemistry, v. 269, no. 19, p. 14303–14306.

Castoldi, R., Jucknischke, U., Pradel, L.P., Arnold, E., Klein, C., Scheiblich, S., Niederfellner, G., and Sustmann, C., 2012, Molecular characterization of novel trispecific ErbB-cMet-IGF1R antibodies and their antigen-binding properties: Protein Engineering Design and Selection,, doi: 10.1093/protein/gzs048.

Chen, Y.-J.J., Johnson, M.A., Lieberman, M.D., Goodchild, R.E., Schobel, S., Lewandowski, N., Rosoklija, G., Liu, R.-C., Gingrich, J.A., Small, S., Moore, H., Dwork, A.J., Talmage, D.A., and Role, L.W., 2008, Type III neuregulin-1 is required for normal sensorimotor gating, memory-related behaviors, and corticostriatal circuit components: The Journal of neuroscience: the official journal of the Society for Neuroscience, v. 28, no. 27, p. 6872–6883, doi: 10.1523/JNEUROSCI.1815-08.2008.

Chen, S.-K., Tvrdik, P., Peden, E., Cho, S., Wu, S., Spangrude, G., and Capecchi, M.R., 2010, Hematopoietic origin of pathological grooming in Hoxb8 mutant mice: Cell, v. 141, no. 5, p. 775–785, doi: 10.1016/j.cell.2010.03.055.

Cheng, K.C.-C., and Inglese, J., 2012, A coincidence reporter-gene system for high-throughput screening: Nature methods, v. 9, no. 10, p. 937, doi: 10.1038/nmeth.2170.

Clower, W.T., and Finger, S., 2001, Discovering trepanation: the contribution of Paul Broca: Neurosurgery, v. 49, no. 6, p. 1417–1425; discussion 1425–1426.

Davis, K.L., Kahn, R.S., Ko, G., and Davidson, M., 1991, Dopamine in schizophrenia: a review and reconceptualization: The American journal of psychiatry, v. 148, no. 11, p. 1474–1486.

Desbonnet, L., Waddington, J.L., and O'Tuathaigh, C.M.P., 2009, Mutant models for genes associated with schizophrenia: Biochemical Society transactions, v. 37, no. Pt 1, p. 308–312, doi: 10.1042/BST0370308.

Djannatian, M.S., Galinski, S., Fischer, T.M., and Rossner, M.J., 2011, Studying G protein-coupled receptor activation using split-tobacco etch virus assays: Analytical biochemistry, v. 412, no. 2, p. 141–152, doi: 10.1016/j.ab.2011.01.042.

Eaton, W.W., Hall, A.L.F., Macdonald, R., and McKibben, J., 2007, Case identification in psychiatric epidemiology: a review: International review of psychiatry (Abingdon, England), v. 19, no. 5, p. 497–507, doi: 10.1080/09540260701564906.

Eitner, K., and Koch, U., 2009, From fragment screening to potent binders: strategies for fragment-to-lead evolution: Mini reviews in medicinal chemistry, v. 9, no. 8, p. 956–961.

Elenius, K., Choi, C.J., Paul, S., Santiestevan, E., Nishi, E., and Klagsbrun, M., 1999, Characterization of a naturally occurring ErbB4 isoform that does not bind or activate phosphatidyl inositol 3-kinase: Oncogene, v. 18, no. 16, p. 2607–2615, doi: 10.1038/sj.onc.1202612.

Ellard, J., 1987, Did schizophrenia exist before the eighteenth century?: The Australian and New Zealand journal of psychiatry, v. 21, no. 3, p. 306–318.

Emamian, E.S., 2012, AKT/GSK3 signaling pathway and schizophrenia: Frontiers in molecular neuroscience, v. 5, p. 33, doi: 10.3389/fnmol.2012.00033.

Eyjolfsson, E.M., Brenner, E., Kondziella, D., and Sonnewald, U., 2006, Repeated injection of MK801: an animal model of schizophrenia?: Neurochemistry international, v. 48, no. 6-7, p. 541–546, doi: 10.1016/j.neuint.2005.11.019.

Fagart, J., Hillisch, A., Huyet, J., Bärfacker, L., Fay, M., Pleiss, U., Pook, E., Schäfer, S., Rafestin-Oblin, M.-E., and Kolkhof, P., 2010, A new mode of mineralocorticoid receptor antagonism by a potent and selective nonsteroidal molecule: The Journal of biological chemistry, v. 285, no. 39, p. 29932–29940, doi: 10.1074/jbc.M110.131342.

Falls, D.L., 2003, Neuregulins: functions, forms, and signaling strategies: Experimental cell research, v. 284, no. 1, p. 14–30.

Fazzari, P., Paternain, A.V., Valiente, M., Pla, R., Luján, R., Lloyd, K., Lerma, J., Marín, O., and Rico, B., 2010, Control of cortical GABA circuitry development by Nrg1 and ErbB4 signalling: Nature, v. 464, no. 7293, p. 1376–1380, doi: 10.1038/nature08928.

Ferentinos, P., and Dikeos, D., 2012, Genetic correlates of medical comorbidity associated with schizophrenia and treatment with antipsychotics: Current opinion in psychiatry, v. 25, no. 5, p. 381–390, doi: 10.1097/YCO.0b013e3283568537.

Di Fiore, P.P., Segatto, O., Lonardo, F., Fazioli, F., Pierce, J.H., and Aaronson, S.A., 1990, The carboxy-terminal domains of erbB-2 and epidermal growth factor receptor exert different regulatory effects on intrinsic receptor tyrosine kinase function and transforming activity: Molecular and cellular biology, v. 10, no. 6, p. 2749–2756.

Fisahn, A., Neddens, J., Yan, L., and Buonanno, A., 2009, Neuregulin-1 modulates hippocampal gamma oscillations: implications for schizophrenia: Cerebral cortex (New York, N.Y.: 1991), v. 19, no. 3, p. 612–618, doi: 10.1093/cercor/bhn107.

Fishman, M.C., and Porter, J.A., 2005, Pharmaceuticals: a new grammar for drug discovery: Nature, v. 437, no. 7058, p. 491–493, doi: 10.1038/437491a.

Flames, N., Long, J.E., Garratt, A.N., Fischer, T.M., Gassmann, M., Birchmeier, C., Lai, C., Rubenstein, J.L.R., and Marín, O., 2004, Short- and long-range attraction of cortical GABAergic interneurons by neuregulin-1: Neuron, v. 44, no. 2, p. 251–261, doi: 10.1016/j.neuron.2004.09.028.

Fleck, D., Garratt, A.N., Haass, C., and Willem, M., 2011, BACE1 Dependent Neuregulin Proteolysis: Current Alzheimer research,.

Flores, C., and Coyle, J.T., 2003, Regulation of glutamate carboxypeptidase II function in corticolimbic regions of rat brain by phencyclidine, haloperidol, and clozapine: Neuropsychopharmacology: official publication of the American College of Neuropsychopharmacology, v. 28, no. 7, p. 1227–1234, doi: 10.1038/sj.npp.1300129.

Fornito, A., Zalesky, A., Pantelis, C., and Bullmore, E.T., 2012, Schizophrenia, neuroimaging and connectomics: NeuroImage, v. 62, no. 4, p. 2296–2314, doi: 10.1016/j.neuroimage.2011.12.090.

Freyer, M.W., and Lewis, E.A., 2008, Isothermal titration calorimetry: experimental design, data analysis, and probing macromolecule/ligand binding and kinetic interactions: Methods in cell biology, v. 84, p. 79–113, doi: 10.1016/S0091-679X(07)84004-0.

Fried, K., Risling, M., Tidcombe, H., Gassmann, M., and Lillesaar, C., 2002, Expression of ErbB3, ErbB4, and neuregulin-1 mRNA during tooth development: Developmental dynamics: an official publication of the American Association of Anatomists, v. 224, no. 3, p. 356–360, doi: 10.1002/dvdy.10114.

Fuller, P.J., Yao, Y., Yang, J., and Young, M.J., 2012, Mechanisms of ligand specificity of the mineralocorticoid receptor: The Journal of endocrinology, v. 213, no. 1, p. 15–24, doi: 10.1530/JOE-11-0372.

Gao, Z., and Jacobson, K.A., 2002, 2-Chloro-N(6)-cyclopentyladenosine, adenosine A(1) receptor agonist, antagonizes the adenosine A(3) receptor: European journal of pharmacology, v. 443, no. 1-3, p. 39–42.

Gaunitz, F., and Papke, M., 1998, Gene transfer and expression: Methods in molecular biology (Clifton, N.J.), v. 107, p. 361–370, doi: 10.1385/0-89603-519-0:361.

Geerling, J.C., and Loewy, A.D., 2009, Aldosterone in the brain: American journal of physiology. Renal physiology, v. 297, no. 3, p. F559–576, doi: 10.1152/ajprenal.90399.2008.

Goff, D.C., and Coyle, J.T., 2001, The emerging role of glutamate in the pathophysiology and treatment of schizophrenia: The American journal of psychiatry, v. 158, no. 9, p. 1367–1377.

Goldman-Rakic, P.S., Castner, S.A., Svensson, T.H., Siever, L.J., and Williams, G.V., 2004, Targeting the dopamine D1 receptor in schizophrenia: insights for cognitive

dysfunction: Psychopharmacology, v. 174, no. 1, p. 3–16, doi: 10.1007/s00213-004-1793-y.

Greene, L.A., and Tischler, A.S., 1976, Establishment of a noradrenergic clonal line of rat adrenal pheochromocytoma cells which respond to nerve growth factor: Proceedings of the National Academy of Sciences of the United States of America, v. 73, no. 7, p. 2424–2428.

Gromova, I.I., Kjeldsen, E., Svejstrup, J.Q., Alsner, J., Christiansen, K., and Westergaard, O., 1993, Characterization of an altered DNA catalysis of a camptothecin-resistant eukaryotic topoisomerase I: Nucleic acids research, v. 21, no. 3, p. 593–600.

Grossmann, C., Ruhs, S., Langenbruch, L., Mildenberger, S., Strätz, N., Schumann, K., and Gekle, M., 2012, Nuclear shuttling precedes dimerization in mineralocorticoid receptor signaling: Chemistry & biology, v. 19, no. 6, p. 742–751, doi: 10.1016/j.chembiol.2012.04.014.

Grossmann, K.S., Wende, H., Paul, F.E., Cheret, C., Garratt, A.N., Zurborg, S., Feinberg, K., Besser, D., Schulz, H., Peles, E., Selbach, M., Birchmeier, W., and Birchmeier, C., 2009, The tyrosine phosphatase Shp2 (PTPN11) directs Neuregulin-1/ErbB signaling throughout Schwann cell development: Proceedings of the National Academy of Sciences of the United States of America, v. 106, no. 39, p. 16704–16709, doi: 10.1073/pnas.0904336106.

Grunze, H.C., Rainnie, D.G., Hasselmo, M.E., Barkai, E., Hearn, E.F., McCarley, R.W., and Greene, R.W., 1996, NMDA-dependent modulation of CA1 local circuit inhibition: The Journal of neuroscience: the official journal of the Society for Neuroscience, v. 16, no. 6, p. 2034–2043.

Gunduz-Bruce, H., 2009, The acute effects of NMDA antagonism: from the rodent to the human brain: Brain research reviews, v. 60, no. 2, p. 279–286, doi: 10.1016/j.brainresrev.2008.07.006.

Haenschel, C., Bittner, R.A., Waltz, J., Haertling, F., Wibral, M., Singer, W., Linden, D.E.J., and Rodriguez, E., 2009, Cortical oscillatory activity is critical for working memory as revealed by deficits in early-onset schizophrenia: The Journal of neuroscience: the official journal of the Society for Neuroscience, v. 29, no. 30, p. 9481–9489, doi: 10.1523/JNEUROSCI.1428-09.2009.

Hall, J., Whalley, H.C., Job, D.E., Baig, B.J., McIntosh, A.M., Evans, K.L., Thomson, P.A., Porteous, D.J., Cunningham-Owens, D.G., Johnstone, E.C., and Lawrie, S.M., 2006, A neuregulin 1 variant associated with abnormal cortical function and psychotic symptoms: Nature neuroscience, v. 9, no. 12, p. 1477–1478, doi: 10.1038/nn1795.

Hancock, M.L., Canetta, S.E., Role, L.W., and Talmage, D.A., 2008, Presynaptic type III neuregulin1-ErbB signaling targets alpha7 nicotinic acetylcholine receptors to axons: The Journal of general physiology, v. 131, no. 6, p. i4, doi: 10.1085/JGP1316OIA4.

Hanisch, U.-K., and Kettenmann, H., 2007, Microglia: active sensor and versatile effector cells in the normal and pathologic brain: Nature neuroscience, v. 10, no. 11, p. 1387–1394, doi: 10.1038/nn1997.

Harrison, P.J., and Weinberger, D.R., 2005, Schizophrenia genes, gene expression, and neuropathology: on the matter of their convergence: Molecular psychiatry, v. 10, no. 1, p. 40–68; image 5, doi: 10.1038/sj.mp.4001558.

Hartley, J.L., Temple, G.F., and Brasch, M.A., 2000, DNA cloning using in vitro site-specific recombination: Genome research, v. 10, no. 11, p. 1788–1795.

Hashimoto, T., Volk, D.W., Eggan, S.M., Mirnics, K., Pierri, J.N., Sun, Z., Sampson, A.R., and Lewis, D.A., 2003, Gene expression deficits in a subclass of GABA neurons in the prefrontal cortex of subjects with schizophrenia: The Journal of neuroscience: the official journal of the Society for Neuroscience, v. 23, no. 15, p. 6315–6326.

Höistad, M., Segal, D., Takahashi, N., Sakurai, T., Buxbaum, J.D., and Hof, P.R., 2009, Linking white and grey matter in schizophrenia: oligodendrocyte and neuron pathology in the prefrontal cortex: Frontiers in neuroanatomy, v. 3, p. 9, doi: 10.3389/neuro.05.009.2009.

Holdgate, G.A., Anderson, M., Edfeldt, F., and Geschwindner, S., 2010, Affinity-based, biophysical methods to detect and analyze ligand binding to recombinant proteins: matching high information content with high throughput: Journal of structural biology, v. 172, no. 1, p. 142–157, doi: 10.1016/j.jsb.2010.06.024.

Holsboer, F., 1999, The rationale for corticotropin-releasing hormone receptor (CRH-R) antagonists to treat depression and anxiety: Journal of psychiatric research, v. 33, no. 3, p. 181–214.

Homayoun, H., and Moghaddam, B., 2007, NMDA Receptor Hypofunction Produces Opposite Effects on Prefrontal Cortex Interneurons and Pyramidal Neurons: The Journal of Neuroscience, v. 27, no. 43, p. 11496–11500, doi: 10.1523/JNEUROSCI.2213-07.2007.

Honea, R.A., Meyer-Lindenberg, A., Hobbs, K.B., Pezawas, L., Mattay, V.S., Egan, M.F., Verchinski, B., Passingham, R.E., Weinberger, D.R., and Callicott, J.H., 2008, Is gray matter volume an intermediate phenotype for schizophrenia? A voxel-based morphometry study of patients with schizophrenia and their healthy siblings: Biological psychiatry, v. 63, no. 5, p. 465–474, doi: 10.1016/j.biopsych.2007.05.027.

Hong, L.E., Wonodi, I., Stine, O.C., Mitchell, B.D., and Thaker, G.K., 2008, Evidence of missense mutations on the neuregulin 1 gene affecting function of prepulse inhibition: Biological psychiatry, v. 63, no. 1, p. 17–23, doi: 10.1016/j.biopsych.2007.05.011.

Houghton, P.J., Cheshire, P.J., Hallman, J.D., 2nd, Lutz, L., Friedman, H.S., Danks, M.K., and Houghton, J.A., 1995, Efficacy of topoisomerase I inhibitors, topotecan and irinotecan, administered at low dose levels in protracted schedules to mice bearing xenografts of human tumors: Cancer chemotherapy and pharmacology, v. 36, no. 5, p. 393–403.

Hsiang, Y.H., Liu, L.F., Wall, M.E., Wani, M.C., Nicholas, A.W., Manikumar, G., Kirschenbaum, S., Silber, R., and Potmesil, M., 1989, DNA topoisomerase I-mediated DNA cleavage and cytotoxicity of camptothecin analogues: Cancer research, v. 49, no. 16, p. 4385–4389.

Huber, W., 2005, A new strategy for improved secondary screening and lead optimization using high-resolution SPR characterization of compound-target interactions: Journal of molecular recognition: JMR, v. 18, no. 4, p. 273–281, doi: 10.1002/jmr.744.

Hudepohl, N.S., and Nasrallah, H.A., 2012, Antipsychotic drugs: Handbook of clinical neurology / edited by P.J. Vinken and G.W. Bruyn, v. 106, p. 657–667, doi: 10.1016/B978-0-444-52002-9.00039-5.

Hudis, C.A., 2007, Trastuzumab--mechanism of action and use in clinical practice: The New England journal of medicine, v. 357, no. 1, p. 39–51, doi: 10.1056/NEJMra043186.

Inglese, J., Johnson, R.L., Simeonov, A., Xia, M., Zheng, W., Austin, C.P., and Auld, D.S., 2007, High-throughput screening assays for the identification of chemical probes: Nature chemical biology, v. 3, no. 8, p. 466–479, doi: 10.1038/nchembio.2007.17.

Ishii, R., Takahashi, H., Kurimoto, R., Aoki, Y., Ikeda, S., Hata, M., Ikezawa, K., Canuet, L., Nakahachi, T., Iwase, M., and Takeda, M., 2012, [Endophenotypes in schizophrenia: a review of electrophysiological studies]: Seishin shinkeigaku zasshi = Psychiatria et neurologia Japonica, v. 114, no. 6, p. 629–646.

Jaaro-Peled, H., Hayashi-Takagi, A., Seshadri, S., Kamiya, A., Brandon, N.J., and Sawa, A., 2009, Neurodevelopmental mechanisms of schizophrenia: understanding disturbed postnatal brain maturation through neuregulin-1-ErbB4 and DISC1: Trends in neurosciences, v. 32, no. 9, p. 485–495, doi: 10.1016/j.tins.2009.05.007.

Javitt, D.C., and Zukin, S.R., 1991, Recent advances in the phencyclidine model of schizophrenia: The American journal of psychiatry, v. 148, no. 10, p. 1301–1308.

Jeste, D.V., del Carmen, R., Lohr, J.B., and Wyatt, R.J., 1985, Did schizophrenia exist before the eighteenth century?: Comprehensive psychiatry, v. 26, no. 6, p. 493–503.

Jia, P., Sun, J., Guo, A.Y., and Zhao, Z., 2010, SZGR: a comprehensive schizophrenia gene resource: Molecular psychiatry, v. 15, no. 5, p. 453–462, doi: 10.1038/mp.2009.93.

Jones, R.B., Gordus, A., Krall, J.A., and MacBeath, G., 2006, A quantitative protein interaction network for the ErbB receptors using protein microarrays: Nature, v. 439, no. 7073, p. 168–174, doi: 10.1038/nature04177.

Jordan, M.A., Himes, R.H., and Wilson, L., 1985, Comparison of the effects of vinblastine, vincristine, vindesine, and vinepidine on microtubule dynamics and cell proliferation in vitro: Cancer research, v. 45, no. 6, p. 2741–2747.

Kang, E., Burdick, K.E., Kim, J.Y., Duan, X., Guo, J.U., Sailor, K.A., Jung, D.-E., Ganesan, S., Choi, S., Pradhan, D., Lu, B., Avramopoulos, D., Christian, K., Malhotra, A.K., et al., 2011, Interaction between FEZ1 and DISC1 in regulation of neuronal development and risk for schizophrenia: Neuron, v. 72, no. 4, p. 559–571, doi: 10.1016/j.neuron.2011.09.032.

Karam, C.S., Ballon, J.S., Bivens, N.M., Freyberg, Z., Girgis, R.R., Lizardi-Ortiz, J.E., Markx, S., Lieberman, J.A., and Javitch, J.A., 2010, Signaling pathways in schizophrenia: emerging targets and therapeutic strategies: Trends in pharmacological sciences, v. 31, no. 8, p. 381–390, doi: 10.1016/j.tips.2010.05.004.

Karaman, M.W., Herrgard, S., Treiber, D.K., Gallant, P., Atteridge, C.E., Campbell, B.T., Chan, K.W., Ciceri, P., Davis, M.I., Edeen, P.T., Faraoni, R., Floyd, M., Hunt, J.P., Lockhart, D.J., et al., 2008, A quantitative analysis of kinase inhibitor selectivity: Nature biotechnology, v. 26, no. 1, p. 127–132, doi: 10.1038/nbt1358.

Kato, T., Kasai, A., Mizuno, M., Fengyi, L., Shintani, N., Maeda, S., Yokoyama, M., Ozaki, M., and Nawa, H., 2010, Phenotypic characterization of transgenic mice overexpressing neuregulin-1: PloS one, v. 5, no. 12, p. e14185, doi: 10.1371/journal.pone.0014185.

Kawato, Y., Aonuma, M., Hirota, Y., Kuga, H., and Sato, K., 1991, Intracellular roles of SN-38, a metabolite of the camptothecin derivative CPT-11, in the antitumor effect of CPT-11: Cancer research, v. 51, no. 16, p. 4187–4191.

Keely, S.J., Calandrella, S.O., and Barrett, K.E., 2000, Carbachol-stimulated transactivation of epidermal growth factor receptor and mitogen-activated protein kinase in T(84) cells is mediated by intracellular ca(2+), PYK-2, and p60(src): The Journal of biological chemistry, v. 275, no. 17, p. 12619–12625.

Kellendonk, C., Simpson, E.H., and Kandel, E.R., 2009, Modeling cognitive endophenotypes of schizophrenia in mice: Trends in neurosciences, v. 32, no. 6, p. 347–358, doi: 10.1016/j.tins.2009.02.003.

Keshavan, M.S., Tandon, R., Boutros, N.N., and Nasrallah, H.A., 2008, Schizophrenia, “just the facts”: what we know in 2008 Part 3: neurobiology: Schizophrenia research, v. 106, no. 2-3, p. 89–107, doi: 10.1016/j.schres.2008.07.020.

Kibbe, W.A., 2007, OligoCalc: an online oligonucleotide properties calculator: Nucleic acids research, v. 35, no. Web Server issue, p. W43–46, doi: 10.1093/nar/gkm234.

Kirkbride, J.B., Fearon, P., Morgan, C., Dazzan, P., Morgan, K., Tarrant, J., Lloyd, T., Holloway, J., Hutchinson, G., Leff, J.P., Mallett, R.M., Harrison, G.L., Murray, R.M., and Jones, P.B., 2006, Heterogeneity in incidence rates of schizophrenia and other psychotic syndromes: findings from the 3-center AeSOP study: Archives of general psychiatry, v. 63, no. 3, p. 250–258, doi: 10.1001/archpsyc.63.3.250.

Kisseleva, T., Bhattacharya, S., Braunstein, J., and Schindler, C.W., 2002, Signaling through the JAK/STAT pathway, recent advances and future challenges: Gene, v. 285, no. 1-2, p. 1–24.

Kleinman, J.E., Law, A.J., Lipska, B.K., Hyde, T.M., Ellis, J.K., Harrison, P.J., and Weinberger, D.R., 2011, Genetic neuropathology of schizophrenia: new approaches to an old question and new uses for postmortem human brains: Biological psychiatry, v. 69, no. 2, p. 140–145, doi: 10.1016/j.biopsych.2010.10.032.

Klosterkötter, J., 2008, Indicated prevention of schizophrenia: Deutsches Ärzteblatt international, v. 105, no. 30, p. 532–539, doi: 10.3238/arztebl.2008.0532.

Kocisko, D.A., Baron, G.S., Rubenstein, R., Chen, J., Kuizon, S., and Caughey, B., 2003, New inhibitors of scrapie-associated prion protein formation in a library of 2000 drugs and natural products: Journal of virology, v. 77, no. 19, p. 10288–10294.

Kodesh, A., Goldshtein, I., Gelkopf, M., Goren, I., Chodick, G., and Shalev, V., 2012, Epidemiology and comorbidity of severe mental illnesses in the community: findings

from a computerized mental health registry in a large Israeli health organization: Social psychiatry and psychiatric epidemiology,, doi: 10.1007/s00127-012-0478-9.

Konradi, C., Yang, C.K., Zimmerman, E.I., Lohmann, K.M., Gresch, P., Pantazopoulos, H., Berretta, S., and Heckers, S., 2011, Hippocampal interneurons are abnormal in schizophrenia: Schizophrenia research, v. 131, no. 1-3, p. 165–173, doi: 10.1016/j.schres.2011.06.007.

Kraepelin, E. 1896: Psychiatrie: Ein Lehrbuch für Studierende und Ärzte.
Fünfte, vollständig umgearbeitete Auflage. Leipzig.

Kuai, L., Ong, S.-E., Madison, J.M., Wang, X., Duvall, J.R., Lewis, T.A., Luce, C.J., Conner, S.D., Pearlman, D.A., Wood, J.L., Schreiber, S.L., Carr, S.A., Scolnick, E.M., and Haggarty, S.J., 2011, AAK1 identified as an inhibitor of neuregulin-1/ErbB4-dependent neurotrophic factor signaling using integrative chemical genomics and proteomics: Chemistry & biology, v. 18, no. 7, p. 891–906, doi: 10.1016/j.chembiol.2011.03.017.

Kuai, L., Wang, X., Madison, J.M., Schreiber, S.L., Scolnick, E.M., and Haggarty, S.J., 2010, Chemical genetics identifies small-molecule modulators of neuritogenesis involving neuregulin-1/ErbB4 signaling: ACS chemical neuroscience, v. 1, no. 4, p. 325–342, doi: 10.1021/cn900046a.

Kuhn, J.G., 1998, Pharmacology of irinotecan: Oncology (Williston Park, N.Y.), v. 12, no. 8 Suppl 6, p. 39–42.

Kwon, O.B., Paredes, D., Gonzalez, C.M., Neddens, J., Hernandez, L., Vullhorst, D., and Buonanno, A., 2008, Neuregulin-1 regulates LTP at CA1 hippocampal synapses through activation of dopamine D4 receptors: Proceedings of the National Academy of Sciences of the United States of America, v. 105, no. 40, p. 15587–15592, doi: 10.1073/pnas.0805722105.

Law, A.J., Kleinman, J.E., Weinberger, D.R., and Weickert, C.S., 2007, Disease-associated intronic variants in the ErbB4 gene are related to altered ErbB4 splice-variant expression in the brain in schizophrenia: Human molecular genetics, v. 16, no. 2, p. 129–141, doi: 10.1093/hmg/ddl449.

Law, A.J., Wang, Y., Sei, Y., O'Donnell, P., Piantadosi, P., Papaleo, F., Straub, R.E., Huang, W., Thomas, C.J., Vakkalanka, R., Besterman, A.D., Lipska, B.K., Hyde, T.M., Harrison, P.J., et al., 2012b, Neuregulin 1-ErbB4-PI3K signaling in schizophrenia and phosphoinositide 3-kinase-p110δ inhibition as a potential therapeutic strategy: Proceedings of the National Academy of Sciences of the United States of America,, doi: 10.1073/pnas.1206118109.

Leevers, S.J., Vanhaesebroeck, B., and Waterfield, M.D., 1999, Signalling through phosphoinositide 3-kinases: the lipids take centre stage: Current opinion in cell biology, v. 11, no. 2, p. 219–225.

Lewis, D.A., and González-Burgos, G., 2008, Neuroplasticity of neocortical circuits in schizophrenia: Neuropsychopharmacology: official publication of the American College of Neuropsychopharmacology, v. 33, no. 1, p. 141–165, doi: 10.1038/sj.npp.1301563.

Lewis, D.A., Hashimoto, T., and Volk, D.W., 2005, Cortical inhibitory neurons and schizophrenia: Nature reviews. Neuroscience, v. 6, no. 4, p. 312–324, doi: 10.1038/nrn1648.

Lewis, D.A., and Levitt, P., 2002, Schizophrenia as a disorder of neurodevelopment: Annual review of neuroscience, v. 25, p. 409–432, doi: 10.1146/annurev.neuro.25.112701.142754.

Lewis, D.A., and Lieberman, J.A., 2000, Catching up on schizophrenia: natural history and neurobiology: Neuron, v. 28, no. 2, p. 325–334.

Li, D., Collier, D.A., and He, L., 2006, Meta-analysis shows strong positive association of the neuregulin 1 (NRG1) gene with schizophrenia: Human molecular genetics, v. 15, no. 12, p. 1995–2002, doi: 10.1093/hmg/ddl122.

Li, T., Stefansson, H., Gudfinnsson, E., Cai, G., Liu, X., Murray, R.M., Steinthorsdottir, V., Januel, D., Gudnadottir, V.G., Petursson, H., Ingason, A., Gulcher, J.R., Stefansson, K., and Collier, D.A., 2004, Identification of a novel neuregulin 1 at-risk haplotype in Han schizophrenia Chinese patients, but no association with the Icelandic/Scottish risk haplotype: Molecular psychiatry, v. 9, no. 7, p. 698–704, doi: 10.1038/sj.mp.4001485.

Lievens, S., Caligiuri, M., Kley, N., and Tavernier, J., 2012, The use of mammalian two-hybrid technologies for high-throughput drug screening: Methods (San Diego, Calif.),, doi: 10.1016/j.ymeth.2012.08.003.

Liu, P., Cleveland, T.E., 4th, Bouyain, S., Byrne, P.O., Longo, P.A., and Leahy, D.J., 2012, A single ligand is sufficient to activate EGFR dimers: Proceedings of the National Academy of Sciences of the United States of America, v. 109, no. 27, p. 10861–10866, doi: 10.1073/pnas.1201114109.

Liu, X., Robinson, G.W., Wagner, K.U., Garrett, L., Wynshaw-Boris, A., and Hennighausen, L., 1997, Stat5a is mandatory for adult mammary gland development and lactogenesis: Genes & development, v. 11, no. 2, p. 179–186.

Lodge, D., and Anis, N.A., 1982, Effects of phencyclidine on excitatory amino acid activation of spinal interneurones in the cat: European journal of pharmacology, v. 77, no. 2-3, p. 203–204.

Lonardo, F., Di Marco, E., King, C.R., Pierce, J.H., Segatto, O., Aaronson, S.A., and Di Fiore, P.P., 1990, The normal erbB-2 product is an atypical receptor-like tyrosine kinase with constitutive activity in the absence of ligand: The New biologist, v. 2, no. 11, p. 992–1003.

Lu, C.-L., Wang, Y.-C., Chen, J.-Y., Lai, I.-C., and Liou, Y.-J., 2010, Support for the involvement of the ERBB4 gene in schizophrenia: a genetic association analysis: Neuroscience letters, v. 481, no. 2, p. 120–125, doi: 10.1016/j.neulet.2010.06.067.

LUBY, E.D., COHEN, B.D., ROSENBAUM, G., GOTTLIEB, J.S., and KELLEY, R., 1959, Study of a new schizophrenomimetic drug; sernyl: A.M.A. archives of neurology and psychiatry, v. 81, no. 3, p. 363–369.

Luo, X., Prior, M., He, W., Hu, X., Tang, X., Shen, W., Yadav, S., Kiryu-Seo, S., Miller, R., Trapp, B.D., and Yan, R., 2011, Cleavage of neuregulin-1 by BACE1 or ADAM10

protein produces differential effects on myelination: The Journal of biological chemistry, v. 286, no. 27, p. 23967–23974, doi: 10.1074/jbc.M111.251538.

Macarron, R., Banks, M.N., Bojanic, D., Burns, D.J., Cirovic, D.A., Garyantes, T., Green, D.V.S., Hertzberg, R.P., Janzen, W.P., Paslay, J.W., Schopfer, U., and Sittampalam, G.S., 2011, Impact of high-throughput screening in biomedical research: Nature reviews. Drug discovery, v. 10, no. 3, p. 188–195, doi: 10.1038/nrd3368.

Man, H.-Y., Wang, Q., Lu, W.-Y., Ju, W., Ahmadian, G., Liu, L., D'Souza, S., Wong, T.P., Taghibiglou, C., Lu, J., Becker, L.E., Pei, L., Liu, F., Wymann, M.P., et al., 2003, Activation of PI3-kinase is required for AMPA receptor insertion during LTP of mEPSCs in cultured hippocampal neurons: Neuron, v. 38, no. 4, p. 611–624.

Maniatis,T., Fritsch, E.F., Sambrook, J., 1982, Molecular cloning : a laboratory manual, Cold Spring Harbour Laboratory

Marín, O., 2012, Interneuron dysfunction in psychiatric disorders: Nature Reviews Neuroscience, v. 13, no. 2, p. 107–120, doi: 10.1038/nrn3155.

Marmor, M.D., Skaria, K.B., and Yarden, Y., 2004, Signal transduction and oncogenesis by ErbB/HER receptors: International journal of radiation oncology, biology, physics, v. 58, no. 3, p. 903–913, doi: 10.1016/j.ijrobp.2003.06.002.

Marzolla, V., Armani, A., Zennaro, M.-C., Cinti, F., Mammi, C., Fabbri, A., Rosano, G.M.C., and Caprio, M., 2012, The role of the mineralocorticoid receptor in adipocyte biology and fat metabolism: Molecular and cellular endocrinology, v. 350, no. 2, p. 281–288, doi: 10.1016/j.mce.2011.09.011.

Maynard, T.M., Sikich, L., Lieberman, J.A., and LaMantia, A.S., 2001, Neural development, cell-cell signaling, and the "two-hit" hypothesis of schizophrenia: Schizophrenia bulletin, v. 27, no. 3, p. 457–476.

McGrath, J.J., 2007, The surprisingly rich contours of schizophrenia epidemiology: Archives of general psychiatry, v. 64, no. 1, p. 14–16, doi: 10.1001/archpsyc.64.1.14.

McIntosh, A.M., Moorhead, T.W.J., Job, D., Lymer, G.K.S., Muñoz Maniega, S., McKirdy, J., Sussmann, J.E.D., Baig, B.J., Bastin, M.E., Porteous, D., Evans, K.L., Johnstone, E.C., Lawrie, S.M., and Hall, J., 2008, The effects of a neuregulin 1 variant on white matter density and integrity: Molecular psychiatry, v. 13, no. 11, p. 1054–1059, doi: 10.1038/sj.mp.4002103.

Medina, P.J., and Goodin, S., 2008, Lapatinib: a dual inhibitor of human epidermal growth factor receptor tyrosine kinases: Clinical therapeutics, v. 30, no. 8, p. 1426–1447, doi: 10.1016/j.clinthera.2008.08.008.

Mei, L., and Xiong, W.-C., 2008, Neuregulin 1 in neural development, synaptic plasticity and schizophrenia: Nature reviews. Neuroscience, v. 9, no. 6, p. 437–452, doi: 10.1038/nrn2392.

Meyer, D., and Birchmeier, C., 1995, Multiple essential functions of neuregulin in development: Nature, v. 378, no. 6555, p. 386–390, doi: 10.1038/378386a0.

Meyer-Lindenberg, A., 2011, Neuroimaging and the question of neurodegeneration in schizophrenia: Progress in neurobiology, v. 95, no. 4, p. 514–516, doi: 10.1016/j.pneurobio.2011.07.007.

Mezler, M., Geneste, H., Gault, L., and Marek, G.J., 2010, LY-2140023, a prodrug of the group II metabotropic glutamate receptor agonist LY-404039 for the potential treatment of schizophrenia: Current opinion in investigational drugs (London, England: 2000), v. 11, no. 7, p. 833–845.

Michailov, G.V., Sereda, M.W., Brinkmann, B.G., Fischer, T.M., Haug, B., Birchmeier, C., Role, L., Lai, C., Schwab, M.H., and Nave, K.-A., 2004, Axonal neuregulin-1 regulates myelin sheath thickness: Science (New York, N.Y.), v. 304, no. 5671, p. 700–703, doi: 10.1126/science.1095862.

Millar, J.K., Wilson-Annan, J.C., Anderson, S., Christie, S., Taylor, M.S., Semple, C.A., Devon, R.S., St Clair, D.M., Muir, W.J., Blackwood, D.H., and Porteous, D.J., 2000, Disruption of two novel genes by a translocation co-segregating with schizophrenia: Human molecular genetics, v. 9, no. 9, p. 1415–1423.

Missios, S., 2007, Hippocrates, Galen, and the uses of trepanation in the ancient classical world: Neurosurgical focus, v. 23, no. 1, p. E11, doi: 10.3171/foc.2007.23.1.11.

Mohit, A., 2001, Mental health and psychiatry in the Middle East: historical development: Eastern Mediterranean health journal = La revue de santé de la Méditerranée orientale = al-Majallah al-ṣiḥḥīyah li-sharq al-mutawassiṭ, v. 7, no. 3, p. 336–347.

Monji, A., Kato, T., and Kanba, S., 2009, Cytokines and schizophrenia: Microglia hypothesis of schizophrenia: Psychiatry and clinical neurosciences, v. 63, no. 3, p. 257–265.

Morton, J.F., 1968, Medicinal plants--old and new: Bulletin of the Medical Library Association, v. 56, no. 2, p. 161–167.

Mülhardt, C., 2003, Der Experimentator, Molekularbiologie/Genomics, Spektrum

Mullis, K.B., and Faloona, F.A., 1987, Specific synthesis of DNA in vitro via a polymerase-catalyzed chain reaction: Methods in enzymology, v. 155, p. 335–350.

Mullis, K., Faloona, F., Scharf, S., Saiki, R., Horn, G., and Erlich, H., 1992, Specific enzymatic amplification of DNA in vitro: the polymerase chain reaction. 1986: Biotechnology (Reading, Mass.), v. 24, p. 17–27.

Munafò, M.R., Thiselton, D.L., Clark, T.G., and Flint, J., 2006, Association of the NRG1 gene and schizophrenia: a meta-analysis: Molecular psychiatry, v. 11, no. 6, p. 539–546, doi: 10.1038/sj.mp.4001817.

Nayak, A., Gayen, P., Saini, P., Maitra, S., and Sinha Babu, S.P., 2011, Albendazole induces apoptosis in adults and microfilariae of Setaria cervi: Experimental parasitology, v. 128, no. 3, p. 236–242, doi: 10.1016/j.exppara.2011.03.005.

Neddens, J., and Buonanno, A., 2011, Expression of the neuregulin receptor ErbB4 in the brain of the rhesus monkey (Macaca mulatta): PloS one, v. 6, no. 11, p. e27337, doi: 10.1371/journal.pone.0027337.

Neddens, J., and Buonanno, A., 2010, Selective populations of hippocampal interneurons express ErbB4 and their number and distribution is altered in ErbB4 knockout mice: Hippocampus, v. 20, no. 6, p. 724–744, doi: 10.1002/hipo.20675.

Neddens, J., Fish, K.N., Tricoire, L., Vullhorst, D., Shamir, A., Chung, W., Lewis, D.A., McBain, C.J., and Buonanno, A., 2011, Conserved interneuron-specific ErbB4 expression in frontal cortex of rodents, monkeys, and humans: implications for schizophrenia: Biological psychiatry, v. 70, no. 7, p. 636–645, doi: 10.1016/j.biopsych.2011.04.016.

Nestler, E.J., and Hyman, S.E., 2010, Animal models of neuropsychiatric disorders: Nature neuroscience, v. 13, no. 10, p. 1161–1169, doi: 10.1038/nn.2647.

Ni, C.Y., Murphy, M.P., Golde, T.E., and Carpenter, G., 2001, gamma -Secretase cleavage and nuclear localization of ErbB-4 receptor tyrosine kinase: Science (New York, N.Y.), v. 294, no. 5549, p. 2179–2181, doi: 10.1126/science.1065412.

Nicodemus, K.K., Marenco, S., Batten, A.J., Vakkalanka, R., Egan, M.F., Straub, R.E., and Weinberger, D.R., 2008, Serious obstetric complications interact with hypoxia-regulated/vascular-expression genes to influence schizophrenia risk: Molecular psychiatry, v. 13, no. 9, p. 873–877, doi: 10.1038/sj.mp.4002153.

Nilsson, M., Carlsson, A., Markinhuhta, K.R., Sonesson, C., Pettersson, F., Gullme, M., and Carlsson, M.L., 2004, The dopaminergic stabiliser ACR16 counteracts the behavioural primitivization induced by the NMDA receptor antagonist MK-801 in mice: implications for cognition: Progress in neuro-psychopharmacology & biological psychiatry, v. 28, no. 4, p. 677–685, doi: 10.1016/j.pnpbp.2004.05.004.

Nitsche, M.A., Müller-Dahlhaus, F., Paulus, W., and Ziemann, U., 2012, The pharmacology of neuroplasticity induced by non-invasive brain stimulation: building models for the clinical use of CNS active drugs: The Journal of physiology,, doi: 10.1113/jphysiol.2012.232975.

O'Leary, J., and Muggia, F.M., 1998a, Camptothecins: a review of their development and schedules of administration: European journal of cancer (Oxford, England: 1990), v. 34, no. 10, p. 1500–1508.

Oda, K., Matsuoka, Y., Funahashi, A., and Kitano, H., 2005, A comprehensive pathway map of epidermal growth factor receptor signaling: Molecular Systems Biology, v. 1, p. 2005.0010, doi: 10.1038/msb4100014.

Ogden, D.A., Scherr, L., Spritz, N., and Rubin, A.L., 1961, A comparison of the properties of chlorothiazide, spironolactone and a combination of both as diuretic agents: The New England journal of medicine, v. 265, p. 358–362, doi: 10.1056/NEJM196108242650802.

Ohlmeyer, M., and Zhou, M.-M., 2010, Integration of small-molecule discovery in academic biomedical research: The Mount Sinai journal of medicine, New York, v. 77, no. 4, p. 350–357, doi: 10.1002/msj.20197.

Okasha, A., 2001, Egyptian contribution to the concept of mental health: Eastern Mediterranean health journal = La revue de santé de la Méditerranée orientale = al-Majallah al-ṣiḥḥīyah li-sharq al-mutawassiṭ, v. 7, no. 3, p. 377–380.

Okasha, A., 1999, Mental health in the Middle East: an Egyptian perspective: Clinical psychology review, v. 19, no. 8, p. 917–933.

Olayioye, M.A., Beuvink, I., Horsch, K., Daly, J.M., and Hynes, N.E., 1999, ErbB receptor-induced activation of stat transcription factors is mediated by Src tyrosine kinases: The Journal of biological chemistry, v. 274, no. 24, p. 17209–17218.

Olney, J.W., and Farber, N.B., 1995, NMDA antagonists as neurotherapeutic drugs, psychotogens, neurotoxins, and research tools for studying schizophrenia: Neuropsychopharmacology: official publication of the American College of Neuropsychopharmacology, v. 13, no. 4, p. 335–345, doi: 10.1016/0893-133X(95)00079-S.

Oyamada, N., Sone, M., Miyashita, K., Park, K., Taura, D., Inuzuka, M., Sonoyama, T., Tsujimoto, H., Fukunaga, Y., Tamura, N., Itoh, H., and Nakao, K., 2008, The role of mineralocorticoid receptor expression in brain remodeling after cerebral ischemia: Endocrinology, v. 149, no. 8, p. 3764–3777, doi: 10.1210/en.2007-1770.

Ozaki, M., Sasner, M., Yano, R., Lu, H.S., and Buonanno, A., 1997, Neuregulin-beta induces expression of an NMDA-receptor subunit: Nature, v. 390, no. 6661, p. 691–694, doi: 10.1038/37795.

Pelicci, G., Lanfrancone, L., Grignani, F., McGlade, J., Cavallo, F., Forni, G., Nicoletti, I., Grignani, F., Pawson, T., and Pelicci, P.G., 1992, A novel transforming protein (SHC) with an SH2 domain is implicated in mitogenic signal transduction: Cell, v. 70, no. 1, p. 93–104.

Penzes, P., Cahill, M.E., Jones, K.A., VanLeeuwen, J.-E., and Woolfrey, K.M., 2011, Dendritic spine pathology in neuropsychiatric disorders: Nature neuroscience, v. 14, no. 3, p. 285–293, doi: 10.1038/nn.2741.

Pippal, J.B., and Fuller, P.J., 2008, Structure-function relationships in the mineralocorticoid receptor: Journal of molecular endocrinology, v. 41, no. 6, p. 405–413, doi: 10.1677/JME-08-0093.

Plowman, G.D., Culouscou, J.M., Whitney, G.S., Green, J.M., Carlton, G.W., Foy, L., Neubauer, M.G., and Shoyab, M., 1993, Ligand-specific activation of HER4/p180erbB4, a fourth member of the epidermal growth factor receptor family: Proceedings of the National Academy of Sciences of the United States of America, v. 90, no. 5, p. 1746–1750.

Pommier, Y., 2004, Camptothecins and topoisomerase I: a foot in the door. Targeting the genome beyond topoisomerase I with camptothecins and novel anticancer drugs: importance of DNA replication, repair and cell cycle checkpoints: Current medicinal chemistry. Anti-cancer agents, v. 4, no. 5, p. 429–434.

Pommier, Y., 2006, Topoisomerase I inhibitors: camptothecins and beyond: Nature reviews. Cancer, v. 6, no. 10, p. 789–802, doi: 10.1038/nrc1977.

Pratt, J., Winchester, C., Dawson, N., and Morris, B., 2012, Advancing schizophrenia drug discovery: optimizing rodent models to bridge the translational gap: Nature reviews. Drug discovery, v. 11, no. 7, p. 560–579, doi: 10.1038/nrd3649.

Ravichandran, K.S., 2001, Signaling via Shc family adapter proteins: Oncogene, v. 20, no. 44, p. 6322–6330, doi: 10.1038/sj.onc.1204776.

Redinbo, M.R., Stewart, L., Kuhn, P., Champoux, J.J., and Hol, W.G., 1998, Crystal structures of human topoisomerase I in covalent and noncovalent complexes with DNA: Science (New York, N.Y.), v. 279, no. 5356, p. 1504–1513.

Rio, C., Buxbaum, J.D., Peschon, J.J., and Corfas, G., 2000, Tumor necrosis factor-alpha-converting enzyme is required for cleavage of erbB4/HER4: The Journal of biological chemistry, v. 275, no. 14, p. 10379–10387.

Rogerson, F.M., Yao, Y.-Z., Smith, B.J., Dimopoulos, N., and Fuller, P.J., 2003, Determinants of spironolactone binding specificity in the mineralocorticoid receptor: Journal of molecular endocrinology, v. 31, no. 3, p. 573–582.

van Rossum, J.M., 1967, [The effect of psychostimulants on the central and autonomic nervous system]: Schweizerische Zeitschrift für Sportmedizin, v. 15, no. 1, p. 26–40.

van Rossum, J.M., 1966, The significance of dopamine-receptor blockade for the mechanism of action of neuroleptic drugs: Archives internationales de pharmacodynamie et de thérapie, v. 160, no. 2, p. 492–494.

Rowinsky, E.K., Adjei, A., Donehower, R.C., Gore, S.D., Jones, R.J., Burke, P.J., Cheng, Y.C., Grochow, L.B., and Kaufmann, S.H., 1994, Phase I and pharmacodynamic study of the topoisomerase I-inhibitor topotecan in patients with refractory acute leukemia: Journal of clinical oncology: official journal of the American Society of Clinical Oncology, v. 12, no. 10, p. 2193–2203.

Rund, B.R., 2009, Is there a degenerative process going on in the brain of people with Schizophrenia?: Frontiers in human neuroscience, v. 3, p. 36, doi: 10.3389/neuro.09.036.2009.

Russel, J., Cohn, R., History of schizophrenia, Bookvika publishing

Rumsey, D., 2010, Statistik für Dummies, Wiley

Saha, S., Chant, D., Welham, J., and McGrath, J., 2005, A systematic review of the prevalence of schizophrenia: PLoS medicine, v. 2, no. 5, p. e141, doi: 10.1371/journal.pmed.0020141.

Sams-Dodd, F., Lipska, B.K., and Weinberger, D.R., 1997, Neonatal lesions of the rat ventral hippocampus result in hyperlocomotion and deficits in social behaviour in adulthood: Psychopharmacology, v. 132, no. 3, p. 303–310.

Sanyal, S., and Van Tol, H.H., 1997, Review the role of dopamine D4 receptors in schizophrenia and antipsychotic action: Journal of psychiatric research, v. 31, no. 2, p. 219–232.

Sato, K., Kimoto, M., Kakumoto, M., Horiuchi, D., Iwasaki, T., Tokmakov, A.A., and Fukami, Y., 2000, Adaptor protein Shc undergoes translocation and mediates up-regulation of the tyrosine kinase c-Src in EGF-stimulated A431 cells: Genes to cells: devoted to molecular & cellular mechanisms, v. 5, no. 9, p. 749–764.

van Schalkwyk, P.C., Geyser, T.L., Récio, M., and Erasmus, F.P., 1979, The anthelmintic efficacy of albendazole against gastrointestinal roundworms, tapeworms, lungworms

and liverflukes in sheep: Journal of the South African Veterinary Association, v. 50, no. 1, p. 31–35.

Schulze, W.X., Deng, L., and Mann, M., 2005, Phosphotyrosine interactome of the ErbB-receptor kinase family: Molecular systems biology, v. 1, p. 2005.0008, doi: 10.1038/msb4100012.

Sebat, J., Levy, D.L., and McCarthy, S.E., 2009, Rare structural variants in schizophrenia: one disorder, multiple mutations; one mutation, multiple disorders: Trends in genetics: TIG, v. 25, no. 12, p. 528–535, doi: 10.1016/j.tig.2009.10.004.

Seeman, P., and Lee, T., 1975, Antipsychotic drugs: direct correlation between clinical potency and presynaptic action on dopamine neurons: Science (New York, N.Y.), v. 188, no. 4194, p. 1217–1219.

Silberberg, G., Darvasi, A., Pinkas-Kramarski, R., and Navon, R., 2006, The involvement of ErbB4 with schizophrenia: association and expression studies: American journal of medical genetics. Part B, Neuropsychiatric genetics: the official publication of the International Society of Psychiatric Genetics, v. 141B, no. 2, p. 142–148, doi: 10.1002/ajmg.b.30275.

Sink, R., Gobec, S., Pečar, S., and Zega, A., 2010, False positives in the early stages of drug discovery: Current medicinal chemistry, v. 17, no. 34, p. 4231–4255.

Slichenmyer, W.J., Elliott, W.L., and Fry, D.W., 2001, CI-1033, a pan-erbB tyrosine kinase inhibitor: Seminars in oncology, v. 28, no. 5 Suppl 16, p. 80–85.

Snyder, S.H., 1980, Phencyclidine: Nature, v. 285, no. 5764, p. 355–356.

St Clair, D., Blackwood, D., Muir, W., Carothers, A., Walker, M., Spowart, G., Gosden, C., and Evans, H.J., 1990, Association within a family of a balanced autosomal translocation with major mental illness: Lancet, v. 336, no. 8706, p. 13–16.

Stagljar, I., Korostensky, C., Johnsson, N., and te Heesen, S., 1998, A genetic system based on split-ubiquitin for the analysis of interactions between membrane proteins in vivo: Proceedings of the National Academy of Sciences of the United States of America, v. 95, no. 9, p. 5187–5192.

Stallings-Mann, M., Jamieson, L., Regala, R.P., Weems, C., Murray, N.R., and Fields, A.P., 2006, A novel small-molecule inhibitor of protein kinase Ciota blocks transformed growth of non-small-cell lung cancer cells: Cancer research, v. 66, no. 3, p. 1767–1774, doi: 10.1158/0008-5472.CAN-05-3405.

Stefansson, H., Sarginson, J., Kong, A., Yates, P., Steinthorsdottir, V., Gudfinnsson, E., Gunnarsdottir, S., Walker, N., Petursson, H., Crombie, C., Ingason, A., Gulcher, J.R., Stefansson, K., and St Clair, D., 2003, Association of neuregulin 1 with schizophrenia confirmed in a Scottish population: American journal of human genetics, v. 72, no. 1, p. 83–87.

Stefansson, H., Sigurdsson, E., Steinthorsdottir, V., Bjornsdottir, S., Sigmundsson, T., Ghosh, S., Brynjolfsson, J., Gunnarsdottir, S., Ivarsson, O., Chou, T.T., Hjaltason, O., Birgisdottir, B., Jonsson, H., Gudnadottir, V.G., et al., 2002, Neuregulin 1 and

susceptibility to schizophrenia: American journal of human genetics, v. 71, no. 4, p. 877–892, doi: 10.1086/342734.

Stefánsson, H., Thorgeirsson, T.E., Gulcher, J.R., and Stefánsson, K., 2003, Neuregulin 1 in schizophrenia: out of Iceland: Molecular psychiatry, v. 8, no. 7, p. 639–640, doi: 10.1038/sj.mp.4001384.

Steurer, J., Bachmann, L.M., and Miettinen, O.S., 2006, Etiology in a taxonomy of illnesses: European journal of epidemiology, v. 21, no. 2, p. 85–89, doi: 10.1007/s10654-005-5925-4.

Streltsov, S., Oleinikov, V., Ermishov, M., Mochalov, K., Sukhanova, A., Nechipurenko, Y., Grokhovsky, S., Zhuze, A., Pluot, M., and Nabiev, I., 2003, Interaction of clinically important human DNA topoisomerase I poison, topotecan, with double-stranded DNA: Biopolymers, v. 72, no. 6, p. 442–454, doi: 10.1002/bip.10479.

Stryer,L., Berg,M., Tymoczko, L., 2007 Biochemie, Spektrum Akademischer Verlag

Sui, Y., and Wu, Z., 2007, Alternative statistical parameter for high-throughput screening assay quality assessment: Journal of biomolecular screening, v. 12, no. 2, p. 229–234, doi: 10.1177/1087057106296498.

Sullivan, P.F., Kendler, K.S., and Neale, M.C., 2003, Schizophrenia as a complex trait: evidence from a meta-analysis of twin studies: Archives of general psychiatry, v. 60, no. 12, p. 1187–1192, doi: 10.1001/archpsyc.60.12.1187.

Sun, H., Liu, X., Xiong, Q., Shikano, S., and Li, M., 2006, Chronic inhibition of cardiac Kir2.1 and HERG potassium channels by celastrol with dual effects on both ion conductivity and protein trafficking: The Journal of biological chemistry, v. 281, no. 9, p. 5877–5884, doi: 10.1074/jbc.M600072200.

Taguchi, T., Wakui, A., Hasegawa, K., Niitani, H., Furue, H., Ohta, K., and Hattori, T., 1990, [Phase I clinical study of CPT-11. Research group of CPT-11]: Gan to kagaku ryoho. Cancer & chemotherapy, v. 17, no. 1, p. 115–120.

Takimoto, C.H., and Arbuck, S.G., 1997a, Clinical status and optimal use of topotecan: Oncology (Williston Park, N.Y.), v. 11, no. 11, p. 1635–1646; discussion 1649–1651, 1655–1657.

Takimoto, C.H., and Arbuck, S.G., 1997b, Clinical status and optimal use of topotecan: Oncology (Williston Park, N.Y.), v. 11, no. 11, p. 1635–1646; discussion 1649–1651, 1655–1657.

Tandon, R., Keshavan, M.S., and Nasrallah, H.A., 2008a, Schizophrenia, “just the facts” what we know in 2008. 2. Epidemiology and etiology: Schizophrenia research, v. 102, no. 1-3, p. 1–18, doi: 10.1016/j.schres.2008.04.011.

Tandon, R., Keshavan, M.S., and Nasrallah, H.A., 2008b, Schizophrenia, “Just the Facts”: What we know in 2008: Part 1: Overview: Schizophrenia Research, v. 100, no. 1–3, p. 4–19, doi: 10.1016/j.schres.2008.01.022.

Tandon, R., Nasrallah, H.A., and Keshavan, M.S., 2009, Schizophrenia, “just the facts” 4. Clinical features and conceptualization: Schizophrenia research, v. 110, no. 1-3, p. 1–23, doi: 10.1016/j.schres.2009.03.005.

Tandon, R., Nasrallah, H.A., and Keshavan, M.S., 2010, Schizophrenia, “just the facts” 5. Treatment and prevention. Past, present, and future: Schizophrenia research, v. 122, no. 1-3, p. 1–23, doi: 10.1016/j.schres.2010.05.025.

Taniguchi, C.M., Emanuelli, B., and Kahn, C.R., 2006, Critical nodes in signalling pathways: insights into insulin action: Nature reviews. Molecular cell biology, v. 7, no. 2, p. 85–96, doi: 10.1038/nrm1837.

Taveggia, C., Thaker, P., Petrylak, A., Caporaso, G.L., Toews, A., Falls, D.L., Einheber, S., and Salzer, J.L., 2008, Type III neuregulin-1 promotes oligodendrocyte myelination: Glia, v. 56, no. 3, p. 284–293, doi: 10.1002/glia.20612.

Taveggia, C., Zanazzi, G., Petrylak, A., Yano, H., Rosenbluth, J., Einheber, S., Xu, X., Esper, R.M., Loeb, J.A., Shrager, P., Chao, M.V., Falls, D.L., Role, L., and Salzer, J.L., 2005, Neuregulin-1 type III determines the ensheathment fate of axons: Neuron, v. 47, no. 5, p. 681–694, doi: 10.1016/j.neuron.2005.08.017.

Tidcombe, H., Jackson-Fisher, A., Mathers, K., Stern, D.F., Gassmann, M., and Golding, J.P., 2003, Neural and mammary gland defects in ErbB4 knockout mice genetically rescued from embryonic lethality: Proceedings of the National Academy of Sciences of the United States of America, v. 100, no. 14, p. 8281–8286, doi: 10.1073/pnas.1436402100.

Ting, A.K., Chen, Y., Wen, L., Yin, D.-M., Shen, C., Tao, Y., Liu, X., Xiong, W.-C., and Mei, L., 2011, Neuregulin 1 promotes excitatory synapse development and function in GABAergic interneurons: The Journal of neuroscience: the official journal of the Society for Neuroscience, v. 31, no. 1, p. 15–25, doi: 10.1523/JNEUROSCI.2538-10.2011.

Towbin, H., Staehelin, T., and Gordon, J., 1992, Electrophoretic transfer of proteins from polyacrylamide gels to nitrocellulose sheets: procedure and some applications. 1979: Biotechnology (Reading, Mass.), v. 24, p. 145–149.

Tsai, G., and Coyle, J.T., 2002, Glutamatergic mechanisms in schizophrenia: Annual review of pharmacology and toxicology, v. 42, p. 165–179, doi: 10.1146/annurev.pharmtox.42.082701.160735.

Tzahar, E., Waterman, H., Chen, X., Levkowitz, G., Karunagaran, D., Lavi, S., Ratzkin, B.J., and Yarden, Y., 1996, A hierarchical network of interreceptor interactions determines signal transduction by Neu differentiation factor/neuregulin and epidermal growth factor: Molecular and cellular biology, v. 16, no. 10, p. 5276–5287.

Uetz, P., and Hughes, R.E., 2000, Systematic and large-scale two-hybrid screens: Current opinion in microbiology, v. 3, no. 3, p. 303–308.

Uhlhaas, P.J., and Singer, W., 2010, Abnormal neural oscillations and synchrony in schizophrenia: Nature reviews. Neuroscience, v. 11, no. 2, p. 100–113, doi: 10.1038/nrn2774.

Velanac, V., Unterbarnscheidt, T., Hinrichs, W., Gummert, M.N., Fischer, T.M., Rossner, M.J., Trimarco, A., Brivio, V., Taveggia, C., Willem, M., Haass, C., Möbius, W., Nave, K.-A., and Schwab, M.H., 2012, Bace1 processing of NRG1 type III produces a myelin-inducing signal but is not essential for the stimulation of myelination: Glia, v. 60, no. 2, p. 203–217, doi: 10.1002/glia.21255.

Vidal, G.A., Naresh, A., Marrero, L., and Jones, F.E., 2005, Presenilin-dependent gamma-secretase processing regulates multiple ERBB4/HER4 activities: The Journal of biological chemistry, v. 280, no. 20, p. 19777–19783, doi: 10.1074/jbc.M412457200.

Vigano, D., Guidali, C., Petrosino, S., Realini, N., Rubino, T., Di Marzo, V., and Parolaro, D., 2009, Involvement of the endocannabinoid system in phencyclidine-induced cognitive deficits modelling schizophrenia: The international journal of neuropsychopharmacology / official scientific journal of the Collegium Internationale Neuropsychopharmacologicum (CINP), v. 12, no. 5, p. 599–614, doi: 10.1017/S1461145708009371.

Wehr, M.C., Laage, R., Bolz, U., Fischer, T.M., Grünewald, S., Scheek, S., Bach, A., Nave, K.-A., and Rossner, M.J., 2006, Monitoring regulated protein-protein interactions using split TEV: Nature methods, v. 3, no. 12, p. 985–993, doi: 10.1038/nmeth967.

Wehr, M.C., Reinecke, L., Botvinnik, A., and Rossner, M.J., 2008a, Analysis of transient phosphorylation-dependent protein-protein interactions in living mammalian cells using split-TEV: BMC biotechnology, v. 8, p. 55, doi: 10.1186/1472-6750-8-55.

Weickert, C.S., Tiwari, Y., Schofield, P.R., Mowry, B.J., and Fullerton, J.M., 2012, Schizophrenia-associated HapICE haplotype is associated with increased NRG1 type III expression and high nucleotide diversity: Translational Psychiatry, v. 2, no. 4, p. e104, doi: 10.1038/tp.2012.25.

Weisman, J.L., Liou, A.P., Shelat, A.A., Cohen, F.E., Guy, R.K., and DeRisi, J.L., 2006, Searching for new antimalarial therapeutics amongst known drugs: Chemical biology & drug design, v. 67, no. 6, p. 409–416, doi: 10.1111/j.1747-0285.2006.00391.x.

Weissmann, C., and Aguzzi, A., 2005, Approaches to therapy of prion diseases: Annual review of medicine, v. 56, p. 321–344, doi: 10.1146/annurev.med.56.062404.172936.

Wen, L., Lu, Y.-S., Zhu, X.-H., Li, X.-M., Woo, R.-S., Chen, Y.-J., Yin, D.-M., Lai, C., Terry, A.V., Jr, Vazdarjanova, A., Xiong, W.-C., and Mei, L., 2010, Neuregulin 1 regulates pyramidal neuron activity via ErbB4 in parvalbumin-positive interneurons: Proceedings of the National Academy of Sciences of the United States of America, v. 107, no. 3, p. 1211–1216, doi: 10.1073/pnas.0910302107.

Wexler, E.M., and Geschwind, D.H., 2011, DISC1: a schizophrenia gene with multiple personalities: Neuron, v. 72, no. 4, p. 501–503, doi: 10.1016/j.neuron.2011.10.023.

Whalley, H.C., Papmeyer, M., Sprooten, E., Lawrie, S.M., Sussmann, J.E., and McIntosh, A.M., 2012, Review of functional magnetic resonance imaging studies comparing bipolar disorder and schizophrenia: Bipolar disorders, v. 14, no. 4, p. 411–431, doi: 10.1111/j.1399-5618.2012.01016.x.

Williams, C.C., Allison, J.G., Vidal, G.A., Burow, M.E., Beckman, B.S., Marrero, L., and Jones, F.E., 2004, The ERBB4/HER4 receptor tyrosine kinase regulates gene expression by

functioning as a STAT5A nuclear chaperone: The Journal of cell biology, v. 167, no. 3, p. 469–478, doi: 10.1083/jcb.200403155.

Williams, R., Berndt, A., Miller, S., Hon, W.-C., and Zhang, X., 2009, Form and flexibility in phosphoinositide 3-kinases: Biochemical Society transactions, v. 37, no. Pt 4, p. 615–626, doi: 10.1042/BST0370615.

Williamson, P, 2005, Mind Brain and Schiziophrenia, Oxford University Press

Winterer, G., Konrad, A., Vucurevic, G., Musso, F., Stoeter, P., and Dahmen, N., 2008, Association of 5' end neuregulin-1 (NRG1) gene variation with subcortical medial frontal microstructure in humans: NeuroImage, v. 40, no. 2, p. 712–718, doi: 10.1016/j.neuroimage.2007.12.041.

Woo, T.U., Whitehead, R.E., Melchitzky, D.S., and Lewis, D.A., 1998, A subclass of prefrontal gamma-aminobutyric acid axon terminals are selectively altered in schizophrenia: Proceedings of the National Academy of Sciences of the United States of America, v. 95, no. 9, p. 5341–5346.

Xie, M., Yang, D., Wu, M., Xue, B., and Yan, B., 2003, Mouse liver and kidney carboxylesterase (M-LK) rapidly hydrolyzes antitumor prodrug irinotecan and the N-terminal three quarter sequence determines substrate selectivity: Drug metabolism and disposition: the biological fate of chemicals, v. 31, no. 1, p. 21–27.

Yap, T.A., Garrett, M.D., Walton, M.I., Raynaud, F., de Bono, J.S., and Workman, P., 2008, Targeting the PI3K-AKT-mTOR pathway: progress, pitfalls, and promises: Current opinion in pharmacology, v. 8, no. 4, p. 393–412, doi: 10.1016/j.coph.2008.08.004.

Yarden, Y., and Pines, G., 2012, The ERBB network: at last, cancer therapy meets systems biology: Nature Reviews. Cancer, v. 12, no. 8, p. 553–563, doi: 10.1038/nrc3309.

Yarden, Y., and Sliwkowski, M.X., 2001, Untangling the ErbB signalling network: Nature reviews. Molecular cell biology, v. 2, no. 2, p. 127–137, doi: 10.1038/35052073.

Zamboni, W.C., Houghton, P.J., Thompson, J., Cheshire, P.J., Hanna, S.K., Richmond, L.B., Lou, X., and Stewart, C.F., 1998, Altered irinotecan and SN-38 disposition after intravenous and oral administration of irinotecan in mice bearing human neuroblastoma xenografts: Clinical cancer research: an official journal of the American Association for Cancer Research, v. 4, no. 2, p. 455–462.

Zeng, F., Zhang, M.-Z., Singh, A.B., Zent, R., and Harris, R.C., 2007a, ErbB4 isoforms selectively regulate growth factor induced Madin-Darby canine kidney cell tubulogenesis: Molecular biology of the cell, v. 18, no. 11, p. 4446–4456, doi: 10.1091/mbc.E07-03-0223.

Zhang, X.D., 2008, Novel analytic criteria and effective plate designs for quality control in genome-scale RNAi screens: Journal of biomolecular screening, v. 13, no. 5, p. 363–377, doi: 10.1177/1087057108317062.

Zhang, Chung, and Oldenburg, 1999, A Simple Statistical Parameter for Use in Evaluation and Validation of High Throughput Screening Assays: Journal of biomolecular screening, v. 4, no. 2, p. 67–73.

Zhang, X.D., Espeseth, A.S., Johnson, E.N., Chin, J., Gates, A., Mitnaul, L.J., Marine, S.D., Tian, J., Stec, E.M., Kunapuli, P., Holder, D.J., Heyse, J.F., Strulovici, B., and Ferrer, M., 2008, Integrating experimental and analytic approaches to improve data quality in genome-wide RNAi screens: Journal of biomolecular screening, v. 13, no. 5, p. 378–389, doi: 10.1177/1087057108317145.